MATRIX ANALYSIS OF WAVE PROPAGATION IN PERIODIC SYSTEMS

A Thesis

Presented for the Degree

of

DOCTOR OF PHILOSOPHY

of the

UNIVERSITY OF SOUTHAMPTON

in the

Faculty of Engineering and Applied Science

by

AHMED Y.A. ABDEL-RAHMAN

July, 1979.

UNIVERSITY OF SOUTHAMPTON

ABSTRACT

FACULTY OF ENGINEERING AND APPLIED SCIENCE
INSTITUTE OF SOUND AND VIBRATION RESEARCH

Doctor of Philosophy

MATRIX ANALYSIS OF WAVE PROPAGATION IN PERIODIC SYSTEMS

by Ahmed Y.A. ABDEL-RAHMAN

This work presents a method for studying the dynamical behaviour of periodic systems in one, two and three dimensions by matrix formulation which can exploit digital computer techniques for the analysis of complex structures.

It is shown that free and forced wave-propagation in periodic systems can be understood by examining the variation of their characteristic propagation constants with frequency. General computer programs have been written to represent an arbitrary periodic system by a finite element model and to determine the variation of its propagation constants with frequency of propagation. The natural frequencies of some finite periodic systems are calculated from the propagation constants/frequency curves.

The response of periodic systems to homogeneous random pressure fields is examined using periodic structure theory and finite elements. Examples of typical aircraft substructures and other engineering structures have been used throughout, and graphs showing the variation of the propagation constants with frequency and associated wave-forms and the response of these structures to random loading are presented.

The response of general structures to random pressure fields using finite element techniques and the standard modal analysis is also presented. Examples of finite periodic structures are used and the results are compared with those obtained using the periodic structure method.

This analysis provides an automatic means of investigating the vibration characteristics of any complex periodic structure by making use of existing finite element programs.

ACKNOWLEDGEMENTS

The author wishes to express his deep sense of gratitude to the following.

To Dr. M. Petyt for giving all possible assistance, guidance and encouragement at all stages of this work.

To Professor B.L. Clarkson for many words of encouragement and appreciation.

To all colleagues in the Structural Dynamics Group, especially to Dr. D.J. Mead for many interesting and useful discussions and to Dr. S. Fahmy for his help with the computing.

To Miss Mavis Bull for her help in locating many references.

Finally to Mrs. Maureen Strickland for typing the manuscript neatly and efficiently.

CONTENTS

NOTATION

Most of the symbols used in this text are listed below. Other notation are defined where they appear.

General.

$[\ ]$	Matrix
$\lfloor\ \rfloor$	Row matrix
$\{\ \}$	Column matrix
$[\ ]^T$	Transpose of a matrix
$[\ ]^{-T}$	Inverse of the transpose of a matrix
$[\ ]^*$	Conjugate of a complex matrix
$[\ ]^i$	Imaginary part of a complex matrix
$[\ ]^r$	Real part of a complex matrix
$[I]$	Unit matrix
$[\nwarrow x \searrow]$	Diagonal matrix
$\|a\|$	Absolute value of a
$\|i\|$	Reference number i
$[C]$	Damping matrix
$[K]$	Stiffness matrix
$[M]$	Inertia matrix
$\{q\}$	Column matrix of generalised degrees of freedom
$\{F\}$	Column matrix of generalised nodal forces
α, β	Angles
ν	Frequency in Hz
ω	Angular frequency
Ω	Non-dimensional angular frequency
σ	Poisson's ratio
ϕ	Propagation property
ρ	Density
λ_w	Wave-length
λ_s	Shortest wave-length
$\theta_x, \theta_y, \theta_z$	Rotations about the x, y, z axes
$\underline{a}$	Wave-number
D	Modulus of rigidity

E	Young's modulus
h	Plate thickness
i	$\sqrt{-1}$
I_{zz}	Second moment of area of cross-section about the z axis through the centroid
K_r	Rotational stiffness
K_t	Translational stiffness
t	time
u,v,w	Displacements along the x, y, z directions
u_y,v_y,w_y	First derivatives of u, v, w with respect to y

Chapters I, II.

μ	Propagation constant
μ_r	Real part of μ
μ_i	Imaginary part of μ
$u(r,t)$	Displacement field within an element
$[N(\underline{r})]$	Matrix of shape functions for an element
$\{\varepsilon(\underline{r})\}$	Strain components for an element
$[B(\underline{r})]$	Differential of the element shape functions
$[D]$	Matrix of material constants
$[k]$	Stiffness matrix for an element
$[m]$	Mass matrix for an element
$\{f\}$	Column matrix of nodal forces for an element
$[R],[a],[T]$	Transformation matrices
ℓ	Periodic length
L	Lagrangian
T	Kinetic energy
U	Potential energy
Q	Generalised non-conservative forces
v	Volume

Chapters III, IV.

μ_1,μ_2,μ_3	Propagation constants along the d_1, d_2, d_3 directions
a_1,a_2,a_3	Components of the wave-number $\underline{a}$ along the d_1, d_2, d_3 directions
ℓ_1,ℓ_2,ℓ_3	Periodic distances (dimensions of a cell) along the d_1, d_2, d_3 directions
∇^2	Operator $= \frac{\partial^2}{\partial x^2} + \frac{\partial^2}{\partial y^2}$

Chapter V

S_ϕ	Power spectral density of a response quantity ϕ
S_p	Power spectral density of the pressure field
U_p	Convection velocity (phase velocity) of the pressure field
CV	Non-dimensional convection velocity of the pressure field
v_w	Free wave speed (phase velocity)
V_w	Non-dimensional free wave speed
σ_m	Mean square response
$\underline{k}$	Angular wave-number
k_1, k_2	Components of the wave-number $\underline{k}$ along the d_1 and d_2 directions
ε	$=-k\ell$
ε_1, ε_2	$=-k_1.\ell_1$, $-k_2.\ell_2$
η	Material loss factor
ξ	Modal damping
$P(\underline{r}, t)$	Pressure field
$\{\eta\}$	Column matrix of generalised degrees of freedom
$[V]$	Transformation matrix
ℓ	Periodic length (length of a cell) for one-dimensional systems
ℓ_1, ℓ_2	Periodic lengths (dimensions of a cell) along the d_1 and d_2 directions

CHAPTER I

1.1 Introduction

A periodic system consists of identical cells, where a cell represents one period of the system, joined together in identical manner in one, two or three dimensions. There are many examples of such systems in physical and engineering structures: crystal lattices in solid state physics, a tall building having identical storeys, a flat or curved plate with stiffeners or supports at regular intervals in one or two dimensions (e.g., in aircraft and ship structures), a pipe-line system with stiffeners and supports placed at equal spacings, etc. Modular type multi-storey buildings can be regarded as three-dimensional periodic structures.

Such structures are considered as finite periodic systems. Their natural frequencies fall into groups |40|, and the number of frequencies in each group equals the number of periods in the structure. When the number of periods is large, the natural frequencies are closely spaced. Calculating the response of these structures to dynamic excitation using the modal method of solution |35|, |37| requires modelling the whole structure and finding a large number of natural frequencies and associated normal modes. Such a procedure needs a lot of time for modelling and data preparation. Also the computer time and storage needed for the analysis can be very large. High modal density and some types of damping add further complications to the modal analysis |35|, |37|.

The dynamical behaviour of such systems can be studied with great simplicity and accurately if we consider them as infinitely periodic and apply the periodic structure theory. For one-dimensional systems it can be stated as follows.

A property ϕ can propagate as a wave in an infinite one-dimensional periodic system if the physical problem admits a solution of the type

$$\begin{aligned} \phi_n &= Ae^{2\pi i(\nu t - an\ell)} \\ &= Ae^{i(\omega t + n\mu)} \end{aligned} \tag{1.1}$$

where $a = \frac{1}{\lambda_w}$, $\mu = -2\pi a\ell$, $\omega = 2\pi\nu$ (1.2)

a is the wave-number, λ_w is the wave-length

ϕ_n is the value of the property ϕ associated with cell number n,

ν is the frequency, ℓ the periodic length,

ω the angular frequency and A is a constant.

The quantity μ is known as the propagation constant. It represents the change in phase in passing from one cell n to its neighbouring cell $n + 1$:

$$\phi_{n+1} = \phi_n e^{i\mu} \tag{1.3}$$

Relations (1.1) and (1.3) can be used to describe attenuating waves |3|. In this case μ will be a complex quantity. Its real part represents the change in phase while the imaginary part represents the attenuation in passing from one cell to the next. This theorem can be generalised for two and three-dimensional periodic systems. This will be investigated in Chapters III and IV.

The study of wave propagation in periodic systems dates back to the eighteenth century, as Brillouin has discussed in his classic work |3| on the mathematical physics of wave propagation. His work covers a wide range of problems that occur in solid state physics, optics, electronics and electrical engineering.

The dynamical behaviour of periodic systems that consist of beams and plates has been recently investigated by employing the periodic structure theory. Heckel |19|, Ungar |60| and Bobrovnitskii and Maslov |5| studied the flexural wave motion in periodic beam structures. Mead and Wilby |27| considered the effects of damping on such structures. Mead |28, 31|, Sen Gupta |55, 56| and Mead and Sen Gupta |29, 30| studied the free and forced vibration of periodic beams and rib-skin structures. They showed that the response of one-dimensional periodic structures of five bays or more to random pressure fields is close to the response of infinite structures. Similar results have been obtained experimentally |43|.

Approximate methods of solution have been employed by Abrahamson |1| and Mead |32|. They used an extension of the Rayleigh Method and the Rayleigh-Ritz method to study the nature of waves propagating in non-

uniform periodic structures. Lindberg and Olson |24| and Orris and Petyt |46 , 47| used the finite element method to study free wave propagation and the response of one-dimensional periodic structures to convected random pressure fields.

The purpose of this work is to present a general method to study the dynamical characteristics of any periodic system in one, two or three dimensions using the finite element method and the periodic structure theory. First the structure is divided into cells, where a cell represents one period of the structure. One cell is represented by a finite element model with interior and boundary degrees of freedom. The linear equation of motion of the cell is given by

$$[M]\{\ddot{q}\} + [C]\{\dot{q}\} + [K]\{q\} = \{F\} \qquad (1.4)$$

where

$[K]$, $[M]$ and $[C]$ are the stiffness, inertia and damping matrices respectively,

$\{q\}$ and $\{F\}$ are the generalised nodal degrees of freedom and forces.

Free and forced waves propagating in the structure can be investigated by solving equation (1.4) after applying the appropriate constraint relations between the boundary degrees of freedom and forces given by equation (1.3).

Chapters II, III and IV deal with free wave propagation in one, two and three-dimensional periodic systems. In Chapter V the response of one and two-dimensional periodic systems to random pressure fields is investigated. Also the response of general structures to random forces using the standard modal method of solution is presented and examples of finite periodic structures in one and two dimensions are used. Conclusions, general discussion and suggestions for future work are presented in Chapter VI.

1.2 Theoretical Background to the Finite Element Method

The equations of motion of systems composed of particles and rigid bodies can be formulated using Newton's laws of motion, where physical

coordinates and forces acting on the individual components of the system are employed. A more general approach referred to as Variational Mechanics can be used to investigate the dynamical characteristics of any system whether discrete or continuous. It considers the system as a whole instead of its individual components, and formulates its equations of motion by considering two scalar quantities only, namely the kinetic and potential energies, and using Lagrange's equations which can be written as

$$\frac{d}{dt}\left(\frac{\partial L}{\partial \dot{q}_i}\right) - \frac{\partial L}{\partial q_i} = Q_i \qquad (i = 1,2,\ldots, n) \quad (1.5)$$

where L is known as the Lagrangian of the system and is defined by

$$L = T - U \qquad (1.6)$$

T and U are the kinetic and potential energies of the system,
q_i are the generalised degrees of freedom in the system,
n is the number of degrees of freedom,
Q_i represents the generalised nonconservative forces in the system.

In order to derive the equation of motion of complex continuous structures some approximate methods must be employed. One of the most reliable methods is the Finite Element Technique, which is in fact an extension of the Rayleigh-Ritz method.

The main idea behind the finite element method is to represent any system by a mathematical model that can exploit the capacities of digital computers. It regards any continuous system as an assemblage of finite number of discrete elements, where each element is a continuous part of the system. These elements are joined together at a selected number of node points. At these nodes the displacements should be compatible and the internal forces be in equilibrium. The basic features of the method can be summarised in the following steps.

i) The structure is divided into a number of elements, where each element is defined by a set of node points. These node points can be shared by several elements.

ii) The stiffness, inertia and consistent load matrices are calculated for each element.

iii) The system stiffness, inertia and consistent load matrices are formed by assembling the individual matrices for each element.

iv) The physical boundary conditions are applied on the system matrices.

The element matrices are calculated as follows.

a) Define the element by a set of node points (usually sited on the element's boundary) with a certain number of degrees of freedom at each node.

b) Represent the displacement field in the element by a set of functions such that each one corresponds to a unit value of one of the degrees of freedom at the nodes.

The displacement field u at any point $\underline{r}$ within an element i can be written as

$$\{u(\underline{r}, t)\}_i = [N(\underline{r})]_i \{q(t)\}_i \tag{1.7}$$

where

$[N(\underline{r})]_i$ is a matrix containing the element shape functions,
$\{q(t)\}_i$ is a vector of the element nodal degrees of freedom.

The element strain components can be written in the form

$$\{\varepsilon(\underline{r}, t)\}_i = [B(\underline{r})]_i \{q(t)\}_i \tag{1.8}$$

where

$[B(\underline{r})]_i$ is a differential of the element shape functions.

The element kinetic and strain energies can be written in the form

$$T_i = \tfrac{1}{2} \int_{V_i} \rho_i \{\dot{u}\}_i^T \{\dot{u}\}_i \, dv \tag{1.9}$$

$$U_i = \tfrac{1}{2} \int_{V_i} \{\varepsilon\}_i^T [D]_i \{\varepsilon\}_i \, dv \tag{1.10}$$

where

ρ_i is the density, v_i is the volume and $[D]_i$ is a matrix of material constants for element i.

Substituting (1.7) into (1.9) gives

$$T_i = \tfrac{1}{2} \int_{V_i} \rho_i \{\dot{q}(t)\}_i^T [N(\underline{r})]_i^T [N(\underline{r})]_i \{q(t)\}_i \, dv$$

or

$$T_i = \tfrac{1}{2} \{\dot{q}\}_i^T [m]_i \{\dot{q}\}_i \tag{1.11}$$

$[m]_i$ is known as the element consistent inertia matrix where

$$[m]_i = \int_{V_i} \rho_i [N(\underline{r})]_i^T [N(\underline{r})]_i \, dv \tag{1.12}$$

Similarly, substituting (1.8) into (1.10) gives

$$U_i = \tfrac{1}{2} \int_{V_i} \{q(t)\}_i^T [B(\underline{r})]_i^T [D]_i [B(\underline{r})]_i \{q(t)\}_i \, dv$$

or

$$U_i = \tfrac{1}{2} \{q\}_i^T [k]_i \{q\}_i \tag{1.13}$$

$[k]_i$ is known as the element consistent stiffness matrix, where

$$[k]_i = \int_{V_i} [B(\underline{r})]_i^T [D]_i [B(\underline{r})]_i \, dv \tag{1.14}$$

If external forces $P(\underline{r}, t)$ exist, then the virtual work done by the external forces is given by

$$\delta W_i = \int_{V_i} \{\delta u(\underline{r}, t)\}_i^T \{P(\underline{r}, t)\}_i \, dv \tag{1.15}$$

Introducing (1.7) into (1.15) gives

$$\delta W_i = \int_{V_i} \{\delta q(t)\}_i^T [N(\underline{r})]_i^T \{P(\underline{r}, t)\}_i \, dv$$

or

$$\delta W_i = \{\delta q(t)\}_i^T \{f\}_i \tag{1.16}$$

$\{f\}_i$ is known as the element consistent load vector, where

$$\{f\}_i = \int_{V_i} [N(\underline{r})]_i^T \{P(\underline{r}, t)\}_i \, dv \tag{1.17}$$

The kinetic and strain energies of the complete system can be written as

$$T = \tfrac{1}{2}\{\dot{q}\}^T [M]\{\dot{q}\} \tag{1.18}$$

$$U = \tfrac{1}{2}\{q\}^T [K]\{q\} \tag{1.19}$$

where

$\{q\}$ is a vector of the system nodal degrees of freedom

$[M]$ and $[K]$ are the system inertia and stiffness matrices, where

$$[M] = \sum_{i=1}^{N} [R]_i^T [m]_i [R]_i \tag{1.20}$$

$$[K] = \sum_{i=1}^{N} [R]_i^T [k]_i [R]_i \tag{1.21}$$

N is the total number of elements in the system

$[R]_i$ is a transformation matrix given by

$$[R]_i = [T]_i [R_B]_i [a]_i \tag{1.22}$$

$[a]_i$ is a Boolean matrix relating the degrees of freedom of the individual elements to the degrees of freedom of the complete system.

$[R_B]_i$ is a transformation matrix for the application of the physical boundary condition.

$[T]_i$ is a transformation matrix to transform the element matrices from the element local coordinates to the system global coordinates.

The generalised nodal forces can be obtained by considering the virtual work done by the external forces. This can be written in the form

$$\delta w = \{\delta q\}^T \{F\}. \tag{1.23}$$

$\{F\}$ is the system consistent load vector, where

$$\{F\} = \sum_{i=1}^{N} [R]_i^T \{f\}_i \, . \tag{1.24}$$

Introducing (1.18), (1.19) and (1.24) into Lagrange's equations,

equations (1.5), yields the equations of motion for the undamped system in the form

$$[M]\{\ddot{q}\} + [K]\{q\} = \{F\} \tag{1.25}$$

This equation can be solved for free and forced motion of the structure using standard matrix techniques.

For detailed analysis of the finite element method see Zienkiewicz |69|.

CHAPTER II

FREE WAVE PROPAGATION IN ONE-DIMENSIONAL PERIODIC SYSTEMS

2.1 General

There are many structures in engineering that can be regarded as one-dimensional periodic systems. Examples of such structures are: a tall building consisting of identical storeys, a flat or curved plate with stiffeners at regular spacings, a pipe-line system with supports at equal intervals, electric transmission lines, etc. Recently, as mentioned in the previous chapter, the literature has contained a large number of papers on the wave propagation in one-dimensional periodic structures and their response to dynamic loads. These structures can be considered as an assemblage of identical cells (periods) joined together in identical manner. Their dynamical characteristics can be easily and quickly investigated if their periodic nature is utilised. This can be achieved by considering such structures as infinitely periodic and studying the nature of waves propagating in them using the periodic structure theory. This theorem was mentioned in Chapter I and will be repeated here since the whole mathematical formulation in this work is based on it. For one-dimensional systems it can be stated as follows:

A property ϕ can propagate as a wave in an infinite one-dimensional periodic system if the physical problem admits a solution of the type

$$\phi_n = Ae^{2\pi i(\nu t - an\ell)} \qquad (2.1)$$

or

$$\phi_n = Ae^{i(\omega t + n\mu)}$$

where ϕ_n is the value of the property ϕ at a given point in cell number n (the origin of the system is chosen at the cell defined by $n = 0$). The definitions of the other variables in equation (2.1) were given in Chapter I, Sec. 1.1. This means that the property ϕ_n at a given point in cell n can be related to ϕ_{n+1} at the corresponding point in cell $n + 1$ by the relation

$$\phi_{n+1} = \phi_n e^{-2\pi i a \ell} \qquad (2.2)$$

or

$$\phi_{n+1} = \phi_n e^{i\mu}$$

μ is known as the propagation constant, where

$$\mu = -2\pi a \ell \qquad (2.3)$$

which represents the change in phase in passing from one cell to the next.

Attenuating waves can be described by relations (2.1) and (2.2) but in this case the wave-number a (and hence the propagation constant μ) will be a complex quantity. The real part of μ represents the change in phase while the imaginary part represents the attenuation in passing from one cell n to its neighbouring cell $n + 1$.

In this chapter a matrix formulation for studying the free wave propagation in any one-dimensional periodic system using the finite element technique and the periodic structure method is presented and discussed in detail. The variation of the propagation constant with frequency is obtained by solving the equations of motion of one periodic section (cell) of the system. Examples of simple one-dimensional periodic systems will be discussed first to illustrate the general behaviour of these systems, then the method will be used to study some typical aircraft substructures such as flat and curved stiffened plates. The determination of the natural frequencies of some finite periodic structures from the propagation constant/frequency curves is also investigated.

This analysis provides an automatic means of studying any periodic system by making use of existing finite element routines.

2.2 Mathematical Formulation

Consider a one-dimensional periodic system composed of an infinite number of identical cells (periods) joined together in identical manner as shown in figure (2.1a). Using the finite element technique, a cell can be represented by a model with interior and boundary degrees of freedom. Each cell is coupled to its neighbours on each side (left and right) by a certain number of degrees of freedom and forces. Let $\{q_I\}$, $\{F_I\}$, $\{q_L\}$,

$\{F_L\}$ and $\{q_R\}$, $\{F_R\}$ be the degrees of freedom and forces at the nodes on the interior, left and right of the cell considered. The linear equation of motion of an undamped cell is given by

$$([K] - \omega^2[M])\{q\} = \{F\} \tag{2.4}$$

where

$$\{q\} = \begin{Bmatrix} q_I \\ q_L \\ q_R \end{Bmatrix}, \qquad \{F\} = \begin{Bmatrix} F_I \\ F_L \\ F_R \end{Bmatrix} \tag{2.5}$$

$[K]$ and $[M]$ are the stiffness and inertia matrices for the cell. They can be partitioned according to the interior, left and right degrees of freedom in the cell. Hence

$$[K] = \begin{bmatrix} K_{I,I} & K_{I,L} & K_{I,R} \\ K_{L,I} & K_{L,L} & K_{L,R} \\ K_{R,I} & K_{R,L} & K_{R,R} \end{bmatrix}, \quad [M] = \begin{bmatrix} M_{I,I} & M_{I,L} & M_{I,R} \\ M_{L,I} & M_{L,L} & M_{L,R} \\ M_{R,I} & M_{R,L} & M_{R,R} \end{bmatrix} \tag{2.6}$$

The forces $\{F\}$ are due to the external forces acting on the system and the forces of interaction between the cell and its neighbours. For free wave-motion, i.e., no external forces exist, $\{F_I\}$ equal to zero; however, $\{F_L\}$ and $\{F_R\}$ are not zero since they transmit the wave-motion from one cell to the next. This wave-motion is characterised by relating the degrees of freedom and equivalent nodal forces in one cell to the corresponding degrees of freedom and forces in adjacent cell by the following relations.

$$\begin{aligned} \{q_L\}_{n+1} &= e^{i\mu}\{q_L\}_n, \\ \{F_L\}_{n+1} &= e^{i\mu}\{F_L\}_n \end{aligned} \tag{2.7}$$

where μ is the propagation constant.

At the common boundaries between cell n and the neighbouring cell $n + 1$, the displacements must be equal and the interconnecting forces must be in equilibrium. Hence,

$$\{q_L\}_{n+1} = \{q_R\}_n$$

and (2.8)

$$\{F_L\}_{n+1} + \{F_R\}_n = 0.$$

Substituting (2.7) into (2.8) gives

$$\{q_R\}_n = e^{i\mu}\{q_L\}_n \tag{2.9}$$

$$\{F_R\}_n + e^{i\mu}\{F_L\}_n = 0 \tag{2.10}$$

Since relations (2.9) and (2.10) are the same for any cell, the suffix n can be dropped.

Relation (2.9) can be used to write the relation between the degrees of freedom in the cell in the matrix form:

$$\begin{Bmatrix} q_I \\ q_L \\ q_R \end{Bmatrix} = [W] \begin{Bmatrix} q_I \\ q_L \end{Bmatrix} \tag{2.11}$$

where

$$[W] = \begin{bmatrix} I & 0 \\ 0 & I \\ 0 & e^{i\mu} \end{bmatrix} \tag{2.12}$$

Also relation (2.10) and the condition

$$\{F_I\} = 0,$$

can be written in the matrix form:

$$[W'] \begin{Bmatrix} F_I \\ F_L \\ F_R \end{Bmatrix} = 0 \tag{2.13}$$

where

$$[W'] = \begin{bmatrix} I & 0 & 0 \\ 0 & I & e^{-i\mu} \end{bmatrix} \tag{2.14}$$

Substituting (2.11) and (2.13) into (2.4) results in an equation of the form

$$([\bar{K}(\mu)] - \omega^2[\bar{M}(\mu)]) \begin{Bmatrix} q_I \\ q_L \end{Bmatrix} = 0 \qquad (2.15)$$

where $[\bar{K}(\mu)]$ and $[\bar{M}(\mu)]$ are complex matrices given by

$$[\bar{K}] = \begin{bmatrix} K_{I,I} & \bar{K}_{I,L} \\ \bar{K}_{L,I} & \bar{K}_{L,L} \end{bmatrix} = [W'][K][W],$$

$$[\bar{M}] = \begin{bmatrix} M_{I,L} & \bar{M}_{I,L} \\ \bar{M}_{L,I} & \bar{M}_{L,L} \end{bmatrix} = [W'][M][W] \qquad (2.16)$$

Equation (2.15) represents an eigenvalue problem in ω for a given value of μ. For propagating (unattenuated) waves μ is real. In this case equation (2.15) can be rearranged to give a real symmetric eigenvalue problem in ω for a given value of μ. This will be discussed in Section 2.3. Also, equation (2.15) can be reformulated to give an eigenvalue problem in μ for a given frequency ω, where μ will be generally a complex quantity. This will be discussed in Section 2.5.

2.3 Formulation for the Real Propagation Constant

Free waves can propagate (without attenuation) in one-dimensional undamped periodic systems within certain frequency bands only (called the propagation bands) |3|. In these bands the wave-number a, and hence the propagation constant μ, is a real quantity. In this section a formulation is presented to study the variation of the real propagation constant μ_r with frequency for any one-dimensional linear undamped periodic system.

Before proceeding to the mathematical formulation, some of the properties of one-dimensional periodic systems will be briefly discussed. Detailed discussion can be found in |3|.

As explained in section 2.1, the relation between a propagation property ϕ_n at any point in cell n and ϕ_{n+1} at the corresponding point in the neighbouring cell n + 1 at any instant of time is given by equation (2.2), namely

$$\phi_{n+1} = \phi_n \, e^{-2\pi i a \ell}$$

or

$$\phi_{n+1} = \phi_n \, e^{i\mu}$$

where μ is the propagation constant and is given by relation (2.3), namely,

$$\mu = -2\pi a \ell$$

ℓ is the periodic length (length of the cell) and

a is the wave-number.

For propagating waves (non-attenuating) the wave-number a (and hence μ) is a real quantity where

$$a = 1/\lambda_w \tag{2.17}$$

λ_w is the wave-length.

The relations (2.2) can be satisfied by using a' and μ' instead of a and μ where

$$\begin{aligned} a' &= a \pm m/\ell \\ \mu' &= \mu \pm 2m\pi \end{aligned} \tag{2.18}$$

where m is an integer number.

Solving the equation of motion of the system given by (2.15) must yield the same values of the frequency ω and the corresponding values of the vectors $\{q\}$ for every equivalent μ and μ'. This means that the propagation property ϕ (the vectors $\{q\}$ in equation (2.15)) and its frequency ω are periodic functions of μ with period 2π. Therefore it is sufficient to examine the relation between ω and μ within one period only. The period given by

$$-\pi \leq \mu \leq \pi$$

or

$$-\frac{1}{2\ell} \leq a \leq \frac{1}{2\ell} \tag{2.19}$$

is chosen and is called the fundamental (first) zone of the one-dimensional system. This zone contains a complete period of $\omega(\mu)$ allowing us to examine all the frequencies that can be propagated. Negative values of μ means a wave travelling to the right (see Figure (2.1a)) while positive μ means a wave travelling to the left. Since a wave propagates to the left

or to the right in the same manner, the curve relating ω to μ (or a) must be symmetrical about the origin with a maximum (or minimum) at $\mu = 0$ (or $a = 0$). Also due to the periodicity of the curve there will be another maximum (or minimum) at $\mu = \pm\pi$ (or $a = \pm \frac{1}{2\ell}$). Restricting the values of a and μ inside the zone given by (2.19) means that the wave-length λ_w varies between

$$\lambda_w = \infty \quad (\text{at } \mu = 0; \quad a = 0) \tag{2.20}$$

and

$$\lambda_w = 2\ell \quad (\text{at } \mu = \pm\pi \; ; \quad a = \pm \frac{1}{2\ell}). \tag{2.21}$$

The wave-length given by (2.21) is the shortest wave-length for any wave travelling in the system. See Brillouin |3| for relevant discussion. Frequencies corresponding to $\mu = 0$ ($a = 0$) and $\mu = \pm\pi$ ($a = \pm \frac{1}{2\ell}$) are called critical frequencies. They are characteristic of the periodic system and depend on its physical properties.

Now for a given value of μ (real quantity) the matrices $[\bar{K}]$ and $[\bar{M}]$ in equation (2.11) can be written as

$$\begin{aligned} [\bar{K}(\mu)] &= [\bar{K}^r] + i[\bar{K}^i], \\ [\bar{M}(\mu)] &= [\bar{M}^r] + i[\bar{M}^i]. \end{aligned} \tag{2.22}$$

Substituting (2.22) into (2.15) gives

$$([\bar{K}^r] + i[\bar{K}^i] - \omega^2([\bar{M}^r] + i[\bar{M}^i]))\,\{\{\bar{q}^r\} + i\{\bar{q}^i\}\} = 0 \tag{2.23}$$

where

$$\{\bar{q}^r\} = \begin{Bmatrix} q_I{}^r \\ q_L{}^r \end{Bmatrix}, \qquad \{\bar{q}^i\} = \begin{Bmatrix} q_I{}^i \\ q_L{}^i \end{Bmatrix} \tag{2.24}$$

Separating the real and imaginary parts of (2.23) and combining the two sets of equations together gives

$$\left(\begin{bmatrix} \bar{K}^r & -\bar{K}^i \\ \bar{K}^i & \bar{K}^r \end{bmatrix} - \omega^2 \begin{bmatrix} \bar{M}^r & -\bar{M}^i \\ \bar{M}^i & \bar{M}^r \end{bmatrix} \right) \begin{Bmatrix} \bar{q}^r \\ \bar{q}^i \end{Bmatrix} = 0 \tag{2.25}$$

From (2.12) and (2.13) it is clear that for real values of μ we can write

$$[W'] = [W^*]^T \tag{2.26}$$

where * denotes the complex conjugate, and hence the matrices $[\bar{K}]$ and $[\bar{M}]$ (given by (2.16)) are Hermitian, i.e.,

$$\begin{aligned} [\bar{K}^*]^T &= [\bar{K}], \\ [\bar{M}^*]^T &= [\bar{M}] \end{aligned} \tag{2.27}$$

Therefore, equation (2.25) represents a real symmetric eigenvalue problem since,

$$\begin{aligned} [\bar{K}^i] &= -[\bar{K}^i]^T, \\ [\bar{M}^i] &= -[\bar{M}^i]^T \end{aligned} \tag{2.28}$$

This equation can be solved to find the variation of the frequency ω with the propagation constant μ (where μ is real). For each value of μ equation (2.25) will give a set of frequencies occurring in equal pairs. The corresponding eigenvectors will define the wave motion in the system at these frequencies. The method used in solving this eigenvalue problem is discussed in Appendix A.

2.3.1 Computer programs

A general computer program has been written to represent one period (cell) of any periodic system by a finite element model and to form the matrices in equation (2.25) for different values of the real propagation constant μ. For each value of μ the eigenvalue problem (2.25) is solved to find the corresponding values of the frequency ω and associated wave-forms. The basic flow diagram for the computational procedure is given in Appendix B.

2.3.2 Illustrative examples

This example will be used to explain and illustrate some of the properties of one-dimensional periodic systems discussed at the beginning of this section.

Consider the transverse wave motion in an infinite beam resting on simple supports at regular intervals as shown in figure (2.2a). One cell is represented by a finite element model, figure (2.2b). The beam element

and the data values used in the analysis are given in Appendix D1. The length of the cell ℓ (distance between the supports) is taken equal to unity. The cell is divided into ten beam elements. The degrees of freedom considered at the nodes are the transverse motion v and the rotation θ_z, and hence at the supports only θ_z exists. Figures (2.2b, c and d) show different choices for the basic cell representing the system. Although any one of these choices can be used for the analysis, it is advantageous to choose the cell with the minimum coupling degrees of freedom to its neighbours (figure (2.2b)) since this will, in general, simplify the analysis. Also it should be noted that the number of independent waves that can exist at any frequency equals twice the minimum number of coupling degrees of freedom between the cells $|32|$ (only the rotation θ_z in this case). Each pair of these waves represents two identical waves travelling in opposite directions. The problem is solved for various values of the real propagation constant μ to find the corresponding frequencies of propagation. Figure (2.8) shows the variation of the non-dimensional frequency Ω with the propagation constant μ for values of μ varying between -3π and $+3\pi$ where

$$\Omega = \omega\left(\frac{\rho\ell^4}{EI_{zz}}\right)^{\frac{1}{2}} \tag{2.29}$$

ρ is the beam density per unit length,

ℓ the periodic length,

I_{zz}: the second moment of area of the cross-section about the local z axis (see Appendix D1),

E: Young's modulus.

From the graph it can be seen that the structure allows propagation within some frequency bands only (where the curves $\Omega(\mu)$ exist). These are called the propagation bands and hence the beam acts as a pass-band filter. Waves with frequencies outside these bands are strongly attenuated. This will be discussed in a later section. Also it is clear that the frequency is a periodic function of μ, with period 2π, and symmetrical about the frequency axis (line $\mu = 0.0$). Figures (2.9) and (2.10) show the frequencies of propagation and the corresponding wave-forms in the first and second propagation bands for various values of the propagation constant

μ. These wave-forms are the eigenvectors obtained by solving equation (2.25). It should be noted here that these eigenvectors are complex quantities and only the real part of the solution

$$(q^r + iq^i).e^{i(\omega t+n\mu)} \tag{2.30}$$

should be considered.

When $\mu = 0$ the corresponding wave-form represents a standing wave where adjacent cells are vibrating in phase with one another. In the first band (upper bound) the frequency and the corresponding wave-form coincide with the fundamental natural frequency and associated normal mode of vibration of the single cell with its coupling degrees of freedom (θ_z at the left and right supports in this case) constrained, while in the second band (lower bounding frequency of the band) they coincide with the second natural frequency and associated normal mode of the single cell with its coupling degrees of freedom unconstrained. The wavelength for these waves is given by

$$\lambda_w = 1/|a| = \infty$$

since the wave-number a is equal to zero. As the absolute value of μ increases the wave-length decreases until it reaches the shortest wave-length λ_s when $\mu = \pm \pi$ (or $a = \pm \frac{1}{2\ell}$) where

$$\lambda_s = \frac{1}{|a|} = 2\ell$$

which can be regarded as a wave travelling to the right (corresponding to $\mu = -\pi$) or to the left ($\mu = +\pi$) or even as a standing wave where adjacent cells are vibrating in counter-phase with one another. In the first band (lower bounding frequency of the first band) the frequency of propagation and the corresponding wave-form coincide with the fundamental natural frequency and associated normal mode of vibration of the single cell with its coupling degrees of freedom unconstrained, while in the second band (upper bounding frequency) they coincide with the second natural frequency and normal mode of the single cell with its coupling degrees of freedom constrained. For intermediate values of μ ($0 < |\mu| < \pi$; $0 < |a| < \frac{1}{2\ell}$) the corresponding waves are travelling waves to the right for negative μ and to the left for positive μ. These results were demonstrained on a movie film produced by the computer showing clearly the standing and travelling

waves. Changing the values of μ (or a) to μ' (or a') in the analysis such that

$$\mu' = \mu \pm 2m\pi \qquad \text{or} \qquad a' = a \pm \frac{m}{\ell}$$

where m is any integer number will result in the same waves obtained for the corresponding values of μ (or a) with a wave-length always given by

$$\lambda_w = 1/|a|$$

and direction of propagation determined by the sign of μ. This shows that the restriction on the values of μ inside the fundamental zone given by (2.19) should be observed when determining the wave-length and the direction of propagation.

To check the accuracy of the finite element results produced here, the single cell representing the system is idealised using different numbers of elements and the results are compared with those produced using closed form solution |31, 55|. Table 2.1 shows a comparison of the bounding frequencies for the first three propagation bands obtained using the exact solution and using different finite element idealisation for the cell (frequencies corresponding to $\mu = 0$ or $a = 0$ and $\mu = \pm\pi$ or $a = \pm \frac{1}{2\ell}$). From the table it is clear that even when the cell is idealised with four elements only the finite element results are very close to the exact ones. The same accuracy is obtained for intermediate values of μ $(0 < |\mu| < \pi)$.

The effect of adding rotational stiffness at the supports, figure (2.3a), on the propagation constant/frequency curve is investigated by considering a single cell with half the rotational stiffness at each support, figure (2.3b). The cell is divided into ten beam elements. The beam element and data values used are the same as before. The results are shown in figure (2.11) for values of the rotational stiffness $K_r = 0$, 4, 10 and ∞. The propagation constant μ is varied between 0 and $-\pi$ only. As can be seen from this graph increasing the value of K_r has the effect of narrowing the width of the propagation bands (only the first two bands are shown). Similar to the beam on simple supports ($K_r = 0$), frequencies corresponding to values of μ equal to zero or $\pm\pi$ (bounding frequencies for the various propagation bands) coincide with the natural frequencies of the cell with its coupling degrees of freedom unconstrained or constrained

and hence, as can be seen from figure (2.11), the addition of the rotational stiffness at the supports affects only the bounding frequencies coinciding with the natural frequencies of the unconstrained cell. At the limit when $K_r = \infty$ the propagation bands disappear completely and no propagation occurs in the beam. Similar results were produced in |30, 31 and 55| using closed form solution.

2.3.3 Two examples of typical aircraft substructures

Most aircraft substructures are composed of flat or curved plates with stiffeners at regular spacings. The following two examples are typical of such structures.

a. Stringer stiffened flat panel, figure (2.4a).

Figure (2.4b) shows a finite element idealisation for one cell. The elements and data values used in the analysis are given in Appendix D2. The cell is represented by four flat strip elements and one thin-walled open section beam element. The degrees of freedom considered at each node are the transverse motion w and the rotation θ_x. The variation of the propagation constant with the non-dimensional frequency Ω is shown in figure (2.12) for the first two propagation bands, where μ is restricted between zero and $-\pi$ only. Similar to the beam on simple supports the panel allows propagation within some frequency bands only. The upper and lower bounding frequencies for the bands occur at values of μ equal to zero or $-\pi$. Waves with frequencies outside these bands attenuate rapidly and the panel acts as a pass-band filter.

b. Stringer stiffened curved panel, figure (2.5a).

Figure (2.5b) shows a finite element idealisation for a single cell. The elements and data values used in the analysis are given in Appendix D3. One cell is represented by four curved strip elements for the panel and one open section beam element for the stringer. The degrees of freedom at the nodes are u, u_y, v, v_y, w, w_y. At the stringers only u, v, w and w_y are retained. Figure (2.13) shows the variation of the propagation constant with the non-dimensional frequency Ω in the first two propagation bands. From the graph it is clear that the lower bounding frequency of the second band does not occur at values of μ equal to zero or $\pm\pi$. Otherwise the panel shows similar behaviour to the beam example discussed in Section 2.3.2.

The results obtained here for these two examples are in full agreement, within the readings taken from the plotted results, with those produced in |14| using transfer matrix analysis. The accuracy of the results produced here can be increased by simply increasing the number of elements representing the cell or by using more accurate elements.

2.4 Transition from Non-Periodic to Periodic Systems

In this section, the effect of adding periodic perturbation to a continuous medium on the variation of its propagation constant with frequency is investigated.

Consider the transverse wave-motion in an infinite beam resting on spring supports at regular spacings as shown in figure (2.6a). One cell is represented by a finite element model with ten beam elements, figure (2.6b). The length of the cell (distance between the supports) is taken equal to unity. The beam element and data values used in the analysis are given in Appendix D1. The degrees of freedom at the nodes are the transverse displacement v and the rotation θ_z and hence each cell is coupled to its neighbours on each side by two degrees of freedom. The problem is solved for different values of the spring supports stiffness K_t. For each case the real propagation constant μ is plotted as a function of the non-dimensional frequency Ω as shown in figure (2.14). For $K_t = 0$ the beam allows propagation at all frequencies and the curve relating μ to Ω is the same as the one obtained by considering the equation for the transverse wave motion in an infinite beam given by

$$EI_{zz} \frac{\partial^4 v}{\partial x^4} + \rho \frac{\partial^2 v}{\partial t^2} = 0 \qquad (2.31)$$

and considering

$$v(x) = v_o e^{2\pi i(\nu t - ax)} \qquad (2.32)$$

as a solution to (2.31) results in the relation

$$\nu^2 = 4\pi^2 \frac{EI_{zz}}{\rho} a^4 \qquad (2.33)$$

but

$$\nu = \frac{\omega}{2\pi}, \qquad a = -\frac{\mu}{2\pi\ell} \qquad \text{and} \qquad \Omega = \left(\frac{\omega\rho\ell^4}{EI_{zz}}\right)^{\frac{1}{2}} \qquad (2.34)$$

Substituting (2.34) into (2.33) gives

$$\Omega = \mu^2 \tag{2.35}$$

where

x is the distance along the beam and v_o is a constant.

Table 2.2 shows a comparison between the finite element results and the exact solution obtained by (2.35) where, as can be seen from the table, the finite element results are very close to the exact ones.

Non-zero values for K_t makes the function $\Omega(\mu)$ discontinuous and the beam starts to act as a pass-band filter allowing propagation within some frequency bands only. Increasing the values of K_t simply increases the discontinuity in the curve. The width of the various propagation bands can be varied by varying the value of K_t. For $K_t = 100$ the first band is very narrow while for $K_t = 1000$ the second band occurs at almost a single frequency only. When $K_t = \infty$ the beam acts as the beam on simple supports giving $\Omega(\mu)$ similar to the one obtained for the example in Section 2.3.2, figure (2.8).

The effect of periodic perturbation in the form of point masses placed at equal intervals on the beam, figure (2.7a), on the propagation constant/frequency curve is shown in figure (2.15) for various values of the mass m. A finite element idealisation of one cell is shown in figure (2.7b). The same beam element and data values used in the previous example are used here. The distance between the masses ℓ (periodic length) is taken equal to unity. Here increasing the value of the point mass m increases the discontinuity in the propagation constant/frequency curve and hence narrowing the propagation bands until the limit when $m = \infty$ where the results are equivalent to those obtained in Section 2.3.2 for the beam on simple supports.

It is interesting to compare the difference between the effects of adding translational spring supports or point masses on the propagation constant/frequency curve. This can be explained by the fact that the motion of each cell is due to the forces of interaction with its neighbouring cells and the forces tending to return the cell to its equilibrium position. The latter increases only by the addition of the translational stiffness and not by the point masses.

2.5 Formulation for the Complex Propagation Constant

In Section 2.3 equation (2.15) was solved by considering that the propagation constant μ is a real quantity and the problem was formulated to give an eigenvalue problem in the frequency ω corresponding to a given value of μ. A more general way to solve equation (2.15) is to formulate it to give an eigenvalue problem in μ for a given value of ω. This formulation has the advantage of giving the values of μ at any frequency ω, where μ will be generally complex, enabling us to study the dynamical behaviour of the periodic system at all frequencies. However, it is more complicated to formulate and requires solving an eigenvalue problem with unsymmetric matrices, but on the other hand this eigenvalue problem can, in some cases, be of much smaller order than the one obtained in the formulation for the real propagation constant.

Now for a given value of the frequency ω equation (2.15) can be written in the form

$$[D(\mu)] \begin{Bmatrix} q_I \\ q_L \end{Bmatrix} = 0 \tag{2.36}$$

where

$$[D(\mu)] = [\bar{K}(\mu)] - \omega^2[\bar{M}(\mu)] = \begin{bmatrix} D_{I,I} & D_{I,L} \\ D_{L,I} & D_{L,L} \end{bmatrix} \tag{2.37}$$

The first relation in equation (2.36) gives

$$\{q_I\} = -D_{I,I}^{-1} D_{I,L} \{q_L\} \tag{2.38}$$

Relation (2.38) can be used to eliminate $\{q_I\}$ from equation (2.36). This results in an equation of the form

$$[\bar{D}(\mu)]\{q_L\} = 0 \tag{2.39}$$

where

$$[\bar{D}] = [T'][D][T]. \tag{2.40}$$

The matrices $[T]$ and $[T']$ are given by

$$[T] = \begin{bmatrix} -D_{I,I}^{-1}.D_{I,L} \\ I \end{bmatrix} \tag{2.41}$$

$$[T'] = [-D_{L,I}D_{I,I}^{-1} \quad I] \tag{2.42}$$

Examination of (2.12), (2.13) and (2.16) shows that the propagation constant μ appears in the elements of the matrices $[\bar{K}]$ and $[\bar{M}]$, and hence in $[D]$ and $[\bar{D}]$, only in the form

$$e^{\pm i\mu}$$

(notice that the matrix $D_{I,I}$, and hence $D_{I,I}^{-1}$, does not contain $e^{\pm i\mu}$). Therefore equation (2.39) can be written in the form

$$(e^{i\mu}[B_1] + e^{-i\mu}[B_2] + [B_3])\{q_L\} = 0 \tag{2.43}$$

The matrices $[B_1]$, $[B_2]$ and $[B_3]$ are of the same order as $[\bar{D}]$ where each matrix contains only the elements of $[\bar{D}]$ which are multiplied by $e^{i\mu}$, $e^{-i\mu}$ and those that do not contain $e^{\pm i\mu}$.

Multiplying equation (2.43) by $e^{i\mu}$ and putting $e^{i\mu} = \lambda$ results in an equation of the form

$$(\lambda^2[B_1] + \lambda[B_3] + [B_2])\{q_L\} = 0 \tag{2.44}$$

Equation (2.44) represents a generalised eigenvalue problem of the form

$$(A_n\lambda^n + A_{n-1}\lambda^{n-1} + \ldots + A_o)\{x\} = 0 \tag{2.45}$$

where $n = 2$ in this case.

Appendix A gives the different methods for converting equation (2.45) into a linear eigenvalue problem of the form

$$([G] - \lambda I)\{Y\} = 0 \tag{2.46}$$

if either A_n or A_o is a non-singular matrix, where $[G]$ is a real unsymmetric matrix. Or to the general form

$$([A] - \lambda[B])\{Y\} = 0 \tag{2.47}$$

if both A_n and A_o are singular, where $[A]$ and $[B]$ are real unsymmetric singular matrices. The matrices A_n and A_o will be singular if the number of coupling degrees of freedom of the single cell chosen to represent the system is more than the minimum number that can be obtained

by a different choice of the cell. For example, in the case of the beam on multiple supports discussed in Section 2.3.2, choices of the cell shown in figures (2.2c) and (2.2d) will result in singular A_n and A_o matrices. While the choice shown in figure (2.2b) (cell with minimum coupling degrees of freedom to its neighbours) will result in non-singular matrices. For some complex periodic structures it can be more convenient to represent the structure by a cell with coupling degrees of freedom more than the minimum number that can be obtained by a different choice of the cell. Methods of solving these eigenvalue problems are also discussed in Appendix A.

The eigenvalue problem (2.45) can be formulated and solved for given values of ω to obtain the corresponding values of λ, and hence μ, which will, in general, be a complex quantity.

2.5.1 Computer programs

A general finite element computer program has been written to represent a single cell of the periodic system by a finite element model and form the matrices in equation (2.45) for a given frequency ω. Then the eigenvalue problem (2.46) or (2.47) is formed and solved to find the corresponding propagation constants μ. The basic flow diagram for the computational procedure is given in Appendix B.

2.5.2 Illustrative example

The same example used in Section 2.3.2, that is the infinite beam on simple supports, is used here again to illustrate the general behaviour of one-dimensional periodic systems at any frequency. The same finite element idealisation for the single cell is used here, figure (2.2b). In this system each cell is coupled to its neighbours on each side by one degree of freedom only, namely the rotation θ_z at the supports, and hence only two independent waves can exist at any frequency |32|. (The number of independent waves that can exist at any frequency equals twice the number of coupling degrees of freedom between the cells.) These will be two identical waves but travelling in opposite directions. Figure (2.16) shows the variation of the real and imaginary parts of μ with frequency for the wave travelling to the right where the real part of μ is negative. As can be seen from the graph there are bands of frequencies within which the

imaginary part of μ (μ_i) is alternately positive and zero. When μ_i is non-zero (attenuation bands) the corresponding real part μ_r is either zero or $\pm\pi$ (in some cases, as will be shown in the next sub-section, μ_r can take any value within the attenuation bands). Waves with frequencies within these bands are attenuated waves where the real part of μ (zero or $\pm\pi$ in this case) represents the change in phase while the imaginary part represents the attenuation in passing from one cell to the next (the amplitude of the wave reduces by $e^{-\mu_i}$ per cell). The bands of frequencies where μ_i is zero are called the propagation bands since within these bands waves can propagate (without attenuation). It is clear that these propagation bands coincide with the results obtained in Section 2.3.2, figure (2.8). Figure (2.17) shows the attenuating wave-form corresponding to frequencies below the propagation band (where $\mu_r = \pm\pi$) and above it (where $\mu_r = 0$). Under these conditions, as mentioned above, adjacent cells will vibrate in counter phase or in phase with one another while the amplitude reduces by $e^{-\mu_i}$ per cell.

2.5.3 Applications

The same two examples used in Section 2.3.3 are used here. These are the flat and curved stringer stiffened panels. The same finite element idealisation for the cells representing the panels is used. Figures (2.18) and (2.19) show the variation of the real and imaginary parts of the propagation constant with the non-dimensional frequency Ω for the flat and curved panels respectively.

For the flat panel case, the coupling degrees of freedom between the cells are the lateral displacement w and the rotation θ_x and hence there are two independent pairs of waves that can exist simultaneously at any frequency (curves numbered 1 and 2 in figure (2.18)). For the first wave (curve 1) there are bands of frequencies where the imaginary part of μ is zero (propagation bands). These bands coincide with the results obtained in Section 2.3.3, figure (2.12). Outside these bands the real part of μ is either zero or $\pm\pi$ while the imaginary part is non-zero (attenuation bands). The second wave (curve 2) has a non-zero imaginary part while the real part is $\pm\pi$. This represents an attenuating wave. As can be seen from these results the behaviour of the flat panel shows great similarity to the behaviour of the beam on multiple supports discussed in Section 2.5.2. For the curved panel case, there are four coupling degrees of freedom between the cells (degrees of freedom at the stringers). These are u, v, w and w_y. Therefore there are four independent pairs of waves

that can exist at any frequency (curves numbered 1 to 4 in figure (2.19)). Each pair of these waves represents two identical waves travelling in opposite directions. For wave 1 there are bands where the imaginary part of μ is zero (propagation bands). These bands coincide with the results produced in Section 2.3.3, figure (2.13). For waves 2 and 3 there are bands of frequencies where the imaginary part of μ is non-zero while the real part is neither zero nor $\pm\pi$. These are attenuated waves |33|. Wave 4 has a non-zero imaginary part while the real part is $\pm\pi$ which represents an attenuating wave. These results are in agreement (within the accuracy of the graphs) with the results produced in |14| using the transfer matrix method.

2.6 Natural Frequencies of a Single Periodic Cell

If the single cell representing one period of any one-dimensional periodic system is symmetrical, about a plane through its centre and parallel to its left and right sides, and having only one type of degree of freedom coupling it to its neighbouring cells (say rotation only or translation only) then its natural frequencies with these degrees of freedom constrained or unconstrained can be associated with the propagation frequencies corresponding to propagation constants $\mu = 0.0$ or $\mu = \pm\pi$ (or wave-numbers $a = 0.0$ or $a = \pm \frac{1}{2\ell}$ where ℓ is the periodic length). To prove this, consider the equation of motion of the cell when vibrating freely. This can be written in a matrix form as

$$([K] - \omega^2[M])\{q\} = 0$$

or

$$\begin{bmatrix} K_{II} & K_{IL} & K_{IR} \\ K_{LI} & K_{LL} & K_{LR} \\ K_{RI} & K_{RL} & K_{RR} \end{bmatrix} - \omega^2 \begin{bmatrix} M_{II} & M_{IL} & M_{IR} \\ M_{LI} & M_{LL} & M_{LR} \\ M_{RI} & M_{RL} & M_{RR} \end{bmatrix} \begin{Bmatrix} q_I \\ q_L \\ q_R \end{Bmatrix} = 0 \qquad (2.48)$$

where $[K]$ and $[M]$ are the stiffness and inertia matrices of the cell. $\{q\}$ is a vector of the generalised degrees of freedom in the cell. The matrices $[K]$, $[M]$ and $\{q\}$ are partitioned according to the interior, left and right degrees of freedom in the cell, figure (2.1b).

Let N_I, N_L and N_R $(N_L = N_R)$ be the number of interior, left and right degrees of freedom in the cell.

Since the cell is symmetrical then its natural modes of vibration will be either symmetrical or anti-symmetrical about the centre plane of symmetry. In these modes the degrees of freedom $\{q_L\}$ and $\{q_R\}$ will be either of the same sign or of opposite sign depending on the nature of the degrees of freedom and the mode of vibration. For example if $\{q_L\}$ and $\{q_R\}$ are rotations (say at the supports of a simply supported beam or plate), then they will be of the same sign in anti-symmetric modes and of opposite sign in symmetric modes. While if they are transverse displacements they will be of the same sign in symmetric modes and of opposite sign in anti-symmetric modes. Therefore when the cell is vibrating freely we can write

$$\{q_L\} = \pm \{q_R\} \tag{2.49}$$

Relations (2.49) can be substituted in equation (2.48) to eliminate q_R. This results in an equation of the form

$$([\bar{K}] - \omega^2[\bar{M}]) \begin{Bmatrix} q_I \\ q_L \end{Bmatrix} = 0 \tag{2.50}$$

where

$$\begin{aligned} [\bar{K}] &= [W]^T[K][W] \\ [\bar{M}] &= [W]^T[K][W] \end{aligned} \tag{2.51}$$

where

$$[W] = \begin{bmatrix} I & 0 \\ 0 & I \\ 0 & \pm 1 \end{bmatrix} \tag{2.52}$$

The two sets of equations represented by (2.50) are eigenvalue problems of order $N_I + N_L$. Their solution will give $2(N_I + N_L)$ eigenvalues and eigenvectors satisfying condition (2.49). However, it should be noticed that this condition is also satisfied when

$$\{q_L\} = \pm\{q_R\} = 0.0 \tag{2.53}$$

The original equation (2.48) has only $N_I + N_L + N_R$ or $N_I + 2N_L$ (since $N_L = N_R$ due to the symmetry of the cell) eigenvalues. Their associated normal modes give all the possible modes of vibration such that

$\{q_L\} = \pm\{q_R\} \neq 0.0$. Therefore the two solutions of (2.50) give N_I extra eigenvalues whose eigenvectors must satisfy the condition (2.53). These are the natural frequencies and normal modes of the cell with its boundary degrees of freedom $\{q_L\}$ and $\{q_R\}$ constrained. Now the two sets of equations (2.50) are the same equations obtained from the equation of free-wave propagation in the infinite periodic system given by equation (2.15) corresponding to values of the propagation constant μ given by $\mu = 0$ or $\mu = \pi$ (or $-\pi$) respectively.

From the above discussion it is clear that the frequencies of propagation corresponding to $\mu = 0.0$ and $\mu = \pm\pi$ are indeed the natural frequencies of the periodic section (cell) with its coupling degrees of freedom ($\{q_L\}$ and $\{q_R\}$) constrained or unconstrained. Inspection of the wave-forms (eigenvectors) obtained when solving equation (2.15) for $\mu = 0$ or $\mu = -\pi$ can determine which frequency corresponds to the unconstrained cell and which corresponds to the constrained cell. However, in some cases, like the beam on simple supports, the natural frequencies of the unconstrained cell alternate with the natural frequencies of the constrained cell and the lowest frequency corresponds to the unconstrained cell [25, 31, 62].

The above analysis can be extended to periodic systems with symmetric cells having more than one type of coupling degree of freedom (say rotation and translation) such as beams on spring supports or stiffened plates. In such cases we will find that the frequencies of propagation corresponding to $\mu = 0.0$, where $\{q_L\} = +\{q_R\}$, and $\mu = \pm\pi$, where $\{q_L\} = -\{q_R\}$, will coincide with the natural frequencies of the cell while its boundary degrees of freedom satisfy the conditions (2.49) or (2.53). This can be proved by a similar procedure as above. But in this case $\{q_L\}$ and $\{q_R\}$ will be divided into degrees of freedom that will have the same sign when the cell is vibrating in a symmetrical mode and degrees of freedom that will have opposite sign. Then condition (2.49) is satisfied if the cell is vibrating in a mode such that the degrees of freedom having the same sign are constrained while the degrees of freedom having opposite sign are unconstrained, or vice versa, or when all of them are constrained (condition (2.51)). The resulting eigenvalue problems in these cases will coincide with the equation of free wave propagation (2.15) when substituting $\mu = 0.0$ or $\mu = \pm\pi$.

2.7 Natural Frequencies of Finite Periodic Systems

In this section we will show that the natural frequencies of finite periodic structures of N identical cells, where each cell is symmetrical (about a plane through its centre and parallel to its sides) and coupled to its neighbouring cells by one type of degree of freedom only, can be obtained from the propagation constant/frequency curve.

As explained in the previous section, if we consider a single cell, of length ℓ, as one period of the infinite structure, then frequencies corresponding to values of the propagation constant μ (or wave-number a) given by

$$\mu = 0.0 \quad \text{or} \quad a = 0.0$$

and

$$\mu = \pm\pi \quad \text{or} \quad a = \pm \frac{1}{2\ell} \tag{2.54}$$

will coincide with the natural frequencies of the chosen period with its coupling degrees of freedom unconstrained or constrained.

Now if we consider N cells together as one period, of length $N\ell$, of the infinite structure then, according to the discussion given in the previous section, the natural frequencies of this period with the degrees of freedom at its ends unconstrained or constrained will coincide with the frequencies of propagation corresponding to values of the wavenumber a' given by

$$a' = 0.0 \quad \text{or} \quad a' = \pm \frac{1}{2N\ell} \tag{2.55}$$

where $N\ell$ is the periodic length in this case. Since the frequency of propagation is a periodic function of the wave-number a', with period $1/N\ell$, then condition (2.55) can be written as

$$a' = 0.0 \pm \frac{m}{N\ell} \quad \text{or} \quad a' = \pm \frac{1}{2N\ell} \pm \frac{m}{N\ell}$$

where m is any integer number or zero.

Or in general

$$a' = \pm \frac{m}{2N\ell} \quad (m = 0,1,2,\ldots) \tag{2.56}$$

Regardless of the choice of the period representing the infinite structure, the wave-number/frequency variation must be the same for the same values of the wave-number since such variation is characteristic of the periodic system, and hence frequencies corresponding to values of the wave-number a equal to a' (where a' is given by (2.56)) i.e.,

$$a = a' = \pm \frac{m}{2N\ell} \qquad (m = 0, 1, 2, \ldots)$$

or (2.57)

$$\mu = \pm \frac{m\pi}{N} \qquad (\text{since } \mu = -2\pi a\ell)$$

are indeed the natural frequencies of the N cell period with its end degrees of freedom ($\{q_L\}$ and $\{q_R\}$) constrained or unconstrained.

To illustrate this consider the case of an infinite beam on simple supports at unit distances apart. This is the illustrative example used in Section 2.3.2. Figure (2.20) shows the variation of the frequency of propagation with the wave-number a in the first two bands when only one cell (figure (2.2b)) is chosen as the period representing the structure (curves JE and KL in figure (2.20)). The wave-number a is restricted inside the first zone, hence

$$-\frac{1}{2\ell} < a < \frac{1}{2\ell} \qquad (\text{or } -\pi < \mu < \pi)$$

or

$$-\tfrac{1}{2} < a < \tfrac{1}{2} \qquad (\text{since } \ell = 1.0).$$

Only the positive values of a are considered due to the symmetry of the curve.

Now consider 4 cells together as one period of the structure. The periodic length in this case will be $4\ell = 4.0$ and the first zone is given by

$$-\frac{1}{2N\ell} < a' < \frac{1}{2N\ell}$$

or (2.58)

$$-\tfrac{1}{8} < a' < \tfrac{1}{8} \qquad (\text{since } N = 4;\ \ell = 1.0)$$

Let us call this zone the sub-zone and the corresponding propagation bands are the sub-bands. As can be seen from figure (2.20), due to the fact that the frequency of propagation is a periodic function of the wave-number a' with period $1/N\ell$ and symmetrical about the x axis (line $a = 0.0$ or $\mu = 0.0$) it follows that section AB (which is the first sub-band)

in figure (2.20) is a mirror image of BC and BC is a mirror image of CD and also CD is a mirror image of DE where section DE must coincide with part of the first band JE since in this part (third sub-zone) $a' = a$. This is because, as explained before, the wave-number/frequency variation must be the same for the same values of the wave-number regardless of the choice of the period representing the infinite structure. Similarly the sub-band FI is a mirror image of IG and finally the fourth sub-band JI coincides with part of the first band JE.

Now, according to the previous section, frequencies corresponding to values of $a' = 0.0$ (points A, F and J) and $a' = \frac{1}{2N\ell} = \frac{1}{8}$ (points B and I) are the natural frequencies of the 4 cell period with its boundary degrees of freedom unconstrained or constrained. But frequencies at points A, B and F are the same frequencies at points E, D and G, respectively. Therefore, frequencies corresponding to values of the wave-number a given by

$$a = \pm \frac{m}{2N\ell} \quad \text{or} \quad \mu = \pm \frac{m\pi}{N} \quad (\text{since } \mu = 2\pi a\ell)$$

(where $\ell = 1.0$, $N = 4$ and $m = 0, 1, 2, 3, 4$ in this case, points J, I, G, D and E)
are the natural frequencies of the four cell period with its boundary degrees of freedom (θ_L and θ_R) unconstrained or constrained.

Therefore calculation of the curves JE and KL obtained by choosing a single cell only to represent the infinite system can be used to calculate the natural frequencies of the finite system.

From the above discussion we can conclude the following:

a. The lower bounding frequency of the first sub-band is the lower bounding frequency of the first band while the upper bounding frequency of the N^{th} sub-band (fourth in the above example) is the upper bounding frequency of the first band. Also the upper, or lower, bounding frequencies of any of the intermediate sub-bands (second and third in this example) are the lower, or upper, bounding frequencies of the neighbouring sub-bands. Similar conclusions can be drawn in higher bands.

b. The natural frequencies of a finite periodic structure of N symmetric cells, where each cell is coupled to its neighbours by one type of

degree of freedom, with its boundary degrees of freedom constrained or unconstrained can be obtained from the propagation constant/frequency curve at values of the propagation constant μ given by (2.57), namely

$$\mu = \pm \frac{m\pi}{N} \qquad (m = 0, 1, 2, \ldots, N)$$

For the case of a finite periodic beam on simple supports, its natural frequencies with the boundary degrees of freedom (rotations at the supports) unconstrained alternate with its natural frequencies with the boundary degrees of freedom constrained |25, 33|. For this system, and similar systems, the natural frequencies of the finite structure can be obtained from the propagation constant/frequency curve at values of μ given by (2.57), namely

$$\mu = \pm \frac{m\pi}{N}$$

where N is the number of periods in the structure. The values of m are taken as follows.

(i) If the boundary degrees of freedom are unconstrained
$m = 1, 2, \ldots, N$ for the odd-numbered bands and
$m = 0, 1, \ldots, N-1$ for the even-numbered bands.

(ii) If the boundary degrees of freedom are constrained
$m = 0, 1, \ldots, N-1$ for the odd-numbered bands and
$m = 1, 2, \ldots, N$ for the even-numbered bands.

(iii) If one boundary (say $\{q_L\}$) is constrained while the other boundary ($\{q_R\}$) is unconstrained then the natural frequencies are in fact the natural frequencies corresponding to the symmetric modes (or unsymmetric modes depending on the type of the coupling degree of freedom) of a structure having 2N periods with its boundary degrees of freedom ($\{q_L\}$ and $\{q_R\}$) unconstrained. In this case it should be noticed that the symmetric modes alternate with the antisymmetric modes |25|.

For finite periodic systems with unsymmetric cells, Mead |33| has shown that their natural frequencies (except the first one) can be obtained by a similar procedure as above.

	4 elements idealisation	10 elements idealisation	Exact results
First band	9.8722 22.403	9.8697 22.374	9.8696 22.373
Second band	39.634 62.243	39.483 61.689	39.478 61.622
Third band	90.449 123.49	88.874 121.02	88.838 120.903

Table 2.1

Comparison of the bounding frequencies of the first three propagation bands for an infinite multi-supported beam using exact and finite element solutions.

Upper figures: Lower bounding frequencies.
Lower figures: Upper bounding frequencies.

Propagation Constant μ	Frequency of Propagation	
	Finite Elements	Exact
0.0	0.0	0.0
0.1π	0.09870	0.09870
0.2π	0.39478	0.39478
0.3π	0.88826	0.88826
0.4π	1.5791	1.5791
0.5π	2.4674	2.4674
0.6π	3.5531	3.5531
0.7π	4.8361	4.8361
0.8π	6.3166	6.3165
0.9π	7.9944	7.9944
π	9.8697	9.8696

Table 2.2

Comparison of finite element results (10 beam elements per cell) and exact solution of the propagation constant/ frequency variation for the transverse wave motion in an infinite beam.

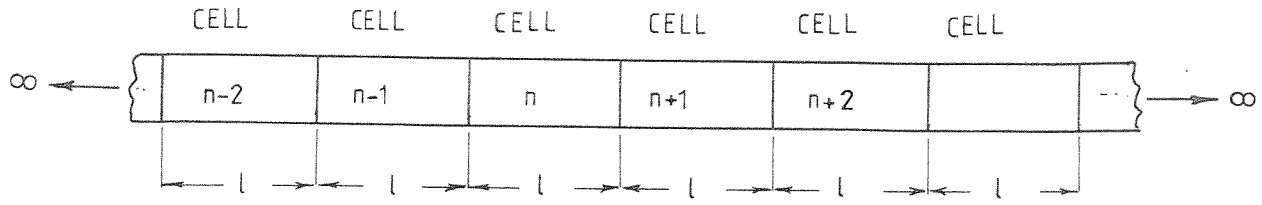

(a)

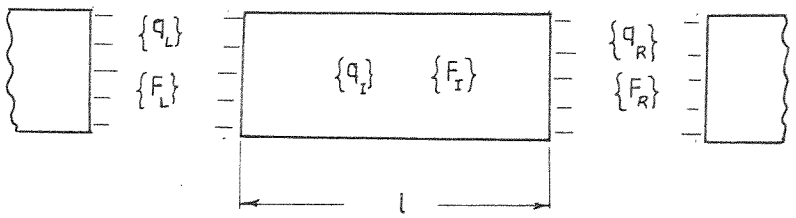

(b)

Figure 2.1.(a)Schematic diagram of part of a one-dimensional periodic system;(b)forces on,and degrees of freedom of a single cell.

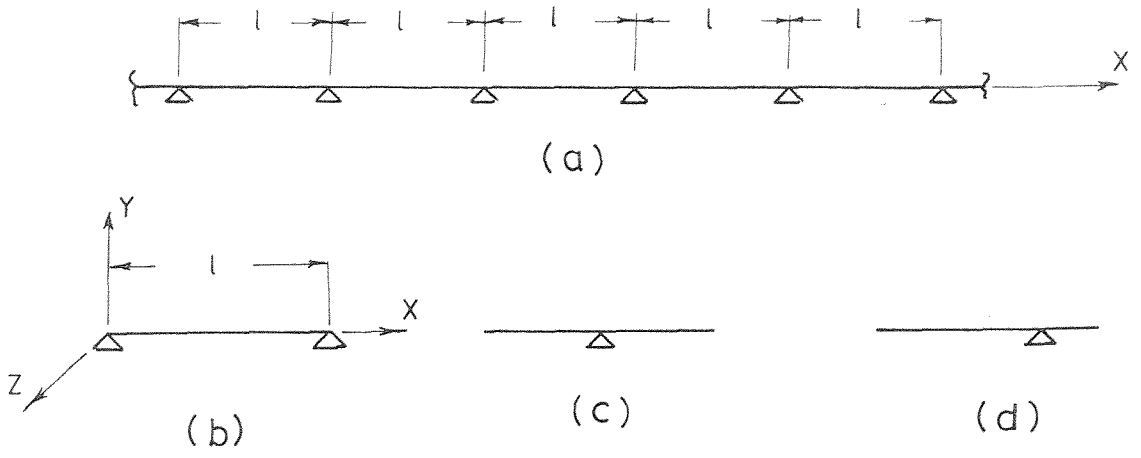

Figure 2.2.(a)Infinite beam on equally spaced simple supports;(b),(c) and(d)various choices for the single cell representing the system.

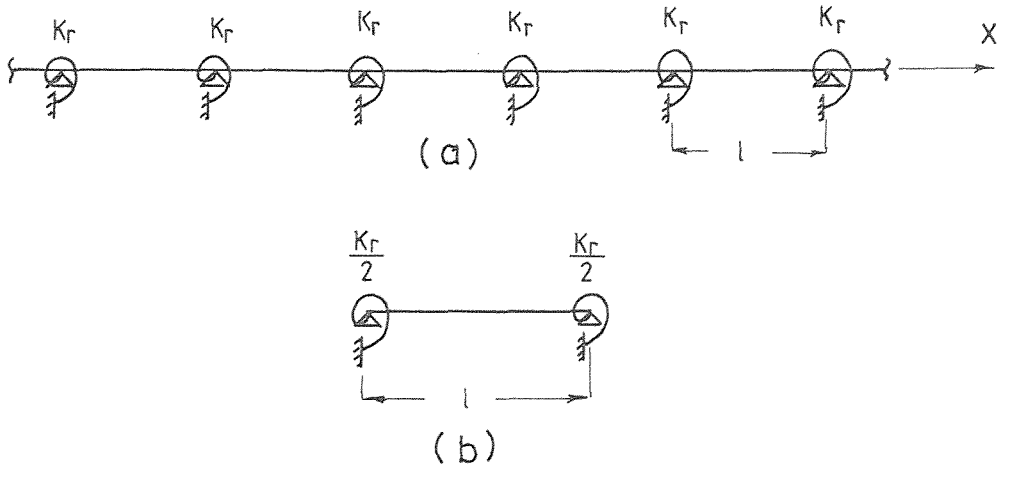

Figure 2.3. (a)Infinite beam on equally spaced supports with rotational stiffness ;(b)single cell representing the system.

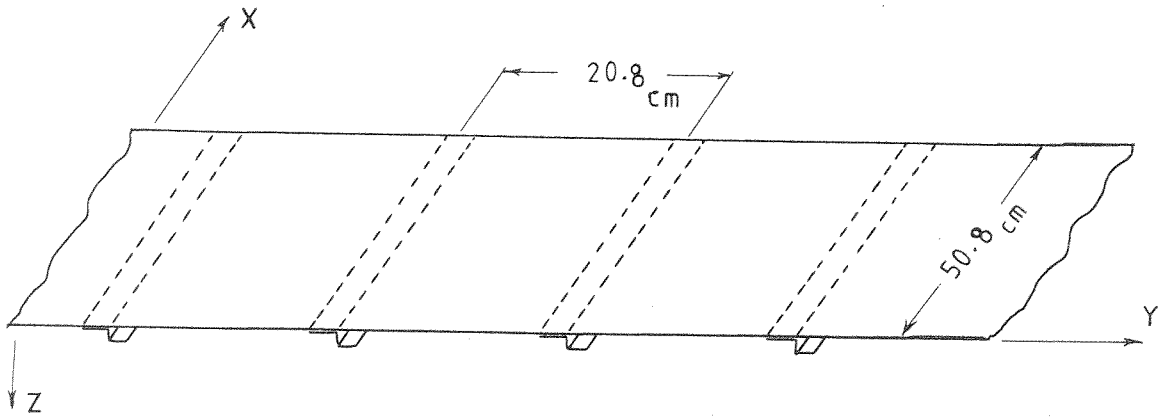

(a)

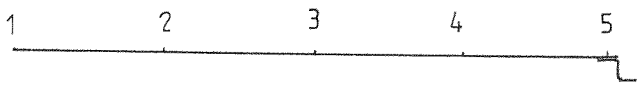

(b)

Figure 2.4.(a)Stringer stiffened flat panel;(b)finite element idealisation of one cell.

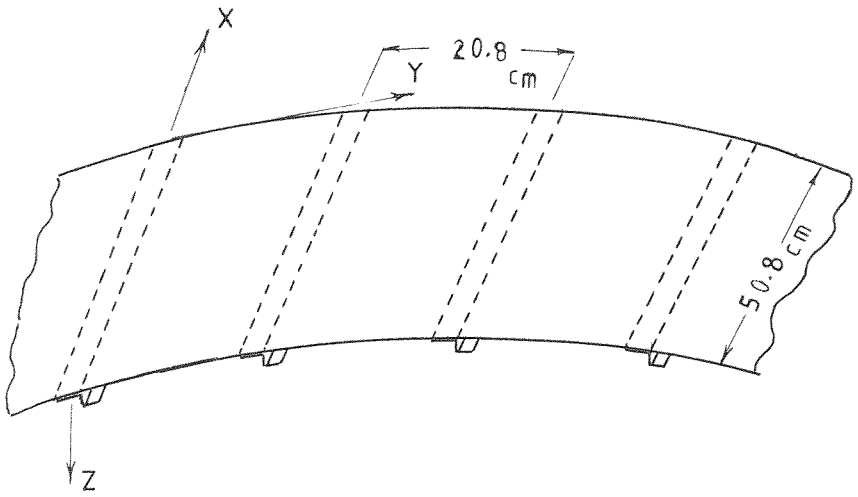

(a)

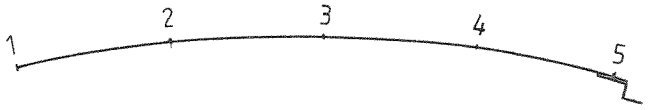

(b)

Figure 2.5.(a)Stringer stiffened curved panel;(b)finite element idealisation of one cell.

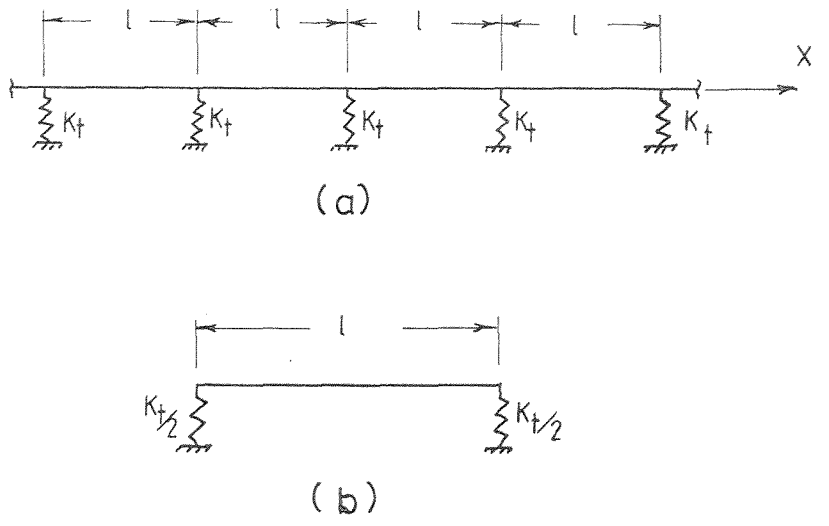

Figure 2.6.(a)Infinite beam on equally spaced translational spring supports,
(b)single cell representing the system.

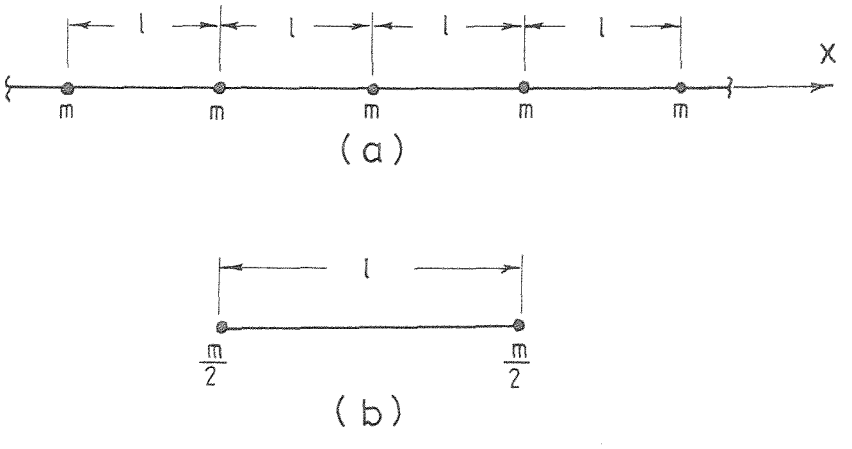

Figure 2.7.(a)Infinite beam with point masses at equal distances,
(b)single cell representing the system.

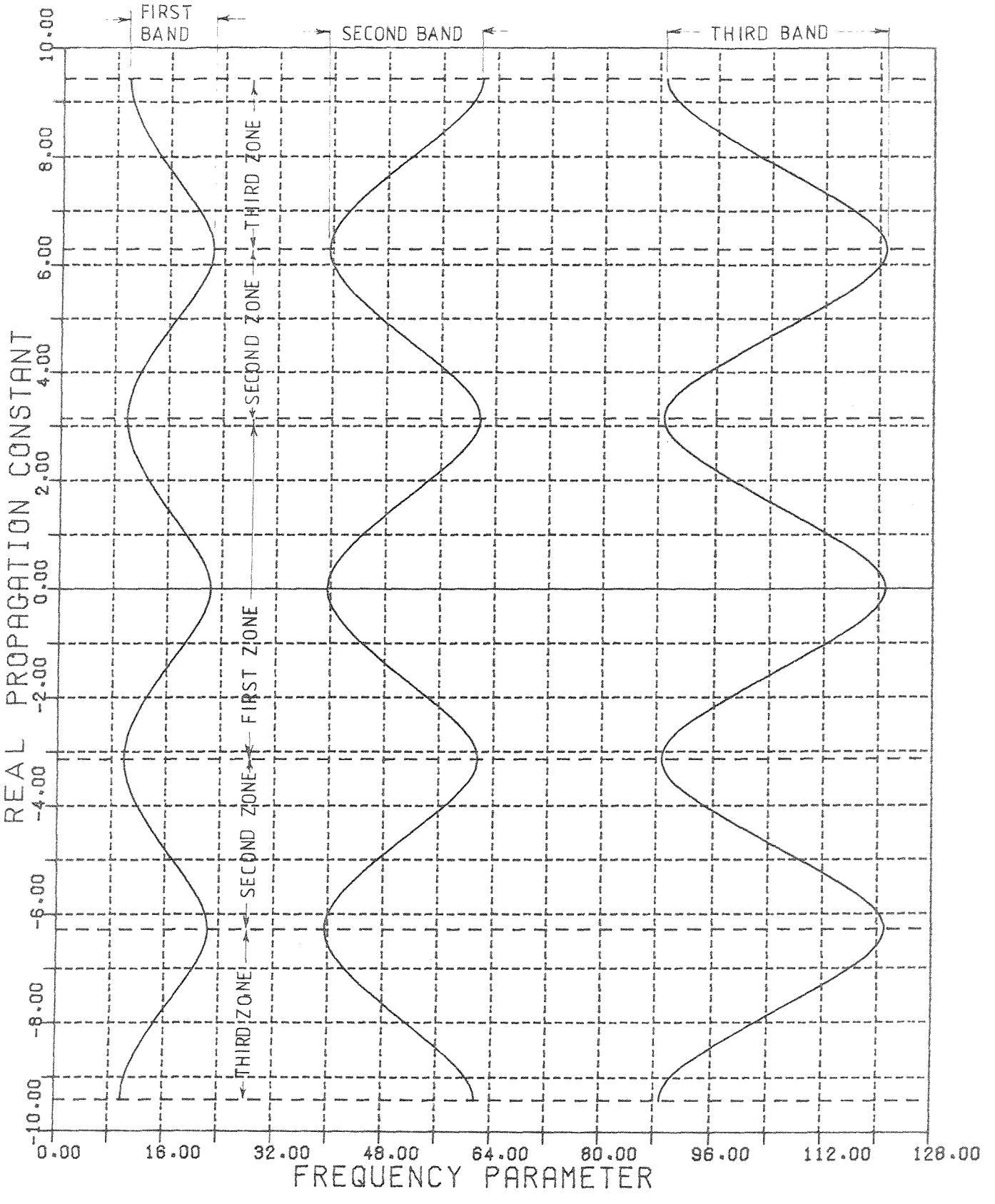

Figure 2.8. Variation of the real propagation constant with frequency for a beam on periodic simple supports.

$\mu = 0.0$ $\Omega = 22.37$

$\mu = \pi/4$ $\Omega = 19.92$

$\mu = \pi/2$ $\Omega = 15.42$

$\mu = 3\pi/4$ $\Omega = 11.51$

$\mu = \pi$ $\Omega = 9.87$

Figure 2.9. Standing and propagating waves of a beam on periodic simple supports. *First propagation band*.

$\mu = 0.0$ $\Omega = 39.48$

$\mu = \pi/4$ $\Omega = 42.85$

$\mu = \pi/2$ $\Omega = 49.97$

$\mu = 3\pi/4$ $\Omega = 57.65$

$\mu = \pi$ $\Omega = 61.69$

Figure 2.10. Standing and propagating waves of a beam on periodic simple supports . Second propagation band .

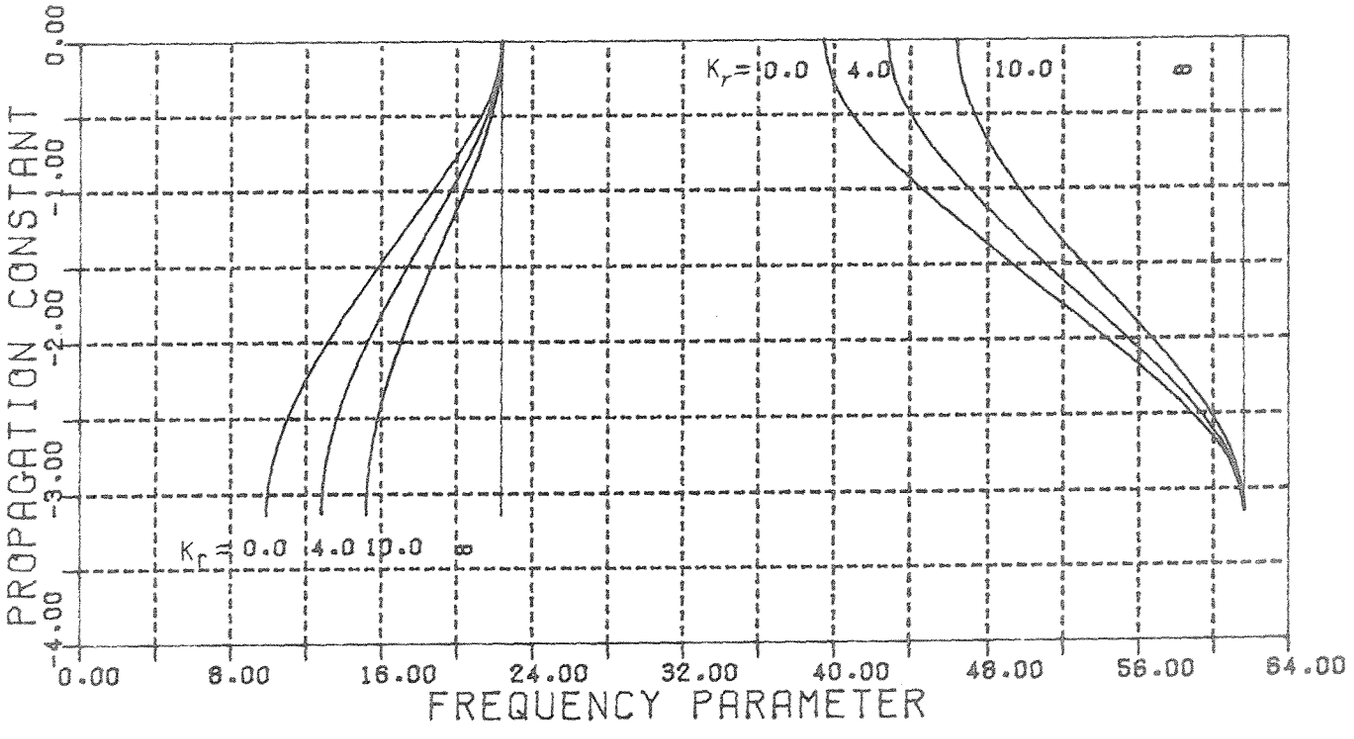

Figure 2.11. Effect of varying the rotational stiffness K_r at the supports of a periodic beam on the propagation constant-frequency variation.

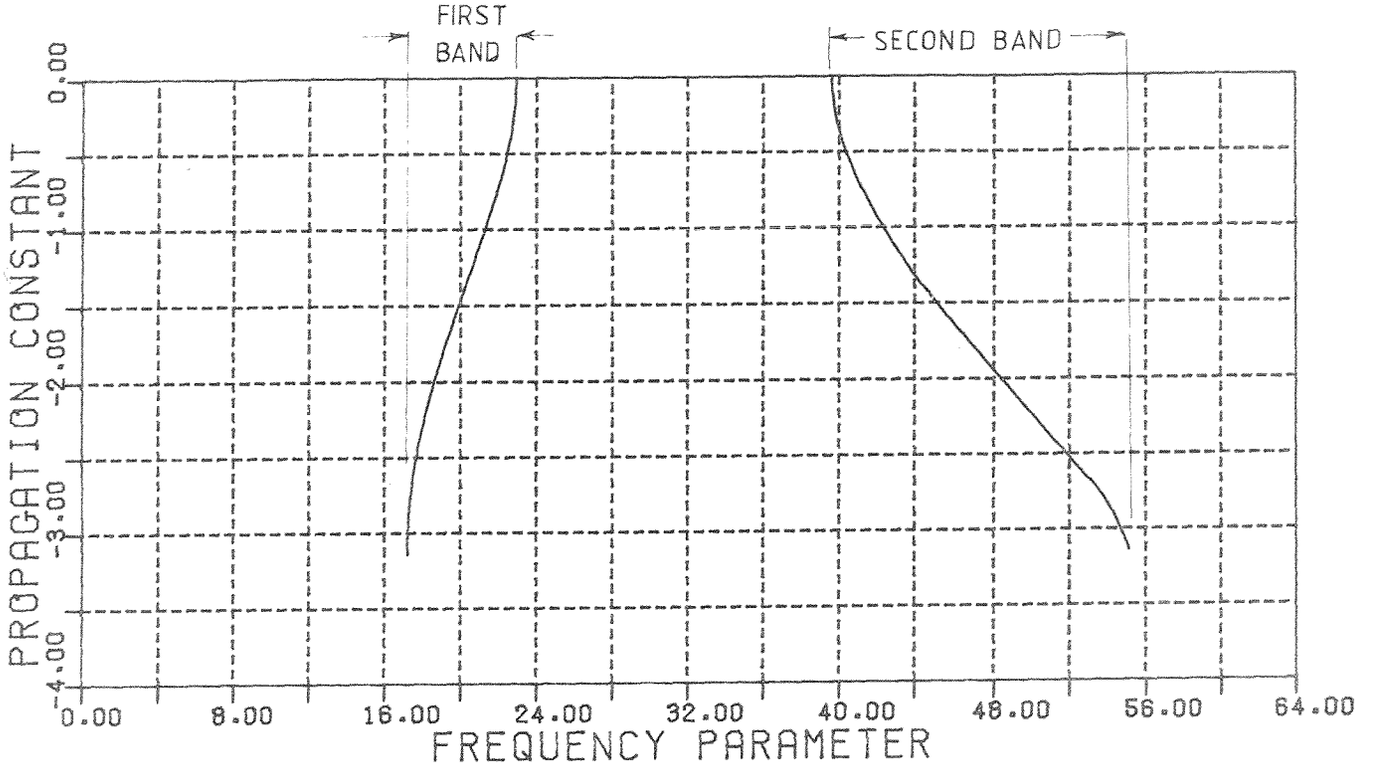

Figure 2.12. Variation of the real propagation constant with frequency for a periodically stiffened flat panel.

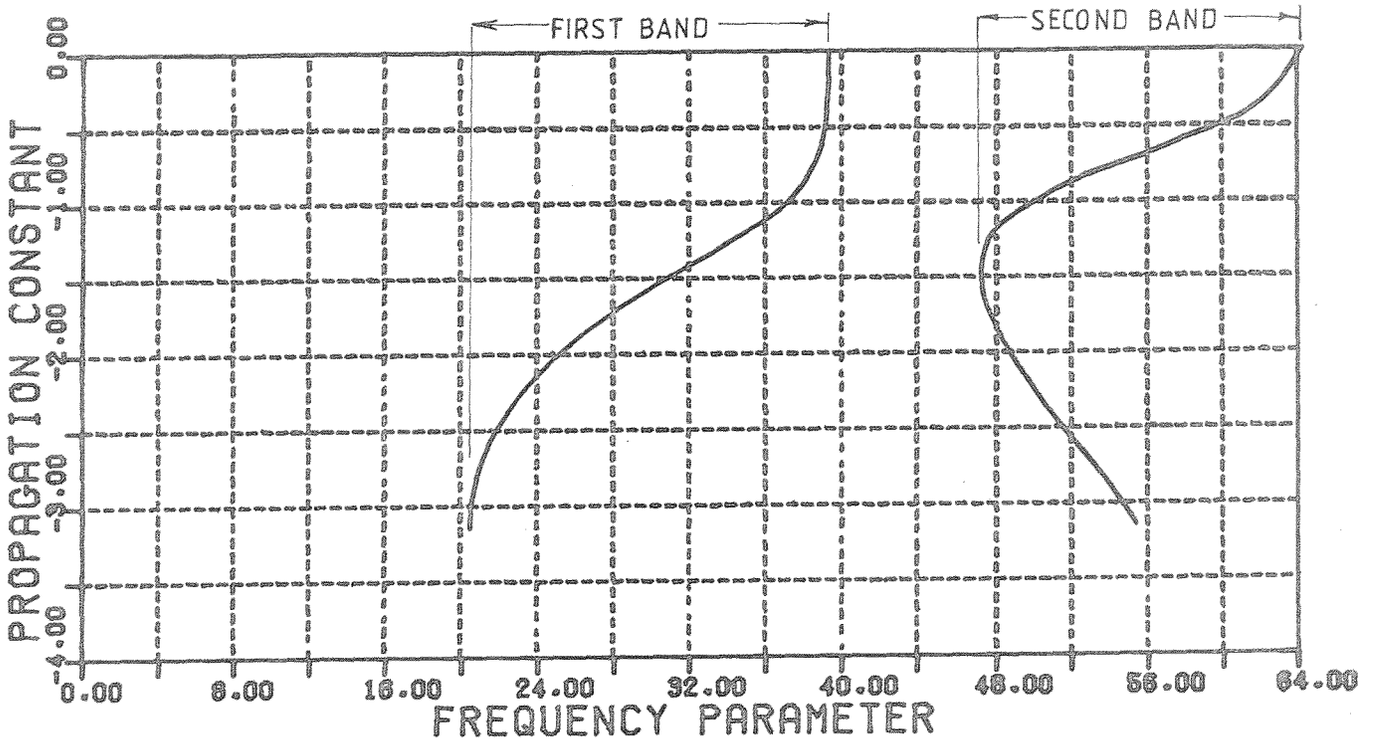

Figure 2.13. Variation of the real propagation constant with frequency for the periodically stiffened panel shown in figure(2.5).

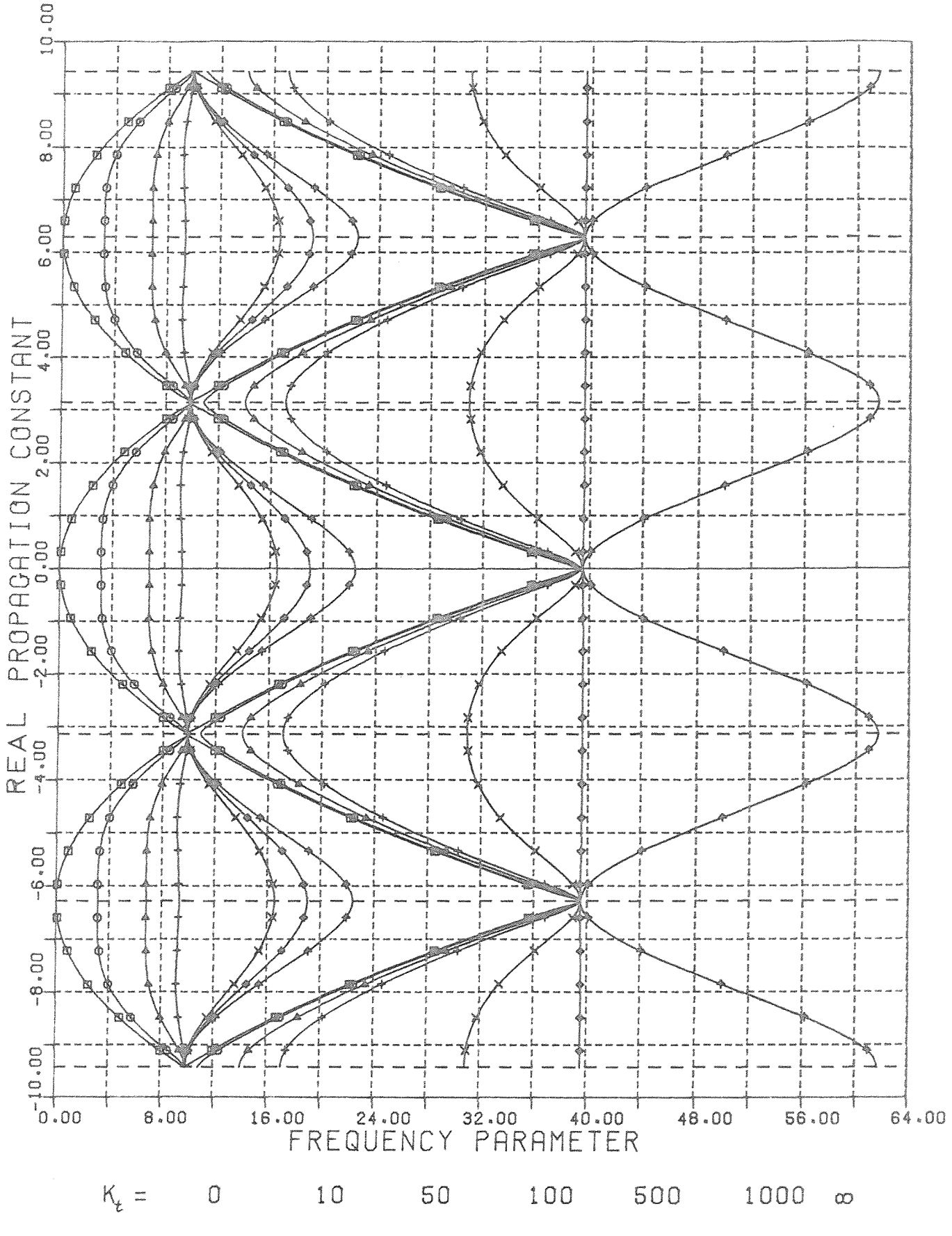

Figure 2.14. Propagation constant-frequency variation for a beam on equally spaced translational spring supports.Various values of the translational spring stiffness $K_t$are chosen.

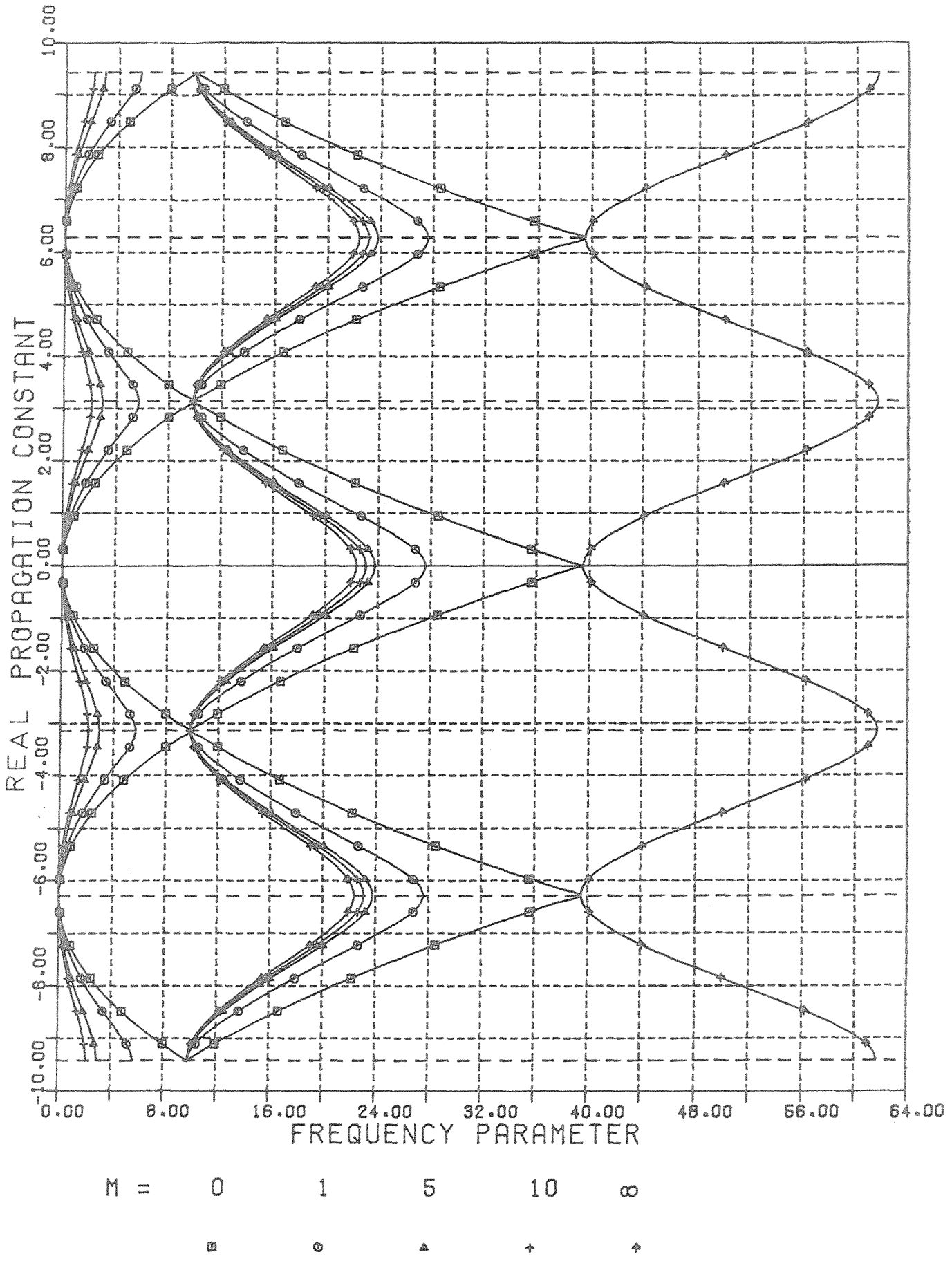

Figure 2.15. Propagation constant-frequency variation for a beam with point masses at equal distances.Various values of the point mass m are chosen.

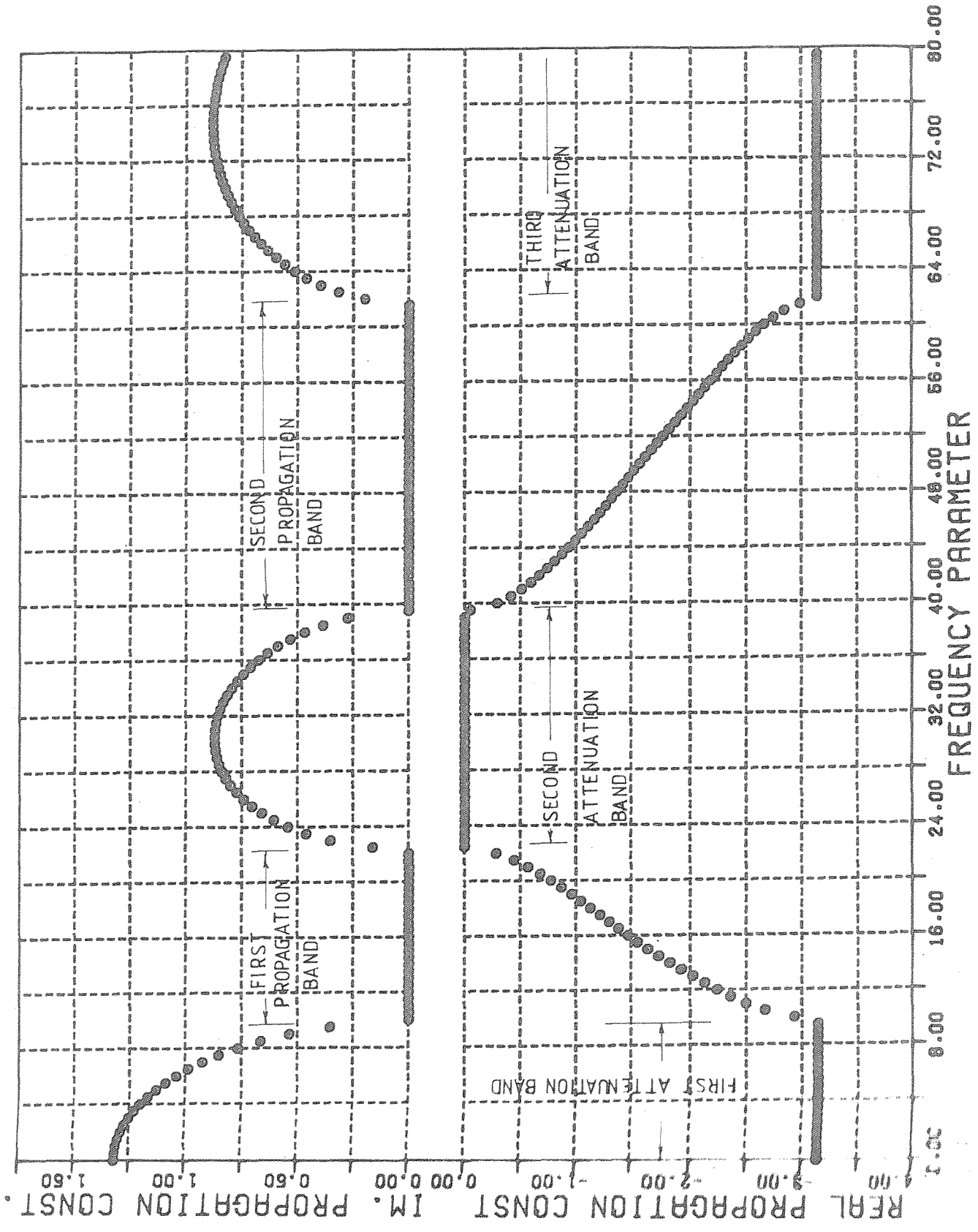

Figure 2.16. Variation of the real and imaginary parts of the propagation constant with frequency for a beam on periodic simple supports.

(a)

(b)

Figure 2.17. Attenuating waves of a beam on periodic simple supports
(a)at a frequency below the first propagation band;
(b)at a frequency above the first propagation band.

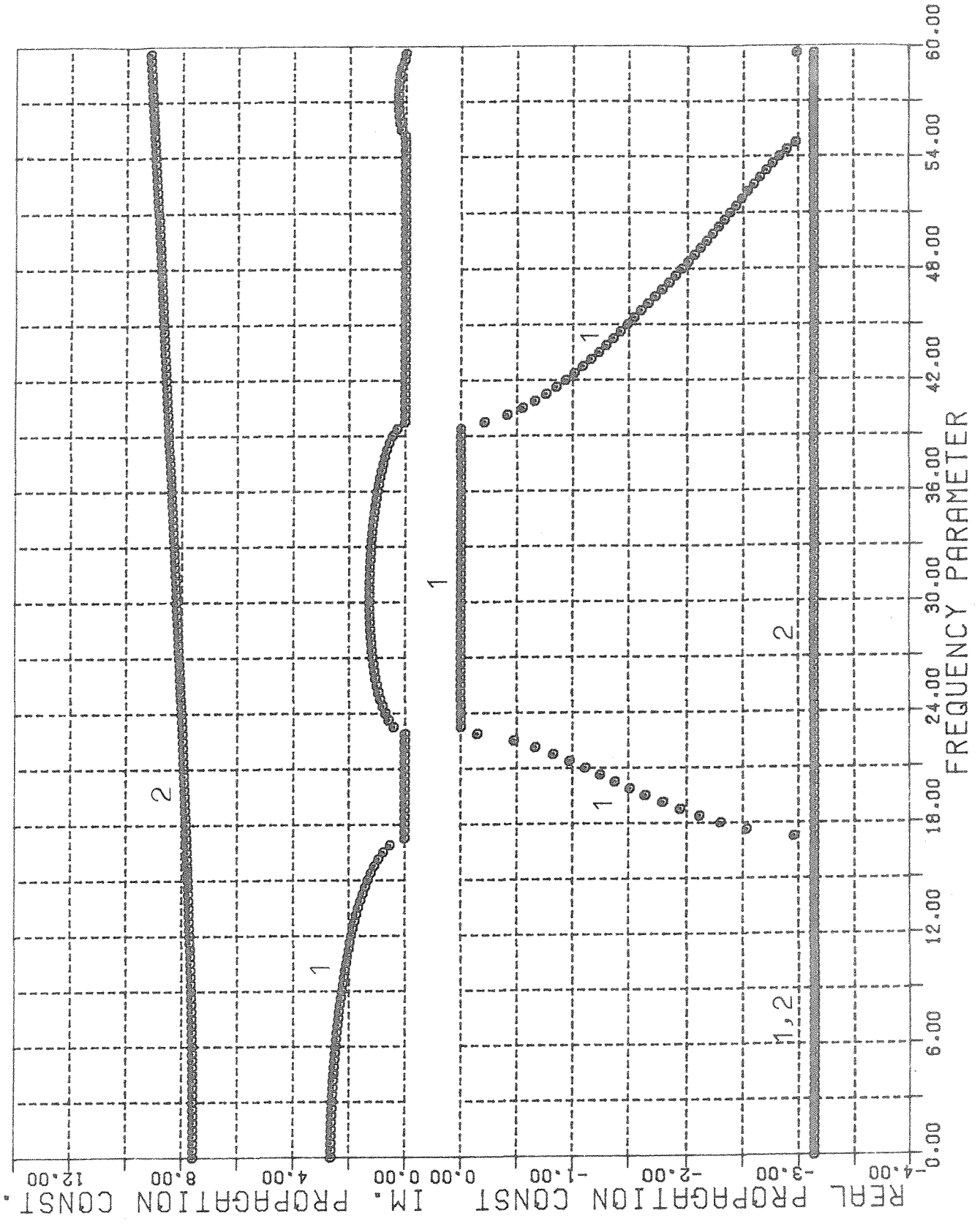

Figure 2.18. Variation of the real and imaginary parts of the propagation constants with frequency for the periodically stiffened panel shown in figure(2.4) .

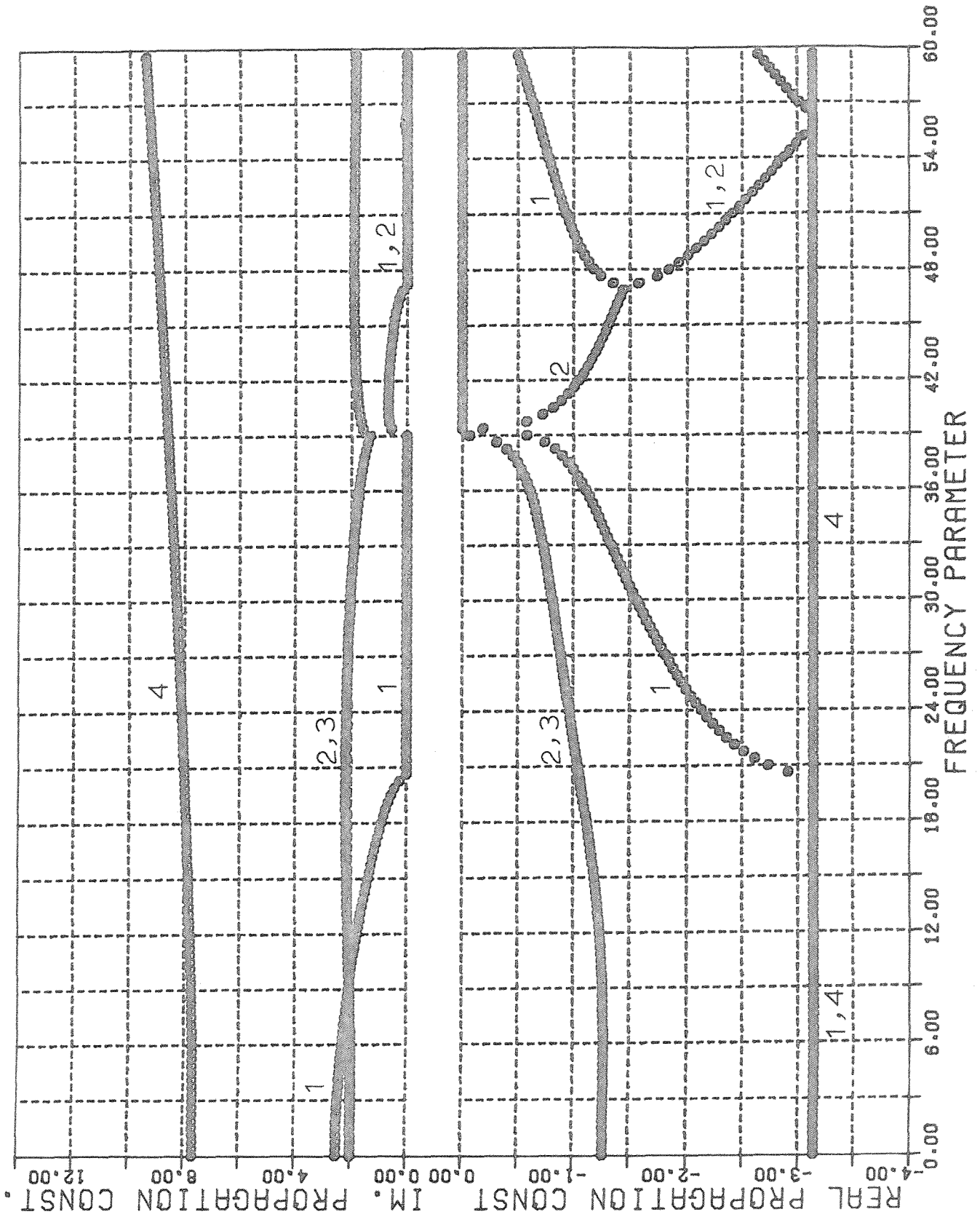

Figure 2.19. Variation of the real and imaginary parts of the propagation constants with frequency for the periodically stiffened curved panel shown in figure(2.5) .

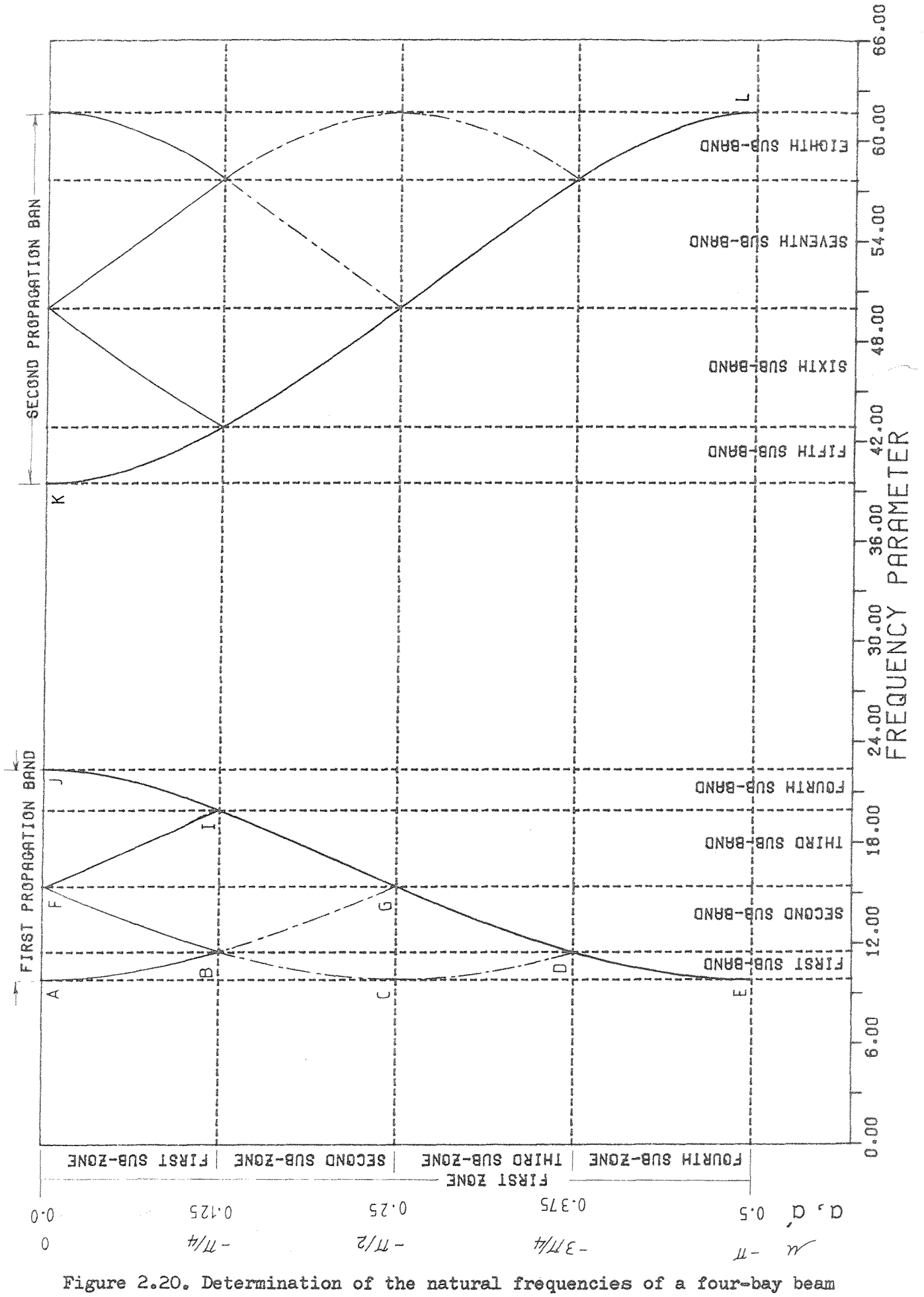

Figure 2.20. Determination of the natural frequencies of a four-bay beam simply supported or clamped at both ends ,from the propagation constant-frequency curve.(The first two groups only are shown).

CHAPTER III

TWO-DIMENSIONAL PERIODIC SYSTEMS

3.1 General

In this chapter a general formulation for studying the free wave propagation in two-dimensional periodic systems is presented. Such systems can be considered as an assemblage of cells (periods) joined together on all sides and corners as shown in figure (3.1a), where a cell represents one repeating period of the system, figure (3.1b).

Waves can propagate in such systems in two different manners, either as circular waves or plane waves depending on the type of forces generating them. Circular waves could be generated by a point force driving a certain point in the system and spreading a circular wave motion, while plane waves could be generated by a line force acting at any angle across the system. This analysis considers only plane wave motion in two-dimensional periodic systems.

Consider a two-dimensional periodic system defined by the two independent directions d_1 and d_2 parallel to the directions of the system's periodicity. Each cell (period) in the system is identified by two numbers n_1 and n_2 defining its position along the d_1 and d_2 directions, where the origin of the system is taken at the cell defined by $n_1 = n_2 = 0$. A property ϕ can propagate as a wave, with wave-number $\underline{a}$ and frequency ν, if the physical system admits a solution of the type

$$\phi_{n_1,n_2} = Ae^{2\pi i(\nu t - n_1 a_1 \ell_1 - n_2 a_2 \ell_2)} = Ae^{i(\omega t + n_1 \mu_1 + n_2 \mu_2)} \qquad (3.1)$$

where

ϕ_{n_1,n_2} is the value of the property ϕ at cell n_1, n_2.

A is a constant, t the time, ω the angular frequency, ℓ_1, ℓ_2 and a_1, a_2 are the dimensions of the cell and the components of the wave-number $\underline{a}$ along the d_1 and d_2 directions, respectively.

μ_1 and μ_2 are known as the propagation constants in the d_1 and d_2 directions, where

$$\mu_1 = -2\pi a_1 \ell_1$$

$$\mu_2 = -2\pi a_2 \ell_2 \tag{3.2}$$

Free waves can propagate, without attenuation, when the propagation constants μ_1 and μ_2 are real quantities. They represent the change in phase between adjacent cells in the d_1 and d_2 directions respectively.

Attenuating waves can be described by (3.1) but in this case the propagation constants μ_1 and μ_2 will be complex quantities |3|. Their real parts represent the change in phase while the imaginary parts represent the attenuation of the wave between adjacent cells in the d_1 and d_2 directions. From the relation (3.1) it can be seen that the relation between the values of the property ϕ at any point in one cell (n_1, n_2) and the corresponding points in adjacent cells can be written as

$$\begin{aligned} \phi_{n_1+1,\, n_2} &= \phi_{n_1,n_2} e^{i\mu_1} \\ \phi_{n_1,n_2+1} &= \phi_{n_1,n_2} e^{i\mu_2} \\ \phi_{n_1+1,n_2+1} &= \phi_{n_1,n_2} e^{i(\mu_1+\mu_2)} \end{aligned} \tag{3.3}$$

For unattenuated waves, where μ_1 and μ_2 are real quantities, relations (3.1) and (3.3) can be satisfied by using μ_1' and μ_2' instead of μ_1 and μ_2 where

$$\mu_1' = \mu_1 \pm 2m_1\pi,$$

$$\mu_2' = \mu_2 \pm 2m_2\pi \tag{3.4}$$

where m_1 and m_2 are any integer numbers.

Equations of motion of the system (equation (3.19) in Section 3.3) must yield the same values for ϕ and ω for a given μ_1 and μ_2 or equivalent μ_1' and μ_2'. This means that the propagating property ϕ, and its frequency ω are periodic functions of the real μ_1 and μ_2 with periods 2π. Therefore it is sufficient to examine the variation of the frequency of propagation ω with the real μ_1 and μ_2 within one period (zone) only. The most suitable choice is

$$-\pi \leq \mu_1 \leq \pi$$

$$-\pi \leq \mu_2 \leq \pi$$

or (3.5)

$$-\frac{1}{2\ell_1} \leq a_1 \leq \frac{1}{2\ell_1}$$

$$-\frac{1}{2\ell_2} \leq a_2 \leq \frac{1}{2\ell_2}$$

Now it remains to determine the boundaries to which the wave-number $\underline{a}$ is to be restricted to allow examining all possible propagating waves in all directions and at the same time satisfy the restrictions (3.5). These restrictions on μ_1 and μ_2 are for the same reasons discussed in Chapter II, Section 2.3 on restricting the propagation constant for one-dimensional systems inside the fundamental zone. This will be discussed in the next section.

3.2 Direct Cells, Recriprocal Cells and Zones in Two Dimensions

In this section we will describe briefly how to construct the zones to which the real wave-number $\underline{a}$ (and hence μ_1 and μ_2) will be confined for any two-dimensional periodic system. This restriction should be observed when determining the direction of propagation or the wave-length λ_w where

$$\lambda_w = 1/|\underline{a}|.$$

Full details and discussions for the zones can be found in |3|.

First we must define what we mean by direct cells and reciprocal cells. One period (cell) of the periodic system is referred to as the direct cell. It describes the periodicity of the medium in space. The reciprocal cell is geometrically identical to the direct cell but of dimensions that are the reciprocal of the corresponding dimensions of the direct cell. It describes the periodicity of the frequency of propagation in the wave-number domain. The direct system is constructed by joining the direct cells together and the reciprocal system is constructed by joining the reciprocal cells together in identical manner to the direct system. To illustrate the meaning of reciprocal cells we will consider first the one-dimensional

systems discussed in Chapter II.

In the one-dimensional case we found that the frequency of propagation is a periodic function of the wave-number $\underline{a}$ with period $1/\ell$ where ℓ is the length of the cell and we restricted the values of $\underline{a}$ within the first zone given by relation (2.19), namely

$$-\frac{1}{2\ell} \leq |\underline{a}| \leq \frac{1}{2\ell}$$

In other words we can say that the periodicity of the frequency in the wave-number domain can be described by a reciprocal cell of length $1/\ell$. Therefore the first (fundamental) zone for one-dimensional systems as given by (2.19) can be constructed by taking its origin at the centre of one of the reciprocal cells in the reciprocal system, figure (3.2). The first zone is bounded by the perpendicular bisectors of the lines drawn from the origin of the zone to the centres of neighbouring reciprocal cells as shown in figure (3.2).

Now we can proceed to find the analogous zones for two-dimensional systems. Zones will be areas in two dimensions and can be constructed as follows:

First define the direct cell and the reciprocal cell for the system. Figure (3.3) shows the reciprocal system corresponding to the oblique two-dimensional system shown in figure (3.1). Taking the centre of one of the reciprocal cells as the origin of the zone, then the boundaries of the first zone are defined by the smallest closed polygon formed by drawing perpendicular bisectors to all the lines drawn from the origin of the zone to the centres of neighbouring reciprocal cells as illustrated in figure (3.3).

The first zone for two-dimensional periodic systems with rectangular cells of dimensions ℓ_1 and ℓ_2 will be another rectangle of dimensions $1/\ell_1$ and $1/\ell_2$ with the origin at its centre as shown in figure (3.4). Higher zones can be constructed in a similar manner. However, for the purpose of this work it is enough to discuss the construction of the first zone only.

Similar to the one-dimensional periodic systems, frequencies corres-

ponding to values of $\underline{a}$ on the boundaries of the first zone for two-dimensional periodic systems are characteristic of the medium and depend on its physical properties. Also propagation will occur within some frequency bands only with possible overlapping of the bands. The width of these bands will vary with the direction of propagation. Solving the system's equations of motion for values of the wave-number $\underline{a}$ outside the fundamental (first) zone will always result in a wave-motion that can be obtained with a wave-number inside the fundamental zone. The shortest wave-length for any wave travelling in a two-dimensional periodic system will correspond to the wave with the largest absolute value of the wave-number $\underline{a}$ inside the first zone since

$$\lambda_w = 1/|\underline{a}|.$$

3.3 Mathematical Formulation

Consider a two-dimensional periodic system composed of an infinite number of identical cells joined together in identical manner as shown in figure (3.5a). A cell contains one period of the system, figure (3.5b). Using the finite element technique, a cell can be represented by a model with interior and boundary degrees of freedom. Each cell is coupled to its neighbours on all sides and corners. Let $\{q_I\}$, $\{F_I\}$ be the degrees of freedom and forces at the interior nodes of the cell, $\{q_L\}$, $\{F_L\}$, $\{q_R\}$, $\{F_R\}$, $\{q_B\}$, $\{F_B\}$ and $\{q_T\}$, $\{F_T\}$ be the degree of freedom and forces at the left, right, bottom and top sides of the cell, $\{q_{LB}\}$, $\{F_{LB}\}$, $\{q_{RB}\}$, $\{F_{RB}\}$, $\{q_{LT}\}$, $\{F_{LT}\}$ and $\{q_{RT}\}$, $\{F_{RT}\}$ be the degrees of freedom and forces at the left bottom, right bottom, left top and right top corners of the cell. The linear equation of motion of an undamped cell is given by

$$([K] - \omega^2[M])\{q\} = \{F\} \tag{3.6}$$

$[K]$ and $[M]$ are the stiffness and inertia matrices for the cell, $\{q\}$ and $\{F\}$ are the nodal degrees of freedom and forces, where

$$\begin{aligned} \{q\} &= \lfloor q_I \;\; q_L \;\; q_R \;\; q_B \;\; q_T \;\; q_{LB} \;\; q_{RB} \;\; q_{LT} \;\; q_{RT} \rfloor^T , \\ \{F\} &= \lfloor F_I \;\; F_L \;\; F_R \;\; F_B \;\; F_T \;\; F_{LB} \;\; F_{RB} \;\; F_{LT} \;\; F_{RT} \rfloor^T . \end{aligned} \tag{3.7}$$

The matrices $[K]$ and $[M]$ can be partitioned according to the interior left, right, bottom, top and corners degrees of freedom, hence

$$[K] = \begin{bmatrix} K_{I,I} & K_{I,L} & K_{I,R} & K_{I,B} & K_{I,T} & K_{I,LB} & K_{I,RB} & K_{I,LT} & K_{I,RT} \\ K_{L,I} & & & & & & & & \\ K_{R,I} & & & & & & & & \\ K_{B,I} & & & & & & & & \\ K_{T,I} & & & & & & & & \\ K_{LB,I} & & & & & & & & \\ K_{RB,I} & & & & & & & & \\ K_{LT,I} & & & & & & & & \\ K_{RT,I} & & & & & & & & K_{RT,RT} \end{bmatrix} \qquad (3.8)$$

A similar expression can be written for $[M]$.

The nodal forces $\{F\}$ are due to any external forces acting on the system and the forces of interaction between the cell and its neighbouring cells. For free wave motion, i.e., no external forces exist, then $\{F_I\} = 0$. However the forces on the boundaries of the cell (forces of interaction between the cell and its neighbouring cells) are not zero since they transmit the wave motion from one cell to its neighbours. This wave motion is characterised by relating the degrees of freedom and equivalent nodal forces in one cell (n_1, n_2) to the corresponding degrees of freedom and forces in adjacent cells, figure (3.5). The relations between the nodal forces can be written as follows:

$$\begin{aligned} \{F_L\}_{n_1+1,n_2} &= e^{i\mu_1}\{F_L\}_{n_1,n_2} \\ \{F_B\}_{n_1,n_2+1} &= e^{i\mu_2}\{F_B\}_{n_1,n_2} \\ \{F_{LT}\}_{n_1+1,n_2} &= e^{i\mu_1}\{F_{LT}\}_{n_1,n_2} \end{aligned} \qquad (3.9)$$

$$\{F_{RB}\}_{n_1,n_2+1} = e^{i\mu_2}\{F_{RB}\}_{n_1,n_2}$$

$$\{F_{LB}\}_{n_1+1,n_2+1} = e^{i(\mu_1+\mu_2)}\{F_{LB}\}_{n_1,n_2} \qquad (3.9)$$

For equilibrium of the interconnecting forces between cell (n_1, n_2) and the neighbouring cells, the following conditions must be satisfied

$$\{F_R\}_{n_1,n_2} + \{F_L\}_{n_1+1,n_2} = 0 \quad \text{(left and right)}$$

$$\{F_T\}_{n_1,n_2} + \{F_B\}_{n_1,n_2+1} = 0 \quad \text{(bottom and top)} \qquad (3.10)$$

$$\{F_{RT}\}_{n_1,n_2} + \{F_{LT}\}_{n_1+1,n_2} + \{F_{RB}\}_{n_1,n_2+1} + \{F_{LB}\}_{n_1+1,n_2+1} = 0 \quad \text{(corner)}$$

Substituting (3.9) into (3.10) gives

$$\{F_R\}_{n_1,n_2} + e^{i\mu_1}\{F_L\}_{n_1,n_2} = 0$$

$$\{F_T\}_{n_1,n_2} + e^{i\mu_2}\{F_B\}_{n_1,n_2} = 0 \qquad (3.11)$$

$$\{F_{RT}\}_{n_1,n_2} + e^{i\mu_1}\{F_{LT}\}_{n_1,n_2} + e^{i\mu_2}\{F_{RB}\}_{n_1,n_2} + e^{i(\mu_1+\mu_2)}\{F_{LB}\}_{n_1,n_2} = 0$$

Also the degrees of freedom can be related as follows

$$\{q_L\}_{n_1+1,n_2} = e^{i\mu_1}\{q_L\}_{n_1,n_2}$$

$$\{q_B\}_{n_1,n_2+1} = e^{i\mu_2}\{q_B\}_{n_1,n_2}$$

$$\{q_{LB}\}_{n_1+1,n_2} = e^{i\mu_1}\{q_{LB}\}_{n_1,n_2} \qquad (3.12)$$

$$\{q_{LB}\}_{n_1,n_2+1} = e^{i\mu_2}\{q_{LB}\}_{n_1,n_2}$$

$$\{q_{LB}\}_{n_1+1,n_2+1} = e^{i(\mu_1+\mu_2)}\{q_{LB}\}_{n_1,n_2}$$

At the common boundaries between cell n_1, n_2 and its neighbouring cells the displacements must be equal, hence,

$$\begin{aligned}
\{q_L\}_{n_1+1,n_2} &= \{q_R\}_{n_1,n_2} \\
\{q_B\}_{n_1,n_2+1} &= \{q_T\}_{n_1,n_2} \\
\{q_{LB}\}_{n_1+1,n_2} &= \{q_{RB}\}_{n_1,n_2} \\
\{q_{LB}\}_{n_1,n_2+1} &= \{q_{LT}\}_{n_1,n_2} \\
\{q_{LB}\}_{n_1+1,n_2+1} &= \{q_{RT}\}_{n_1,n_2}
\end{aligned} \tag{3.13}$$

Substituting (3.13) into (3.12) gives

$$\begin{aligned}
\{q_R\}_{n_1,n_2} &= e^{i\mu_1}\{q_L\}_{n_1,n_2} \\
\{q_T\}_{n_1,n_2} &= e^{i\mu_2}\{q_B\}_{n_1,n_2} \\
\{q_{RB}\}_{n_1,n_2} &= e^{i\mu_1}\{q_{LB}\}_{n_1,n_2} \\
\{q_{LT}\}_{n_1,n_2} &= e^{i\mu_2}\{q_{LB}\}_{n_1,n_2} \\
\{q_{RT}\}_{n_1,n_2} &= e^{i(\mu_1+\mu_2)}\{q_{LB}\}_{n_1,n_2}
\end{aligned} \tag{3.14}$$

Relations (3.11) and (3.14) are the same for any cell and hence the suffix n_1, n_2 can be dropped. Relations (3.14) can be used to write the relation between the degrees of freedom in the cell in the matrix form

$$\{q\} = [w]\{\bar{q}\} \tag{3.15}$$

where

$$\{q\} = \lfloor q_I \;\; q_L \;\; q_R \;\; q_B \;\; q_T \;\; q_{LB} \;\; q_{RB} \;\; q_{LT} \;\; q_{RT} \rfloor^T,$$

$$\{\bar{q}\} = \lfloor q_I \;\; q_L \;\; q_B \;\; q_{LB} \rfloor^T,$$

$$[W] = \begin{bmatrix} I & 0 & 0 & 0 \\ 0 & I & 0 & 0 \\ 0 & e^{i\mu_1} & 0 & 0 \\ 0 & 0 & I & 0 \\ 0 & 0 & e^{i\mu_2} & 0 \\ 0 & 0 & 0 & I \\ 0 & 0 & 0 & e^{i\mu_1} \\ 0 & 0 & 0 & e^{i\mu_2} \\ 0 & 0 & 0 & e^{i(\mu_1+\mu_2)} \end{bmatrix} \tag{3.16}$$

Also the equilibrium conditions (3.11) and the condition

$$\{F_I\} = 0 ,$$

can be written in the matrix form,

$$[W']\{F\} = 0 \tag{3.17}$$

where

$$\{F\} = \lfloor F_I \quad F_L \quad F_R \quad F_B \quad F_T \quad F_{LB} \quad F_{RB} \quad F_{LT} \quad F_{RT} \rfloor^T ,$$

$$[W'] = \begin{bmatrix} I & 0 & 0 & 0 & 0 & 0 & 0 & 0 & 0 \\ 0 & I & e^{-i\mu_1} & 0 & 0 & 0 & 0 & 0 & 0 \\ 0 & 0 & 0 & I & e^{-i\mu_2} & 0 & 0 & 0 & 0 \\ 0 & 0 & 0 & 0 & 0 & I & e^{-i\mu_1} & e^{-i\mu_2} & e^{-i(\mu_1+\mu_2)} \end{bmatrix} \tag{3.18}$$

Substituting (3.15) and (3.17) into equation (3.6) results in an equation of the form

$$([\bar{K}(\mu_1, \mu_2)] - \omega^2[\bar{M}(\mu_1, \mu_2)])\{\bar{q}\} = 0 \tag{3.19}$$

where $[\bar{K}]$ and $[\bar{M}]$ are complex matrices given by

$$[\bar{K}] = \begin{bmatrix} K_{I,I} & \bar{K}_{I,L} & \bar{K}_{I,B} & \bar{K}_{I,LB} \\ \bar{K}_{L,I} & & & \\ \bar{K}_{B,I} & & & \\ \bar{K}_{LB,I} & & & \bar{K}_{LB,LB} \end{bmatrix} = [W'][K][W], \qquad (3.20)$$

$$[\bar{M}] = \begin{bmatrix} M_{I,I} & \bar{M}_{I,L} & \bar{M}_{I,B} & \bar{M}_{I,LB} \\ \bar{M}_{L,I} & & & \\ \bar{M}_{B,I} & & & \\ \bar{M}_{LB,I} & & & \bar{M}_{LB,LB} \end{bmatrix} = [W'][M][W]$$

$[K]$ and $[M]$ are the stiffness and inertia matrices in equation (3.6).

Equation (3.19) represents an eigenvalue problem in ω for given values of μ_1 and μ_2. When μ_1 and μ_2 are real quantities, equation (3.19) can be rearranged to give a real symmetric eigenvalue problem in ω. This will be discussed in Section 3.4. Also this equation can be reformulated to give an eigenvalue problem in μ_1 and μ_2 for given values of ω, where μ_1 and μ_2 will be generally complex quantities. This will be discussed in Section 3.5.

3.4 Formulation for the Real Propagation Constants

As mentioned in Section 3.1, waves can propagate in two-dimensional periodic systems, without attenuation, when the propagation constants μ_1 and μ_2 are real quantities. In this case the frequency of propagation is a periodic function of μ_1 and μ_2 with periods 2π and hence the variation of the frequency with the real propagation constants can be examined by solving equation (3.19) for given values of μ_1 and μ_2 within one period only. In this case equation (3.19) can be reformulated to give a real symmetric eigenvalue problem in ω for given real values of μ_1 and μ_2.

Now the matrices $[\bar{K}(\mu_1, \mu_2)]$ and $[\bar{M}(\mu_1, \mu_2)]$ in equation (3.19) can be written as

$$[\bar{K}(\mu_1, \mu_2)] = [\bar{K}^r] + i[\bar{K}^i]$$
$$[\bar{M}(\mu_1, \mu_2)] = [\bar{M}^r] + i[\bar{M}^i] \tag{3.21}$$

Substituting (3.21) into (3.19) gives

$$([\bar{K}^r] + i[\bar{K}^i] - \omega^2([\bar{M}^r] + i[\bar{M}^i]))\{\{\bar{q}^r\} + i\{\bar{q}^i\}\} = 0 \tag{3.22}$$

where

$$\{\bar{q}^r\} = \begin{Bmatrix} q_I \\ q_L \\ q_B \\ q_{LB} \end{Bmatrix}^r , \qquad \{\bar{q}^i\} = \begin{Bmatrix} q_I \\ q_L \\ q_B \\ q_{LB} \end{Bmatrix}^i \tag{3.23}$$

Separating the real and imaginary parts of (3.22) and combining the two equations together gives

$$\left(\begin{bmatrix} \bar{K}^r & -\bar{K}^i \\ \bar{K}^i & \bar{K}^r \end{bmatrix} - \omega^2 \begin{bmatrix} \bar{M}^r & -\bar{M}^i \\ \bar{M}^i & \bar{M}^r \end{bmatrix} \right) \begin{Bmatrix} \bar{q}^r \\ \bar{q}^i \end{Bmatrix} = 0 \tag{3.24}$$

From (3.16) and (3.18) it is clear that for real values of μ_1 and μ_2 we can write

$$[W'] = [W^*]^T$$

where $*$ denotes the complex conjugate, and hence the matrices $[\bar{K}]$ and $[\bar{M}]$ (given by (3.20)) are Hermitian, i.e.,

$$[\bar{K}^*]^T = [\bar{K}]$$
$$[\bar{M}^*]^T = [\bar{M}] \tag{3.25}$$

Therefore equation (3.24) represents a real symmetric eigenvalue problem since

$$[\bar{K}^i] = -[\bar{K}^i]^T$$
$$[\bar{M}^i] = -[\bar{M}^i]^T \tag{3.26}$$

This equation can be solved for different values of the propagation constants μ_1 and μ_2 (where μ_1 and μ_2 are real) to find the corresponding frequencies of propagation and associated wave forms.

3.4.1 Computer programs

A general computer program has been written to analyse any two-dimensional periodic system. One period (cell) of the system is represented by a finite element model and the matrices in equation (3.24) are formed for given real values of μ_1 and μ_2. Then the problem is solved as a standard eigenvalue problem. The basic flow diagram for the computational procedure is given in Appendix B. The method used to solve the eigenvalue problem (3.24) is given in Appendix A.

3.4.2 Illustrative examples

Two examples are used here to illustrate the general behaviour of two-dimensional periodic systems, and to explain some of the points discussed in Section 3.1.

Consider the flexural wave-motion in an infinite plate resting on simple line supports along orthogonal, equally spaced lines, figure (3.6a). In this case the system can be defined by the cartesian axes x and y. Let $\underline{a}$ be the wave-number for a wave travelling across the plate at a direction making an angle α to the x-axis, then the components of the wave-number $\underline{a}$ along the x and y directions are

$$a_x = |\underline{a}| \cos \alpha \quad , \qquad a_y = |\underline{a}| \sin \alpha \tag{3.27}$$

If ℓ_x and ℓ_y are the dimensions of the cell representing one period of the plate (distances between the supports), figure (3.5b), then, from relations (3.2), we can write

$$\mu_x = -2\pi a_x \ell_x \quad , \qquad \mu_y = -2\pi a_y \ell_y \tag{3.28}$$

where μ_x and μ_y are the propagation constants along the x and y directions respectively.

The first zone to which the wave number $\underline{a}$ (and hence the propagation constants μ_1 and μ_2) will be restricted is a rectangle of dimensions $1/\ell_x$ and $1/\ell_y$ as shown in figure (3.4). This was discussed in Section 3.2. The shortest wave-length for a wave travelling along the x direction will correspond to a wave-number $\underline{a} = a_x = 1/2\ell_x$ and hence

$$\lambda_x = \frac{1}{|\underline{a}|} = 2\ell_x \tag{3.28}$$

Similarly the shortest wave-length for a wave travelling along the y direction is

$$\lambda_y = 2\ell_y. \tag{3.30}$$

The shortest wave-length λ_s for any wave travelling in the system will correspond to a wave having the largest absolute value of $\underline{a}$ inside the zone as its wave-number, hence

$$\lambda_s = \frac{1}{|\underline{a}|_{max}} = \frac{1}{\sqrt{|a_x|^2_{max} + |a_y|^2_{max}}}$$

or

$$\lambda_s = \frac{1}{\sqrt{(\frac{1}{2\ell_x})^2 + (\frac{1}{2\ell_y})^2}} = \frac{2\ell_x\ell_y}{\sqrt{\ell_x^2 + \ell_y^2}} \tag{3.31}$$

The directions of propagation for this wave are given by

$$\alpha = \tan^{-1}(\frac{a_y}{a_x}) = \tan^{-1}(\pm \frac{\ell_x}{\ell_y}) \tag{3.32}$$

Propagation bands will be surfaces in the a_x, a_y (or μ_x, μ_y) domain. The width of the first propagation band, as will be shown later, is largest along the directions given by (3.32) and hence these directions can be called the preferred directions of propagation. These are directions normal to the diagonals of the cells. Frequencies corresponding to waves with wave-length given by (3.29), (3.30) and (3.31) are characteristic of the periodic system. They depend on the dimensions of the cells and their physical properties.

Now consider a plate with square cells of dimensions $\ell_x = \ell_y = 1.0$ (distances between the line supports). One cell (a square plate simply supported along its sides) is represented by a finite element model,

figure (3.6b). The cell is divided into 16 plate elements. The plate element and the data values used in the analysis are given in Appendix D4. The degrees of freedom at the nodes are the transverse displacement w and the two rotations θ_x and θ_y, and hence at the left and right sides only θ_y exists while at the bottom and top sides only θ_x exists. No degrees of freedom exist at the corners. The problem is solved for different values of the propagation constants μ_x and μ_y. Figure (3.13) shows the variation of the non-dimensional frequency Ω, in the first propagation band, for values of μ_x and μ_y in the range

$$-3\pi \leq \mu_x \leq 3\pi$$

$$-3\pi \leq \mu_y \leq 3\pi$$

The non-dimensional frequency Ω is defined as

$$\Omega = \omega \ell_x^2 (\frac{\rho h}{D})^{\frac{1}{2}} \tag{3.33}$$

where

$$D = Eh^3/12(1 - \sigma^2).$$

ω is the angular frequency, ρ,h, D, E, σ are the density, the thickness, the modulus of rigidity, Young's modulus and Poisson's ratio of the plate.

As can be seen from the graph, the propagation band is a surface with periodic variation in the μ_x, μ_y domain of periods 2π and symmetrical about the lines $\mu_x = 0$ and $\mu_y = 0$. Therefore it must terminate at the boundaries of the first zone (a square bounded by $\mu_x = \pm\pi$ and $\mu_y = \pm\pi$) with zero normal derivatives. Also shown on the graph the values of the components of the wave-number $\underline{a}$ (a_x and a_y) alongside μ_x and μ_y. Due to the periodicity of the frequency with μ_x and μ_y, as explained in Section 3.3, it is enough to examine the variation of the frequency with μ_x and μ_y inside the first zone only. Figures (3.14), (3.15) and (3.16) show the first, second and third propagation bands where μ_x and μ_y are restricted within the first zone only. Cross-sections along the x direction ($\mu_y = 0.0$) or the y direction ($\mu_x = 0.0$) or along a direction given by $\mu_x = \mu_y$ (a direction making 45 degrees to the x axis in this case) will yield curves similar to those obtained for one-dimensional systems. This is shown in figure (3.17) for the first three propagation bands.

The limiting (cut-off) frequencies for the propagation bands depend on the direction of propagation and occur at the centre of the zone

($\mu_x = \mu_y = 0.0$) and at the boundaries of the zone ($\mu_x = \pm\pi$ and/or $\mu_y = \pm\pi$). However in some cases, as will be shown later, the limiting frequencies for the propagation bands can occur at different values for μ_x and μ_y.

Another way of showing the variation of the frequency of propagation inside the first zone can be obtained in a polar plot by drawing lines joining the frequencies corresponding to wave-numbers drawn from the centre of the zone at all directions and terminating on the boundaries of one of the concentric polygons drawn inside the zone with sides parallel to the boundaries of the zone (squares in this case) as shown in figure (3.7). Figure (3.18) shows the first three propagation bands in the polar plot for the plate with square cells. This representation has the advantage of showing clearly the variation in the width of the different bands and the limiting (cut off) frequencies with the direction of propagation. It also shows that the width of the first band is largest along a direction of propagation making an angle 45 degrees to the x axis which is the preferred direction of propagation. Also the overlapping of the second and third bands is very clear on this plot.

Figures (3.19 a, b), (3.20 a, b), (3.21a, b) and (3.22a, b) show the frequencies of propagation and the associated wave-forms (These are the eigenvectors in equation (3.24)) in the first and second propagation bands corresponding to some values of μ_x and μ_y (only 5 x 5 cells are shown.) For μ_x equal to 0 or $\pm\pi$ the corresponding wave components along the x direction are standing waves with wave-length equal to ∞ or $2\ell_x$ respectively. Similarly for μ_y equal to 0 or $\pm\pi$ the corresponding wave components along the y direction are standing waves with wave-length equal to ∞ or $2\ell_y$. Frequencies corresponding to $\mu_x = 0.0$ or $\pm\pi$ and $\mu_y = 0.0$ or $\pm\pi$ are the bounding frequencies for the propagation bands along the x direction, the y direction and the preferred direction of propagation. These frequencies and associated wave-forms, as can be seen from figures (3.19) to (3.21), can be associated with the natural frequencies of the single cell with various boundary conditions. This will be discussed in detail in Section 3.6.

For $0 < |\mu_x| < \pi$ or $0 < |\mu_y| < \pi$ the corresponding wave components are travelling waves along the x-direction or the y-direction respectively. The shortest wave-length and the corresponding direction of propagation

are obtained from relations (3.31) and (3.32), hence

$$\lambda_s = \frac{2\ell_x \ell_y}{\sqrt{\ell_x^2 + \ell_y^2}} = \sqrt{2}$$

and

$$\alpha = \tan^{-1}\left(\frac{\ell_x}{\ell_y}\right) = 45^o$$

which is the preferred direction of propagation. This wave corresponds to the lowest frequency of propagation in the first band (cut-off frequency).

The second example is similar to the previous one except that the distances between the supports are taken as

$$\ell_x = 1.0, \qquad \ell_y = 2.0$$

and hence the basic cell representing the system is a rectangular plate of dimension $\ell_x = 1.0$, $\ell_y = 2.0$ with simply supported edges. Figures (3.23) and (3.24) show the variation of the frequency of propagation in the first two propagation bands where μ_x and μ_y are restricted within the fundamental zone (μ_x and μ_y vary between $\pm\pi$). Figure (3.25) shows cross-sections in these bands along the x direction, the y direction and the preferred direction of propagation (a direction making an angle equal to 26.56 degrees to the x axis in this case, where $\mu_x = \mu_y$). Figure (3.26) shows a polar plot for the frequency variation in the first two bands. Comparing this graph with the one for the plate with square cells (figure (3.18)) it can be seen how the dimensions of the cells affect the variation in the width of the various propagation bands with direction of propagation. Also it is clear that the first and second bands overlap in this case. Figures (3.27), (3.28), (3.29) and (3.30) show the frequencies of propagation and the associated wave-forms in the first and second propagation bands corresponding to values of μ_x and μ_y equal to 0 or $\pm\pi$. Inspection of these figures shows that these frequencies and associated wave-forms coincide with the natural frequencies and associated normal modes of the cell with various boundary conditions. This will be discussed in Section 3.6. The shortest wave-length and the corresponding direction of propagation (preferred direction of propagation) are obtained from relations (3.31) and (3.32), hence

$$\lambda_s = \frac{2\ell_x \ell_y}{\sqrt{\ell_x^2 + \ell_y^2}} = 4/\sqrt{5}$$

and

$$\alpha = \tan^{-1}\left(\frac{\ell_x}{\ell_y}\right) = 26.56^o$$

This corresponds to the lowest frequency of propagation in the first band (cut-off frequency).

A movie film showing clearly the standing and propagating waves described above has been produced using the computer.

3.4.3 Transition from non-periodic to periodic two-dimensional systems

To illustrate the effect of periodic discontinuities on the propagation of waves in a homogeneous two-dimensional medium, consider the transverse wave-motion in an infinite plate resting on orthogonal, equally spaced line spring supports (translational only) as shown in figure (3.8a). A finite element idealisation of one cell is shown in figure (3.8b). The dimensions of the cell (distances between the line supports) are

$$\ell_x = \ell_y = 1.0.$$

The plate element and data values used in the analysis are given in Appendix D4. Figure (3.31a, b) shows the variation of the frequency of propagation with μ_x and μ_y in the first two propagation bands where the spring supports stiffness K_t is taken equal to zero. The values of μ_x and μ_y are restricted inside the first zone (a square bounded by $\mu_x = \pm\pi$ and $\mu_y = \pm\pi$). Similar to the one-dimensional case discussed in Section 2.4 it is clear from the figure that if we plot the propagation surfaces for larger values of μ_x and μ_y (say $-3\pi \leq \mu_x, \mu_y \leq 3\pi$, similar to the one-dimensional case shown in figure (2.14)) then we will find that the propagation bands (surfaces) will join together to form continuous surfaces (paraboloids) allowing propagation at all frequencies and in all directions. These surfaces are the same as those obtained by considering the equation of two-dimensional transverse wave motion w in an infinite plate given by

$$D\nabla^4 w + \rho h \frac{\partial^2 w}{\partial t^2} = 0 \qquad (3.34)$$

where

$$\nabla^4 = \nabla^2 . \nabla^2 \ , \tag{3.34}$$

$$\nabla^2 = \frac{\partial^2}{\partial x^2} + \frac{\partial^2}{\partial y^2}$$

and considering

$$w(x, y) = w_o e^{2\pi i(\nu t - a_x . x - a_y . y)} \tag{3.35}$$

as a solution to (3.34) where w_o is a constant, ν is the frequency, a_x and a_y are the components of the wave-number in the x and y directions, ρ and D are the density and the modulus of rigidity of the plate.

Substituting (3.35) into (3.34) gives

$$\nu^2 = 4\pi^2 . \frac{D}{\rho h} . (a_x^2 + a_y^2)^2$$

or

$$\Omega = \mu_x^2 + \mu_y^2 \tag{3.36}$$

where

$$\mu_x = -2\pi a_x \ell_x \ ,$$

$$\mu_y = -2\pi a_y \ell_y = -2\pi a_y \ell_x \qquad (\ell_x = \ell_y)$$

Ω is the non-dimensional frequency given by

$$\Omega = \omega \ell_x^2 (\frac{\rho h}{D})^{\frac{1}{2}}$$

ω is the angular frequency where

$$\omega = 2\pi\nu .$$

Table 3.1 shows a comparison between the finite element results plotted in figure (3.31) and the exact solution (3.36). The table gives the non-dimensional frequency Ω corresponding to various values of μ_x and μ_y. From these results it is clear that the finite element calculations are very close to the exact ones. More accurate results can be obtained by increasing the number of elements representing the cell. Non-zero values for the translational spring supports stiffness K_t

simply introduce discontinuities into these surfaces allowing propagation in some frequency bands only. At the limit when K_t is equal to ∞ the propagation bands are the same as those obtained for the simply supported plate with square cells discussed in Section 3.4.2.

3.4.4 Oblique two-dimensional periodic systems

In some two-dimensional periodic structures the cell describing the periodicity of the system can be in the form of a parallelogram. These can be found in some aircraft substructures such as stringer stiffened plates in two dimensions where the stringers are not orthogonal. Such systems are referred to as oblique systems. To illustrate how waves propagate in these systems consider the transverse wave motion in an infinite plate resting on simple line supports at equally spaced parallel lines in two directions making a 60° angle between them as shown in figure (3.9a). A finite element idealisation of the cell representing one period of the system is shown in figure (3.9b). The dimensions of the cell sides along the directions d_1 and d_2 defining the system are

$$\ell_1 = 1.0, \quad \ell_2 = 1.0.$$

The plate element and data values used in the analysis are given in Appendix D5. As described in Section 3.2, the first zone, to which the wave-number $\underline{a}$ (and hence μ_1 and μ_2) is to be restricted, for this system will be a hexagon with the origin at its centre as shown in figure (3.10). Figure (3.32) shows a polar plot for the first propagation band. Each curve in this plot corresponds to wave-numbers drawn from the centre of the zone in all directions and terminating at one of the concentric polygons drawn inside the zone with sides parallel to the boundaries of the zone as illustrated in figure (3.10). From the graph it is clear that the width of the propagation band is largest at a direction of propagation along the shorter diagonal of the cell (normal to the longer diagonal) and the lowest bounding frequency for the first band occurring along that direction (preferred direction of propagation). Figure (3.33) shows cross-sections in the first and second propagation bands for waves travelling along the d_1 and d_2 directions (where $\mu_1 \neq 0$, $\mu_2 = 0$ and $\mu_1 = 0$, $\mu_2 \neq 0$ respectively), and along the longer and shorter diagonals of the cell (these are directions making 30° to

the d_1 axis where $\mu_1 = \mu_2$ and 120^o to the d_1 axis where $\mu_1 = -\mu_2$). From this graph it is clear that the upper bounding frequency for the first band does not correspond to zero wave-number ($\mu_1 = \mu_2 = 0$).

A comparison between these results and those obtained in Section 3.4.2 for the plate with square cells, figures (3.17) and (3.18), shows that the propagation bands for the oblique system occur at higher frequencies and the width of the first band is very narrow along the d_1 and d_2 directions.

3.4.5 Wave propagation in two-dimensional point supported periodic plates

In many building structures the floors are supported on columns which are generally located in a regular pattern. Understanding the vibration characteristics of such structures is important if they are subjected to dynamic loads such as machinery resting upon them. This can be easily and quickly estimated if the periodic nature of the structure is utilised. To illustrate this, consider a two-dimensional plate resting on point supports at regular intervals parallel to the x and y directions as shown in figure (3.11a). A finite element idealisation of one cell with point supports at its corners is shown in figure (3.11b). The plate element and data values used in the analysis are given in Appendix D4. The dimensions of the cell (distances between the supports) in the x and y directions are

$$\ell_x = 1.0, \quad \ell_y = 1.0.$$

The degrees of freedom at the nodes are: the transverse displacement w and the two rotations θ_x and θ_y, and hence at the supports only θ_x and θ_y exist. Figures (3.34a, b) show the variation of the frequency of propagation in the first and second propagation bands where the propagation constants μ_x and μ_y are restricted inside the first zone (a square bounded by $\mu_x = \pm\pi$ and $\mu_y = \pm\pi$). Figure (3.34c) shows cross-sections in the first, second and third propagation bands along the x direction ($\mu_x \neq 0.0$, $\mu_y = 0.0$) and along the diagonal of the cells (a direction making an angle 45^o to the x axis) which is the preferred direction of propagation in this case ($\mu_x = \mu_y$). From these graphs it can be seen that the bounding frequencies for the bands at some directions (e.g., preferred direction of propagation) do not necessarily correspond to wave-numbers at the centre or the boundaries of the zone.

A comparison between these results and those obtained in Section 3.4.2 for the plate on line supports with square cells, figures (3.14), (3.15), (3.16) and (3.17) shows that the propagation bands for the point supported plate occur at lower frequencies. Also it is clear that the highest bounding frequency for the first band (along the preferred direction of propagation) is the lowest bounding frequency for the second band and hence, contrary to the plate on line supports, there is no stopping band between the first and second bands along the preferred direction of propagation.

3.4.6 Wave propagation in periodically stiffened plates

Many aircraft substructures are composed of flat or curved plates stiffened at regular spacings in one or two directions. Here we will consider the transverse wave motion in a two-dimensional flat plate stiffened with frames and stringers at equally spaced orthogonal lines as shown in figure (3.12a). The structural data and elements used in the analysis are given in Appendix D6. A finite element idealisation of one cell is shown in figure (3.12b). The dimensions of the cell (distances between the stringers or the frames) are

$$\ell_x = 11.43 \text{ cm}, \ell_y = 22.86 \text{ cm} .$$

The cell is divided into 16 plate elements, 4 frame elements and 4 stringer elements. First the problem was analysed assuming zero transverse motion at the frames and the stringers (this is due to their high transverse rigidity in comparison to the plate). The variation of the frequency of propagation in the first two bands is shown in figures (3.35a, b) where μ_x and μ_y are restricted within the first zone. Figure (3.35c) shows cross-sections in the first, second and third propagation bands for waves travelling along the x direction, the y direction and the preferred direction of propagation (a direction making an angle α to the x axis where

$$\alpha = \tan^{-1} \frac{\ell_x}{\ell_y} = 26.56^{\circ}).$$

Figures (3.36a, b, c) show similar results for the same structure considering non-zero transverse motion at the frames and the stringers. In this case the first propagation band starts from zero frequency. Wave motion corresponding to the first part of the first band, where the wave-number is small, represents waves of large wave-length compared to the distances between the stiffeners, and hence waves are propagated as if

the structure is non-periodic. The rest of the first band is very close to the first band for the plate when considering zero transverse displacement at the stiffeners.

The results obtained here when considering zero transverse displacement at the stiffeners shows great similarity with the results obtained in Section 3.4.2 for the plate on line supports and rectangular cells ($\ell_x = 1.0$, $\ell_y = 2.0$).

3.5 Formulation for the Complex Propagation Constant

Following the formulation for the one-dimensional systems given in Section 2.5, equation (3.19) can be rearranged to give an eigenvalue problem in μ_1 and μ_2 for a given value of the frequency ω, where μ_1 and μ_2 will be generally complex. This formulation has the advantage of giving the values of the propagation constants μ_1 and μ_2 at any frequency. Also, in some cases, it produces an eigenvalue problem of smaller order than the eigenvalue problem obtained in the formulation for the real propagation constants discussed in the previous section. However it is more complicated to formulate.

Equation (3.19) can be written in the form

$$[D(\mu_1, \mu_2)] \begin{Bmatrix} q_I \\ q_L \\ q_B \\ q_{LB} \end{Bmatrix} = 0 \tag{3.37}$$

where

$$[D] = \begin{bmatrix} D_{I,I} & D_{I,L} & D_{I,B} & D_{I,LB} \\ D_{L,I} & D_{L,L} & D_{L,B} & D_{L,LB} \\ D_{B,I} & D_{B,L} & D_{B,B} & D_{B,LB} \\ D_{LB,I} & D_{LB,L} & D_{LB,B} & D_{LB,LB} \end{bmatrix} = [\bar{K}] - \omega^2[\bar{M}] \tag{3.38}$$

The submatrices $D_{i,j}$ are given by

$$D_{i,j} = \bar{K}_{i,j} - \omega^2 \bar{M}_{i,j}$$

where $\bar{K}_{i,j}$ and $\bar{M}_{i,j}$ are the submatrices of $[\bar{K}]$ and $[\bar{M}]$. The first relation in equation (3.37) gives

$$\{q_I\} = -D_{I,I}^{-1}(D_{I,L}\{q_L\} + D_{I,B}\{q_B\} + D_{I,LB}\{q_{LB}\}) \tag{3.39}$$

Relation (3.39) can be used to eliminate $\{q_I\}$ from equation (3.37). This results in an equation of the form

$$[\bar{D}(\mu_1, \mu_2)] \begin{Bmatrix} q_L \\ q_B \\ q_{LB} \end{Bmatrix} = 0 \tag{3.40}$$

where

$$[\bar{D}(\mu_1, \mu_2)] = [T'][D(\mu_1, \mu_2)][T] \tag{3.41}$$

The matrices $[T]$ and $[T']$ are given by

$$[T] = \begin{bmatrix} -D_{I,I}^{-1}D_{I,L} & -D_{I,I}^{-1}D_{I,B} & -D_{I,I}^{-1}D_{I,LB} \\ I & 0 & 0 \\ 0 & I & 0 \\ 0 & 0 & I \end{bmatrix} \tag{3.42}$$

$$[T'] = \begin{bmatrix} -D_{L,I}D_{I,I}^{-1} & I & 0 & 0 \\ -D_{B,I}D_{I,I}^{-1} & 0 & I & 0 \\ -D_{LB,I}D_{I,I}^{-1} & 0 & 0 & I \end{bmatrix} \tag{3.43}$$

Examination of (3.16), (3.18) and (3.20) shows that the propagation constants μ_1 and μ_2 appear in the elements of the matrices $[\bar{K}]$ and $[\bar{M}]$, and hence in $[D]$ and $[\bar{D}]$, only in the form

$$e^{\pm i\mu_1}, \quad e^{\pm i\mu_2} \quad \text{and} \quad e^{\pm i\mu_1 \pm i\mu_2}$$

(notice that the matrix $D_{I,I}$, and hence $D_{I,I}^{-1}$, is a real symmetric matrix).

Therefore equ ation (3.37) can be written in the form

$$(e^{i\mu_1}[B_1] + e^{-i\mu_1}[B_2] + e^{i\mu_2}[B_3] + e^{-i\mu_2}[B_4] + e^{i(\mu_1+\mu_2)}[B_5] + e^{i(\mu_1-\mu_2)}[B_6] + e^{i(\mu_2-\mu_1)}[B_7] + e^{-i(\mu_1+\mu_2)}[B_8] + [B_9]) \begin{Bmatrix} q_L \\ q_B \\ q_{LB} \end{Bmatrix} = 0 \quad (3.44)$$

The matrices $[B_i]$ are of the same order as $[\bar{D}]$ where each matrix contains only the elements of $[\bar{D}]$ which are multiplied by $e^{i\mu_1}$, $e^{-i\mu_1}$, etc. Now if the ratio between μ_1 and μ_2 gives a rational number, then they can be written in the form

$$\mu_1 = n_1\mu$$
$$\mu_2 = n_2\mu \quad (3.45)$$

where n_1 and n_2 are integer numbers or zero.

Substituting (3.45) into (3.44) and putting $e^{i\mu} = \lambda$ gives

$$(\lambda^{n_1}[B_1] + \lambda^{-n_1}[B_2] + \lambda^{n_2}[B_3] + \lambda^{-n_2}[B_4] + \lambda^{n_1+n_2}[B_5] + \lambda^{n_1-n_2}[B_6] + \lambda^{n_2-n_1}[B_7] + \lambda^{-n_1-n_2}[B_8] + [B_9]) \begin{Bmatrix} q_L \\ q_B \\ q_{LB} \end{Bmatrix} = 0 \quad (3.46)$$

If the largest negative power of λ in (3.46) is -m, then multiplying (3.46) by λ^m will eliminate all negative powers of λ. Therefore (3.46) can be written in the form (after multiplying by λ^m and rearranging terms)

$$([A_n]\lambda^n + [A_{n-1}]\lambda^{n-1} + \ldots + [A_o]) \begin{Bmatrix} q_L \\ q_B \\ q_{LB} \end{Bmatrix} \quad (3.47)$$

where n is an integer positive number.

$[A_i]$ are the sum of the matrices $[B_j]$ that are multiplied by λ^i.

Equation (3.47) represents a general eigenvalue problem of order n. This can be solved for various values of the frequency ω and a certain

direction of propagation such that the ratio between μ_1 and μ_2 is a rational number. For example, along the d_1 direction where $\mu_1 \neq 0$ and $\mu_2 = 0$ or along the d_2 direction where $\mu_1 = 0$ and $\mu_2 \neq 0$ or along directions such that $\mu_1 = \mu_2$ or $\mu_1 = 2\mu_2$ etc. Different techniques for solving the eigenvalue problem (3.44) are given in Appendix A.

3.5.1 Computer programs

A general computer program has been written to represent one period (cell) of any two-dimensional periodic system by a finite element model and to formulate the eigenvalue problem given by equation (3.47). This eigenvalue problem is then reformulated to give a standard eigenvalue problem of the form

$$([G] - \lambda[I])\{x\} = 0$$

or

$$([A] - \lambda[B])\{x\} = 0$$

where various eigenvalue solutions can be used. This is discussed in Appendix A. The basic flow diagram for the computational procedure is given in Appendix B.

3.5.2 Applications

Some of the cases used in Section 3.4 will be used here to show that this formulation produces results similar to those obtained using the formulation for the real propagation constants (when μ_1 and μ_2 are real quantities), and also to investigate the behaviour of two-dimensional periodic systems at frequencies outside the propagation bands where the propagation constants will be generally complex.

The following cases are considered.

a. Transverse wave-motion in infinite plates resting on orthogonal, equally spaced simple line supports.

This is the same example used in Section 3.4.2, figure (3.6a). A similar finite element idealisation is used here, figure (3.6b). For the case of square cells ($\ell_x = \ell_y = 1.0$) two directions of propagation are considered, along the x axis and at a direction normal to the diagonal of the cells (preferred direction of propagation). When the waves are propagating along the x direction, relations (3.45) can be

written in the form

$$\mu_x = \mu_1 = \mu$$

$$\mu_y = \mu_2 = 0.0.$$

Therefore the eigenvalue problem (3.47) will be of the form

$$([A_2]\lambda^2 + [A_1]\lambda + [A_o])\{q\} = 0.$$

This has been solved for various values of the non-dimensional frequency Ω. The resulting λ will give conjugate pairs for μ. Each pair represents two identical waves travelling in opposite directions. Figure (3.37) shows the variation of the real and imaginary parts of μ (where $\mu_x = \mu$) with the non-dimensional frequency Ω. Three different waves are shown (numbered 1, 2 and 3). The imaginary parts of μ (attenuation factor) are plotted as positive quantities while the real parts are plotted as negative quantities. It is clear from this figure that the range of frequencies where μ is real (propagation bands for waves 1 and 2) coincide with the results obtained in Section 3.4.2, figure (3.17). Outside this range the real parts of μ are either zero or $\pm\pi$, while the imaginary parts are non-zero. Waves corresponding to these values of μ will attenuate at a rate depending on the values of the imaginary parts of μ (the amplitude of the wave will attenuate by a factor $e^{-\mu_i}$ from one cell to the next). Wave 3 has a large imaginary part within the plotted frequency range and hence it is a heavily attenuated wave.

For waves travelling normal to the diagonal of the cell (a direction making 45^o to the x axis), we can write

$$\mu_x = \mu_y$$

and hence relation (3.45) can be written as

$$\mu_x = \mu_1 = \mu$$

$$\mu_y = \mu_2 = \mu$$

and the eigenvalue problem (3.47) will be of the form

$$([A_4]\lambda^4 + [A_3]\lambda^3 + [A_2]\lambda^2 + [A_1]\lambda + [A_o])\{q\} = 0.$$

However since there are no degrees of freedom at the corners of the cell in this case we will find that the matrices $[A_4]$ and $[A_3]$ are zero.

Figure (3.38) shows six possible waves that can exist at any frequency (numbered 1 to 6 in the figure). The propagation constants for waves 1 and 2 are purely real within some frequency bands (propagation bands). These bands coincide with those produced in figure (3.17) outside these bands the imaginary parts of μ are non-zero and hence waves 1 and 2 will attenuate at these frequencies. The propagation constants corresponding to waves 3, 4, 5 and 6 have non-zero imaginary parts and hence they represent attenuating waves.

Figures (3.39) and (3.40) show similar results for the plate with rectangular cells ($\ell_x = 1.0$, $\ell_y = 2.0$). This is the second example used in Section (3.4.2). These graphs correspond to waves travelling along the x direction and the preferred direction of propagation (a direction making an angle 26.56° to the x axis in this case). In figure (3.39) three waves are shown (numbered 1, 2 and 3), while in figure (3.40) six waves are shown (numbered 1 to 6). Similar to the previous example, within the range of frequencies where the propagation constants for some of these waves are real quantities (propagation bands) coincide with those produced in Section 3.4.2, figure (3.25).

b. Stringer stiffened flat plate.

This example was used in Section 3.4.6, figure (3.12a). The same finite element idealisation for the cell is used here. This is shown in figure (3.12b). Figure (3.41) shows the variation of the complex propagation constants with frequency for waves travelling along the preferred direction of propagation (a direction making an angle 26.56° to the x axis, $\mu_x = \mu_y = \mu$). The transverse displacements at the stiffeners were considered equal to zero (due to the high transverse rigidity of the stiffeners). Four possible waves are shown in figure (3.41) (numbered 1 to 4). Here again it is clear that the range of frequencies where the propagation constants μ are real quantities (propagation bands for waves 1 and 2) coincide with the results obtained in Section 3.4.6, figure (3.35).

3.6 Natural Frequencies of a Single Two-dimensional Periodic Cell

If the single cell of a two-dimensional periodic system is symmetrical (about two planes through its centre and parallel to its sides) and having only one type of degree of freedom coupling it to its neighbouring cells on opposite sides, then its natural frequencies, while some or all of the boundary degrees of freedom are constrained or unconstrained, can be associated with the frequencies of propagation corresponding to wave-numbers (or propagation constants) given by

$$a_x = 0.0, \quad \mu_x = 0.0$$

or

$$a_x = \pm \frac{1}{2\ell_x}, \quad \mu_x = \pm\pi$$

and

$$a_y = 0.0, \quad \mu_y = 0.0$$

or

$$a_y = \pm \frac{1}{2\ell_y}, \quad \mu_y = \pm\pi$$

where a_x, a_y, μ_x, μ_y and ℓ_x, ℓ_y are the components of the wave-number, the propagation constants and the dimensions of the cell along the two directions x and y defining the system, figure (3.6).

To prove this, consider the transverse wave-motion in two-dimensional plates resting on orthogonal, equally spaced line supports as shown in figure (3.6). This is the illustrative example used in Section 3.4.2. This example is chosen to simplify the proof (since there are no degrees of freedom at the corners of the cell in this case). However, the same procedure can be carried out for other cases.

Now consider a single cell, figure (3.6b), vibrating freely. The degrees of freedom at the left and right boundaries ($\{q_L\}$ and $\{q_R\}$) are the rotation θ_y, while at the bottom and top boundaries ($\{q_B\}$ and $\{q_T\}$) only θ_x exist. No degrees of freedom exist at the corners of the cell ($\{q_{LB}\} = \{q_{LT}\} = \{q_{RB}\} = \{q_{RT}\} = 0$). The linear equation of motion of the undamped cell is given by

$$([K] - \omega^2[M])\{q\} = 0 \qquad (3.48)$$

where $[K]$ and $[M]$ are the stiffness and inertia matrices for the cell ,

$\{q\}$ is a vector of generalised degrees of freedom in the cell.

These matrices can be partitioned according to the interior, left, right, bottom and top degrees of freedom in the cell. Hence

$$[K] = \begin{bmatrix} K_{I,I} & & & & \\ K_{L,I} & K_{L,L} & \text{symmetric} & & \\ K_{R,I} & K_{R,L} & K_{R,R} & & \\ K_{B,I} & K_{B,L} & K_{B,R} & K_{B,B} & \\ K_{T,I} & K_{T,L} & K_{T,R} & K_{T,B} & \end{bmatrix} \quad ; \quad \{q\} = \begin{Bmatrix} q_I \\ q_L \\ q_R \\ q_B \\ q_T \end{Bmatrix} \tag{3.49}$$

A similar expression can be written for the matrix $[M]$.

Let N_I, N_L, N_R, N_B and N_T be the number of degrees of freedom at the interior, left, right, bottom and top of the cell (notice that $N_L = N_R$ and $N_B = N_T$ due to symmetry). Since the cell is symmetrical then its normal modes of vibration will be either symmetrical or anti-symmetrical about lines through the cell's centre and parallel to the x and y axis. Four possible combinations of symmetry can exist. For each symmetry condition, the degrees of freedom $\{q_L\}$, $\{q_R\}$, $\{q_B\}$ and $\{q_T\}$ can be related to each other as given in table 3.2 (notice that these degrees of freedom are rotations only).

	symmetry about centre line parallel to the x axis	symmetry about centre line parallel to the y axis
1	Symmetric $\{q_B\} = -\{q_T\}$	Symmetric $\{q_L\} = -\{q_R\}$
2	Symmetric $\{q_B\} = -\{q_T\}$	Anti-symmetric $\{q_L\} = \{q_R\}$
3	Anti-symmetric $\{q_B\} = \{q_T\}$	Anti-symmetric $\{q_L\} = \{q_R\}$
4	Anti-symmetric $\{q_B\} = \{q_T\}$	Symmetric $\{q_L\} = -\{q_R\}$

Table 3.2

Relation between the degrees of freedom on the boundaries of a simply supported rectangular plate in free vibration (figure(3.6B)).

Now the first relations in table (3.2), that is

$$\{q_B\} = -\{q_T\} \quad \text{and} \quad \{q_L\} = -\{q_R\}$$

can be used to eliminate $\{q_T\}$ and $\{q_R\}$ from equation (3.48). This will give an equation of the form

$$\left([\bar{K}] - \omega^2[\bar{M}]\right) \begin{Bmatrix} q_I \\ q_L \\ q_B \end{Bmatrix} = 0 \qquad (3.50)$$

where

$$[\bar{K}] = [W]^T[K][W] \ , \qquad [\bar{M}] = [W]^T[M][W] \qquad (3.51)$$

$[W]$ is a transformation matrix given by

$$[W] = \left[\begin{array}{c|c|c} I & 0 & 0 \\ \hline 0 & I & 0 \\ \hline 0 & -1 \nearrow\searrow & 0 \\ \hline 0 & 0 & I \\ \hline 0 & 0 & -1 \nearrow\searrow \end{array}\right]$$

It is clear that the matrices $[\bar{K}]$ and $[\bar{M}]$ are of the same form as $[\bar{K}]$ and $[\bar{M}]$ in equation (3.19) when substituting $\mu_1 = \mu_2 = \pi$ (notice that there are no degrees of freedom at the corners of the cell and hence the rows and columns corresponding to $\{q_{LB}\}$ in equation (3.19) are eliminated).

Similarly we can use the second, third or fourth relations in table 3.2 to eliminate $\{q_R\}$ and $\{q_T\}$ from equation (3.48). In each case we will obtain an eigenvalue problem similar to (3.50) where the matrices $[\bar{K}]$ and $[\bar{M}]$ will be the same as the matrices obtained in equations (3.19) when substituting the following values for the propagation constants μ_1 and μ_2

(i) $\mu_1 = -\pi, \quad \mu_2 = 0.0$

(ii) $\mu_1 = 0.0, \quad \mu_2 = -\pi$

(iii) $\mu_1 = 0.0, \quad \mu_2 = 0.0$

The eigenvalue problem (3.50) is of order $N_I + N_L + N_B$. Its solution gives all the eigenvalues and eigenvectors satisfying the condition

$$\{q_B\} = -\{q_T\} \quad \text{and} \quad \{q_L\} = -\{q_R\}$$

However it should be noticed that

$$\{q_B\} = -\{q_T\} = 0.0 \quad \text{and/or} \quad \{q_L\} = -\{q_R\} = 0.0$$

are other possible solutions to (3.50).

Similar conclusions can be drawn for the other eigenvalue problems obtained from equation (3.48) when substituting the second, third and fourth relations in table 3.2. Each of these eigenvalue problems is of order $N_I + N_L + N_B$ and hence solving these four eigenvalue problems gives $4(N_I + N_L + N_B)$ eigenvalues and eigenvectors. However, the original equation (3.48) has only $N_I + N_L + N_R + N_B + N_T$ or $N_I + 2N_L + 2N_B$ (since $N_R = N_L$ and $N_T = N_B$) eigenvalues and eigenvectors which are all the possible solutions such that

$$\{q_L\} = \pm\{q_R\} \neq 0.0 \quad \text{and} \quad \{q_B\} = \pm\{q_T\} \neq 0.0$$

Therefore all the other eigenvalues and eigenvectors obtained by solving the four eigenvalue problems mentioned above $(4(N_I + N_L + N_B) - N_I + 2N_L + 2N_B))$ must be solutions satisfying the conditions

$$\{q_L\} = \pm\{q_R\} = 0.0 \quad \text{and/or} \quad \{q_B\} = \pm\{q_T\} = 0.0 \ .$$

From the above discussion it can be concluded that the natural frequencies of the single cell, while one of the conditions

$$\begin{aligned}
&\text{(i)} \quad \{q_L\} = \pm\{q_R\} \neq 0.0 \quad \text{and} \quad \{q_B\} = \pm\{q_T\} \neq 0.0 \\
&\text{(ii)} \quad \{q_L\} = \pm\{q_R\} = 0.0 \quad \text{and} \quad \{q_B\} = \pm\{q_T\} \neq 0.0 \\
&\text{(iii)} \quad \{q_L\} = \pm\{q_R\} \neq 0.0 \quad \text{and} \quad \{q_B\} = \pm\{q_T\} = 0.0 \\
&\text{(iv)} \quad \{q_L\} = \pm\{q_R\} = 0.0 \quad \text{and} \quad \{q_B\} = \pm\{q_T\} = 0.0
\end{aligned} \tag{3.52}$$

is satisfied coincide with the frequencies of propagation corresponding to values of the propagation constants μ_1 and μ_2 equal to zero or $\pm\pi$ (or wave-numbers a_x and a_y equal to zero or $\pm 1/2\ell_x$ and $\pm 1/2\ell_y$).

Tables 3.3 and 3.4 show the propagation frequencies for the plate with square cells ($\ell_x = \ell_y = 1.0$) and rectangular cells ($\ell_x = 1.0$, $\ell_y = 2.0$) corresponding to values of μ_x and μ_y equal to zero or $\pm\pi$

and the boundary condition imposed on the cell such that one of its natural frequencies coincides with that propagation frequency. This is shown for the first three propagation bands. Also shown in the tables are the values of the natural frequencies obtained using Warburton's expressions [61] for comparison.

3.7 Natural Frequencies of Finite Two-dimensional Periodic Systems

In this section we will show that the natural frequencies of finite two-dimensional periodic structures, where each period (cell) is symmetrical (about two planes through its centre and parallel to its sides) and coupled to its neighbours on opposite sides by one type of degree of freedom only, can be obtained from the propagation constants/frequency curves.

Following the same proof given in Section 2.7 for one-dimensional finite periodic systems, consider the case of two-dimensional periodic plates resting on equally spaced orthogonal line supports. As explained in the previous section, if we choose a single cell of dimensions ℓ_x, ℓ_y (distances between the line supports) as one period of the infinite plate, then frequencies corresponding to values of the propagation constants μ_x and μ_y, or wave-numbers a_x and a_y, given by

$$\begin{aligned} &\mu_x = 0.0, && a_x = 0.0 \\ \text{or} \quad &\mu_x = \pm\pi, && a_x = \pm 1/2\ell_x \\ \text{and} \quad & && \qquad (3.53) \\ &\mu_y = 0.0, && a_y = 0.0 \\ \text{or} \quad &\mu_y = \pm\pi, && a_y = \pm 1/2\ell_y \end{aligned}$$

will coincide with the natural frequencies of the chosen period with its coupling degrees of freedom satisfying one of the conditions given by (3.52). Now if we choose the period representing the infinite system as a plate consisting of N_1 cells along the x direction and N_2 cells along the y direction then, according to the discussion given in the previous section, the natural frequencies of this period with its coupling degrees of freedom ($\{q_L\}$, $\{q_R\}$, $\{q_B\}$ and $\{q_T\}$) satisfying one of the conditions

given by (3.52) will coincide with the frequencies of propagation corresponding to wave-numbers given by

$$\begin{aligned} a_x' &= 0.0 \\ \text{or} \quad a_x' &= \pm\, 1/2N_1\ell_x \\ \text{and} \quad a_y' &= 0.0 \\ \text{or} \quad a_y' &= \pm\, 1/2N_2\ell_y \end{aligned} \tag{3.54}$$

where $N_1\ell_x$ and $N_2\ell_y$ are the dimensions of the chosen period representing the system (periodic lengths). Since the frequency of propagation is a periodic function of the wave-number components a_x' and a_y' with periods $1/N_1\ell_x$ and $1/N_2\ell_y$ then (3.54) can be written as

$$\begin{aligned} a_x' &= \pm\, \frac{m_1}{2N_1\ell_x} \quad , \\ a_y' &= \pm\, \frac{m_2}{2N_2\ell_y} \end{aligned} \tag{3.55}$$

$$(m_1, m_2 = 0, 1, 2, \ldots.)$$

Regardless of the choice of the period representing the infinite system, the wave-number/frequency variation must be the same for the same values of the wave-number since such variation is a characteristic of the periodic system and does not depend on the choice of the period. Therefore, frequencies corresponding to values of the wave-number components a_x and a_y (when choosing one cell only representing the system) equal to a_x' and a_y' given by (3.55), i.e.,

$$\begin{aligned} a_x &= \pm\, \frac{m_1}{2N_1\ell_x} \qquad (m_1 = 0, 1, 2 \ldots N_1), \\ a_y &= \pm\, \frac{m_2}{2N_2\ell_y} \qquad (m_2 = 0, 1, 2 \ldots N_2) \end{aligned} \tag{3.56}$$

or propagation constants

$$\begin{aligned} \mu_x &= \pm\, \frac{m_1\pi}{N_1} \quad , \\ \mu_y &= \pm\, \frac{m_2\pi}{N_2} \end{aligned} \tag{3.57}$$

(since $\mu_x = -2\pi a_x\ell_x$ and $\mu_y = -2\pi a_y\ell_y$)

are indeed the natural frequencies of the $N_1 \times N_2$ cell period with its boundary degrees of freedom ($\{q_L\}$, $\{q_R\}$, $\{q_B\}$ and $\{q_T\}$) satisfying one of the conditions given by (3.52).

Similar to the one-dimensional case, the choice of $N_1 \times N_2$ cells as one period of the system will result in sub-zones and sub-bands. The first sub-zone is given by

$$\begin{aligned} -\frac{1}{2N_1\ell_x} \leq a'_x \leq \frac{1}{2N_1\ell_x} \quad , \\ -\frac{1}{2N_2\ell_y} \leq a'_y \leq \frac{1}{2N_2\ell_y} \end{aligned} \tag{3.58}$$

while if we choose one cell only of dimensions ℓ_x, ℓ_y as the period representing the system will result in zones and propagation bands. The first zone is given by

$$\begin{aligned} -\frac{1}{2\ell_x} \leq a_x \leq \frac{1}{2\ell_x} \quad , \\ -\frac{1}{2\ell_y} \leq a_y \leq \frac{1}{2\ell_y} \end{aligned} \tag{3.59}$$

Sub-bands corresponding to (3.58) will construct the bands corresponding to (3.59) in a similar manner as discussed in Section 2.7 for the one-dimensional case.

Inspection of tables 3.3 and 3.4 showing the propagation frequencies corresponding to values of μ_x and μ_y equal to zero or π and the boundary conditions imposed on the period representing the system such that one of its natural frequencies coincides with that propagation frequency, and also inspection of the various wave-forms corresponding to different values of μ_x and μ_y (some of these wave-forms are shown in figures (3.19) to (3.22) and (3.27) to (3.30)). It is found (without proof) that the values of m_1 and m_2 in relation (3.57) can be chosen as given in table 3.5 to calculate the natural frequencies corresponding to the various boundary conditions given by (3.52). This table is for the cases of periodic plates with square cells and rectangular cells ($\ell_x/\ell_y = 0.5$). Tables 3.6 and 3.7 give the variation of the frequency of propagation with the propagation constants μ_x and μ_y, within the first propagation band, for the above two cases. The natural frequencies of finite periodic plates

can be calculated either from these tables or graphically from the propagation constants/frequency surfaces. (The figures in these tables are calculated by idealising a single cell by 25 plate elements of the type given in Appendix D5). The values of m_1 and m_2 in table 3.5 havebeen checked by calculating the natural frequencies of some finite periodic plates (2 x 2 cells and 5 x 5 cells) with various boundary conditions as given by (3.52). In each case the finite periodic plate is idealised by a finite element model and the natural frequencies are calculated using standard eigenvalue routines. The calculated natural frequencies coincided with the frequencies of propagation corresponding to values of μ_x and μ_y given by (3.57) when substituting values of m_1 and m_2 as given in table 3.5.

μ_x \ μ_y	0	0.2π	0.4π	0.6π	0.8π	π
0	0.0 0.0					
0.2π	0.39478 0.39478	0.79038 0.7896				
0.4π	1.5791 1.5791	1.9772 1.9739	3.1713 3.1583			
0.6π	3.5532 3.5531	3.9552 3.9478	5.1615 5.1322	7.1723 7.1061		
0.8π	6.3173 6.3165	6.7249 6.7113	7.9481 7.8957	9.9875 9.8696	12.843 12.633	
π	9.8724 9.8696	10.287 10.264	11.532 11.449	13.608 13.423	16.515 16.186	20.255 19.739

Table 3.1 Comparison between finite element results and the exact solution of the propagation constants/ frequency variation for the transverse wave motion in an infinite plate.

Upper figures: Finite element solution

Lower figures: Exact solution

μ_x, μ_y	First propagation band	Second propagation band	Third propagation band
0, 0	37.437 37.073 36.468 36.133 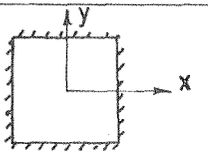	58.095 57.088 55.723 55.065 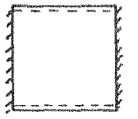	58.095 57.088 55.723 55.065 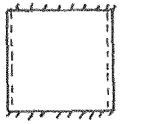
0, π	30.043 29.695 29.252 29.011 	51.574 50.722 49.864 49.348 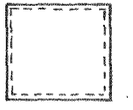	77.453 76.253 74.673 72.205 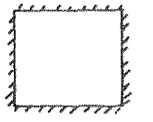
π, 0	30.045 29.695 29.252 29.011 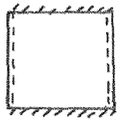	51.574 50.722 49.864 49.348 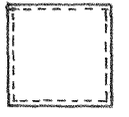	77.453 76.253 74.673 72.205 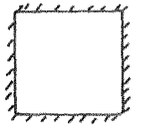
π, π	20.255 20.068 19.867 19.739 	72.652 71.496 70.176 69.354 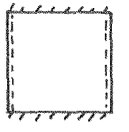	72.652 71.496 70.176 69.354 

Table 3.3 Frequencies of propagation corresponding to values of $\mu_x = 0, \pm\pi$ and $\mu_y = 0, \pm\pi$ for plates with square cells and the boundary condition imposed on the cell such that one of its natural frequencies coincides with that propagation frequency.
Upper figures: finite element results using 16, 25 and 64 elements per cell.
Lower figures: natural frequencies calculated using Warburton's expressions.
=-=-=-simply supported edges; ////// clamped edges.

μ_x, μ_y	First propagation band	Second propagation band	Third propagation band
0, 0	25.402 25.193 24.862 24.663 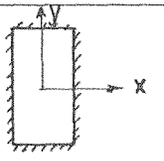	31.402 30.618 29.629 29.011 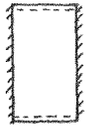	44.158 43.743 43.130 42.813 
0, π	24.321 24.145 23.974 23.832 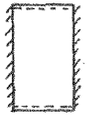	34.646 34.151 32.990 31.969 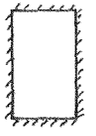	43.064 42.626 40.909 39.259 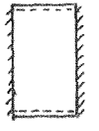
π, 0	14.575 14.349 13.976 13.766 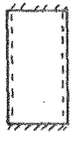	21.713 21.027 20.240 19.739 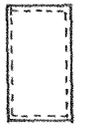	41.646 42.781 40.936 44.987 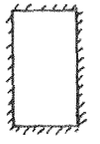
π, π	12.658 12.542 12.417 12.337 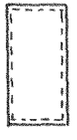	26.113 25.792 24.690 23.709 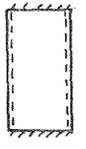	37.460 35.851 33.500 32.076 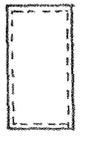

Table 3.4 Frequencies of propagation corresponding to values of $\mu_x = 0, \pm\pi$ and $\mu_y = 0, \pm\pi$ for plates with rectangular cells ($\ell_x/\ell_y = 0.5$) and the boundary condition imposed on the cell such that one of its natural frequencies coincides with that propagation frequency.
Upper figures: finite element results using 16, 25 and 64 elements per cell
Lower figures: natural frequencies calculated using Warburton's expressions.
====== simply supported edges; ~~~~~~~~ clamped edges.

Boundary Condition	First band		Second band		Third band	
	m_1	m_2	m_1	m_2	m_1	m_2
	$1,2...N_1$	$1,2,... N_2$	$0,1,..N_1-1$ $1,2,..N_1$	$1,2,...N_2$ $0,1....N_2-1$	———	———
	$1,2...N_1$	$1,2.... N_2$	$1,2,..N_1$	$0,1,...N_2-1$	$1,2,..N_1$	$1,2,..N_2$
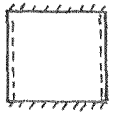	$1,2...N_1$	$0,1....N_2-1$	$1,2...N_1$	$1,2....N_2$	$0,1...N_1-1$	$0,1,..N_2-1$
	$1,2,..N_1$	$0,1....N_2-1$	$1,2...N_1$	$1,2....N_2$	$0,1...N_1-1$	$0,1,..N_2-1$
	$0,1,..N_1-1$	$1,2,...N_2$	$0,1...N_1-1$	$0,1....N_2-1$	$1,2,..N_1$	$1,2,...N_2$
	$0,1,..N_1-1$	$1,2,...N_2$	$0,1...N_1-1$	$0,1....N_2-1$	$0,1...N_1-1$	$1,2,...N_2$
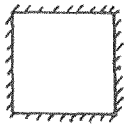	$0,1...N_1-1$	$0,1....N_2-1$	———	———	$0,1...N_1-1$ $1,2,..N_1$	$1,2,...N_2$ $0,1....N_2-1$
	$0,1...N_1-1$	$0,1,...N_2-1$	$0,1...N_1-1$	$1,2,...N_2$	$1,2...N_1$	$0,1,.. N_2-1$

Table 3.5 Values of m_1 and m_2 for the calculation of the natural frequencies of finite periodic plates on simple line supports.
Upper figures for plates with square cells
Lower figures for plates with rectangular cells ($\ell_x/\ell_y = 0.5$).
——— simply supported edge; ———— clamped edges.

μ_x \ μ_y	0.0	0.1π	0.2π	0.3π	0.4π	0.5π	0.6π	0.7π	0.8π	0.9π	π
0.0	36.101										
0.1π	35.832	35.562									
0.2π	34.106	34.830	34.084								
0.3π	34.100	33.816	33.047	31.978				symmetric			
0.4π	32.986	32.693	31.898	30.792	29.563						
0.5π	31.895	31.591	30.769	29.624	28.349	27.088					
0.6π	30.913	30.599	29.751	28.569	27.250	25.942	24.751				
0.7π	30.099	29.777	28.905	27.690	26.332	24.983	23.750	22.712			
0.8π	29.492	29.164	28.274	27.032	25.643	24.261	22.996	21.927	21.117		
0.9π	29.119	28.786	27.884	26.626	25.217	23.814	22.527	21.438	20.612	20.096	
π	28.992	28.658	27.752	26.488	25.073	23.662	22.367	21.272	20.440	19.920	19.743

Table 3.6 Non-dimensional frequencies of propagation for periodic plates with square cells.

μ_x \ μ_y	0.0	0.1π	0.2π	0.3π	0.4π	0.5π	0.6π	0.7π	0.8π	0.9π	π
0.0	24.672	24.644	24.567	24.456	24.329	24.201	24.084	23.987	23.913	23.868	23.853
0.1π	24.263	24.235	24.157	24.045	23.915	23.785	23.666	23.567	23.492	23.446	23.431
0.2π	23.176	23.147	23.066	22.948	22.814	22.678	22.553	22.449	22.371	22.323	22.307
0.3π	21.690	21.659	21.573	21.448	21.305	21.161	21.029	20.918	20.835	20.784	20.767
0.4π	20.045	20.012	19.920	19.787	19.634	19.479	19.338	19.219	19.130	19.076	19.057
0.5π	18.408	18.372	18.273	18.130	17.965	17.799	17.647	17.519	17.424	17.365	17.345
0.6π	16.893	16.854	16.748	16.593	16.416	16.237	16.073	15.936	15.833	15.769	15.747
0.7π	15.592	15.551	15.436	15.270	15.080	14.888	14.712	14.564	14.453	14.384	14.361
0.8π	14.586	14.542	14.420	14.245	14.042	13.838	13.651	13.493	13.375	13.302	13.277
0.9π	13.947	13.901	13.774	13.591	13.380	13.167	12.972	12.807	12.684	12.607	12.581
π	13.727	13.681	13.552	13.366	13.152	12.936	12.737	12.570	12.445	12.367	12.341

Table 3.7 Non-dimensional frequencies of propagation for periodic plates with rectangular cells ($\ell_x/\ell_y = 0.5$)

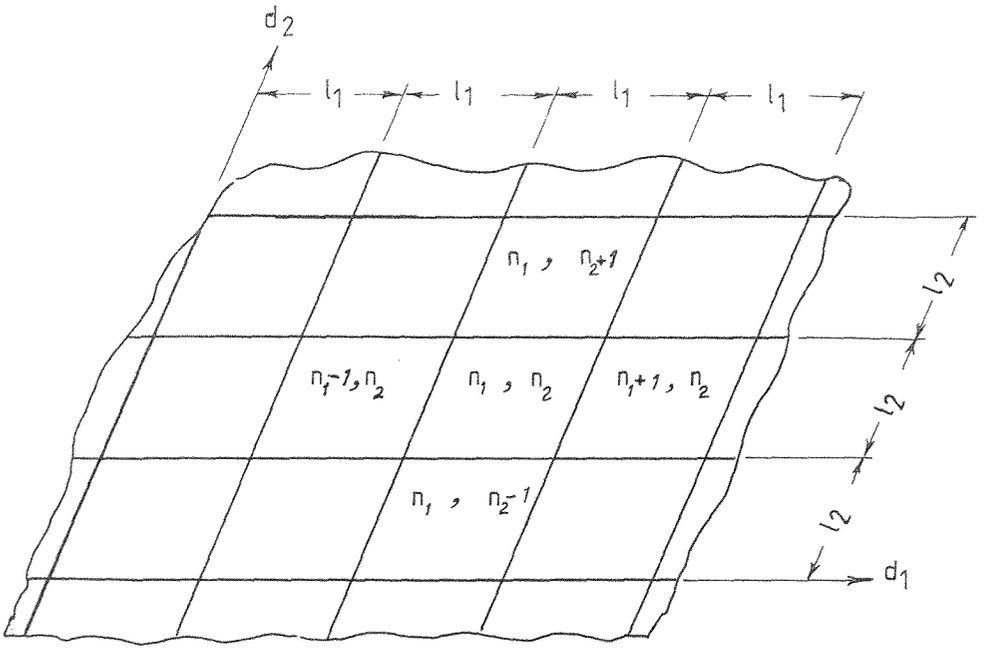

(a)

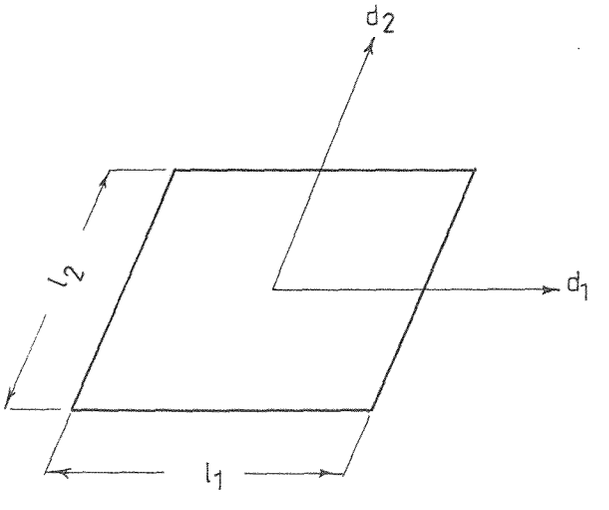

(b)

Figure 3.1.(a) Schematic diagram of part of a two-dimensional periodic system ; (b) single cell representing the system.

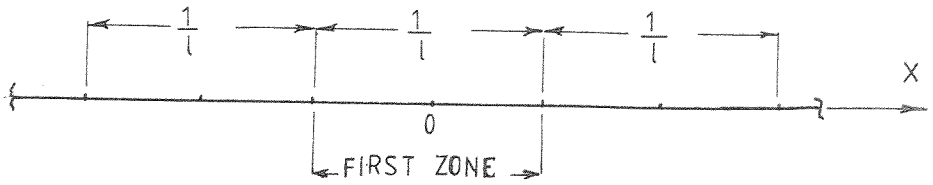

Figure 3.2. Reciprocal cells and first zone for one-dimensional periodic systems.

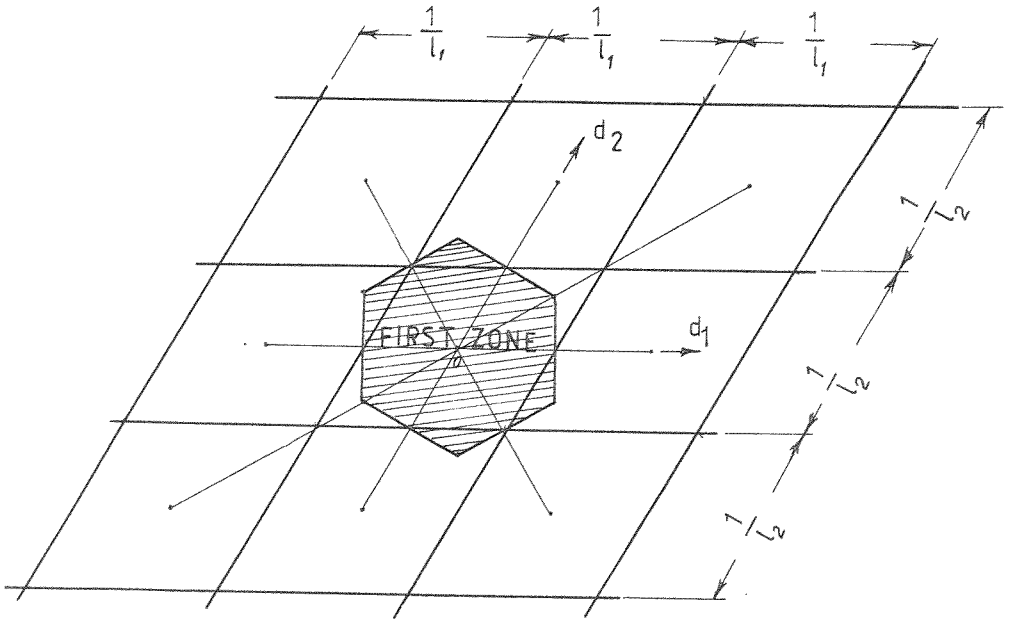

Figure 3.3. Reciprocal system and first zone for the oblique two-dimensional periodic system shown in figure(3.1.).

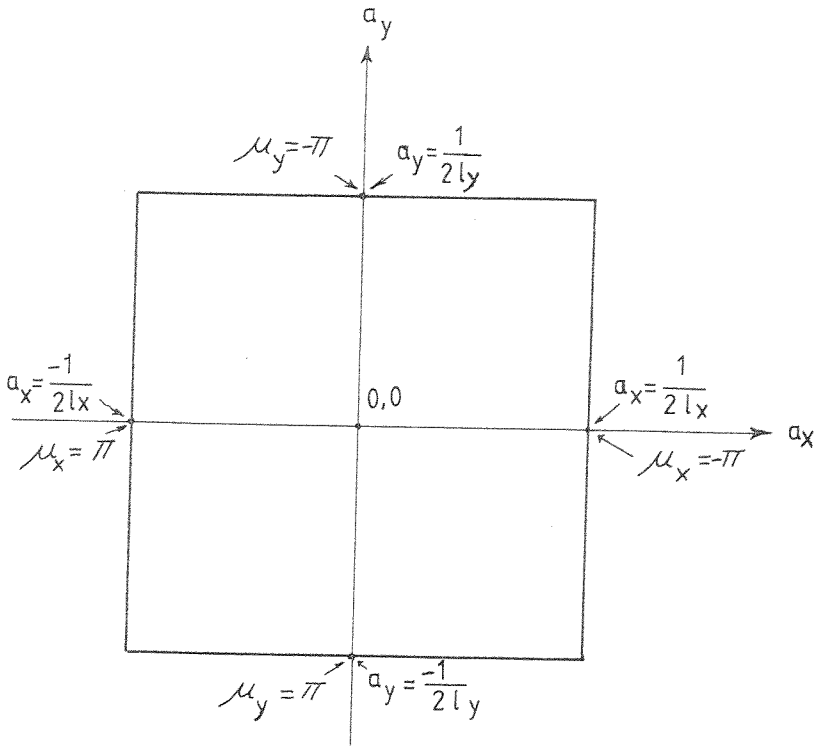

Figure 3.4. First zone for two-dimensional periodic systems with rectangular cells.

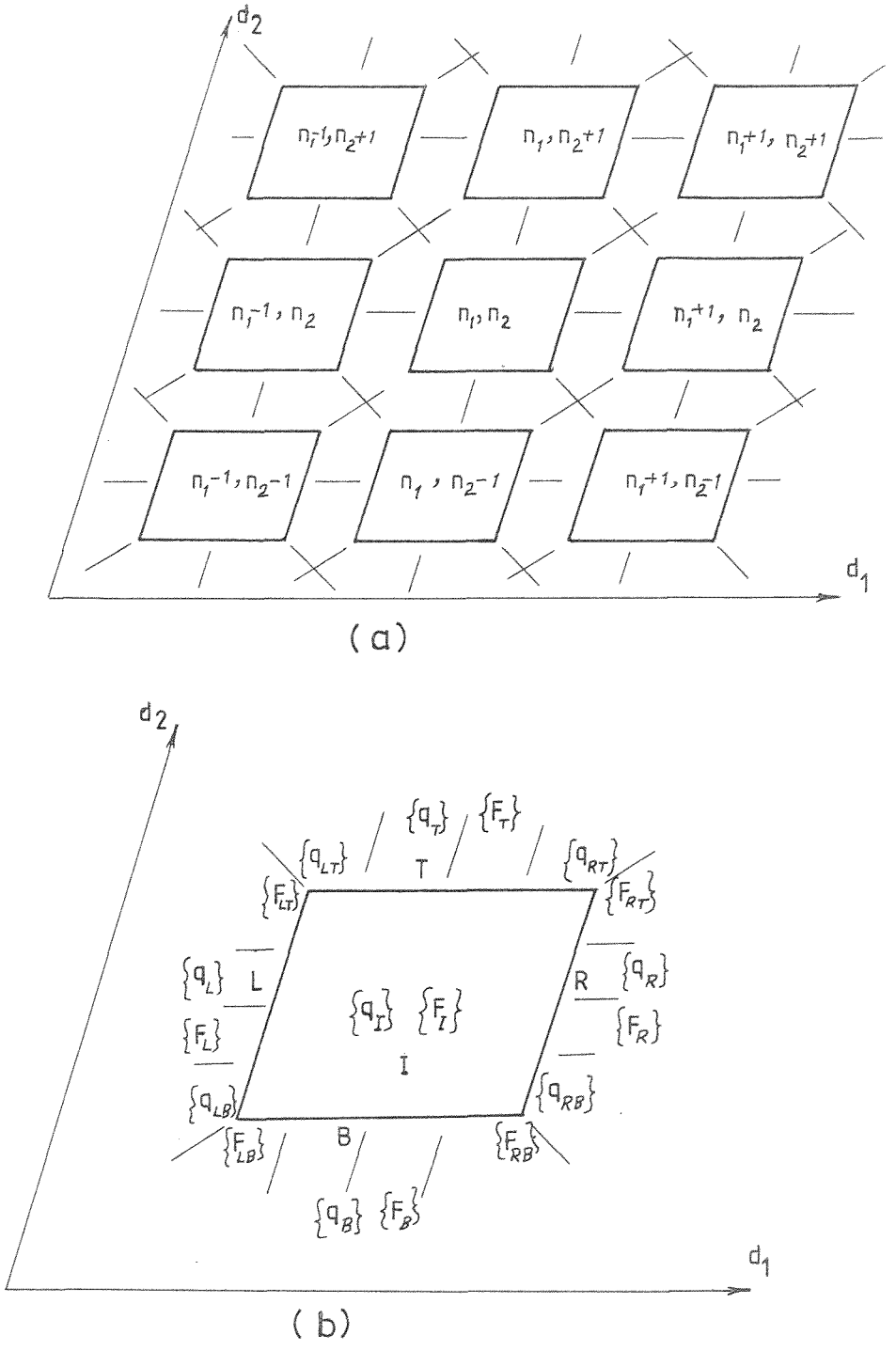

Figure 3.5. (a) Idealisation of a two-dimensional periodic system as an assembly of cells joined together on all sides and corners ;(b)forces on and degrees of freedom of a single cell .

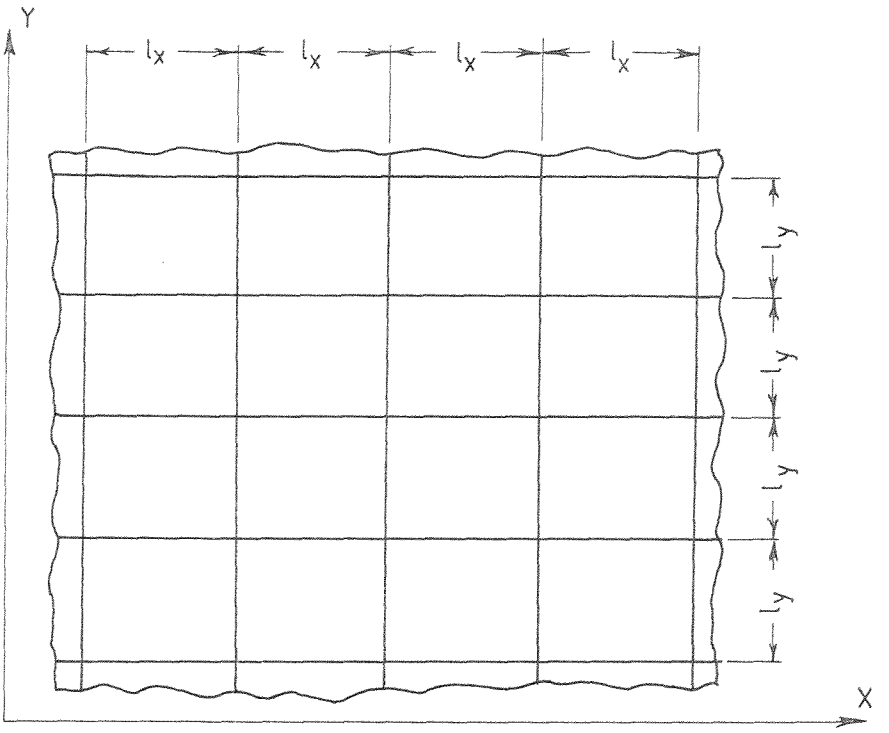

(a)

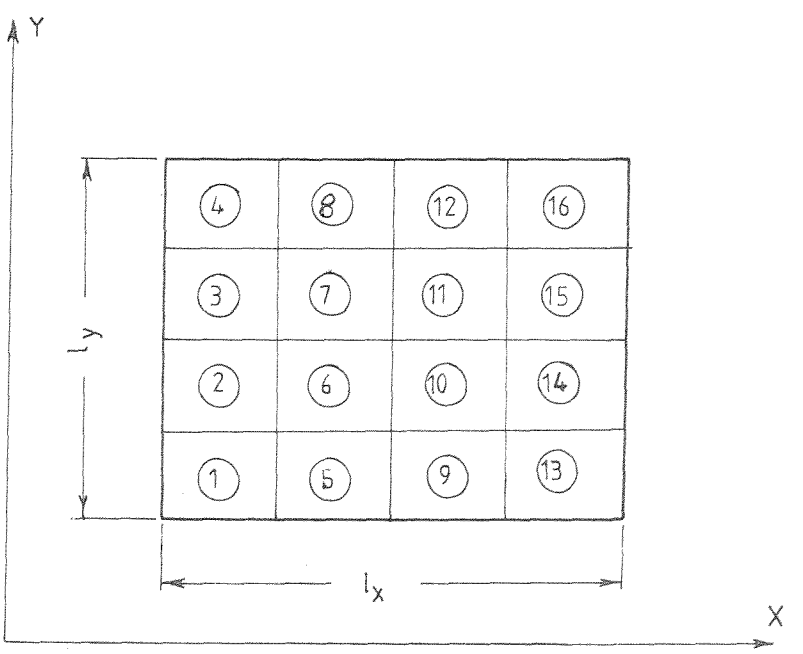

(b)

Figure 3.6. (a) Part of two-dimensional periodic plates on simple orthogonal line supports; (b) finite element idealisation of one cell.

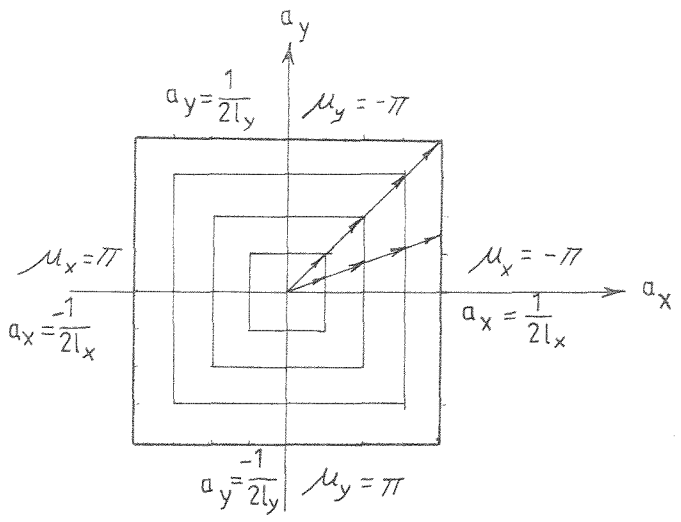

Figure 3.7. Divisions inside the first zone of a two-dimensional periodic system with rectangular cells for polar plotting of the propagation constants-frequency variation.

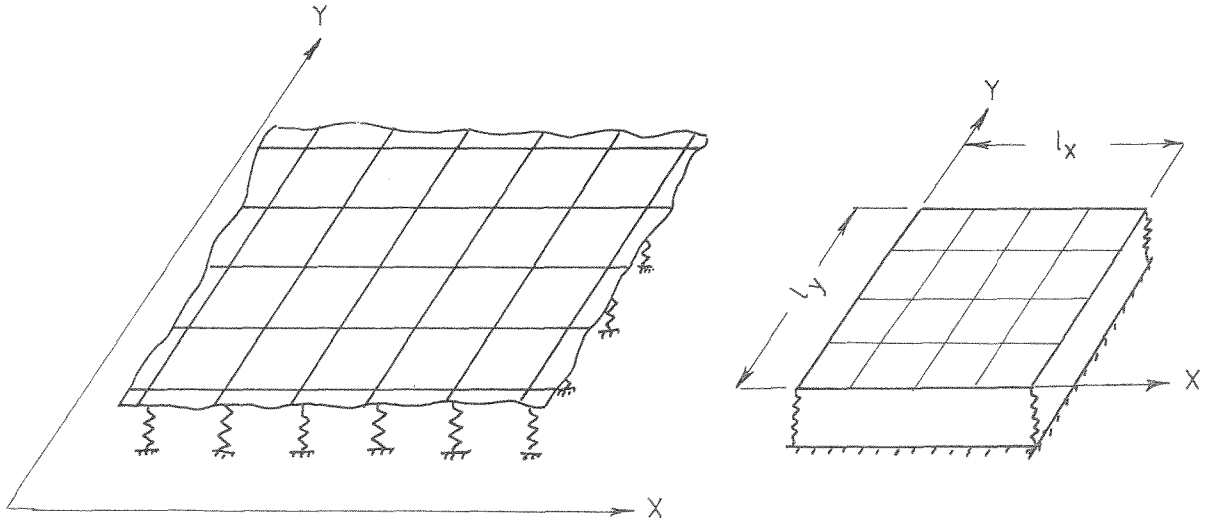

Figure 3.8. (a) Part of two-dimensional periodic plate on orthogonal line spring supports ; (b) finite element idealisation of one cell.

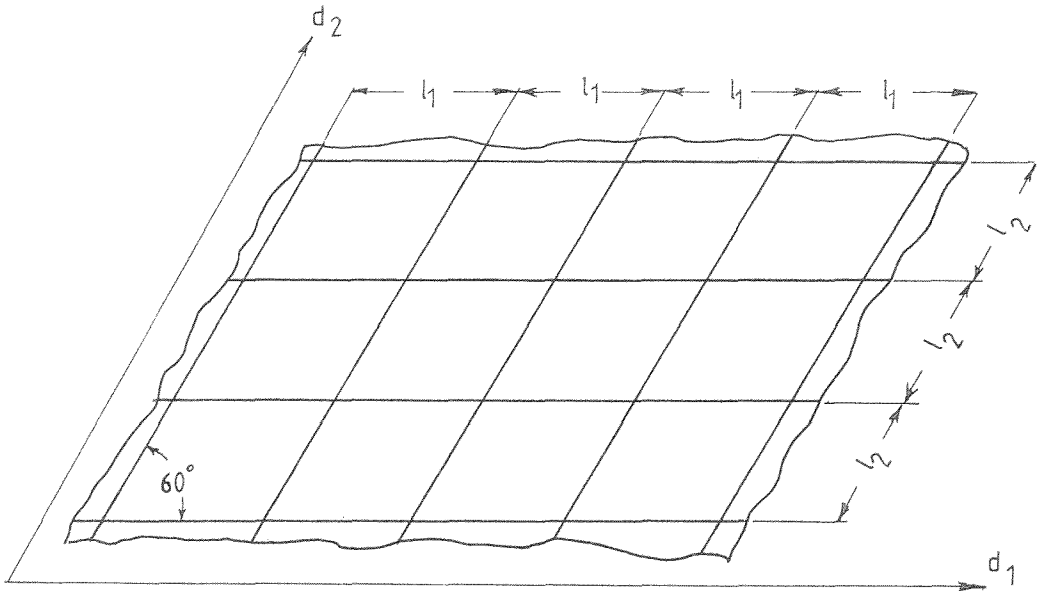

(a)

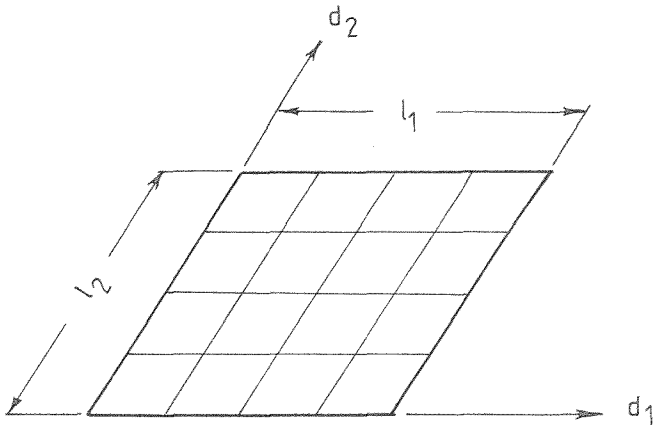

(b)

Figure 3.9. (a) part of two-dimensional periodic plate on oblique simple line supports ; (b) finite element idealisation of one cell.

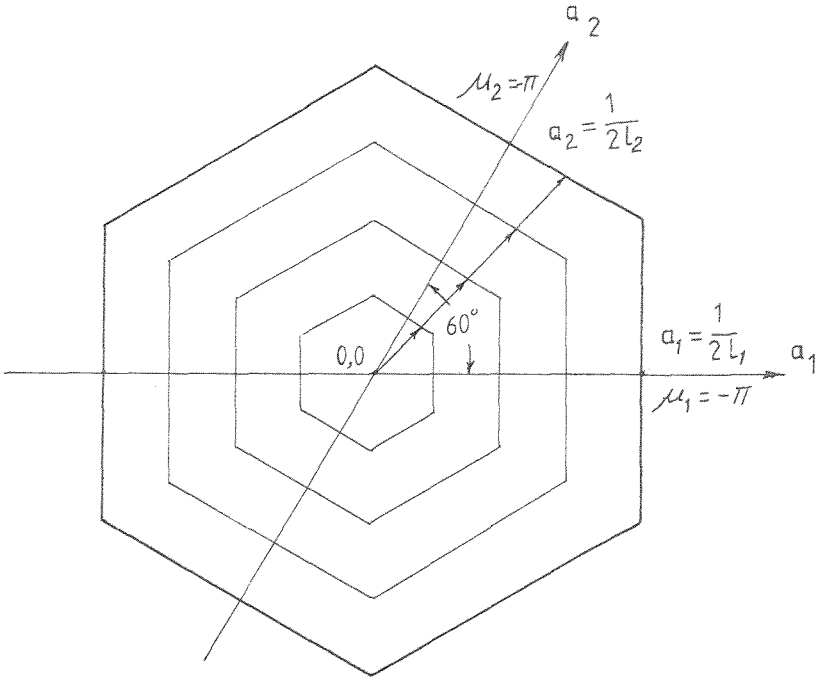

Figure 3.10. Divisions inside the first zone of the two-dimensional periodic system shown in figure (3.9)for polar plotting of the propagation constants-frequency variation.

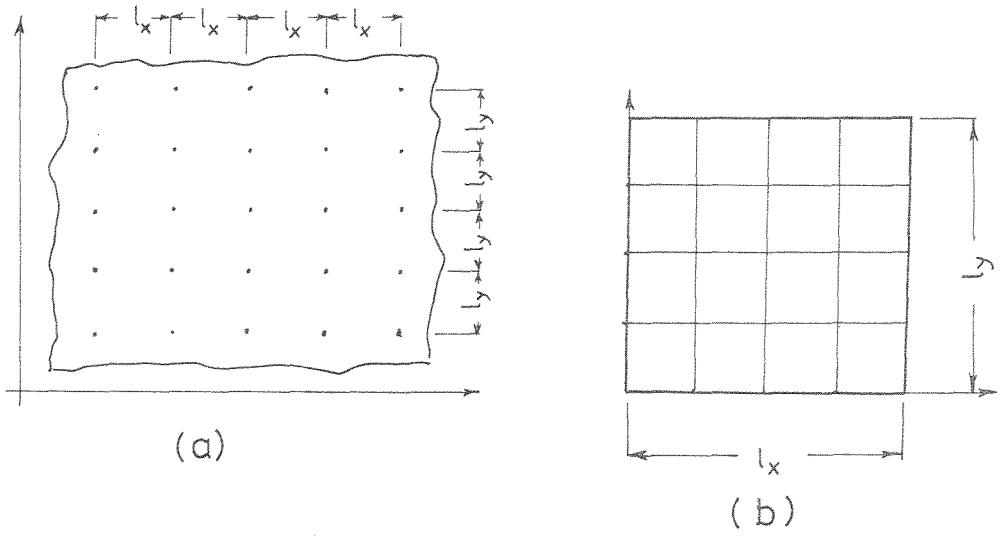

Figure 3.11. (a) Part of a two-dimensional periodic point supported plates ; (b) finite element idealisation of one cell.

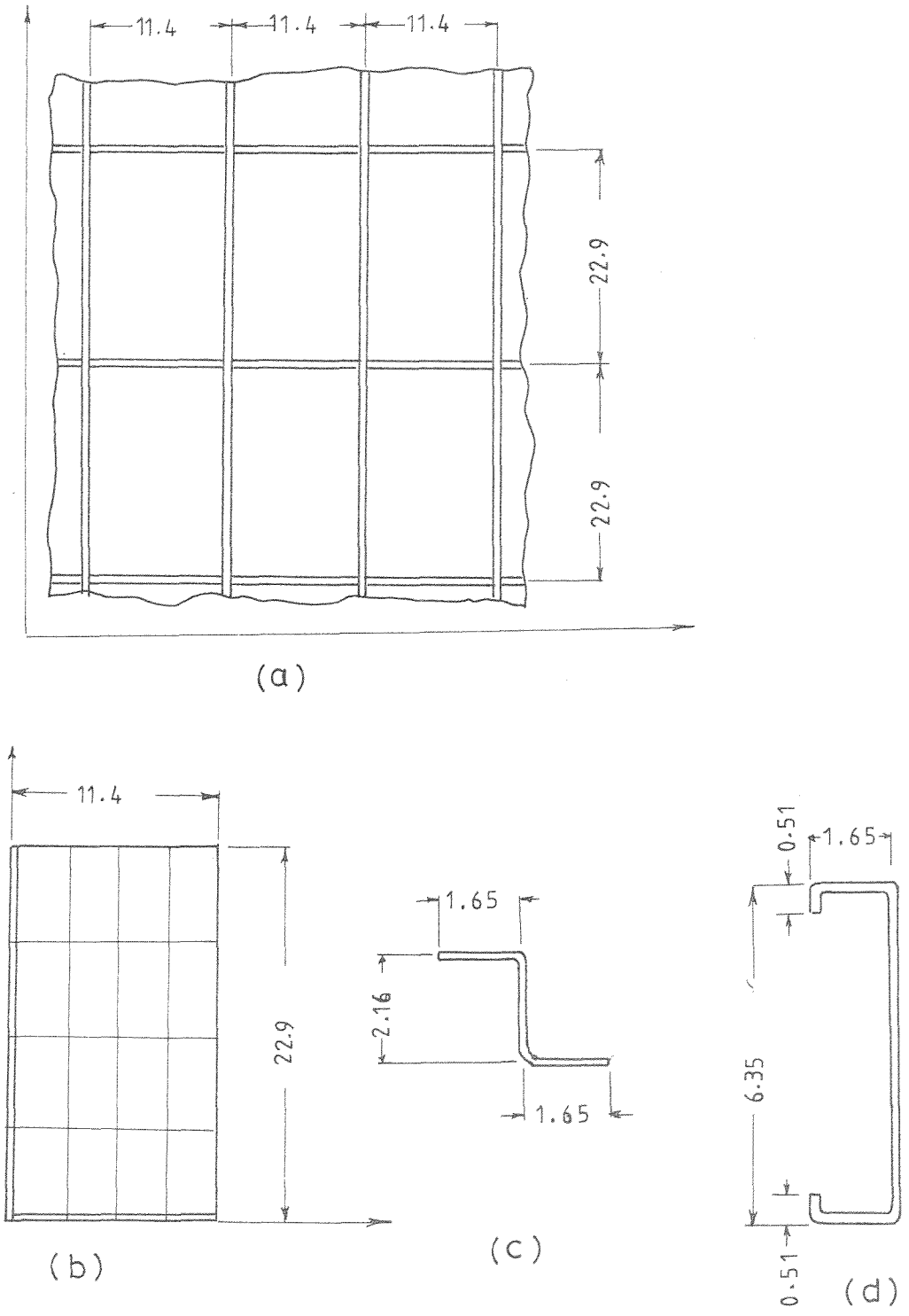

Figure 3.12. (a) Part of a two-dimensional periodically stiffened plate; (b) finite element idealisation of one cell ; (c) stringer cross-section ; (d) frame cross-section. Dimensions in centimeters.

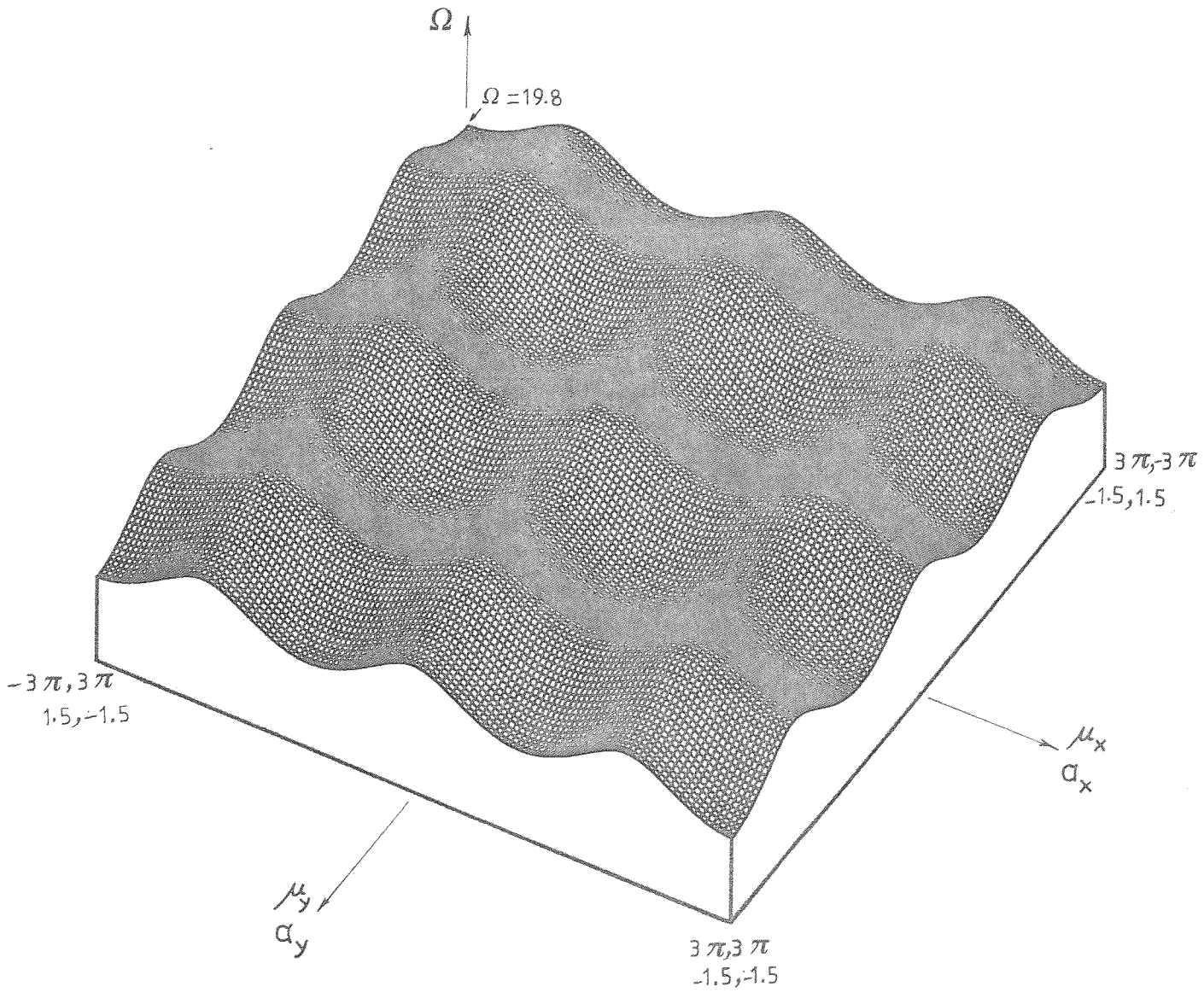

Figure 3.13. Extended first band of the propagation surfaces for a periodic plate on simple line supports with square cells.

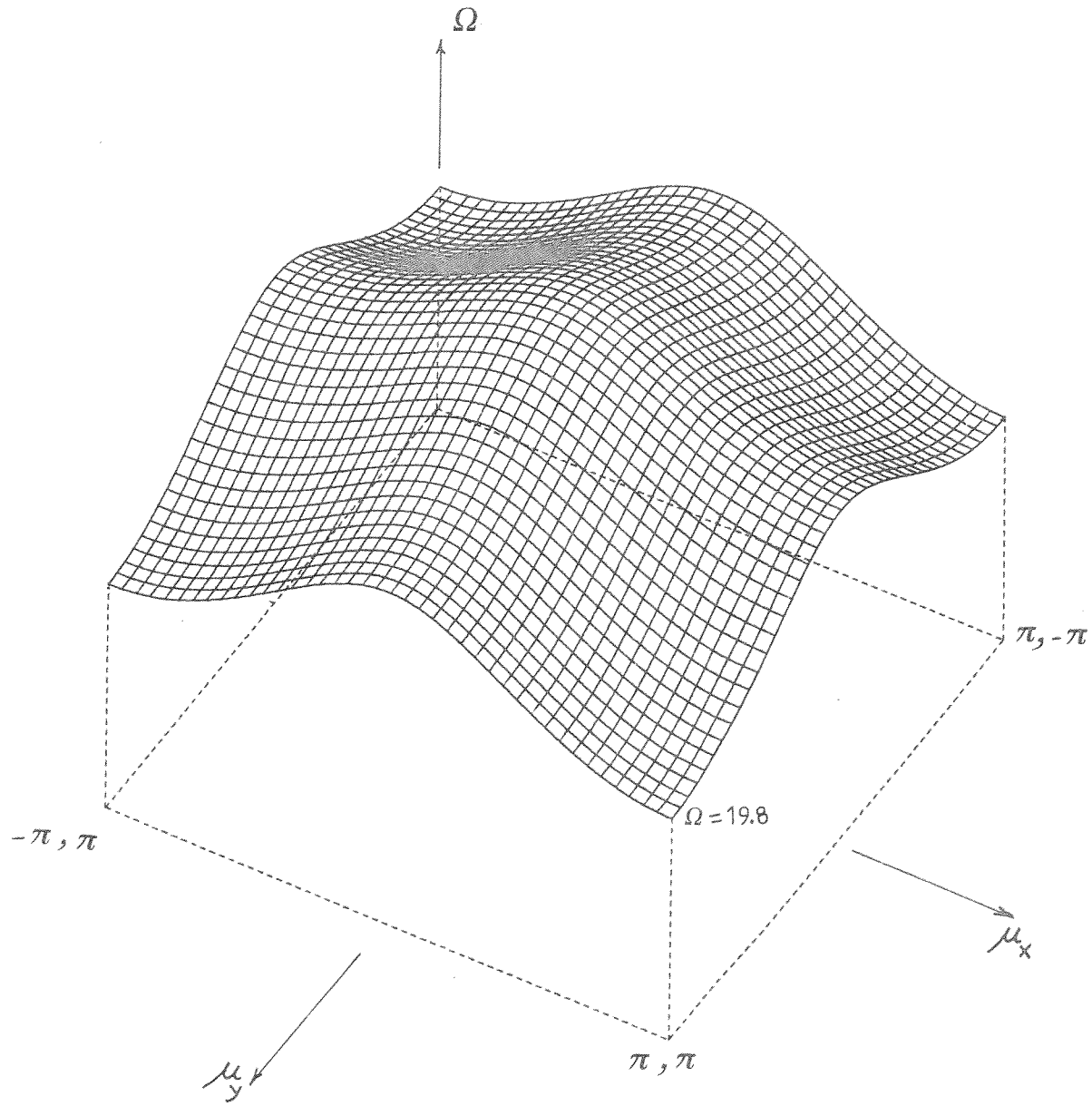

Figure 3.14. First band of the propagation surfaces for a periodic plate on simple line supports with square cells.

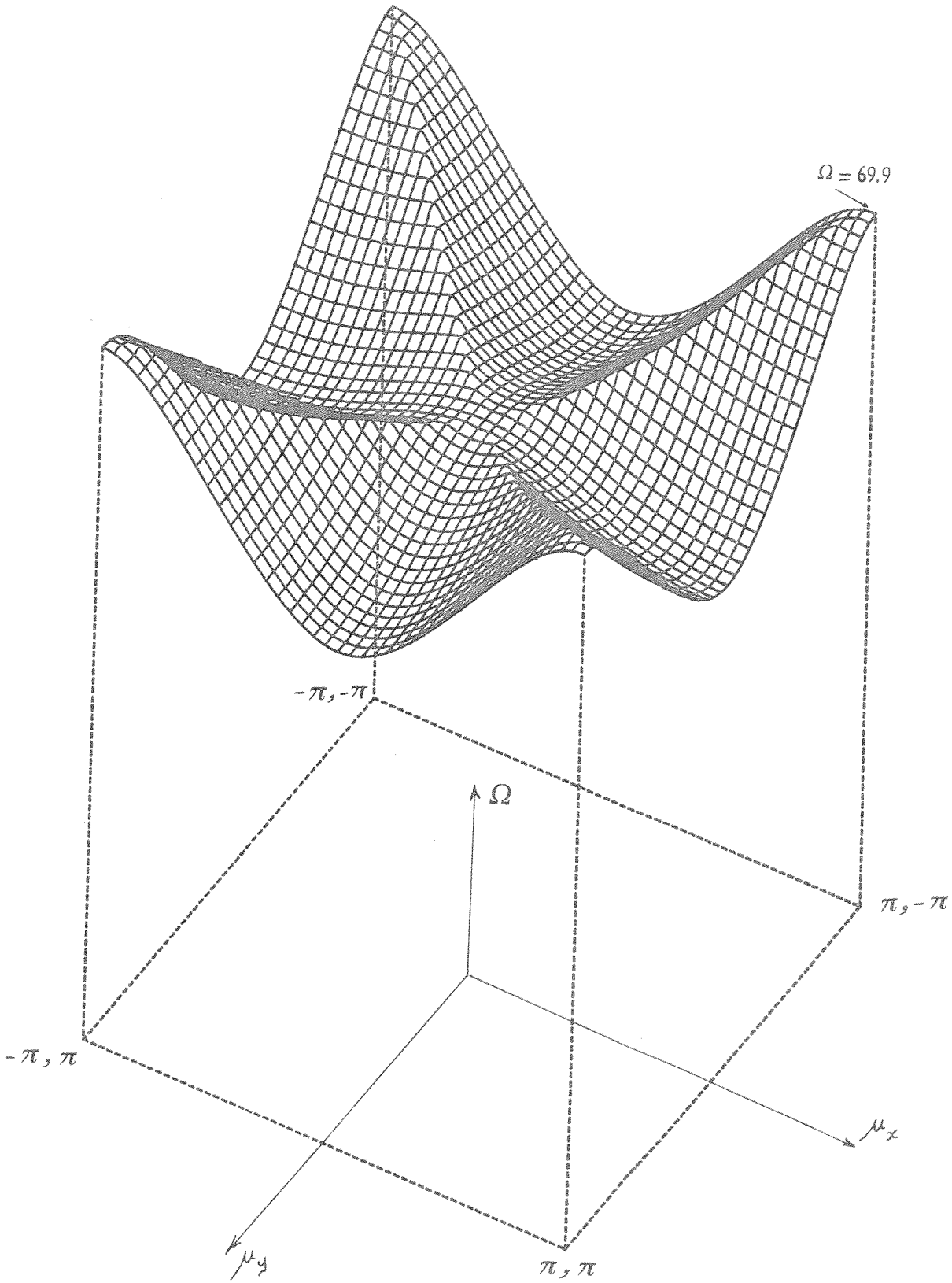

Figure 3.15. Second band of the propagation surfaces for a two-dimensional periodic plate on simple line supports with square cells.

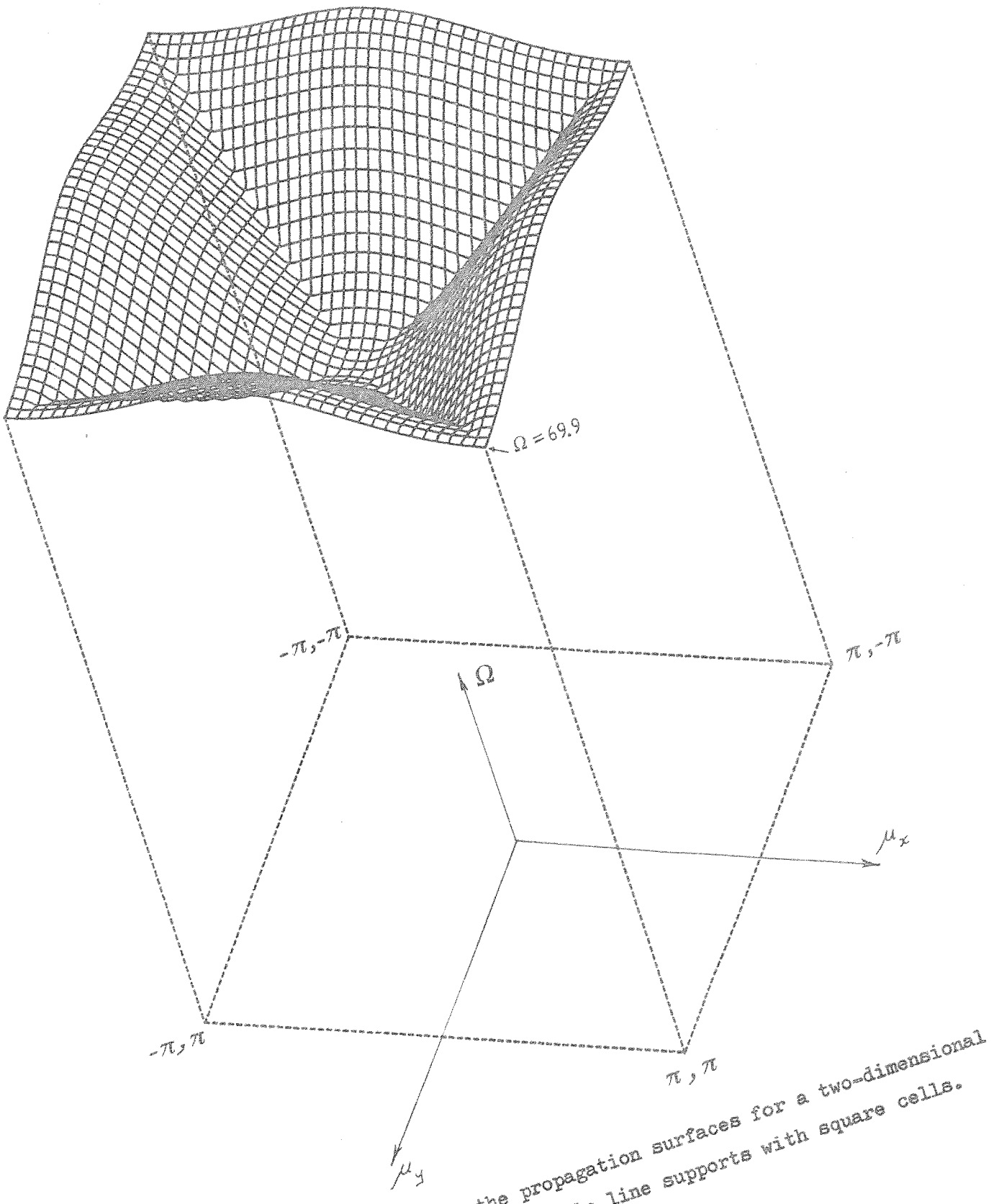

Figure 3.16. Third band of the propagation surfaces for a two-dimensional periodic plate on simple line supports with square cells.

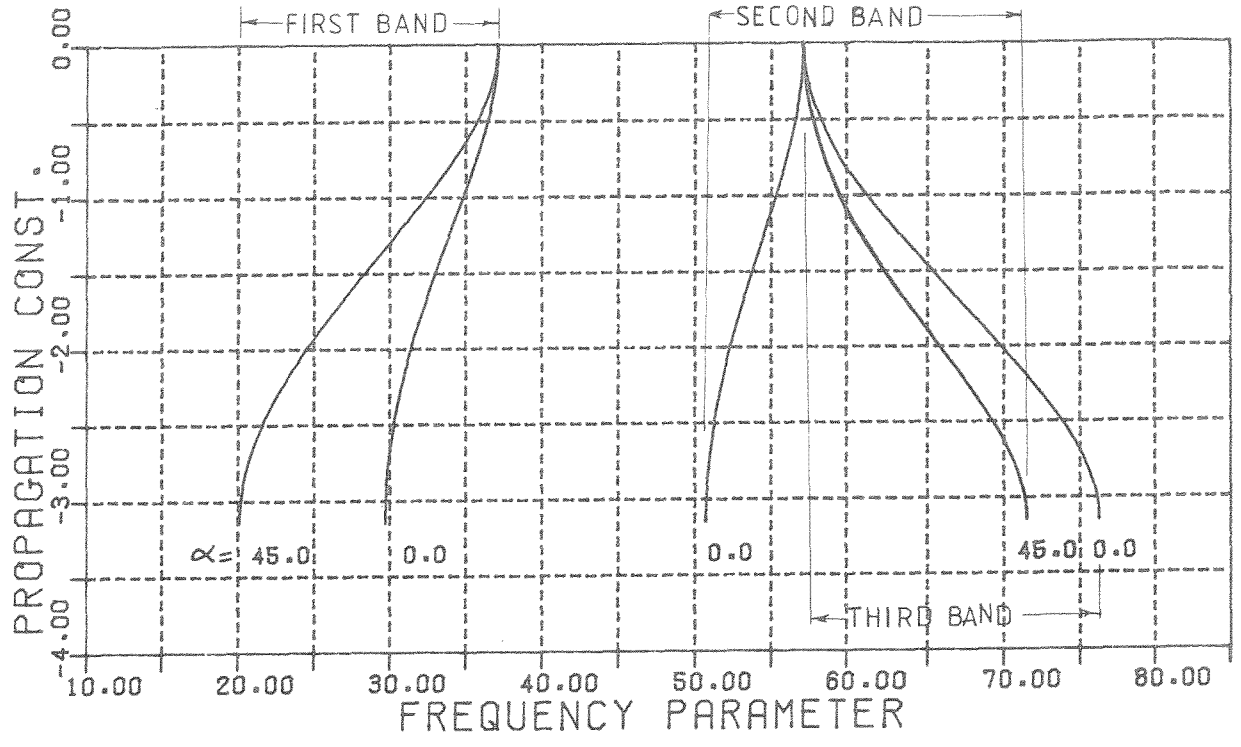

Figure 3.17. Variation of the real propagation constants with frequency, for a two-dimensional periodic plate on simple line supports with square cells, for waves propagating along the X direction ($\alpha = 0.0, \mu_y = 0.0$) and along the preferred direction of propagation ($\alpha = 45.0^{\circ}, \mu_x = \mu_y$) .

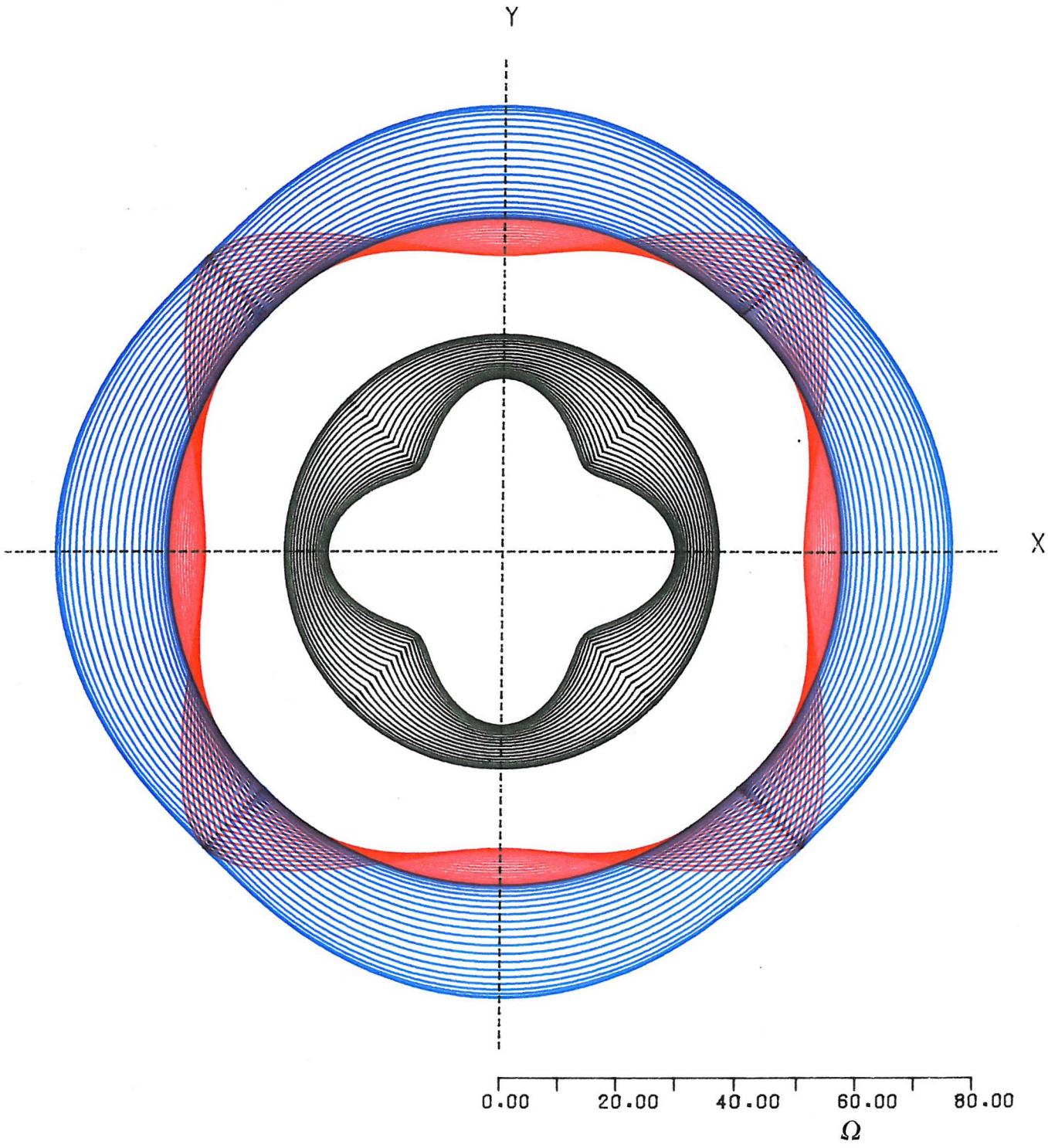

Figure 3.18. Polar representation of the real propagation constants-frequency variation for two-dimensional periodic plates on simple line supports with square cells;first band:black; second band:red;third band:blue .

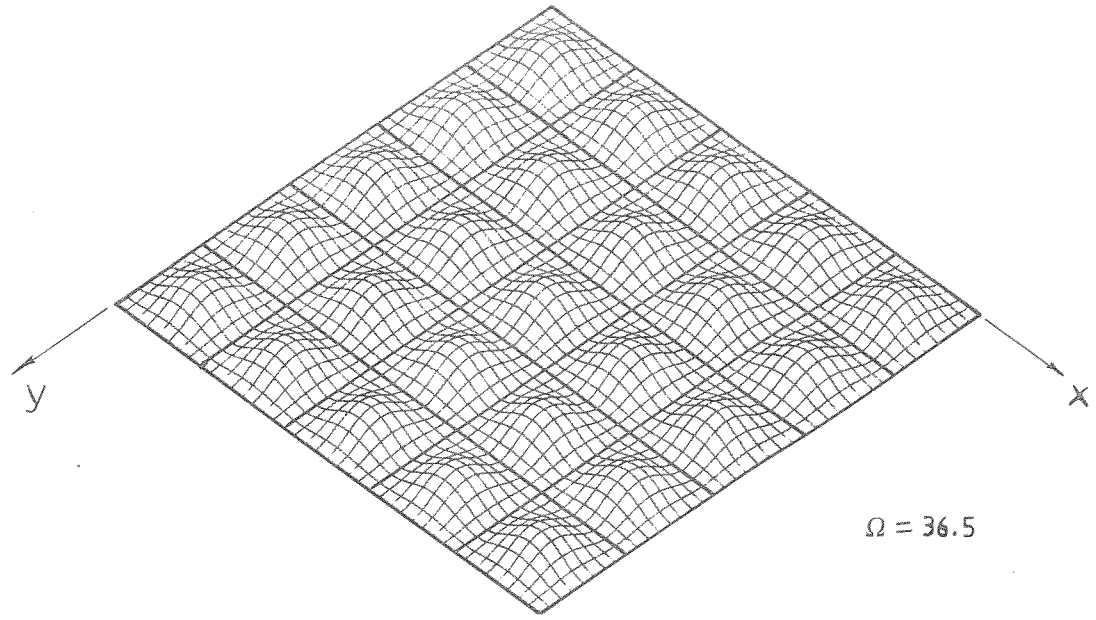

(a)

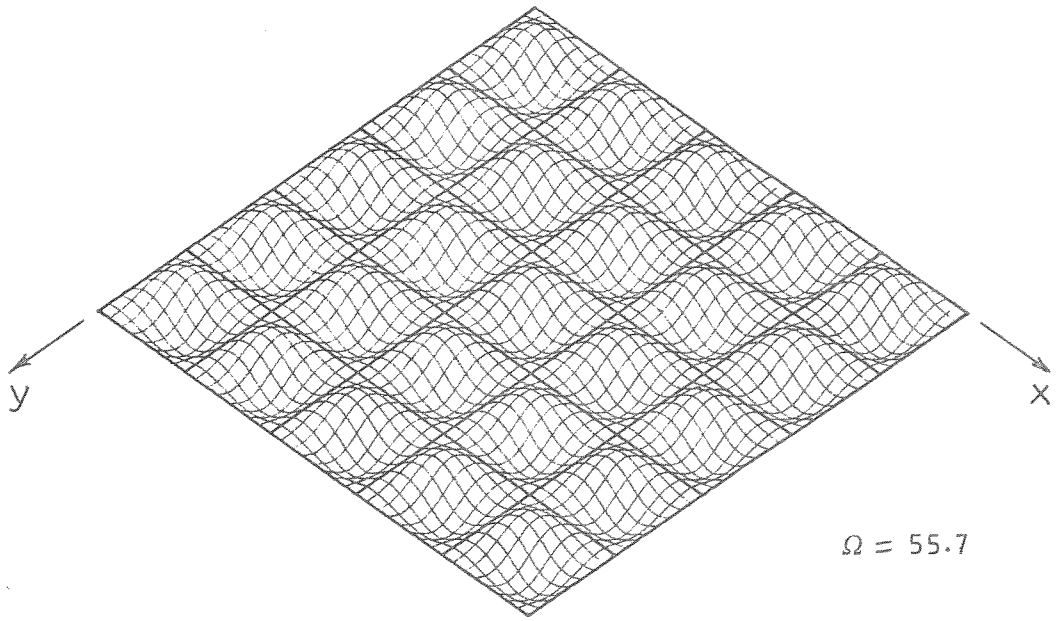

(b)

Figure 3.19. Standing waves of the two-dimensional periodic plate shown in figure(3.6) , $l_x=l_y=1.0$, $\mu_x=\mu_y=0.0$; (a) first band ; (b) second band .

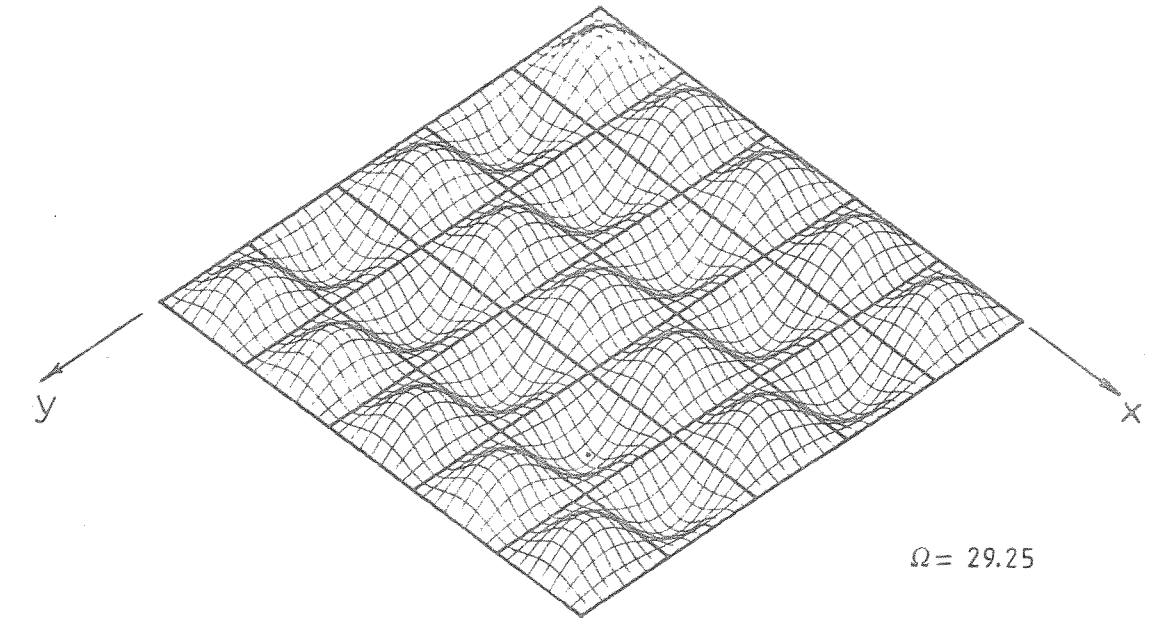

(a)

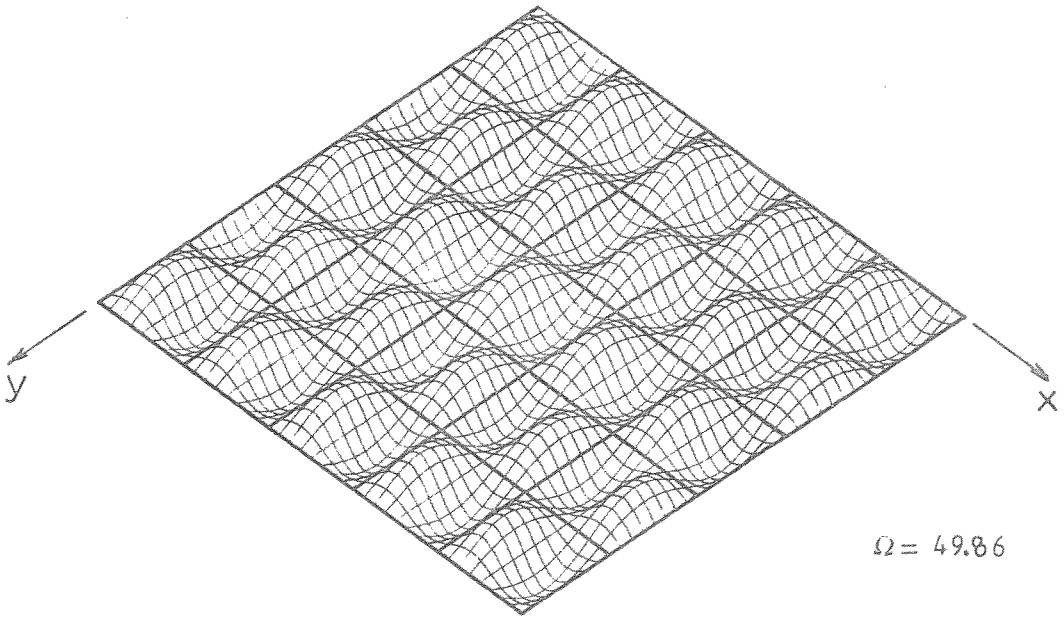

(b)

Figure 3.20. standing waves of the two-dimensional periodic plate shown in figure(3.6) , $l_x=l_y=1.0$, $\mu_x=0.0$, $\mu_y=\pi$; (a) first band ; (b) second band .

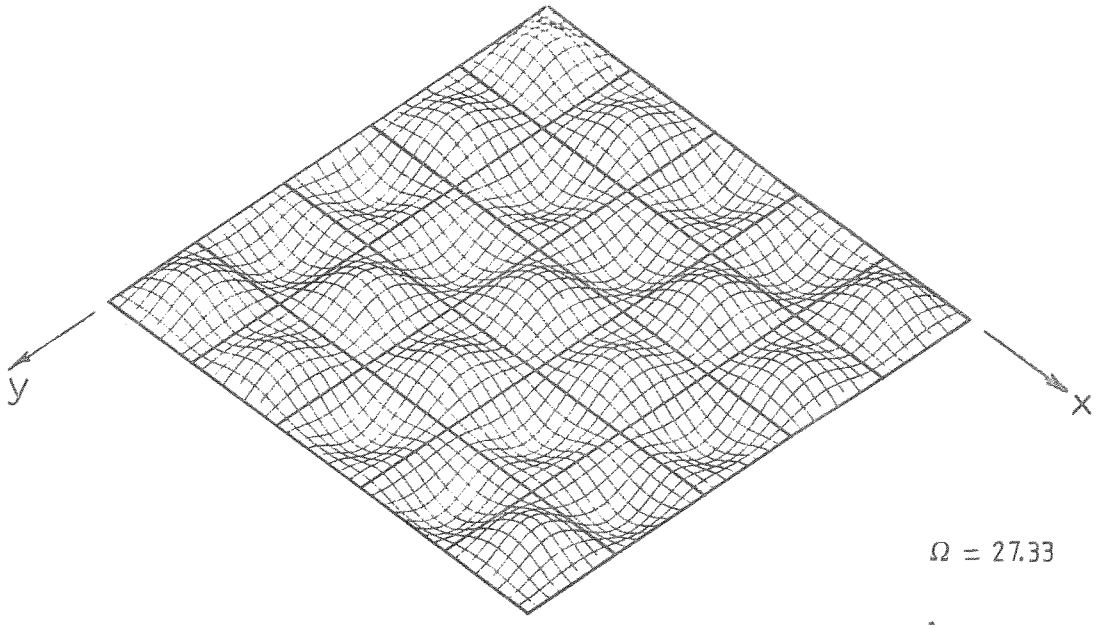

(a)

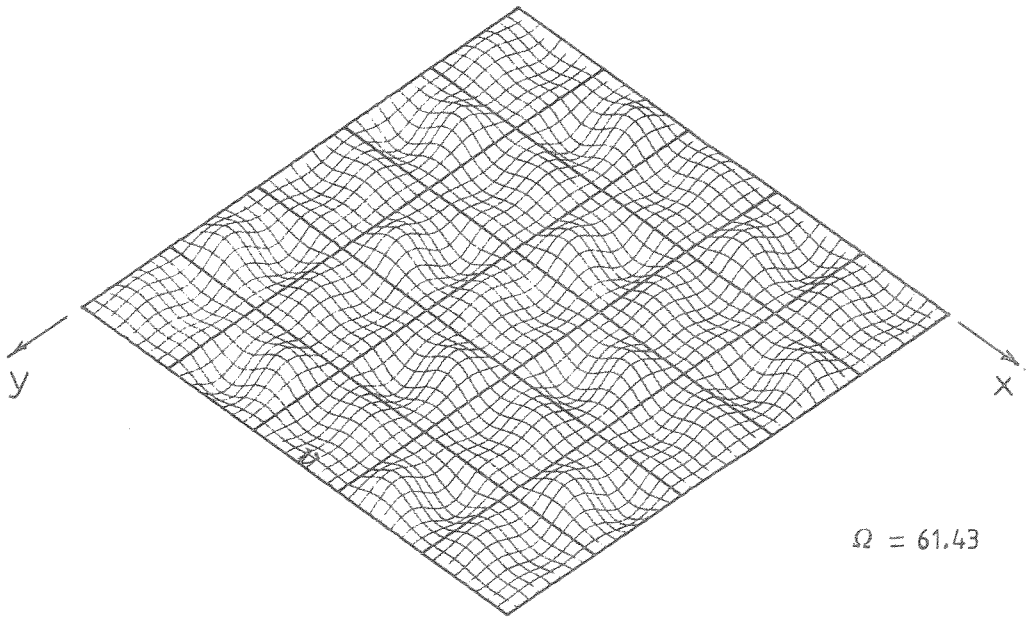

(b)

Figure 3.21. Propagating waves of the two-dimensional periodic plate shown in figure(3.6) , $l_x=l_y=1.0$, $\mu_x=\pi/2$, $\mu_y=\pi/2$; (a) first band ; (b) second band .

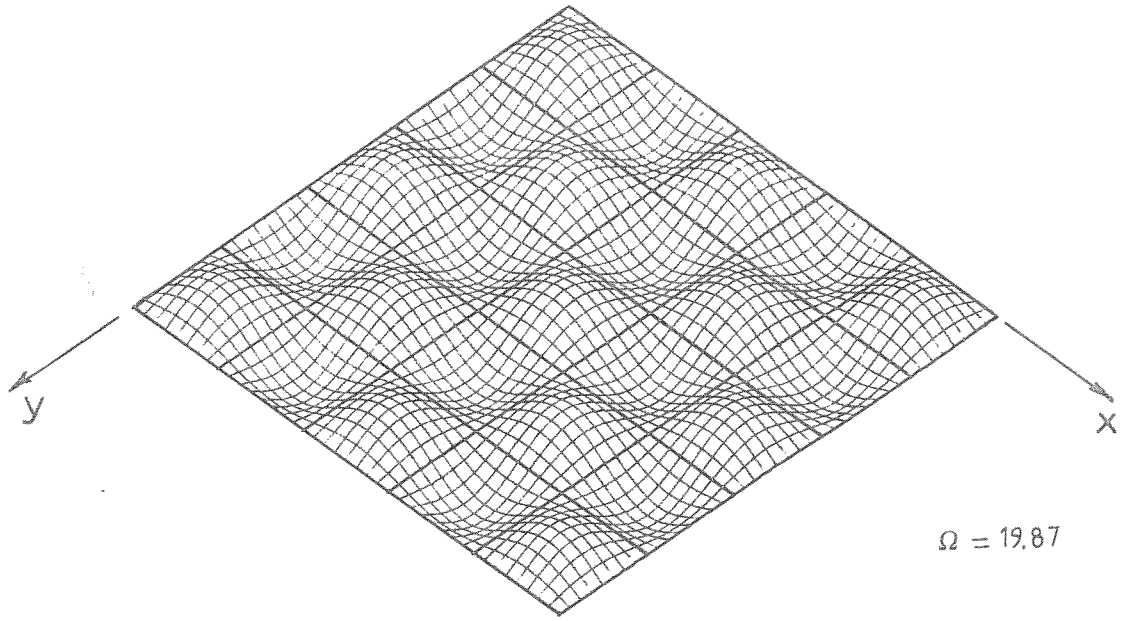

(a)

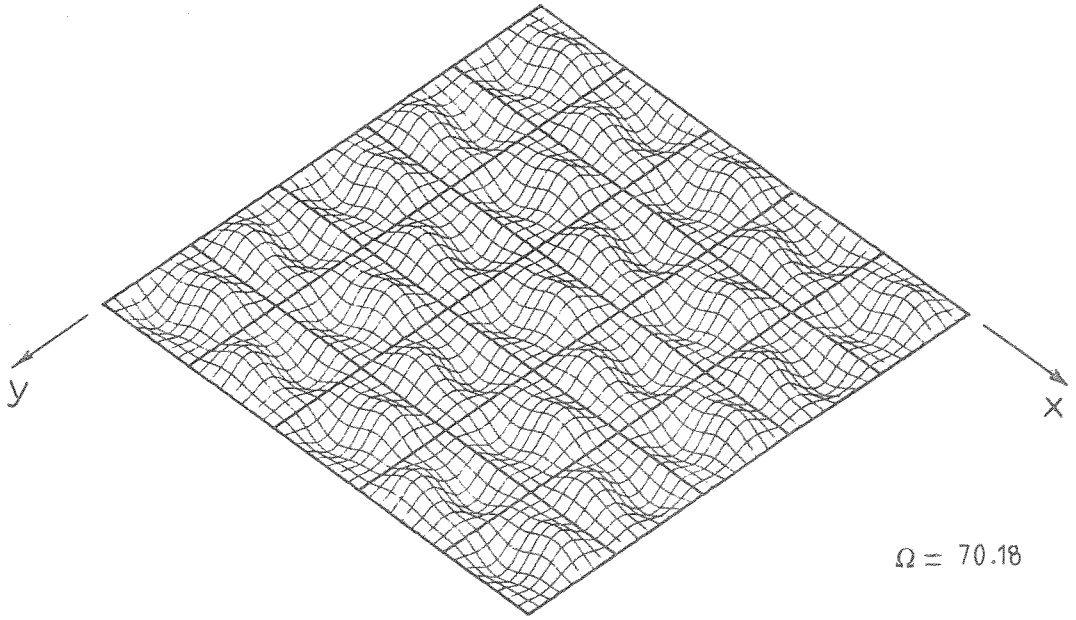

(b)

Figure 3.22. Standing waves of the two-dimensional periodic plate shown in figure(3.6) , $l_x=l_y=1.0$, $\mu_x=\pi$, $\mu_y=\pi$; (a) first band ; (b) second band .

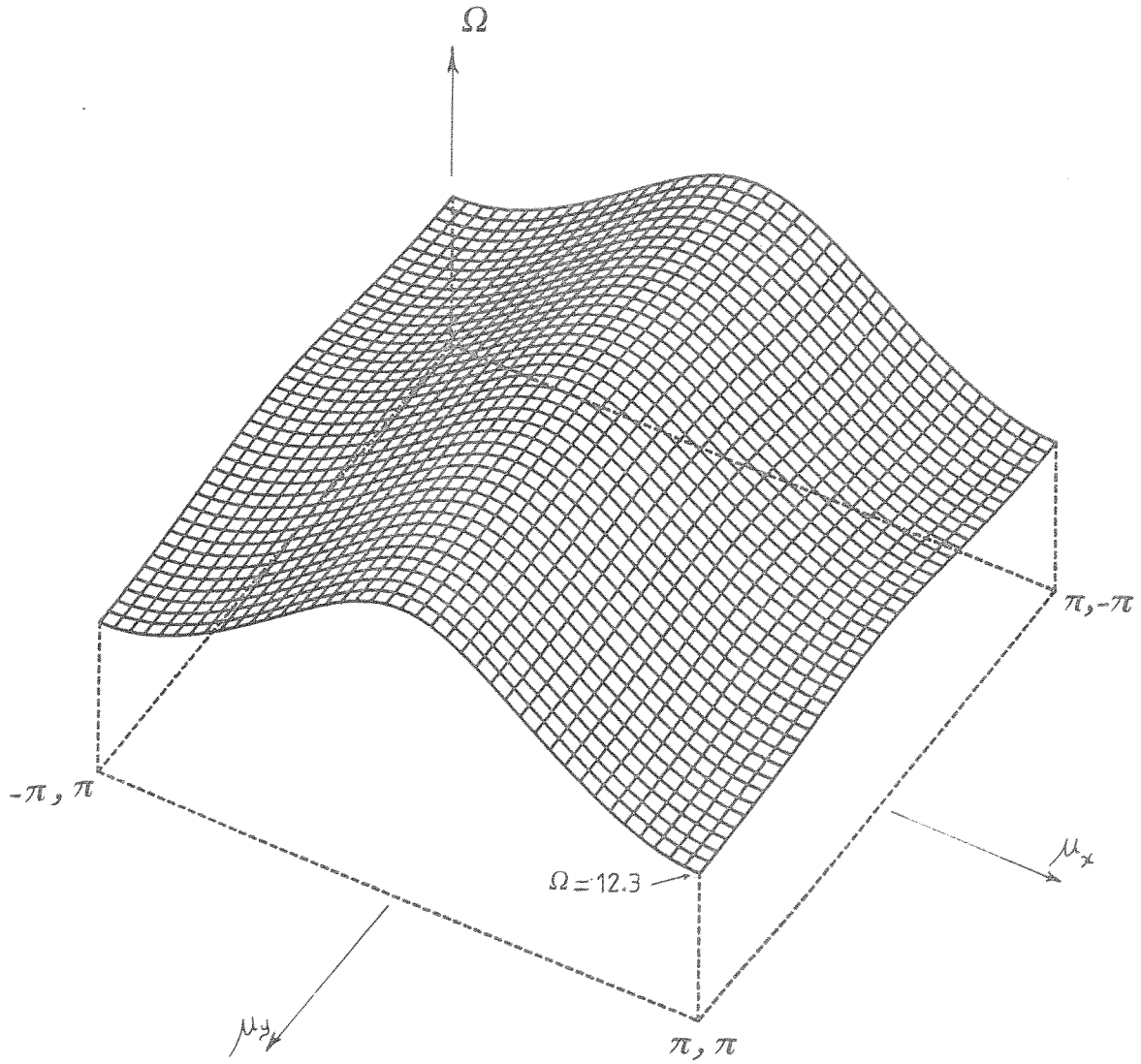

Figure 3.23. First band of the propagation surfaces for a two-dimensional periodic plate on simple line supports with rectangular cells, $l_x/l_y=0.5$.

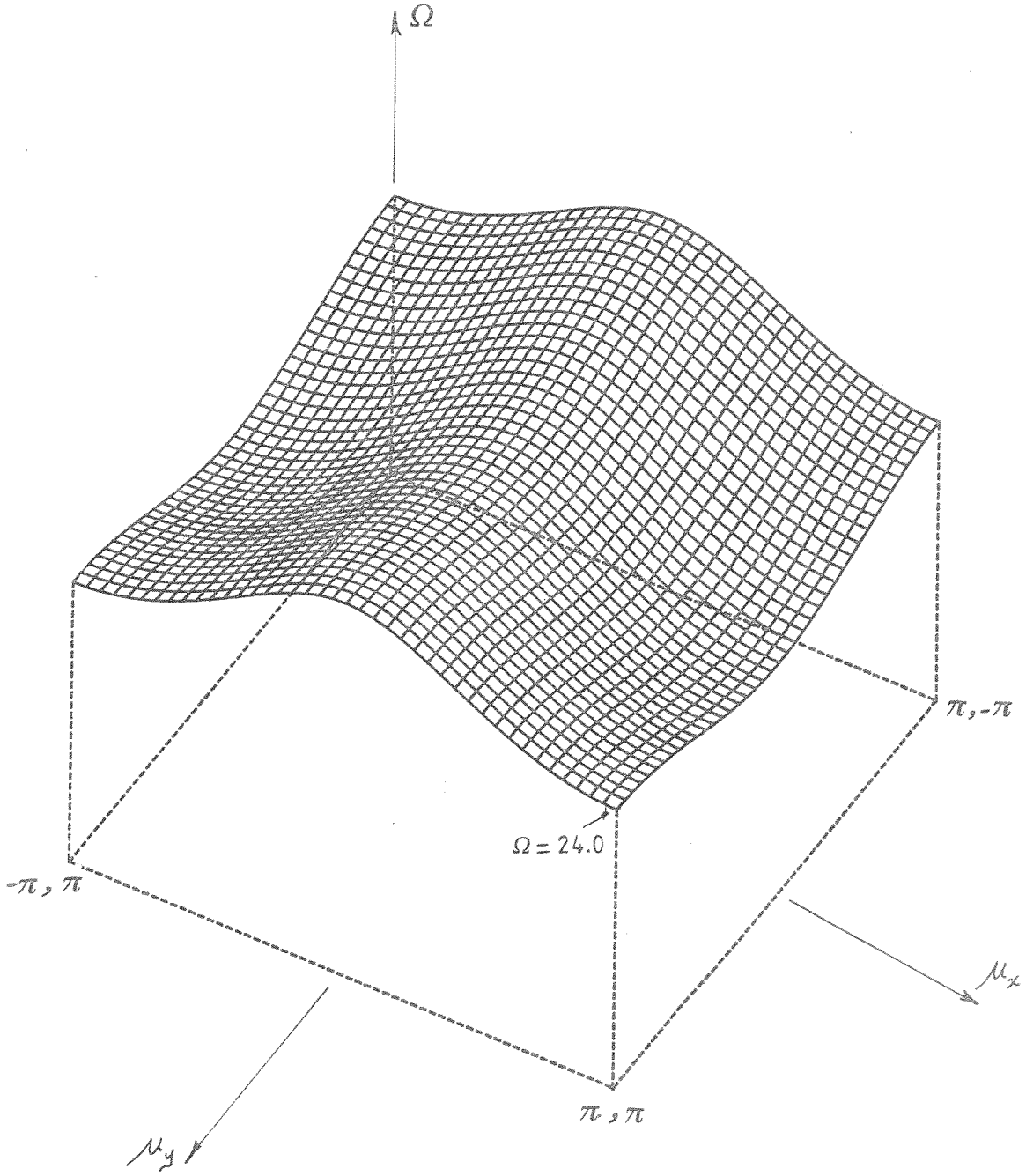

Figure 3.24. Second band of the propagation surfaces for a two-dimensional periodic plate on simple line supports with rectangular cells , $l_x / l_y = 0.5$.

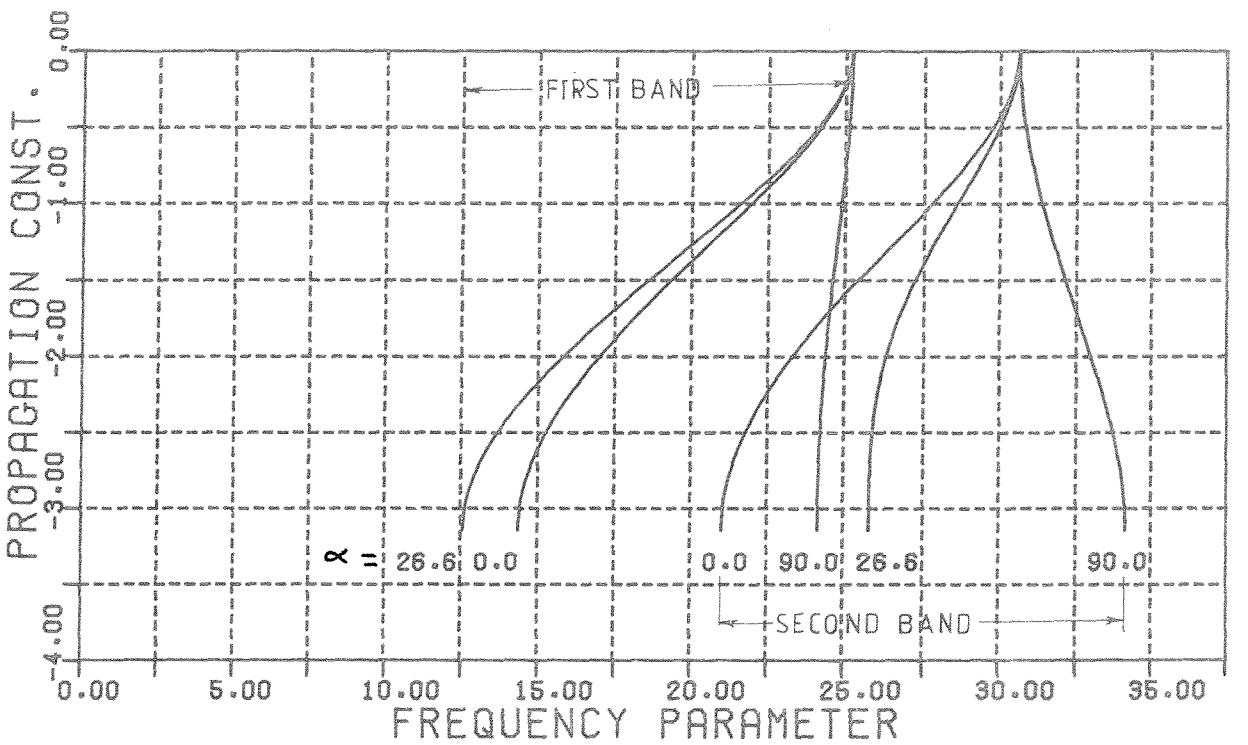

Figure 3.25. Variation of the real propagation constants with frequency, for a two-dimensional periodic plate on simple line supports with rectangular cells($l_x/l_y=0.5$), for waves propagating along the x direction($\alpha=0.0°, \mu_y=0$), along the y direction ($\alpha=90.0°, \mu_x=0$) and along the preferred direction of propagation($\alpha=26.6°, \mu_x=\mu_y$).

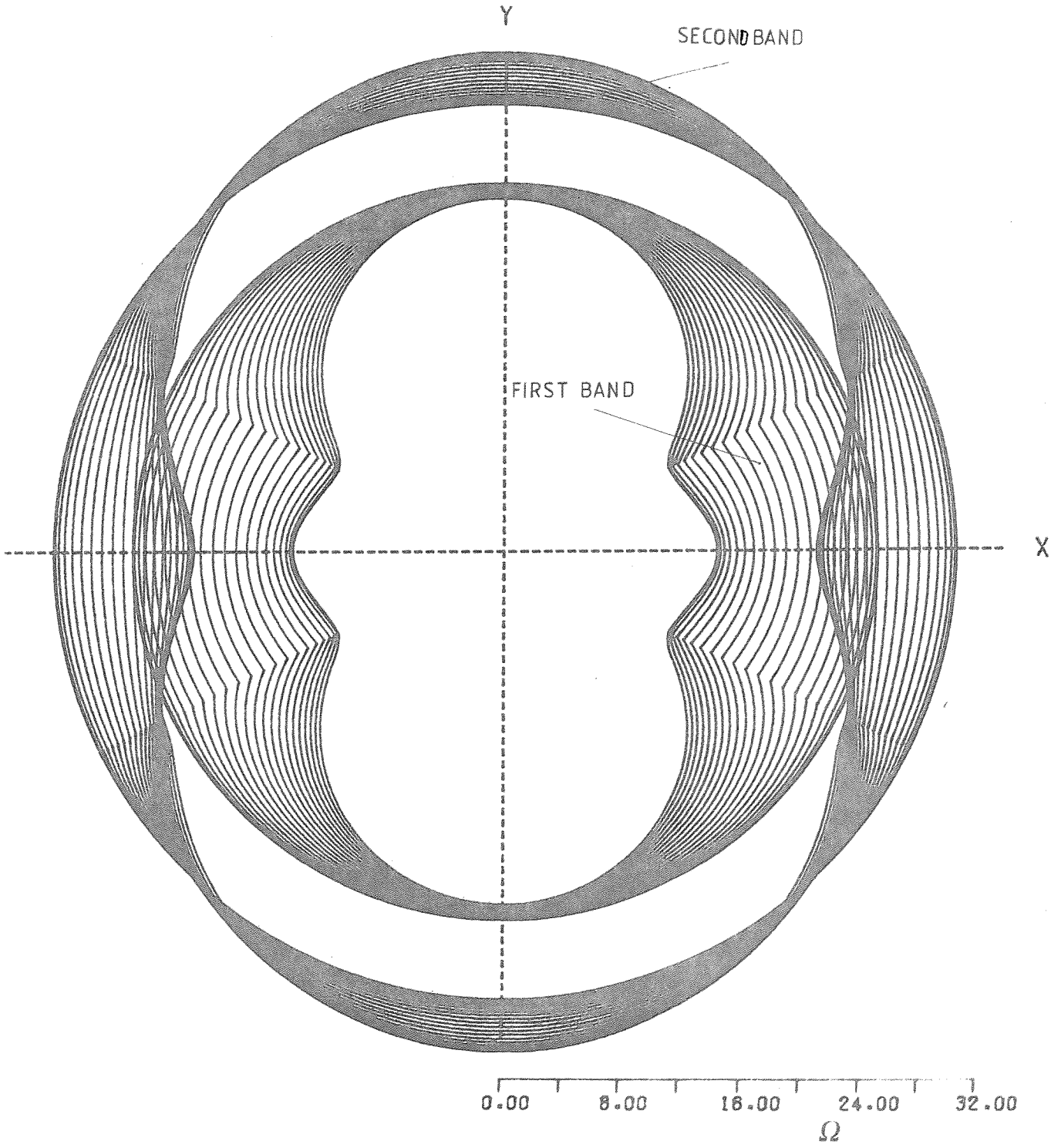

Figure 3.26. Polar representation of the real propagation constants-frequency variation for a two dimensional periodic plate on simple line supports with rectangular cells(l_x/l_y=0.5).

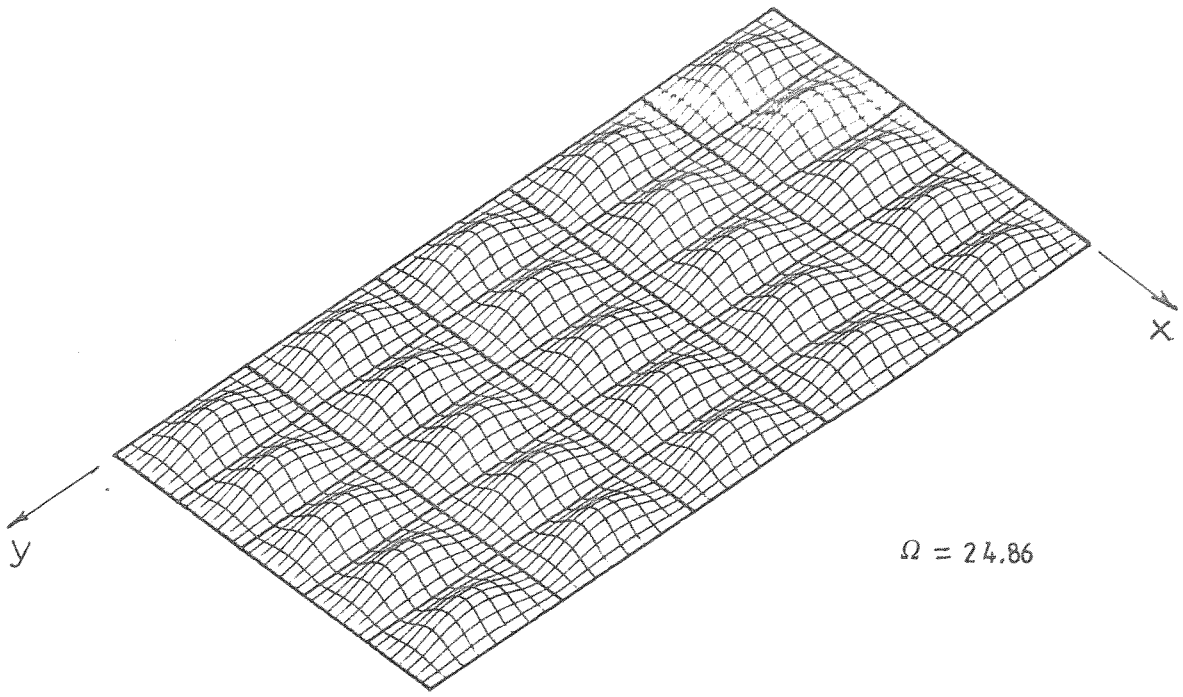

(a)

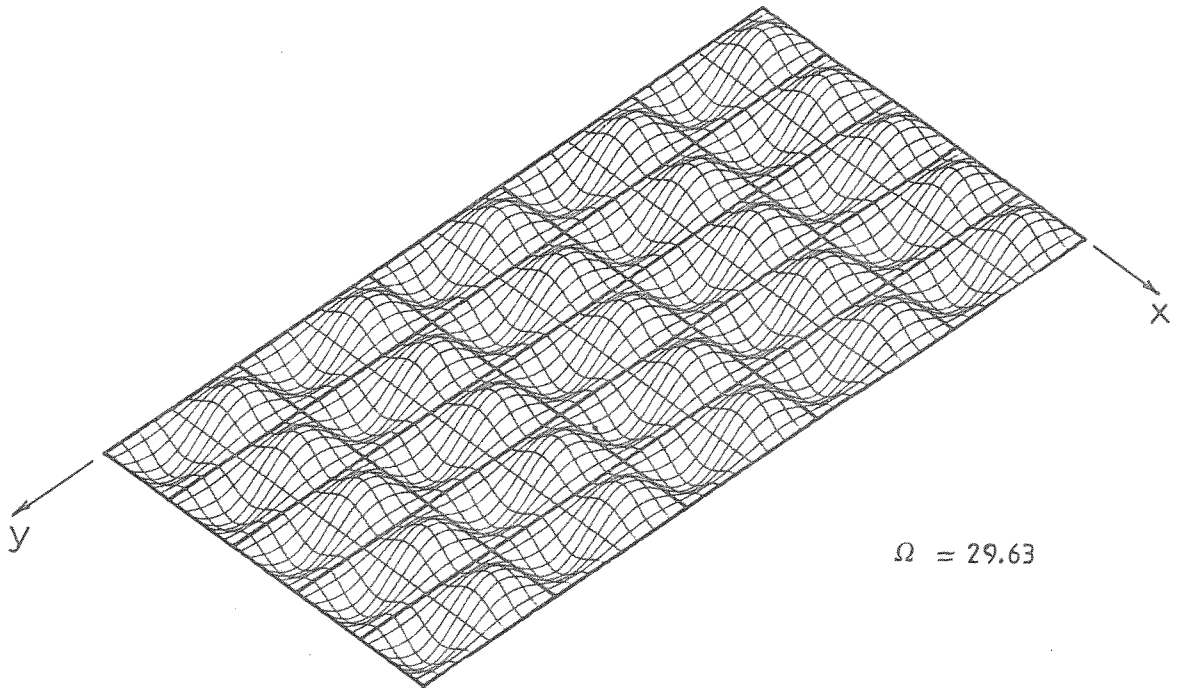

(b)

Figure 3.27. Standing waves of the two-dimensional periodic plate shown in figure(3.6) , $l_x/l_y=0.5$, $\mu_x=\mu_y=0.0$; (a) first band ; (b) second band .

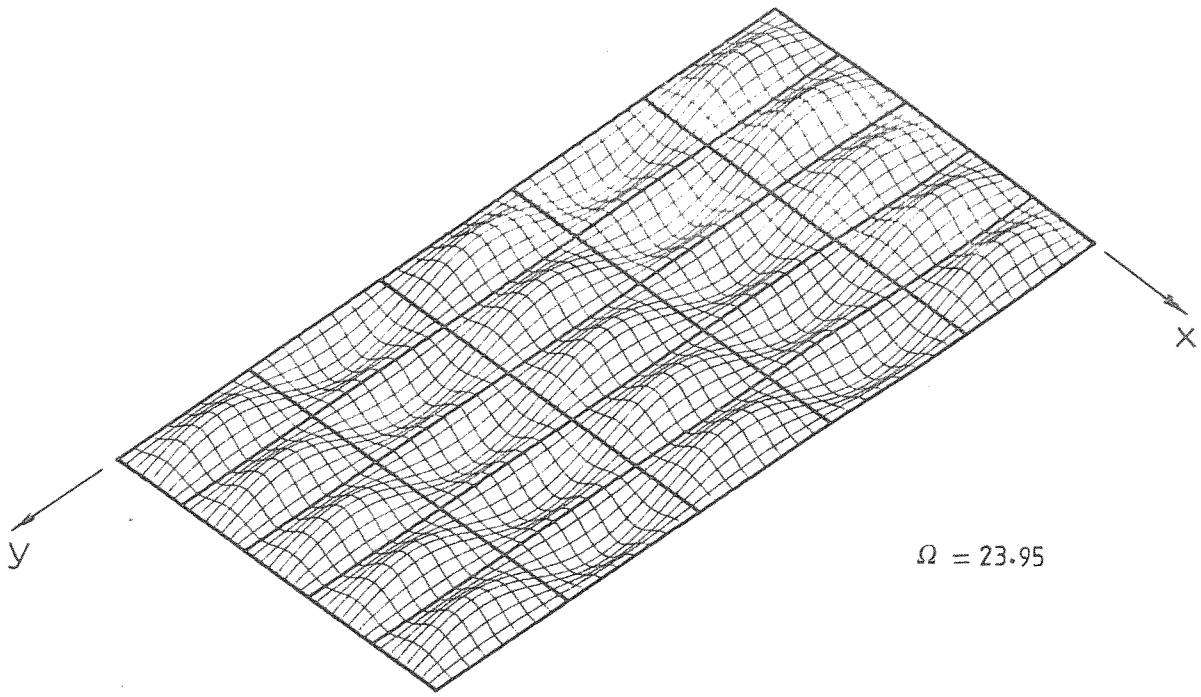

(a)

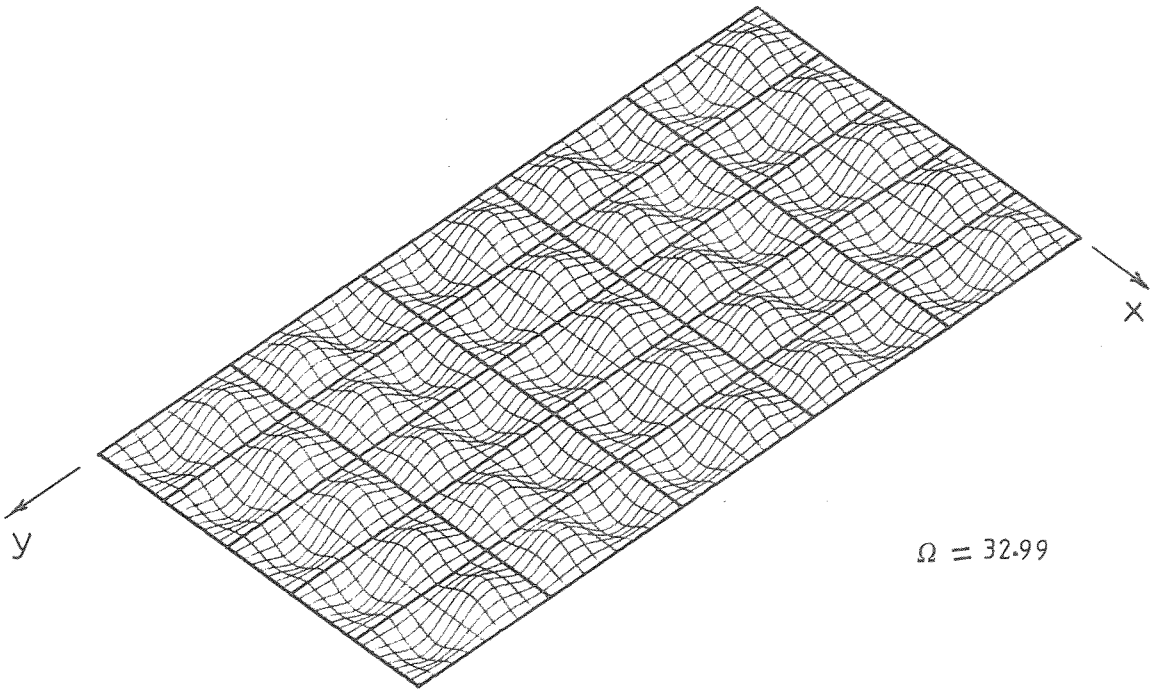

(b)

Figure 3.28. Standing waves of the two-dimensional periodic plate shown in figure(3.6) , $l_x/l_y=0.5$, $\mu_x=0.0$, $\mu_y=\pi$; (a) first band ; (b) second band .

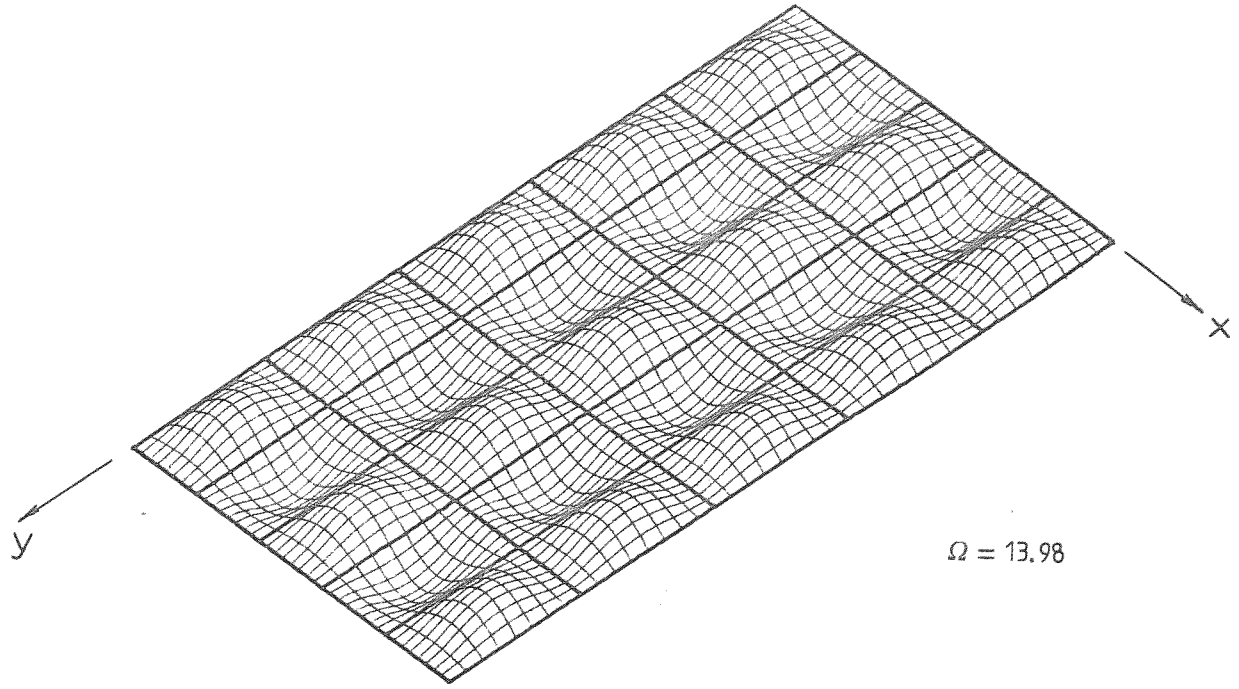

(a)

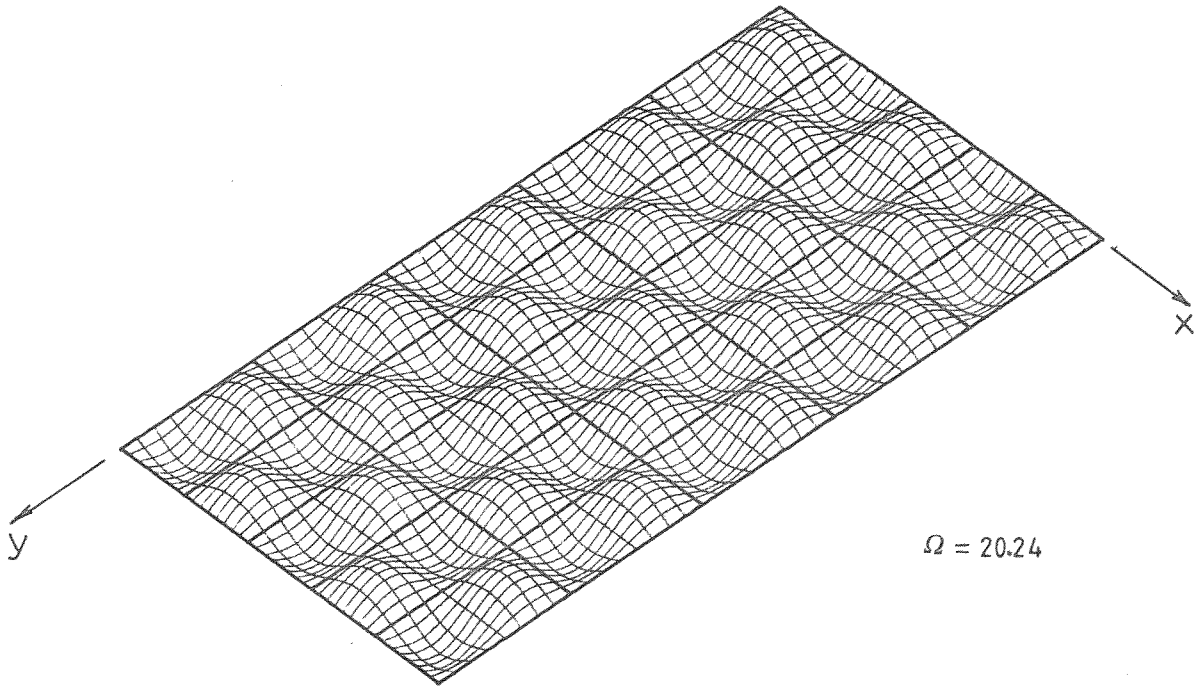

(b)

Figure 3.29. Standing waves of the two-dimensional periodic plate shown in figure(3.6) , $l_x/l_y=0.5$, $\mu_x=\pi$, $\mu_y=0.0$; (a) first band ; (b) second band .

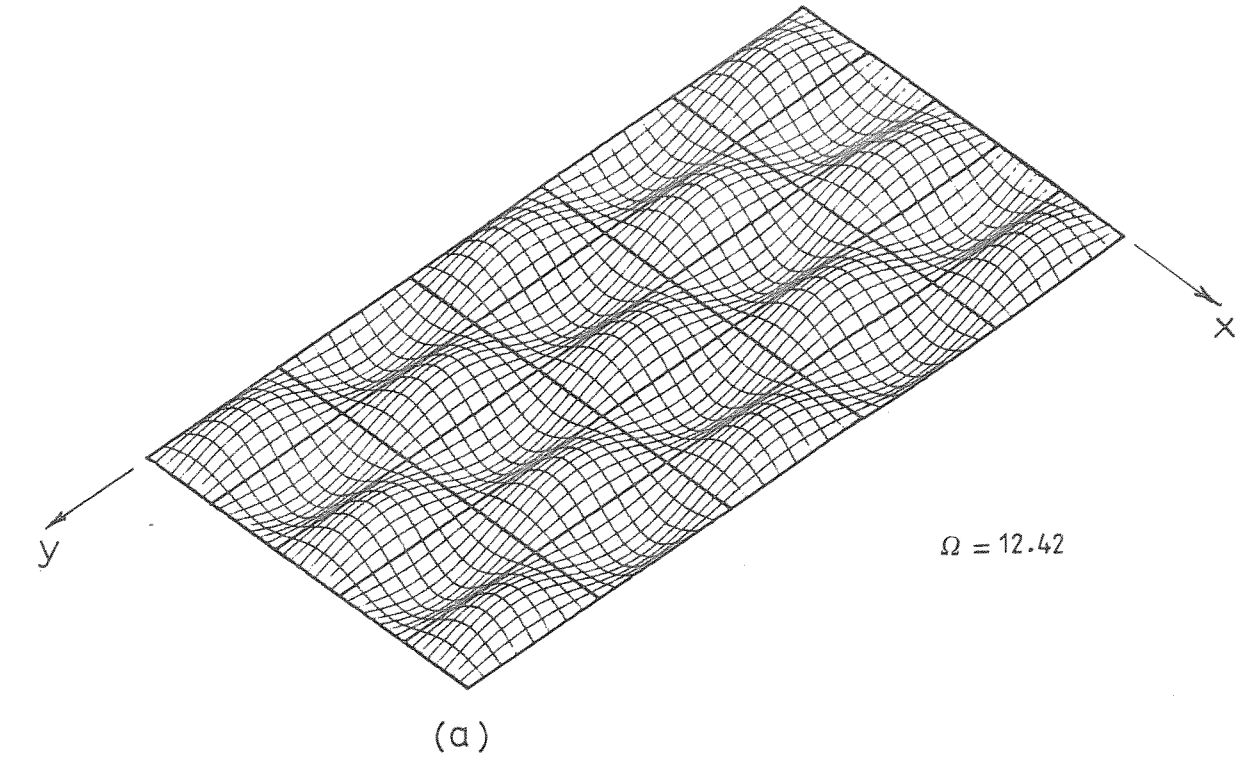

(a)

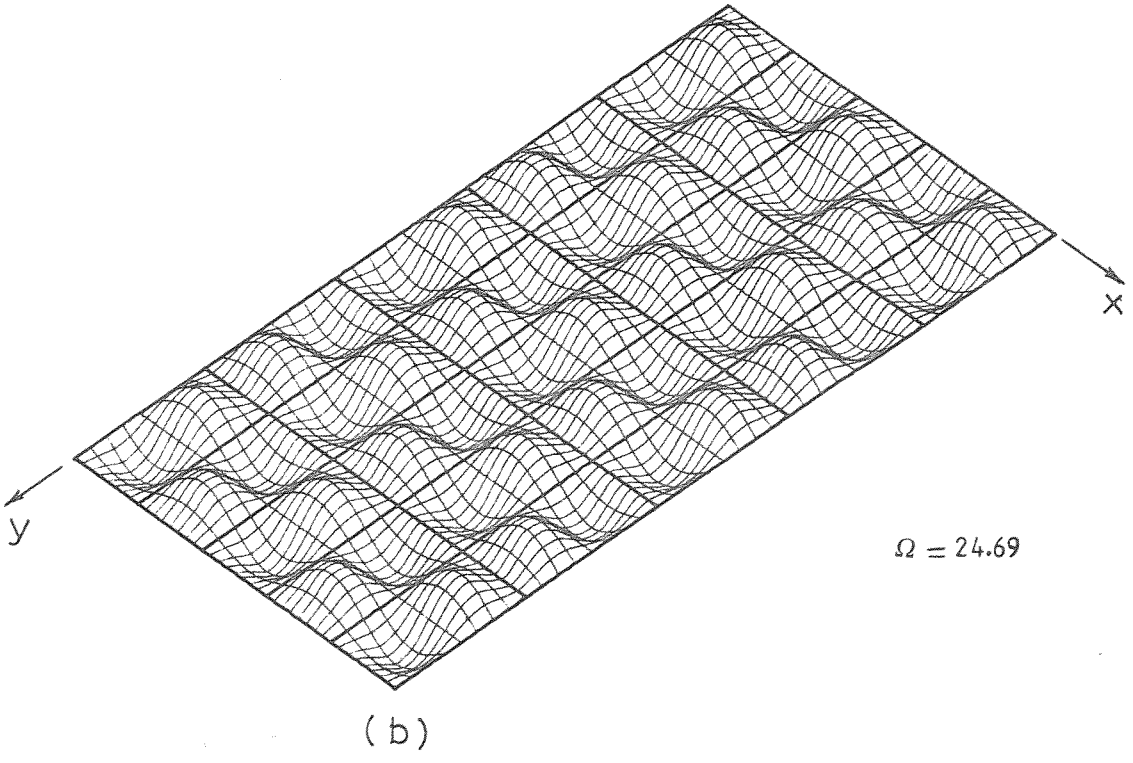

(b)

Figure 3.30. Standing waves of the two-dimensional periodic plate shown in figure(3.6) , $l_x/l_y=0.5$, $\mu_x=\mu_y=\pi$; (a) first band ; (b) second band .

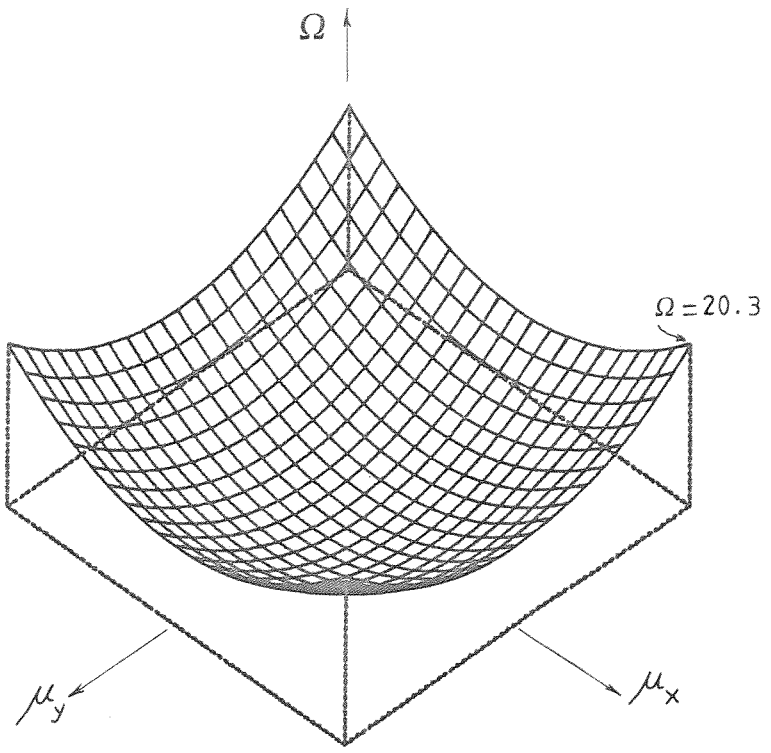

(a)

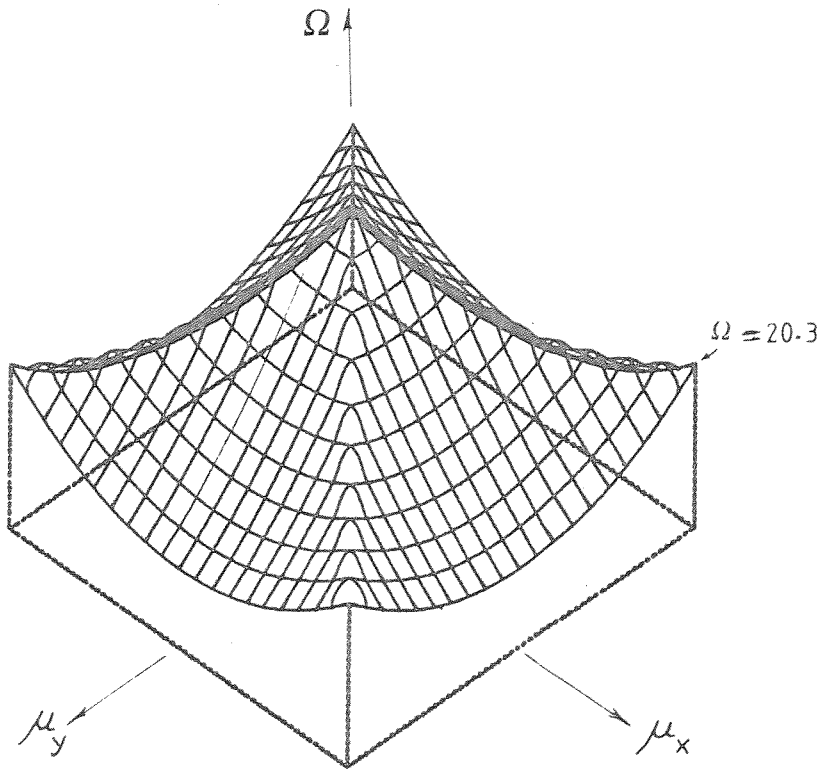

(b)

Figure 3.31. Propagation surfaces for a flat plate; (a) first band ; (b) second band .

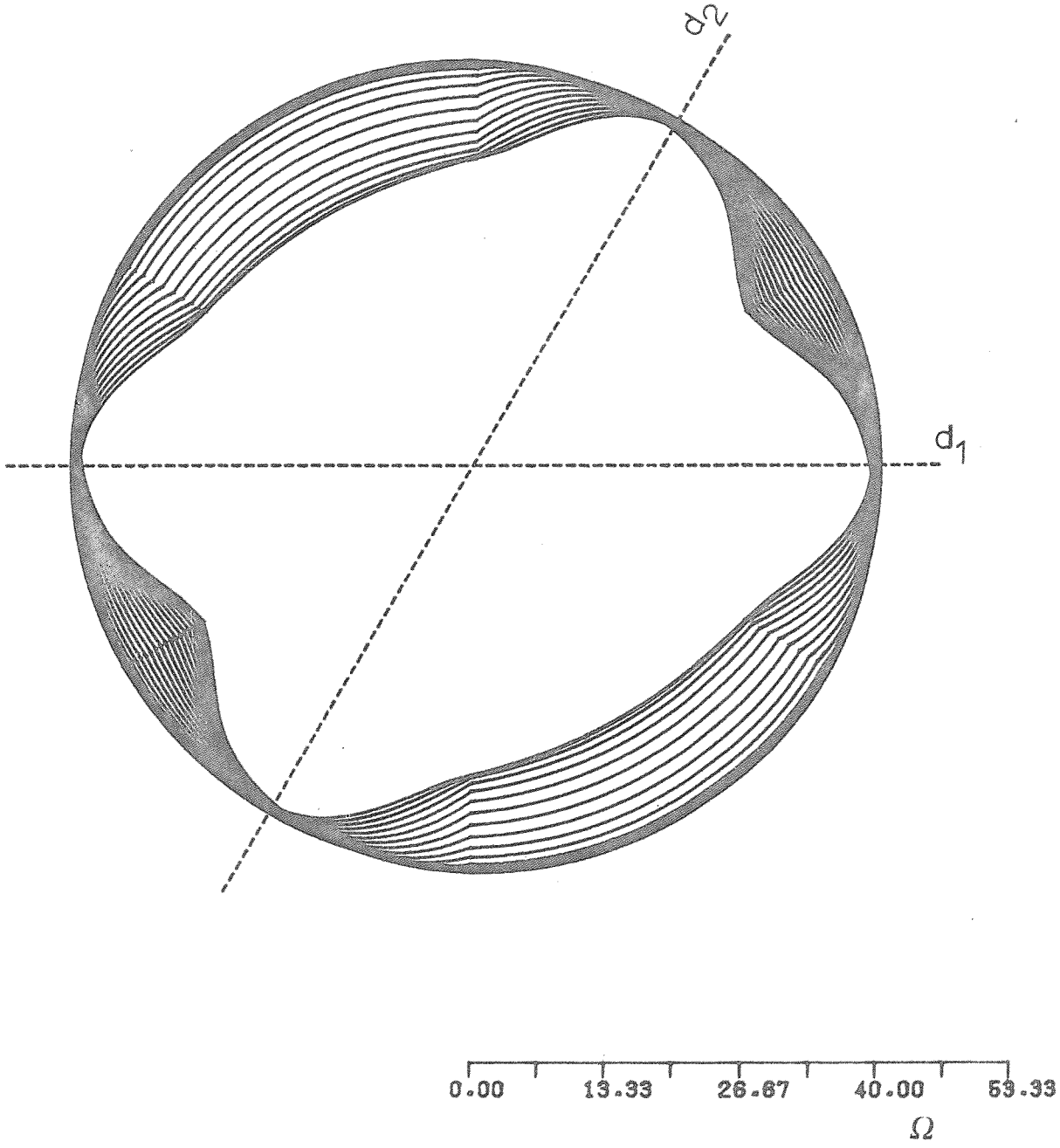

Figure 3.32. Polar representation of the real propagation constants-frequency variation for the two-dimensional periodic plate shown in figure(3.9) .

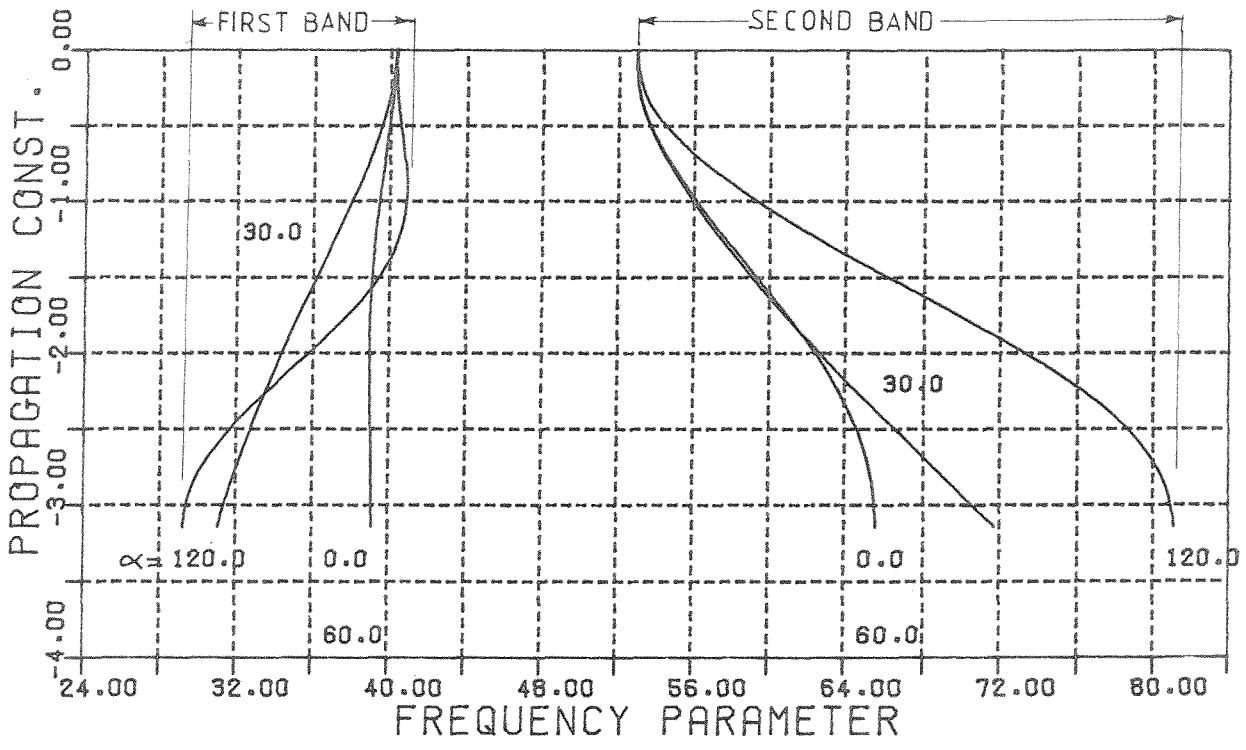

Figure 3.33. Variation of the real propagation constants with frequency, for the two-dimensional periodic plate shown in figure(3.9), $l_1=l_2$, for waves propagating along the d_1 direction($\alpha=0.0$, $\mu_2=0.0$),along the d_2 direction($\alpha=60.0^{\circ}$, $\mu_1=0.0$),normal to the shorter diagonal of the cell($\alpha=30.0^{\circ}$, $\mu_1=\mu_2$) and normal to the longer diagonal of the cell($\alpha=120.0^{\circ}$, $\mu_1=-\mu_2$).

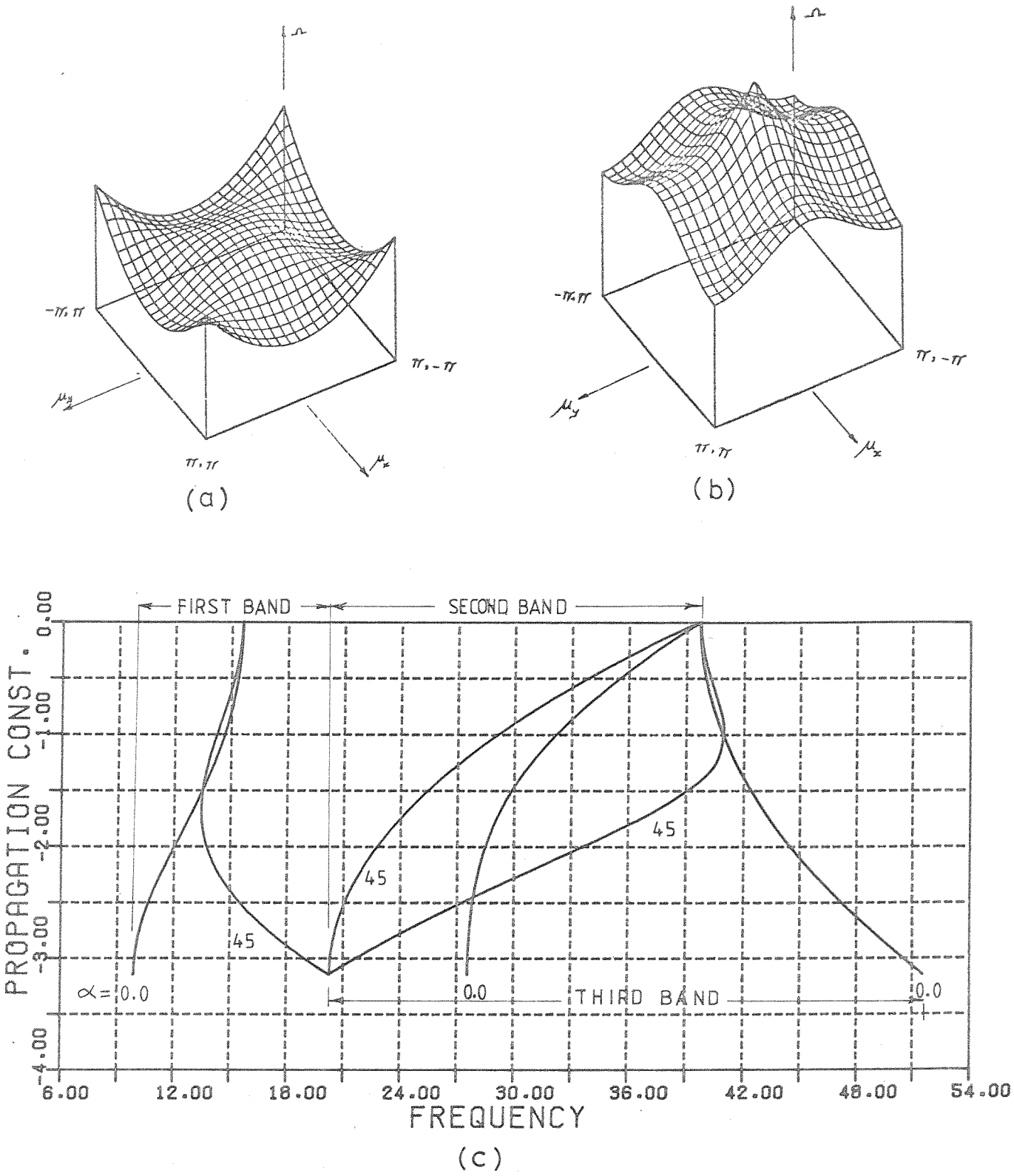

(c)

Figure 3.34. Variation of the real propagation constants with frequency, for the two-dimensional point supported periodic plate shown in figure(3.11), $l_x = l_y = 1.0$; (a) first band ; (b) second band ; (c) variation for waves propagating along the x direction ($\alpha = 0.0$, $\mu_y = 0.0$) and along a direction making 45 degrees to the x direction ($\alpha = 45.0^{\circ}$, $\mu_x = \mu_y$)

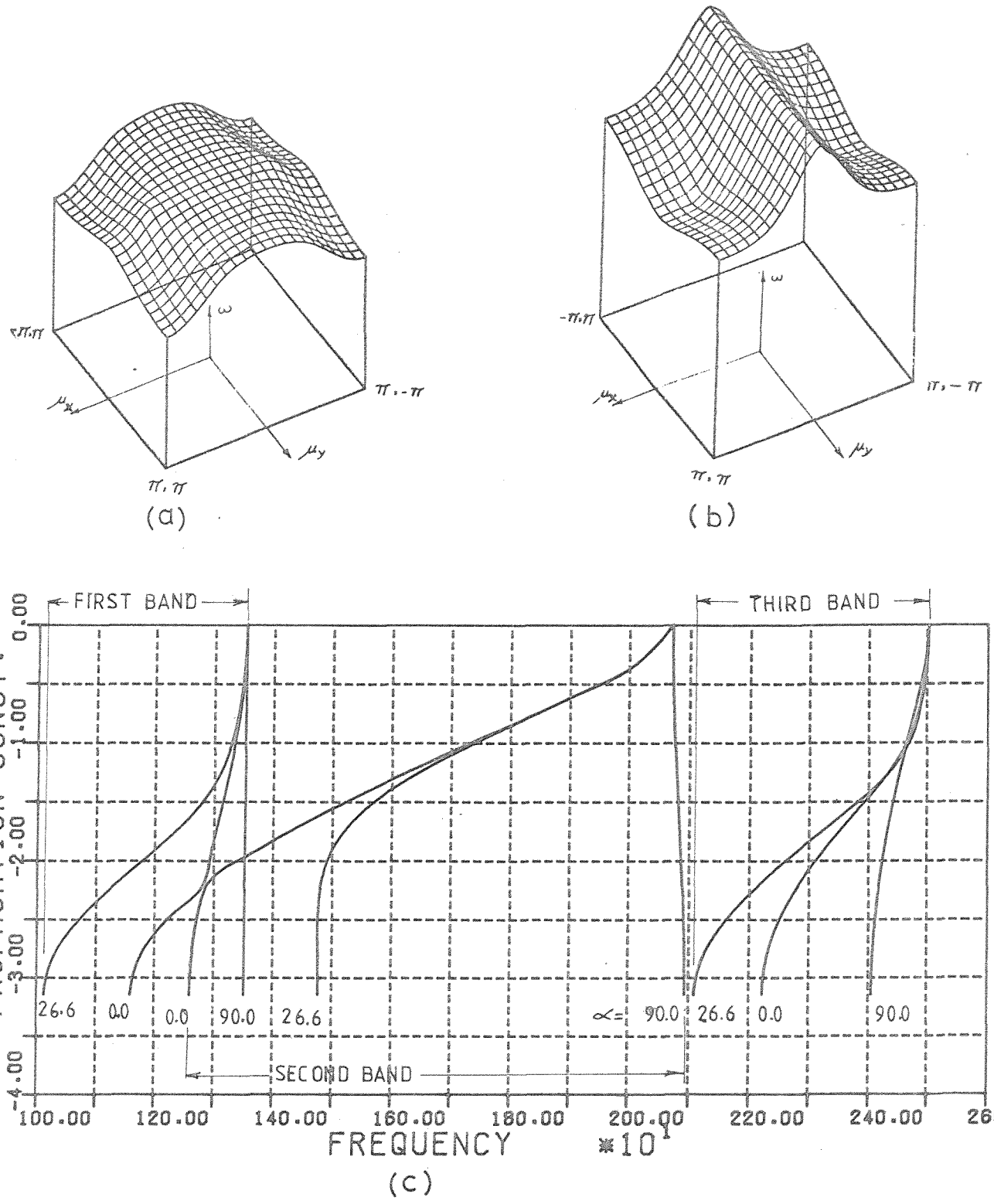

Figure 3.35. Variation of the real propagation constants with frequency, for the two-dimensional periodically stiffened plate shown in figure(3.12) ;(a) first band ;(b) second band ;(c)variation for waves propagating along the X direction(α =0.0, μ_y=0.0), along the y direction(α =90.0°, μ_x=0.0)and along the preferred direction of propagation(α =26.6°, $\mu_x = \mu_y$).The stiffeners are considered transversely rigid .

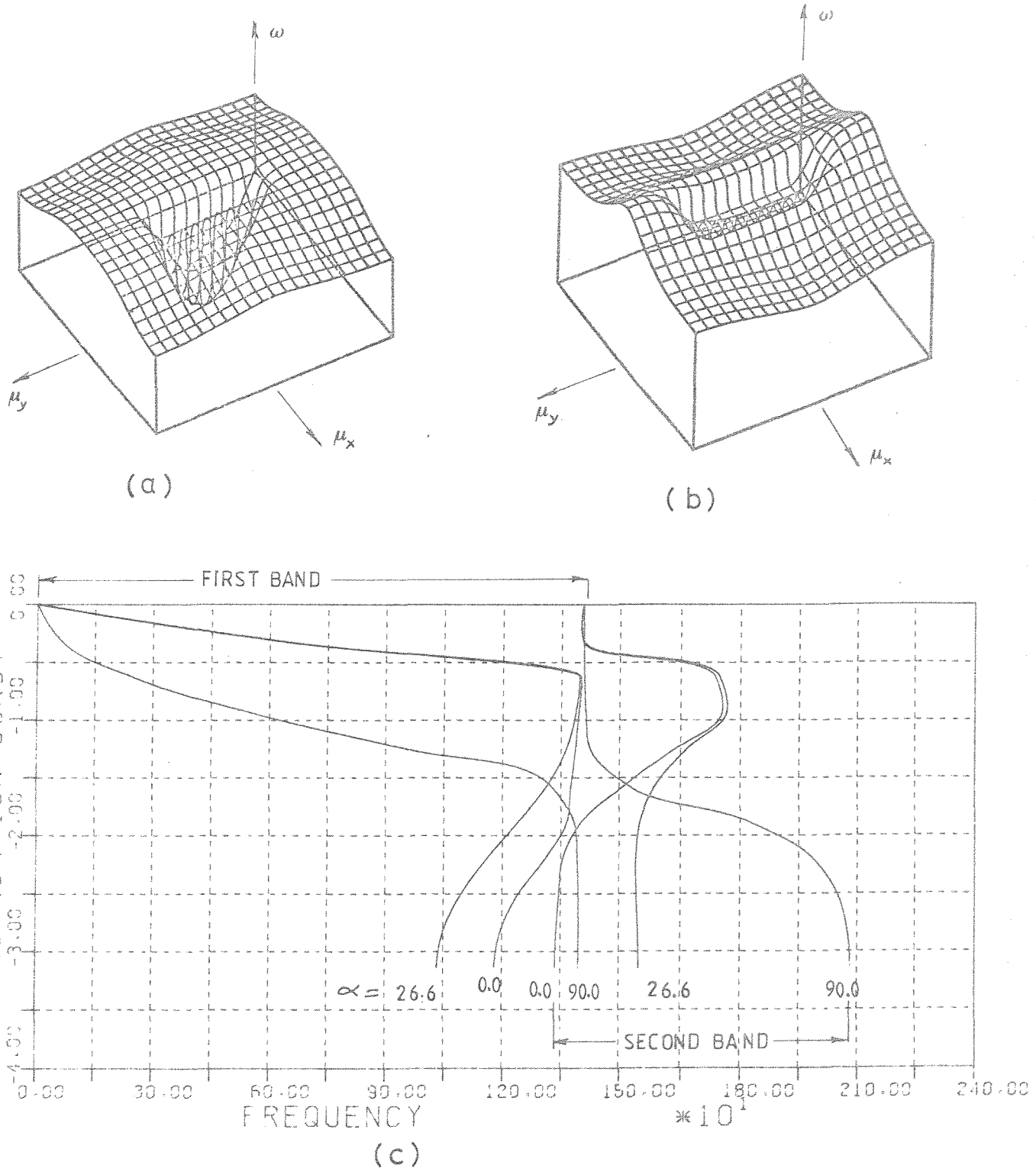

Figure 3.36. Variation of the real propagation constants with frequency, for the two-dimensional periodically stiffened plate shown in figure(3.12) ;(a) first band ;(b)second band ;(c)variation for waves propagating along the X direction(α =0.0, μ_y=0.0), along the Y direction(α =90.0°, μ_x=0.0)and along a direction normal to the diagonal of the cell(α =26.6°, $\mu_x = \mu_y$) . The transverse motion of the stiffeners is considered .

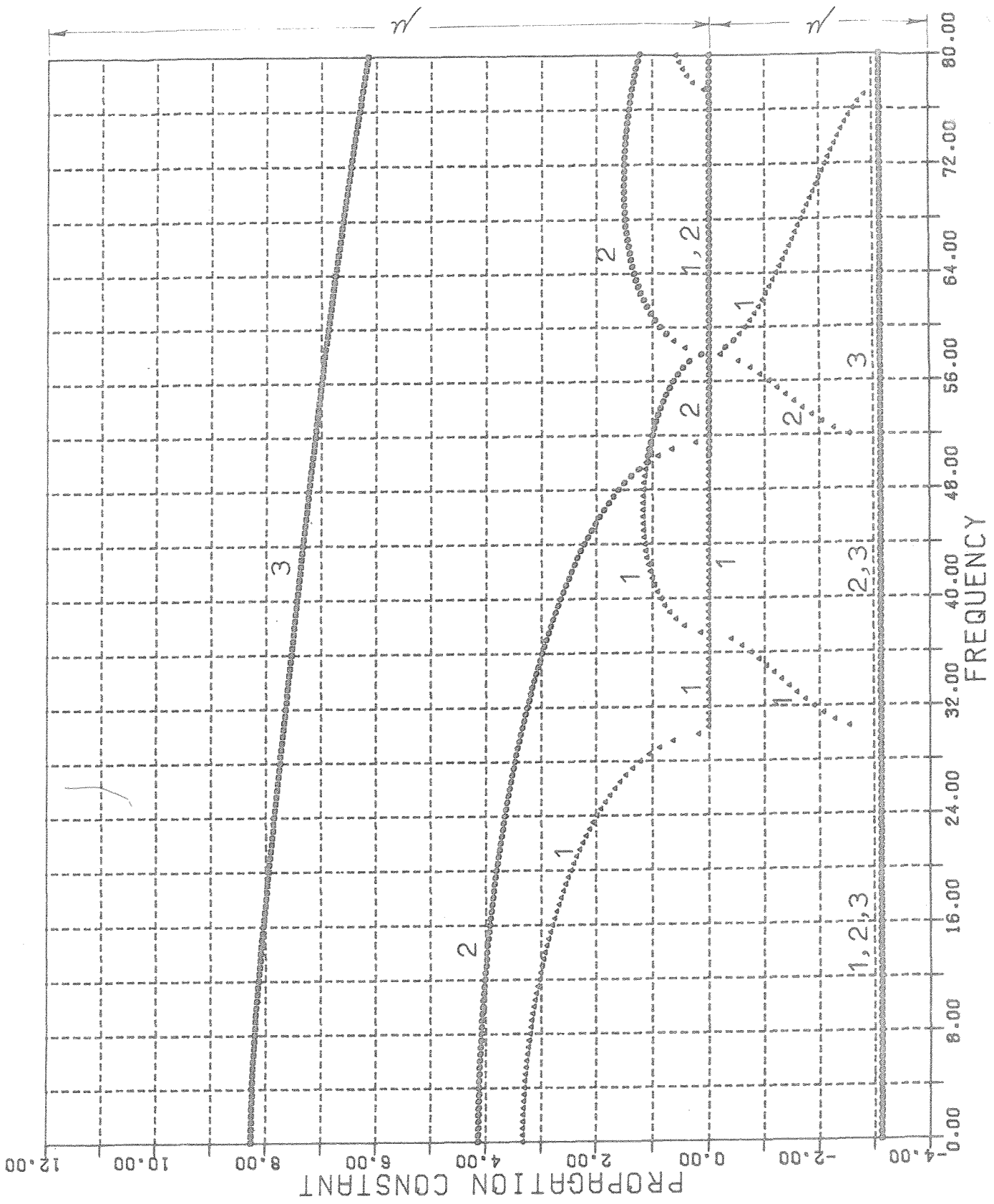

Figure 3.37. Variation of the real and imaginary parts of the propagation constants for a two-dimensional periodic plate on simple line supports with square cells, for waves propagating along the X direction(μ_y=0.0) .

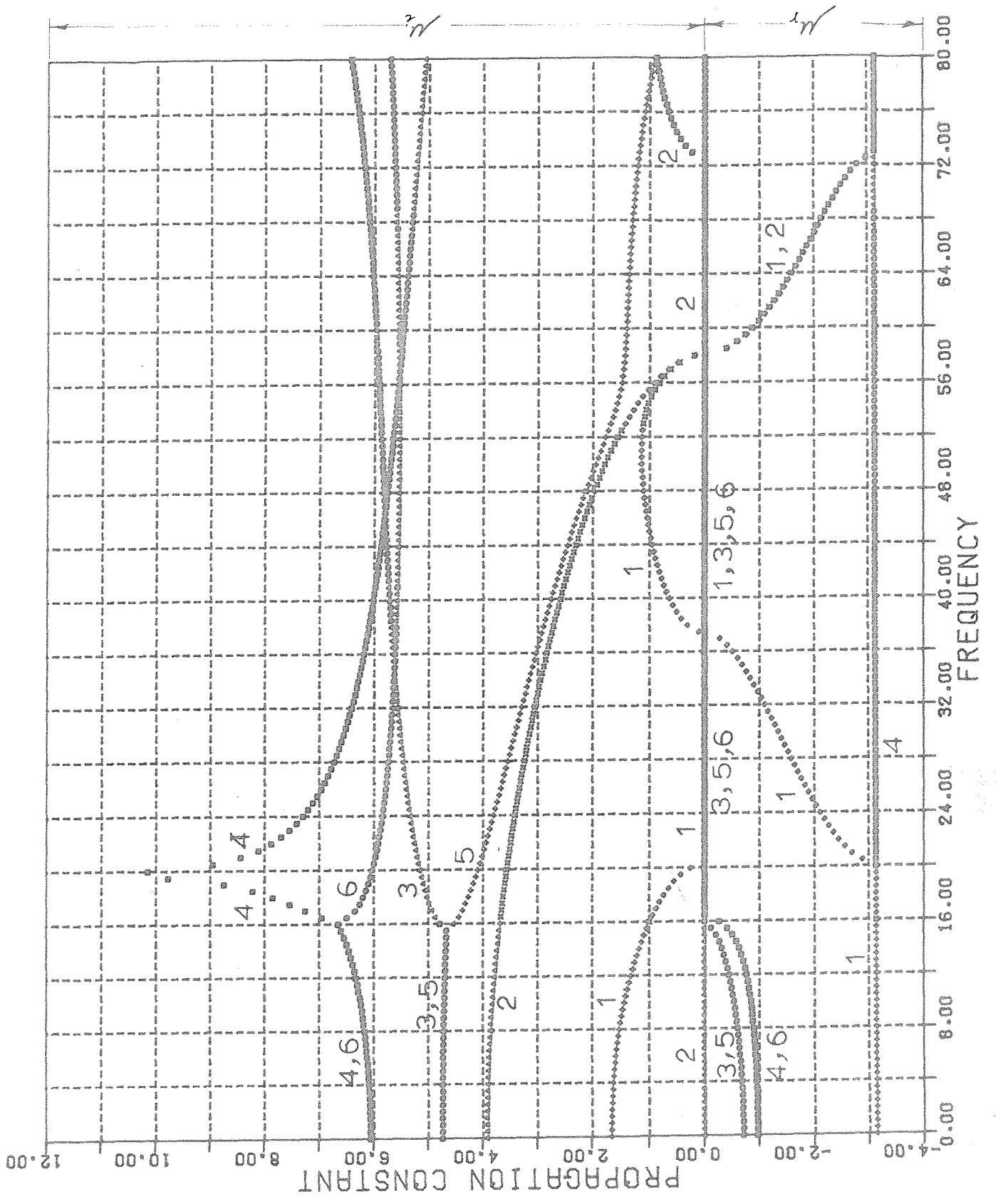

Figure 3.38. Variation of the real and imaginary parts of the propagation constants, for a two-dimensional periodic plate on simple line supports with square cells, for waves propagating along the preferred direction of propagation ($\alpha = 45.0^{\circ}$, $\mu_x = \mu_y$).

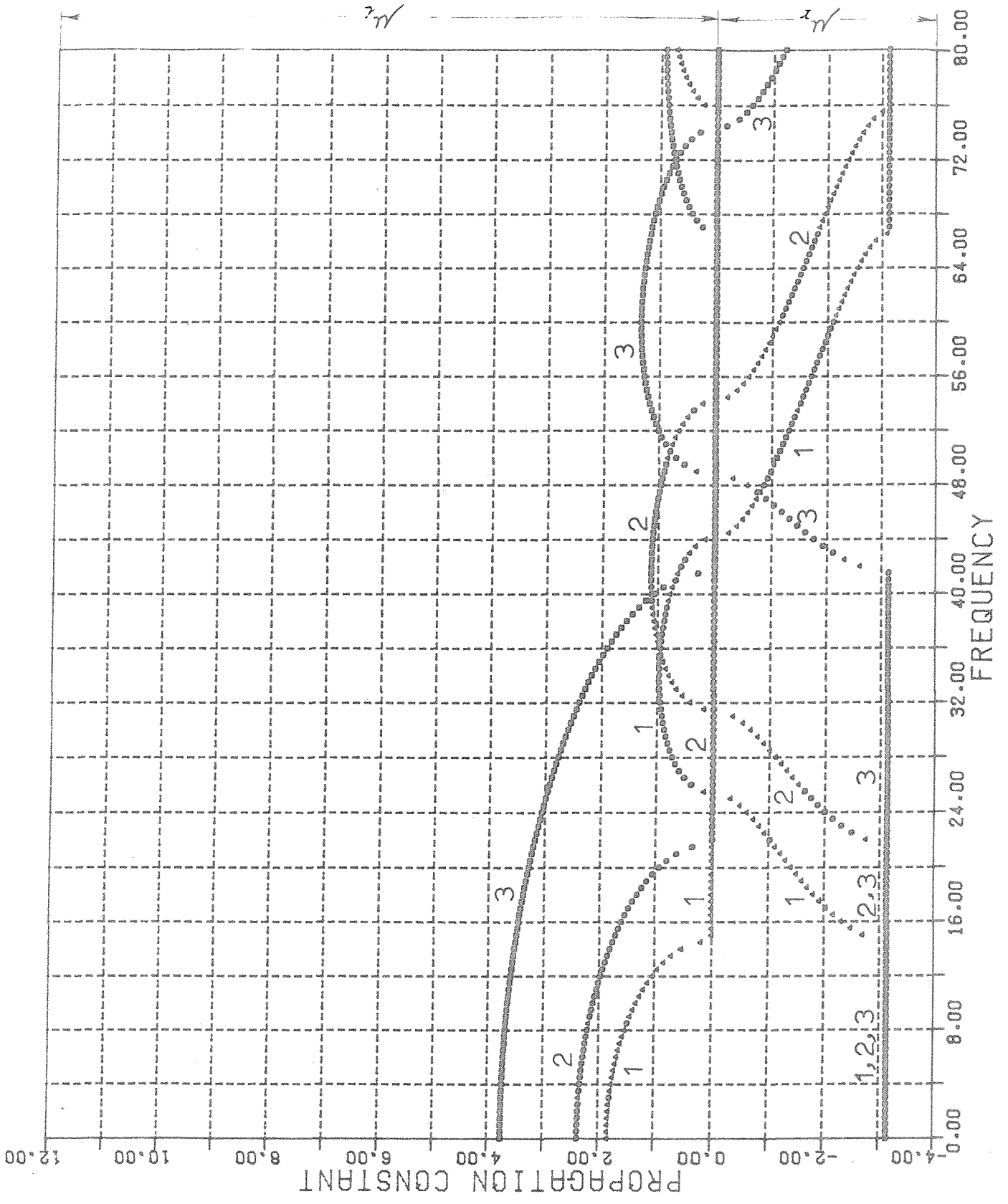

Figure 3.39. Variation of the real and imaginary parts of the propagation constants, for a two-dimensional periodic plate on simple line supports with rectangular cells($l_x/l_y=0.5$), for waves propagating along the X direction($\mu_y=0.0$) .

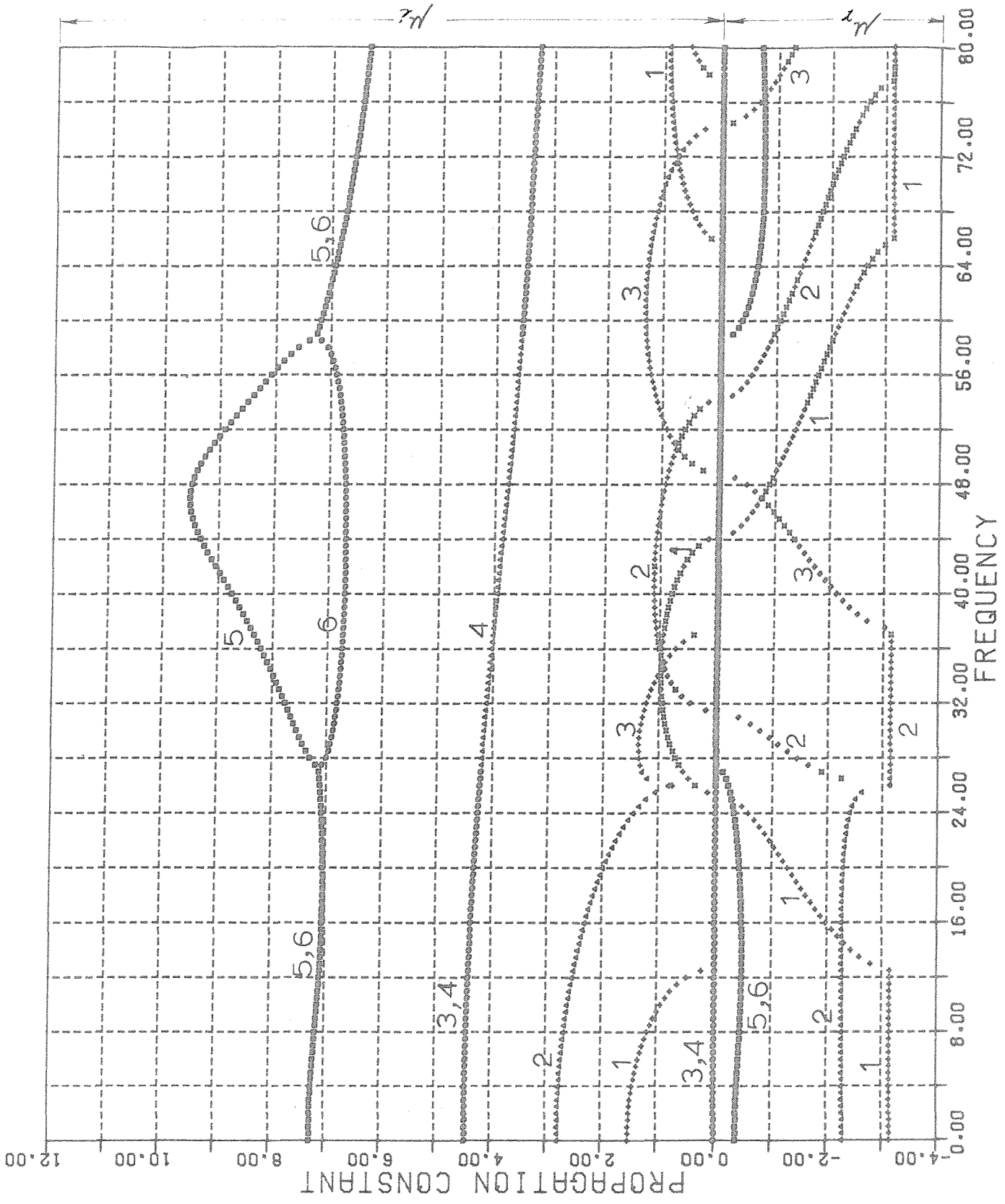

Figure 3.40. Variation of the real and imaginary parts of the propagation constants with frequency, for a two-dimensional periodic plate on simple line supports with rectangular cells($l_x/l_y=0.5$), for waves propagating along the preferred direction of propagation($\alpha=26.6^\circ$, $\mu_x=\mu_y$) .

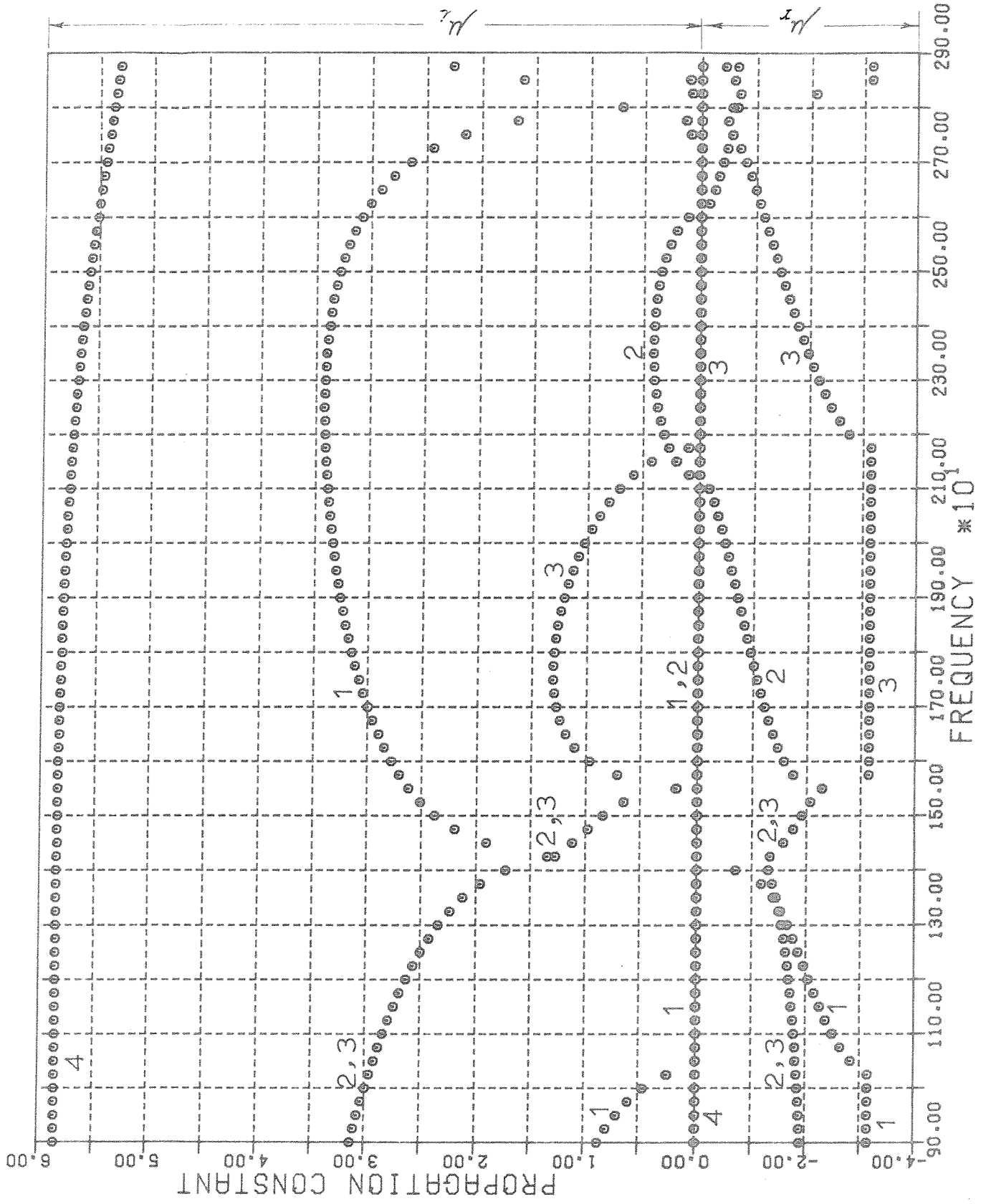

Figure 3.41. Variation of the real and imaginary parts of the propagation constants with frequency ,for the two-dimensional periodically stiffened plate shown in figure(3.12),for waves propagating along the preferred direction of propagation($\alpha = 26.6^{\circ}$, $\mu_x = \mu_y$) .

CHAPTER IV

THREE-DIMENSIONAL PERIODIC SYSTEMS

4.1 General

Periodic systems in three dimensions can be considered as an assemblage of cells (periods) joined together on all faces, edges and corners in identical ways to form the whole system as shown in figure (4.1). Typical examples of such systems are crystal structures in solid state physics and the modern modular type buildings. Waves can travel in these systems in two different manners, either as spherical waves or plane waves depending on the type of forces generating them. This analysis considers only plane wave-motion in three-dimensional periodic systems.

Consider a three-dimensional periodic system defined by three independent directions d_1, d_2 and d_3 parallel to the directions of the system's periodicity. Each cell (period) in the system can be identified by three numbers n_1, n_2 and n_3 defining its position along the d_1, d_2 and d_3 directions respectively, where the origin of the system is taken at the cell defined by $n_1 = n_2 = n_3 = 0$. A property ϕ can propagate as a wave, with wave number $\underline{a}$ and frequency ν, if the physical system admits a solution of the type

$$\phi_{n_1, n_2, n_3} = Ae^{2\pi i(\nu t - n_1 d_1 \ell_1 - n_2 d_2 \ell_2 - n_3 d_3 \ell_3)}$$

$$= Ae^{i(\omega t + n_1 \mu_1 + n_2 \mu_2 + n_3 \mu_3)} \qquad (4.1)$$

where

ϕ_{n_1, n_2, n_3} is the value of the property ϕ associated with cell n_1, n_2, n_3.

A is a constant, t the time, ν the frequency, ω the angular frequency, where

$$\omega = 2\pi\nu$$

ℓ_1, ℓ_2, ℓ_3 and a_1, a_2, a_3 are the dimensions of the cell and the components of the wave-number $\underline{a}$ along the d_1, d_2 and d_3 directions respectively.

μ_1, μ_2 and μ_3 are known as the propagation constants in the d_1, d_2 and d_3 directions, where

$$\begin{aligned} \mu_1 &= -2\pi a_1 \ell_1 \ , \\ \mu_2 &= -2\pi a_2 \ell_2 \ , \\ \mu_3 &= -2\pi a_3 \ell_3 \end{aligned} \tag{4.2}$$

For propagating waves, without attenuation, the propagation constants μ_1, μ_2 and μ_3 are real quantities. They represent the change in phase between adjacent cells in the d_1, d_2 and d_3 directions. Attenuating waves can be described by (4.1) where in this case μ_1, μ_2 and μ_3 will be complex quantities. Their real parts represent the change in phase while the imaginary parts represent the attenuation of the wave as it travels from one cell to the next in the d_1, d_2 and d_3 directions respectively.

From relation (4.1) it can be seen that the relation between the value of the property ϕ at any point in one cell n_1, n_2, n_3 and at the corresponding points in adjacent cells can be written as

$$\begin{aligned} \phi_{n_1+1,\ n_2,n_3} &= \phi_{n_1,n_2,n_3}\, e^{i\mu_1} \ , \\ \phi_{n_1,n_2+1,n_3} &= \phi_{n_1,n_2,n_3}\, e^{i\mu_2} \ , \\ \phi_{n_1,n_2,n_3+1} &= \phi_{n_1,n_2,n_3}\, e^{i\mu_3} \end{aligned} \tag{4.3}$$

For unattenuated waves, where μ_1, μ_2 and μ_3 are real quantities, relations (4.1) and (4.3) can be satisfied by using μ_1', μ_2' and μ_3' instead of μ_1, μ_2 and μ_3 where

$$\begin{aligned} \mu_1' &= \mu_1 \pm 2m_1\pi \ , \\ \mu_2' &= \mu_2 \pm 2m_2\pi \ , \\ \mu_3' &= \mu_3 \pm 2m_3\pi \end{aligned} \tag{4.4}$$

m_1, m_2 and m_3 are any integer numbers.

The equation of motion of the system (equation (4.21), Section 4.3) must yield the same values for ϕ and ω for given μ_1, μ_2 and μ_3 or equivalent μ_1', μ_2' and μ_3'. This means that the property ϕ and its frequency ω are periodic functions of the real μ_1, μ_2 and μ_3 with periods 2π. Therefore it is sufficient to examine the variation of the frequency of propagation ω with the real μ_1, μ_2 and μ_3 along the directions d_1, d_2 and d_3 inside one period (2π) only. The most suitable choice is

$$\begin{aligned} -\pi \leq \mu_1 \leq \pi \ , \\ -\pi \leq \mu_2 \leq \pi \ , \\ -\pi \leq \mu_3 \leq \pi \end{aligned} \qquad (4.5)$$

Similar to the one and two-dimensional systems, we must determine the boundaries to which the wave number $\underline{a}$ (and hence μ_1, μ_2 and μ_3) is to be confined to allow examining all possible propagating waves in all directions in the system and at the same time satisfy the condition (4.5). These restrictions on μ_1, μ_2 and μ_3 are for the same reasons discussed in Chapters II and III for the one and two-dimensional systems and should be observed when determining the wave-length or the direction of propagation. This will be discussed in the next section.

4.2 Reciprocal Cells and Zones in Three Dimensions

The discussion of reciprocal cells and zones given in Chapter III for the two-dimensional systems will be extended here to cover the three-dimensional case.

Zones to which the wave-number $\underline{a}$ (and hence μ_1, μ_2, and μ_3) is to be confined will be volumes in three dimensions and can be constructed in a similar manner as for the two-dimensional systems. This restriction should be observed when determining the direction of propagation or the wave-length λ_w, where

$$\lambda_w = 1/|\underline{a}| .$$

To construct the first (fundamental) zone for a three-dimensional system we will follow the procedure given in Section 3.2 for two-

dimensional systems. First construct the reciprocal cells and the reciprocal system for the three-dimensional system considered. The reciprocal cell is geometrically identical to the direct (original) cell describing the periodicity of the direct (original) system, but of dimensions that are the reciprocal of the corresponding dimensions in the direct cell. The reciprocal system is constructed by joining the reciprocal cells together such that the reciprocal system is geometrically identical to the direct system. Now taking the centre of one of the reciprocal cells as the origin of the zone, then the first zone is the smallest volume bounded by plane perpendicular bisectors of the lines from the origin to the centres of all neighbouring reciprocal cells. To illustrate this, consider a three-dimensional system having rectangular parallelpiped cells, figure (4.2a). Let ℓ_x, ℓ_y and ℓ_z be the dimensions of the cell along the three directions x, y and z defining the system. The first zone will be another rectangular parallelpiped with dimensions $1/\ell_x$, $1/\ell_y$ and $1/\ell_z$ with the origin at its centre as shown in figure (4.2b). The wave-number components, and hence the propagation constants μ_x, μ_y and μ_z, along the three directions x, y and z will be restricted as follows

$$
\begin{aligned}
-\frac{1}{2\ell_x} \leq a_x \leq \frac{1}{2\ell_x}, \qquad & -\pi \leq \mu_x \leq \pi \\
-\frac{1}{2\ell_y} \leq a_y \leq \frac{1}{2\ell_y}, \qquad & -\pi \leq \mu_y \leq \pi \\
-\frac{1}{2\ell_z} \leq a_z \leq \frac{1}{2\ell_z}, \qquad & -\pi \leq \mu_z \leq \pi
\end{aligned}
\tag{4.6}
$$

since $\mu_x = -2\pi a_x \ell_x$, $\mu_y = -2\pi a_y \ell_y$ and $\mu_z = -2\pi a_z \ell_z$. The shortest wavelength for waves travelling along the x, y or z directions will be

$$
\begin{aligned}
\lambda_x &= \frac{1}{|a_x|} = 2\ell_x, \\
\lambda_y &= \frac{1}{|a_y|} = 2\ell_y, \\
\lambda_z &= \frac{1}{|a_z|} = 2\ell_z
\end{aligned}
\tag{4.7}
$$

and the shortest wave-length λ_s for any wave travelling in the system

will correspond to a wave associated with the largest absolute value of the wave-number $\underline{a}$ inside the zone, hence

$$\lambda_s = \frac{1}{|\underline{a}|_{max}} = \frac{1}{\sqrt{|a_x|^2 + |a_y|^2 + |a_z|^2}}$$

$$= \frac{1}{\sqrt{(1/2\ell_x)^2 + (1/2\ell_y)^2 + (1/2\ell_z)^2}}$$

$$= \frac{2\ell_x \ell_y \ell_z}{\sqrt{\ell_x^2 + \ell_y^2 + \ell_z^2}} \qquad (4.8)$$

The directions of propagation of this wave can be defined by two angles α and β as shown in figure (4.3) where

$$\alpha = \pm \tan^{-1} \frac{a_y}{a_x} = \pm \tan^{-1} \frac{\ell_x}{\ell_y}$$

and

$$\beta = \pm \tan^{-1} \frac{\sqrt{a_x^2 + a_y^2}}{a_z} = \pm \tan^{-1} \frac{\ell_z \sqrt{\ell_x^2 + \ell_y^2}}{\ell_x \cdot \ell_y} \qquad (4.9)$$

4.3 Mathematical Formulation

Following the analysis for one and two-dimensional periodic systems, a three-dimensional periodic system can be considered as an assemblage of infinite number of identical cells joined together in identical manner on all sides, edges and corners, as shown in figure (4.1). A cell contains one period of the system. Using the finite element technique, a cell can be represented by a model with interior and boundary degrees of freedom. Let $\{q_I\}$, $\{F_I\}$ be the degrees of freedom and forces at the interior of the cell, $\{q_L\}$, $\{F_L\}$, $\{q_R\}$, $\{F_R\}$, $\{q_B\}$, $\{F_B\}$, $\{q_T\}$, $\{F_T\}$, $\{q_F\}$, $\{F_F\}$ and $\{q_N\}$, $\{F_N\}$ be the degrees of freedom and forces at the left, right, bottom, top, far and near faces of the cell; also let $\{q_{LB}\}$, $\{F_{LB}\}$, ..., etc., and $\{q_{LBN}\}$, $\{F_{LBN}\}$ ...., etc. be the degrees of freedom and forces at the edges and corners (common boundaries between the different faces of the cell) degrees of freedom as shown in figure (4.1b).

The linear equation of motion of the undamped cell is given by

$$([K] - \omega^2[M])\{q\} = \{F\} \tag{4.10}$$

where $[K]$ and $[M]$ are the stiffness and inertia matrices for the cell.

$\{q\}$ and $\{F\}$ are the nodal degrees of freedom and forces. The matrices $[K]$ and $[M]$ and the vectors $\{q\}$ and $\{F\}$ can be partitioned according to the interior, left, right, bottom, top, edges and corners degrees of freedom, hence,

$$[K] = \begin{bmatrix} K_{I,I} & K_{I,L} & \cdots & K_{I,RTN} \\ K_{L,I} & K_{L,L} & & \\ K_{R,I} & & & \\ K_{B,I} & & & \\ K_{T,I} & & & \\ K_{F,I} & & & \\ K_{N,I} & & & \\ K_{LB,I} & & & \\ K_{RB,I} & & & \\ K_{LT,I} & \text{symmetric} & & \\ K_{RT,I} & & & \\ K_{BF,I} & & & \\ K_{TF,I} & & & \\ K_{BN,I} & & & \\ K_{TN,I} & & & \\ K_{LF,I} & & & \\ K_{LN,I} & & & \\ K_{RF,I} & & & \\ K_{RN,I} & & & \\ K_{LBF,I} & & & \\ K_{RBF,I} & & & \\ K_{LTF,I} & & & \\ K_{LBN,I} & & & \\ K_{RTF,I} & & & \\ K_{RBN,I} & & & \\ K_{LTN,I} & & & \\ K_{RTN,I} & & & K_{RTN,RTN} \end{bmatrix}, \quad \{q\} = \begin{Bmatrix} q_I \\ q_L \\ q_R \\ q_B \\ q_T \\ q_F \\ q_N \\ q_{LB} \\ q_{RB} \\ q_{LB} \\ q_{RT} \\ q_{BF} \\ q_{TF} \\ q_{BN} \\ q_{TN} \\ q_{LF} \\ q_{LN} \\ q_{RT} \\ q_{RN} \\ q_{LBF} \\ q_{LTF} \\ q_{RBF} \\ q_{LBN} \\ q_{RTF} \\ q_{RBN} \\ q_{LTN} \\ q_{RTN} \end{Bmatrix} \tag{4.11}$$

Similar expressions can be written for $[M]$ and $\{F\}$.

Free waves propagate through infinite three-dimensional periodic systems (no external forces) when $\{F_I\}$ equal to zero. However the forces on the boundaries of the cell (forces of interaction between the cell and its neighbours) are not zero since they transmit the wave-motion from one cell to its neighbouring cells. This wave-motion is characterised by relating the degrees of freedom and equivalent nodal forces in one cell to the corresponding degrees of freedom and forces in adjacent cells. Let the suffix n_1, n_2, n_3 define the position of the cell along the three directions d_1, d_2 and d_3 defining the system, then we can write

$$
\begin{aligned}
\{F_L\}_{n_1+1,\, n_2,n_3} &= e^{i\mu_1}\{F_L\}_{n_1,n_2,n_3}\,, \\
\{q_L\}_{n_1+1,n_2,n_3} &= e^{i\mu_1}\{q_L\}_{n_1,n_2,n_3}\,, \\
\{F_B\}_{n_1,n_2+1,n_3} &= e^{i\mu_2}\{F_B\}_{n_1,n_2,n_3}\,, \\
\{q_B\}_{n_1,n_2+1,n_3} &= e^{i\mu_2}\{q_B\}_{n_1,n_3,n_3}\,, \\
\{F_F\}_{n_1,n_2,n_3+1} &= e^{i\mu_3}\{F_F\}_{n_1,n_2,n_3}\,, \\
\{q_F\}_{n_1,n_2,n_3+1} &= e^{i\mu_3}\{q_F\}_{n_1,n_2,n_3}\,, \\
\{F_{LB}\}_{n_1+1,n_2+1,n_3} &= e^{i(\mu_1+\mu_2)}\{F_{LB}\}_{n_1,n_2,n_3}\,, \\
\{q_{LB}\}_{n_1+1,n_2+1,n_3} &= e^{i(\mu_1+\mu_2)}\{q_{LB}\}_{n_1,n_2,n_3}\,, \\
\{F_{LBF}\}_{n_1+1,n_2+1,n_3+1} &= e^{i(\mu_1+\mu_2+\mu_3)}\{F_{LBF}\}_{n_1,n_2,n_3}\,, \\
\{q_{LBF}\}_{n_1+1,n_2+1,n_3+1} &= e^{i(\mu_1+\mu_2+\mu_3)}\{q_{LBF}\}_{n_1,n_2,n_3}
\end{aligned}
\qquad (4.12)
$$

etc....

For equilibrium of the interconnecting forces between cell n_1, n_2, n_3 and neighbouring cells, the sum of forces at the common boundaries between the cells must be zero and hence the following equilibrium conditions must be satisifed.

$$\{F_R\}_{n_1,n_2,n_3} + \{F_L\}_{n_1+1,n_2,n_3} = 0 \quad , \qquad \text{(Right face)}$$

$$\{F_T\}_{n_1,n_2,n_3} + \{F_B\}_{n_1,n_2+1,n_3} = 0 \quad , \qquad \text{(Top face)}$$

$$\{F_N\}_{n_1,n_2,n_3} + \{F_F\}_{n_1,n_2,n_3+1} = 0 \quad , \qquad \text{(Near face)}$$

$$\{F_{RT}\}_{n_1,n_2,n_3} + \{F_{LT}\}_{n_1+1,n_2,n_3} + \{F_{RB}\}_{n_1,n_2+1,n_3} + \{F_{LB}\}_{n_1+1,n_2+1,n_3} = 0 \quad ,$$

(edge RT)

$$\{F_{RTN}\}_{n_1,n_2,n_3} + \{F_{LTN}\}_{n_1+1,n_2,n_3} + \{F_{RTF}\}_{n_1,n_2+1,n_3} + \{F_{RBN}\}_{n_1,n_2,n_3+1}$$

$$+ \{F_{LBN}\}_{n_1+1,n_2+1,n_3} + \{F_{RBF}\}_{n_1,n_2+1,n_3+1} + \{F_{LTF}\}_{n_1+1,n_2,n_3+1}$$

$$+ \{F_{LBF}\}_{n_1+1,n_2+1,n_3+1} = 0 \qquad \text{(corner RTN)} \qquad (4.13)$$

Similar expressions can be written for the other edges and corners.

At the common boundaries between cell n_1,n_2,n_3 and neighbouring cells the displacements must be equal, hence

$$\begin{aligned}
\{q_R\}_{n_1,n_2,n_3} &= \{q_L\}_{n_1+1,n_2,n_3} \quad , \\
\{q_T\}_{n_1,n_2,n_3} &= \{q_B\}_{n_1,n_2+1,n_3} \quad , \\
\{q_N\}_{n_1,n_2,n_3} &= \{q_F\}_{n_1,n_2,n_3+1} \quad , \\
\{q_{RT}\}_{n_1,n_2,n_3} &= \{q_{LB}\}_{n_1+1,\ n_2+1,n_3} \quad , \\
\{q_{RTN}\}_{n_1,n_2,n_3} &= \{q_{LBF}\}_{n_1+1,\ n_2+1,n_3+1}
\end{aligned} \qquad (4.14)$$

etc.....

Substituting (4.12) into (4.13) and (4.14) the following relations between the forces and displacements on the boundaries of cell n_1,n_2,n_3 can be obtained (suffix n_1,n_2,n_3 are dropped since these relations hold for any cell).

$$
\begin{aligned}
&\{F_R\} + e^{i\mu_1}\{F_L\} = 0,\\
&\{F_T\} + e^{i\mu_2}\{F_B\} = 0,\\
&\{F_N\} + e^{i\mu_3}\{F_F\} = 0,\\
&\{F_{RT}\} + e^{i\mu_1}\{F_{LT}\} + e^{i\mu_2}\{F_{RB}\} + e^{i(\mu_1+\mu_2)}\{F_{LB}\} = 0,\\
&\{F_{TN}\} + e^{i\mu_2}\{F_{BN}\} + e^{i\mu_3}\{F_{TF}\} + e^{i(\mu_2+\mu_3)}\{F_{BF}\} = 0,\\
&\{F_{RN}\} + e^{i\mu_3}\{F_{RF}\} + e^{i\mu_1}\{F_{LN}\} + e^{i(\mu_3+\mu_1)}\{F_{LF}\} = 0,\\
&\{F_{RTN}\} + e^{i\mu_1}\{F_{LTN}\} + e^{i\mu_2}\{F_{RBN}\} + e^{i\mu_3}\{F_{RTF}\}\\
&\quad + e^{i(\mu_1+\mu_2)}\{F_{LBN}\} + e^{i(\mu_2+\mu_3)}\{F_{RBF}\} + e^{i(\mu_3+\mu_1)}\{F_{LTF}\}\\
&\quad + e^{i(\mu_1+\mu_2+\mu_3)}\{F_{LBF}\} = 0
\end{aligned}
\tag{4.15}
$$

Also

$$
\begin{aligned}
&\begin{Bmatrix} q_R\\ q_{RB}\\ q_{RF}\\ q_{RBF}\end{Bmatrix} = e^{i\mu_1}\begin{Bmatrix} q_L\\ q_{LB}\\ q_{LF}\\ q_{LBF}\end{Bmatrix}, \qquad \begin{Bmatrix} q_T\\ q_{TF}\\ q_{LT}\\ q_{LTF}\end{Bmatrix} = e^{i\mu_2}\begin{Bmatrix} q_B\\ q_{BF}\\ q_{LB}\\ q_{LBF}\end{Bmatrix}\\
&\begin{Bmatrix} q_N\\ q_{BN}\\ q_{LN}\\ q_{LBN}\end{Bmatrix} = e^{i\mu_3}\begin{Bmatrix} q_F\\ q_{BF}\\ q_{LF}\\ q_{LBF}\end{Bmatrix}, \qquad \begin{Bmatrix} q_{RT}\\ q_{RTF}\end{Bmatrix} = e^{i(\mu_1+\mu_2)}\begin{Bmatrix} q_{LB}\\ q_{LBF}\end{Bmatrix}\\
&\begin{Bmatrix} q_{TN}\\ q_{LTN}\end{Bmatrix} = e^{i(\mu_2+\mu_3)}\begin{Bmatrix} q_{BF}\\ q_{LBF}\end{Bmatrix}, \qquad \begin{Bmatrix} q_{RN}\\ q_{RBN}\end{Bmatrix} = e^{i(\mu_3+\mu_1)}\begin{Bmatrix} q_{LF}\\ q_{LBF}\end{Bmatrix}\\
&\{q_{RTN}\} = e^{i(\mu_1+\mu_2+\mu_3)}\{q_{LBF}\}
\end{aligned}
\tag{4.16}
$$

Relations (4.16) can be used to write the relation between the degrees of freedom in the cell in the matrix form

$$\{q\} = [W]\{\bar{q}\} \tag{4.17}$$

where

$\{q\}$ is given by (4.11),

$$\{\bar{q}\} = \lfloor q_I \quad q_L \quad q_B \quad q_F \quad q_{LB} \quad q_{BF} \quad q_{LF} \quad q_{LBF} \rfloor^T \tag{4.18}$$

$[W] =$

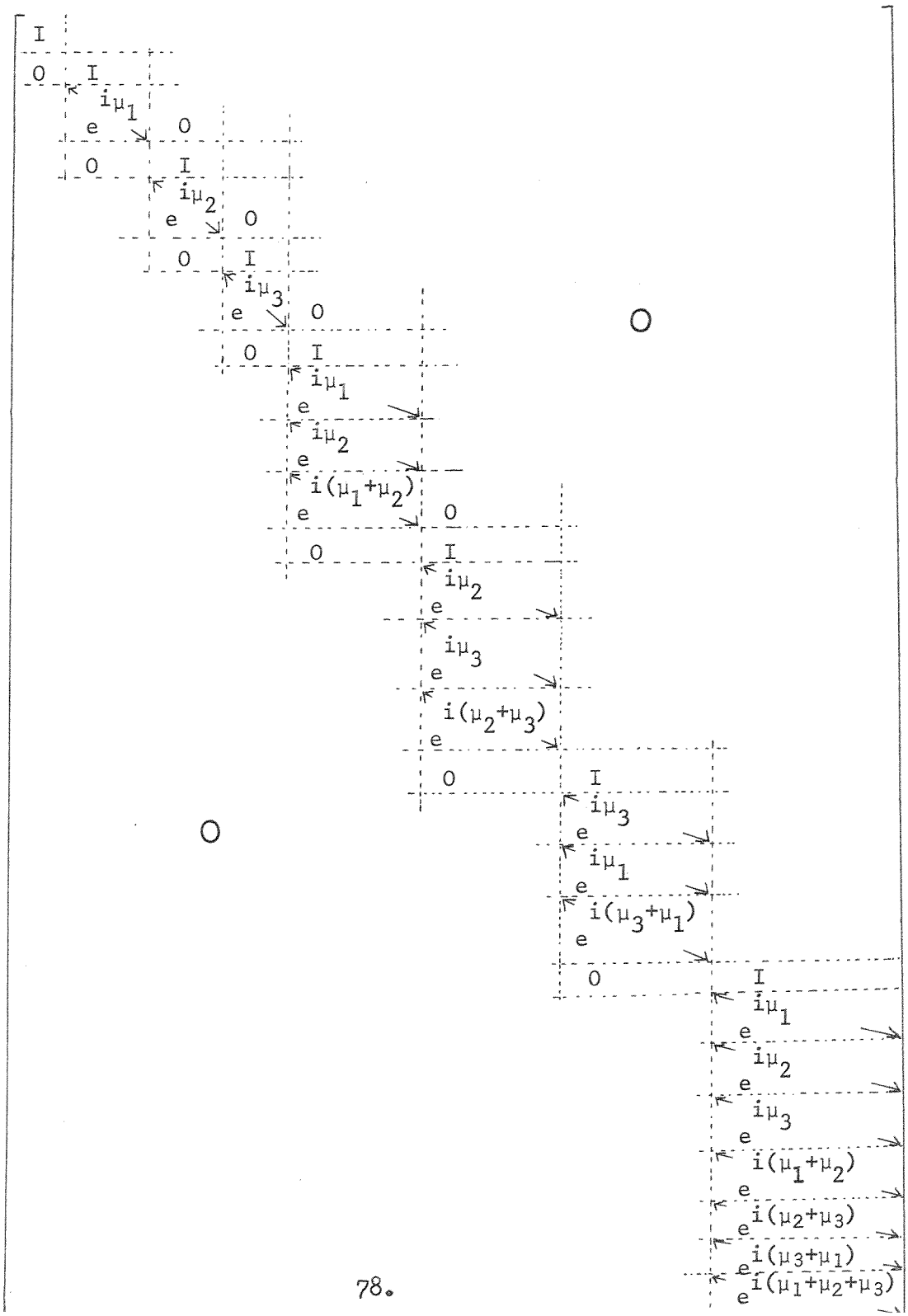

(4.19)

Also the equilibrium conditions (4.15) and the condition

$$\{F_I\} = 0$$

can be written in the matrix form

$$[W']\{F\} = 0 \tag{4.20}$$

where $\{F\}$ are the forces in equation (4.10). The matrix $[W']$ is identical to the transpose of the matrix $[W]$ given by (4.19) while replacing $e^{i\mu' s}$ by $e^{-i\mu' s}$.

Substituting (4.17) and (4.20) into equation (4.10) results in an equation of the form

$$([\bar{K}(\mu_1, \mu_2, \mu_3) - \omega^2 \bar{M}(\mu_1, \mu_2, \mu_3)]\{\bar{q}\} = 0 \tag{4.21}$$

The matrices $[\bar{K}]$ and $[\bar{M}]$ are complex matrices given by

$$\begin{aligned} [\bar{K}] &= [W'][K][W], \\ [\bar{M}] &= [W'][M][W]. \end{aligned} \tag{4.22}$$

$[K]$ and $[M]$ are the matrices in equation (4.10). Equation (4.21) represents an eigenvalue problem in ω for given values of μ_1, μ_2 and μ_3. For real values of the wave-number $\underline{a}$, and hence μ_1, μ_2 and μ_3, equation (4.21) can be rearranged to give a real symmetric eigenvalue problem in ω. This will be discussed in Section 4.4. Also it can be reformulated to give an eigenvalue problem in μ_1, μ_2 and μ_3 for a given value of ω, where μ_1, μ_2 and μ_3 will be generally complex quantities. This will be discussed in Section 4.5.

4.4 Formulation for the Real Propagation Constants

Similar to the one and two-dimensional periodic systems, waves can propagate, without attenuation, in three-dimensional periodic systems when the wave-number $\underline{a}$, and hence μ_1, μ_2 and μ_3, are real quantities. In this case the frequency of propagation is a periodic function of the propagation constants μ_1, μ_2 and μ_3 with periods 2π. Therefore it is enough to study the variation of the frequency ω with μ_1, μ_2 and μ_3 within one period only. In this case equation (4.21) can be formulated

to give a real symmetric eigenvalue problem in ω for given real values of μ_1, μ_2 and μ_3.

Equation (4.21) can be written in the form

$$([\bar{K}^r] + i[\bar{K}^i] - \omega^2([\bar{M}^r] + i[\bar{M}^i]))\{\bar{q}^r + i\bar{q}^i\} = 0 \tag{4.23}$$

where $[\bar{K}^r]$, $[\bar{K}^i]$, $[\bar{M}^r]$, $[\bar{M}^i]$ and $\bar{q}^r$, $\bar{q}^i$ are the real and imaginary parts of $[\bar{K}]$, $[\bar{M}]$ and $\{\bar{q}\}$ respectively. Separating the real and imaginary parts of (4.23) and combining the two sets of equations together gives

$$\left(\begin{bmatrix} \bar{K}^r & -\bar{K}^i \\ \bar{K}^i & \bar{K}^r \end{bmatrix} - \omega^2 \begin{bmatrix} \bar{M}^r & -\bar{M}^i \\ \bar{M}^i & \bar{M}^r \end{bmatrix} \right) \begin{Bmatrix} \bar{q}^r \\ \bar{q}^i \end{Bmatrix} = 0 \tag{4.24}$$

From (4.19) and (4.20) it can be seen that for real values of μ_1, μ_2 and μ_3 we can write

$$[W'] = [W^*]^T \tag{4.25}$$

where * denotes the complex conjugate, and hence the matrices $[\bar{K}]$ and $[\bar{M}]$ (given by (4.22)) are Hermitian, i.e.,

$$\begin{aligned} [\bar{K}^*]^T &= [\bar{K}] \\ [\bar{M}^*]^T &= [\bar{M}] \end{aligned} \tag{4.26}$$

Therefore equation (4.24) represents a real symmetric eigenvalue problem since

$$\begin{aligned} [\bar{K}^i] &= -[\bar{K}^i]^T \\ [\bar{M}^i] &= -[\bar{M}^i]^T \end{aligned} \tag{4.27}$$

This equation can be solved for various values of the propagation constants μ_1, μ_2 and μ_3 (as real quantities) to find the corresponding frequencies of propagation and associated wave-forms. Appendix A gives the method of solving this eigenvalue problem.

4.4.1 Computer programs

A general computer program has been written to represent one period (cell) of any three-dimensional periodic system by a finite element model and form the matrices in equation (4.24) for given real values of the propagation constants μ_1, μ_2 and μ_3. Then the problem is solved to find the corresponding frequencies of propagation and associated wave-forms. The basic flow diagram for the computational procedure is given in Appendix B.

4.4.2 Applications

Consider the flexural wave-motion in a three-dimensional structure consisting of infinite flat plates intersecting orthogonally at equal distances in three directions. This can be regarded as an idealisation of a modular type building. Figure (4.4) shows a finite element idealisation of the cell chosen to represent one period of the structure (the cell is idealised by 12 plate elements). The plate element and data values used in the analysis are given in Appendix D7. The system is defined by the three directions x, y and z parallel to the sides of the cells. The dimensions of the cell (periodic lengths) along these directions are

$$\ell_x = \ell_y = \ell_z = 1.0$$

Therefore the first zone to which the wave-number $\underline{a}$ (and hence the propagation constants μ_x, μ_y and μ_z) will be confined is a rectangular parallelpiped of dimensions $1/\ell_x$, $1/\ell_y$ and $1/\ell_z$ with the origin of the zone at its centre. This was discussed in Section 4.2.

First the problem is solved to find the variation of the frequency of propagation with the propagation constants μ_x, μ_y and μ_z. In polar representation, where the length and direction of the vector from the centre of the plot represents the value of the frequency and the direction of propagation, propagation bands will be volumes enclosed between surfaces which are the upper and lower bounding frequencies for the bands. These surfaces are the frequencies corresponding to zero wave-number ($\underline{a} = 0.0$, $\mu_x = \mu_y = \mu_z = 0.0$) and wave-numbers terminating on the boundaries of the first zone. These surfaces can be defined by lines of constant α and lines of constant β where α and β are the two angles defining the direction of propagation as shown in figure (4.3).

Figure (4.5) shows the upper and lower bounding frequency surfaces for the first propagation band. The upper bounding frequency is the same for all directions of propagation and corresponds to a wave-number $\underline{a}$ equal to zero. This is shown as the spherical surface, figure (4.5d). The lower bounding frequencies surface (corresponding to wave-numbers terminating on the boundaries of the zone) is shown in figures (4.5a,b,c) as the projection of the surface seen from the x, y and z directions. From these figures it is clear that the lower bounding frequencies for the band vary with directions of propagation and the lowest frequency occurs in a direction given by (4.9), hence

$$\alpha = \tan^{-1}\frac{\ell_x}{\ell_y} = \tan^{-1}\left(\frac{1.0}{1.0}\right) = 45^\circ,$$

$$\beta = \tan^{-1}\frac{\ell_z\sqrt{\ell_x^2 + \ell_y^2}}{\ell_x\ell_y} = \tan^{-1}(\sqrt{2}) = 54.74^\circ$$

which can be called the preferred direction of propagation in this case. The wave-length corresponding to this frequency is the shortest wave-length λ_s given by (4.8), hence

$$\lambda_s = \frac{2\ell_x\ell_y\ell_z}{\sqrt{\ell_x^2 + \ell_y^2 + \ell_z^2}} = \frac{2}{\sqrt{3}} = 1.55.$$

Plotting the variation of the frequency of propagation with the wave-number $\underline{a}$ (or with μ_x, μ_y and μ_z) for waves propagating in a certain direction will result in curves similar to those obtained for one-dimensional periodic systems. Figure (4.6) shows the frequency variation for waves travelling along the preferred direction of propagation. This direction is defined by the two angles

$$\alpha = 45^\circ \quad \text{and} \quad \beta = 54.74^\circ$$

(along this direction we have $\mu_x = \mu_y = \mu_z$).

The frequency variation is shown for the first four propagation bands, where the first and second propagation bands coincided with each other (this is because the cell representing the system is cubic).

From these results we can conclude that propagation occurs in three dimensional periodic systems within some frequency bands only. The width of these bands vary with the direction of propagation. Similar to the one and two-dimensional periodic systems, waves with frequencies within these bands propagate in the system without attenuation while waves with frequencies outside these bands are attenuating waves.

The second example is similar to the previous one except that the dimensions of the cells (distances between the plates in the x, y and z directions) are

$$\ell_x = 1.0, \quad \ell_y = 1.5 \quad \text{and} \quad \ell_z = 2.0.$$

Figure (4.7) shows the upper and lower limiting surfaces for the first propagation band. The upper bound is the spherical surface (figure (4.7d)) corresponding to a wave-number $\underline{a} = 0.0$, while the lower bound is the surface shown in figures (4.7a, b and c) corresponding to wave-numbers terminating on the boundaries of the first zone. Similar to the previous example the width of the first band is largest along the direction given by (4.9) where,

$$\alpha = \tan^{-1} \frac{\ell_x}{\ell_y} = 33.69^\circ,$$

$$\beta = \tan^{-1} \frac{\ell_z \sqrt{\ell_x^2 + \ell_y^2}}{\ell_x \ell_y} = 67.41^\circ$$

which is the preferred direction of propagation in this case.

Figure (4.8) shows the variation of the frequency of propagation with the propagation constants along this direction (where $\mu_x = \mu_y = \mu_z$).

Comparing these results with the previous example shows that the width of the propagation bands is dependent on the dimensions of the cells (the first band is wider along the larger dimension). Otherwise the behaviour of the structure is similar to the first case.

4.5 Formulation for the Complex Propagation Constants

The formulation given in Chapter III, Section 3.5 for the two-dimensional systems can be followed here to reformulate equation (4.21) to give an eigenvalue problem in μ_1, μ_2 and μ_3 for a given frequency ω, and hence the wave-number/frequency variation can be examined at any frequency whether within the propagation bands where the propagation constants are real quantities, or outside the bands where the propagation constants (or the wave-number) are complex quantities. Now for a given value of the frequency ω, equation (4.21) can be written in the form

$$[D(\mu_1, \mu_2, \mu_3)]\{\bar{q}\} = 0 \tag{4.28}$$

where

$$[D] = [\bar{K}] - \omega^2[\bar{M}]$$

$$= \begin{bmatrix} D_{I,I} & D_{I,L} & D_{I,B} & D_{I,F} & D_{I,LB} & D_{I,BF} & D_{I,LF} & D_{I,LBF} \\ D_{L,I} & & & & & & & \\ D_{B,I} & & & & & & & \\ D_{F,I} & & & & & & & \\ D_{LB,I} & & & & & & & \\ D_{BF,I} & & & & & & & \\ D_{LF,I} & & & & & & & \\ D_{LBF,I} & & & & & & & D_{LBF,LBF} \end{bmatrix} \tag{4.29}$$

and $$\{\bar{q}\} = \lfloor q_I \quad q_L \quad q_B \quad q_F \quad q_{LB} \quad q_{BF} \quad q_{LF} \quad q_{LBF} \rfloor^T \tag{4.30}$$

From the first relation in equation (4.28) we can write

$$\{q_I\} = -D_{I,I}^{-1}(D_{I,L}\{q_L\} + D_{I,B}\{q_B\} + D_{I,F}\{q_F\} + D_{I,LB}\{q_{LB}\} +$$

$$D_{I,BF}\{q_{BF}\} + D_{I,LF}\{q_{LF}\} + D_{I,LBF}\{q_{LBF}\}) \tag{4.31}$$

Substituting (4.31) into (4.28) to eliminate $\{q_I\}$ gives an equation of the form

$$\left[\bar{D}(\mu_1,\mu_2,\mu_3)\right]\{\bar{q}'\} = 0 \qquad (4.32)$$

where

$$\{\bar{q}'\} = \left\lfloor q_L \quad q_B \quad q_F \quad q_{LB} \quad q_{BF} \quad q_{LF} \quad q_{LBF} \right\rfloor^T \qquad (4.33)$$

The matrix $[\bar{D}]$ is given by

$$[\bar{D}] = [T'][D][T] \qquad (4.34)$$

The matrices $[T]$ and $[T']$ are given by

$$[T] = \begin{bmatrix} E\,D_{I,L} & E\,D_{I,B} & E\,D_{I,F} & E\,D_{I,LB} & E\,D_{I,BF} & E\,D_{I,LF} & E\,D_{I,LBF} \\ I & 0 & 0 & 0 & 0 & 0 & 0 \\ 0 & I & 0 & 0 & 0 & 0 & 0 \\ 0 & 0 & I & 0 & 0 & 0 & 0 \\ 0 & 0 & 0 & I & 0 & 0 & 0 \\ 0 & 0 & 0 & 0 & I & 0 & 0 \\ 0 & 0 & 0 & 0 & 0 & I & 0 \\ 0 & 0 & 0 & 0 & 0 & 0 & I \end{bmatrix} \qquad (4.35)$$

$$[T'] = \begin{bmatrix} D_{L,I}\,E & I & 0 & 0 & 0 & 0 & 0 & 0 \\ D_{B,I}\,E & 0 & I & 0 & 0 & 0 & 0 & 0 \\ D_{F,I}\,E & 0 & 0 & I & 0 & 0 & 0 & 0 \\ D_{LB,I}\,E & 0 & 0 & 0 & I & 0 & 0 & 0 \\ D_{BF,I}\,E & 0 & 0 & 0 & 0 & I & 0 & 0 \\ D_{LF,I}\,E & 0 & 0 & 0 & 0 & 0 & I & 0 \\ D_{LBF,I}\,E & 0 & 0 & 0 & 0 & 0 & 0 & I \end{bmatrix} \qquad (4.36)$$

where

$$E = -D_{I,I}^{-1} \qquad (4.37)$$

From (4.22) we can see that the propagation constants μ_1, μ_2 and μ_3 appear in the elements of the matrices $[\bar{K}]$ and $[\bar{M}]$, and hence in $[D]$ and $[\bar{D}]$, only in the form

$$e^{\pm i\mu_1}, \quad e^{\pm i\mu_2}, \quad e^{\pm i\mu_3}, \quad e^{\pm i(\mu_1 \pm \mu_2)}, \quad e^{\pm i(\mu_2 \pm \mu_3)},$$

$$e^{\pm i(\mu_3 \pm \mu_1)}, \quad \text{and} \quad e^{\pm i(\mu_1 \pm \mu_2 \pm \mu_3)}$$

(notice that the matrix $D_{I,I}$, and hence $D^{-1}_{I,I}$, is a real symmetric matrix).

Now similar to the two-dimensional analysis given in Section 3.5, if the ratios between μ_1, μ_2 and μ_3 give rational numbers, then they can be written in the form

$$\begin{aligned} \mu_1 &= n_1\mu \,, \\ \mu_2 &= n_2\mu \,, \\ \mu_3 &= n_3\mu \end{aligned} \tag{4.38}$$

Substituting (4.38) into equation (4.32) and putting $e^{i\mu} = \lambda$ gives

$$[\bar{D}(\lambda)]\{\bar{q}\} = 0 \tag{4.39}$$

The elements of the matrix $[\bar{D}]$ in equation (4.39) contain λ raised to positive and negative integer powers only. If the largest negative power of λ in (4.39) is $-m$ then multiplying (4.39) by λ^m will eliminate all negative powers of λ. Therefore (4.39) can be written in the form (after multiplying by λ^{-m} and rearranging terms)

$$([A_n]\lambda^n + [A_{n-1}]\lambda^{n-1} + \ldots + [A_o])\{\bar{q}\} = 0 \tag{4.40}$$

where n is a positive integer number.

The matrices $[A_i]$ are of the same order as the matrix $[\bar{D}]$ where each matrix contains only the elements of $[\bar{D}]$ which are multiplied by λ^i. Equation (4.40) represents a general eigenvalue problem of order n. This can be formulated and solved for various values of the frequency ω and a given direction of propagation such that the ratios between the propagation constants μ_1, μ_2 and μ_3 satisfy the condition (4.38). For example, along the d_1, d_2 and d_3 directions where $\mu_2 = \mu_3 = 0$, $\mu_3 = \mu_1 = 0$ and $\mu_1 = \mu_2 = 0$ or along the preferred direction of propagation where $\mu_1 = \mu_2 = \mu_3$, etc. Methods of solving the eigenvalue problem (4.40) are discussed in Appendix A.

4.5.1 Computer programs

A general computer program has been written to represent one cell (period) of any three-dimensional periodic system by a finite element model and to form the eigenvalue problem (4.40) for various values of the frequency ω and a certain direction of propagation satisfying the conditions (4.38). This eigenvalue problem is then solved using one of the methods discussed in Appendix A. The basic flow diagram for the computational procedure is given in Appendix B.

4.5.2 Applications

The same two examples used in Section 4.4.2 are used here. The same finite element idealisation for the cell representing the structure, fig. (4.4), is used. First the case of plates with cubic cells ($\ell_x = \ell_y = \ell_z = 1.0$) is considered. Wave propagation along the preferred direction of propagation is investigated. This direction is defined by

$$\alpha = 45^o \quad \text{and} \quad \beta = 54.74^o$$

Along this direction we have

$$\mu_x = \mu_y = \mu_z$$

and hence relations (4.38) become

$$\mu_1 = \mu_x = \mu \ ,$$

$$\mu_2 = \mu_y = \mu \ ,$$

$$\mu_3 = \mu_z = \mu$$

Figure (4.9) shows two possible waves that can exist at any frequency (numbered 1 and 2 in the figure). The propagation constants for wave 1 are purely real within the frequency range $25.8 \leqslant \omega \leqslant 37.25$ which is the first propagation band. This band coincides with the results produced in Section 4.4.2, figure (4.6). Outside this band the propagation constants are complex quantities with real parts equal to zero or $\pm\pi$. Waves corresponding to these propagation constants are attenuated waves. The propagation constants for the second wave (wave number 2 in the figure) have non-zero imaginary parts (within the plotted frequency range) and hence it represents attenuated waves.

Figure (4.10) shows the variation of the propagation constants with frequency for waves travelling along the preferred direction of propagation for the second example ($\ell_x = 1.0$, $\ell_y = 1.5$, $\ell_z = 2.0$). This direction is defined by

$$\alpha = 33.69^{\circ}, \qquad \beta = 67.41^{\circ}$$

(where $\mu_x = \mu_y = \mu_z$).

Three different waves are shown in the figure (numbered 1, 2 and 3). For each wave there are bands of frequencies where the propagation constant is a real quantity (propagation bands). Also we can notice the overlapping between the higher bands. Similar to the previous example, these propagation bands coincide with the results produced in Section 4.4.2, figure (4.8).

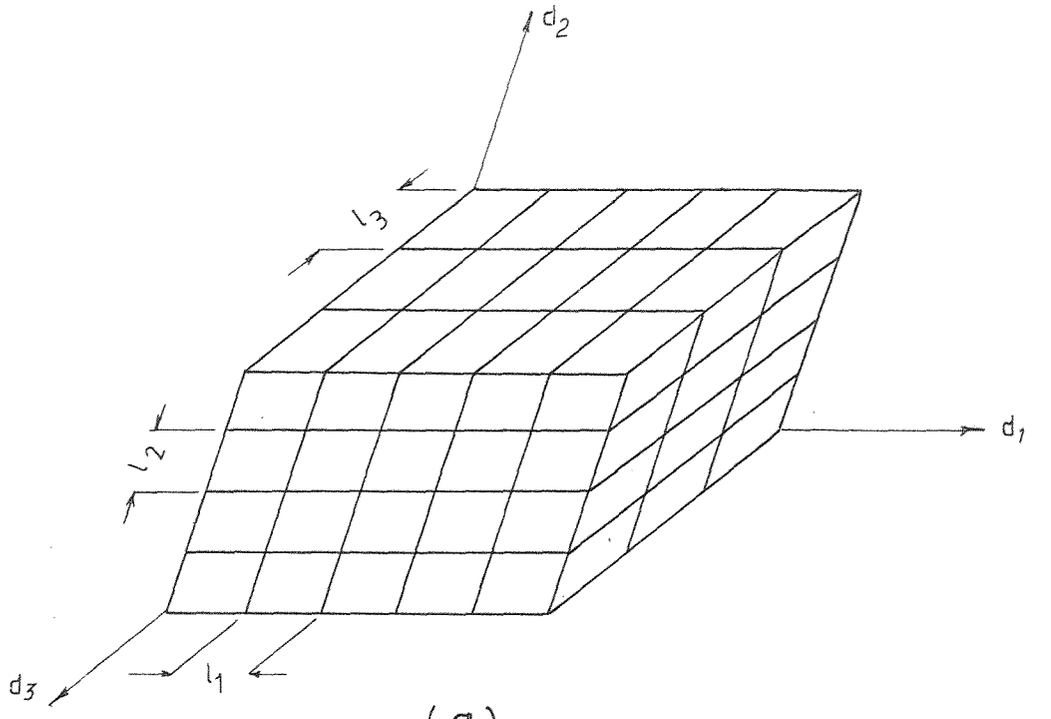

(a)

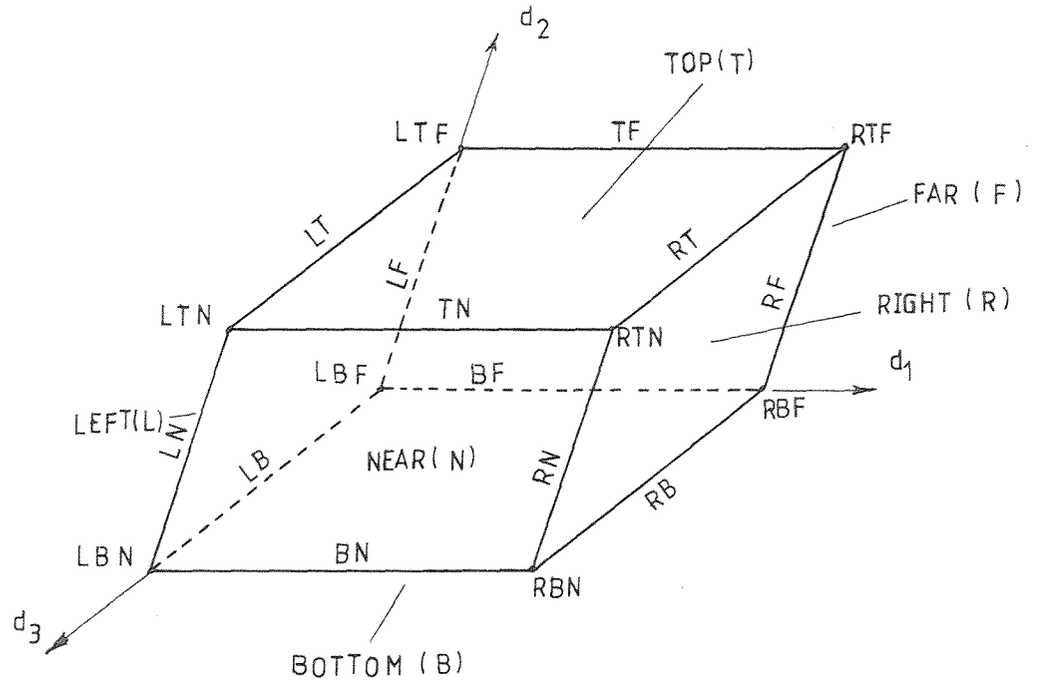

(b)

Figure 4.1.(a)Schematic diagram of a three-dimensional periodic system;
(b)Single cell representing the system .

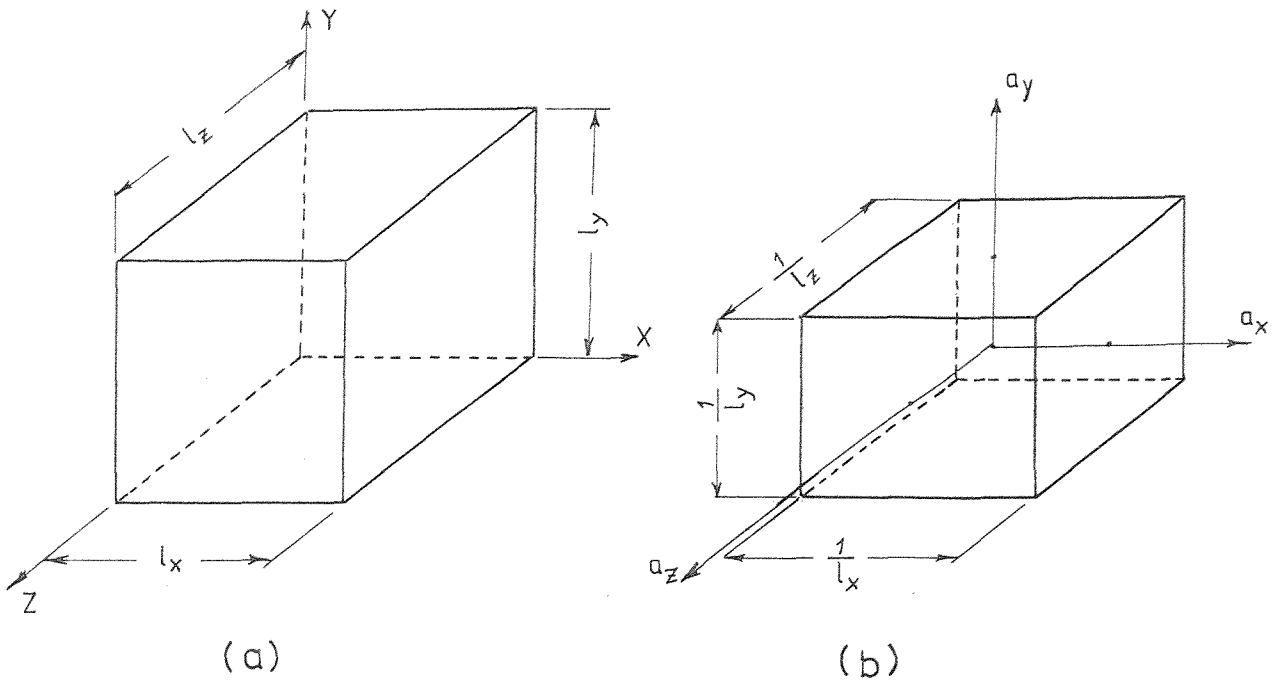

Figure 4.2.(a)Single cell of a three-dimensional periodic system with rectangular parallelepiped cells;(b)the first zone to which the wave number $\underline{a}$ will be confined .

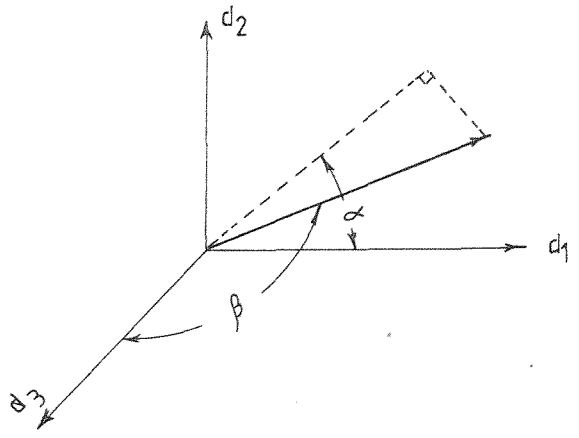

Figure 4.3. The two angles defining the direction of propagation in a three-dimensional periodic system.

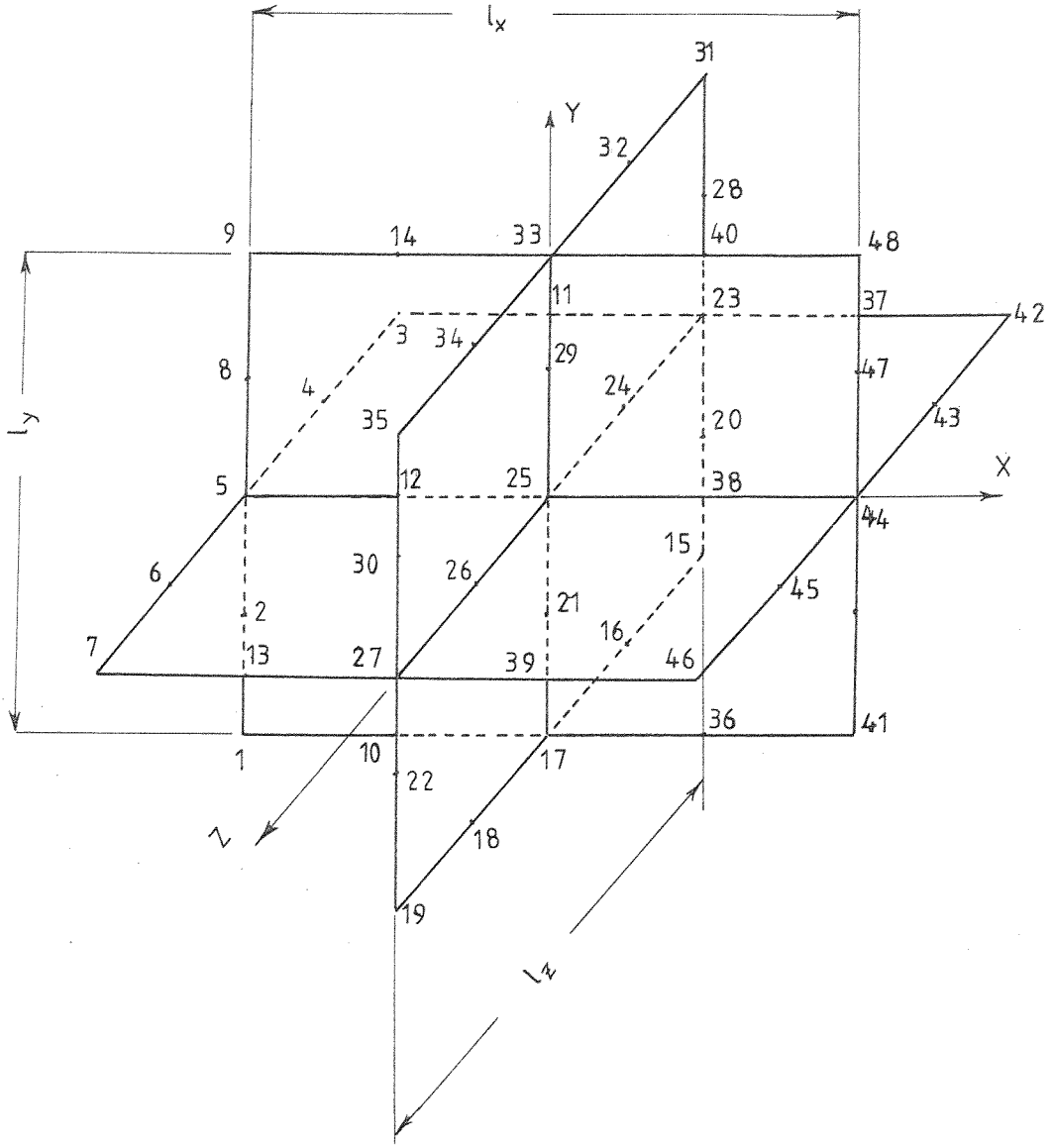

Figure 4.4. Finite element idealisation of the single cell representing an infinite three-dimensional periodic system formed of flat plates .

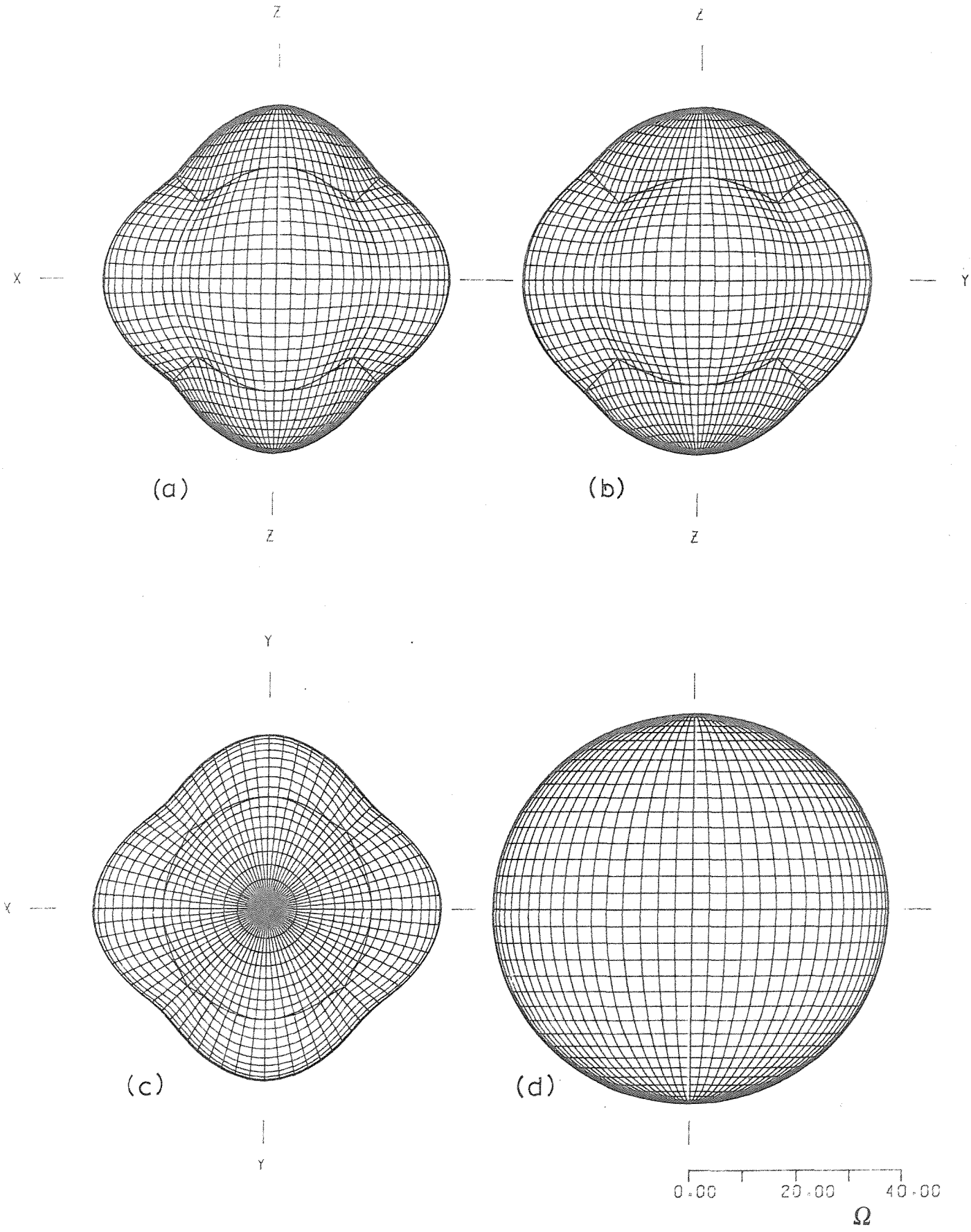

Figure 4.5. Upper and lower bounding surfaces of the first propagation band for the three-dimensional periodic plates of figure(4.4); $l_x=l_y=l_z$;(a),(b),(c)lower bound;(d)upper bound.

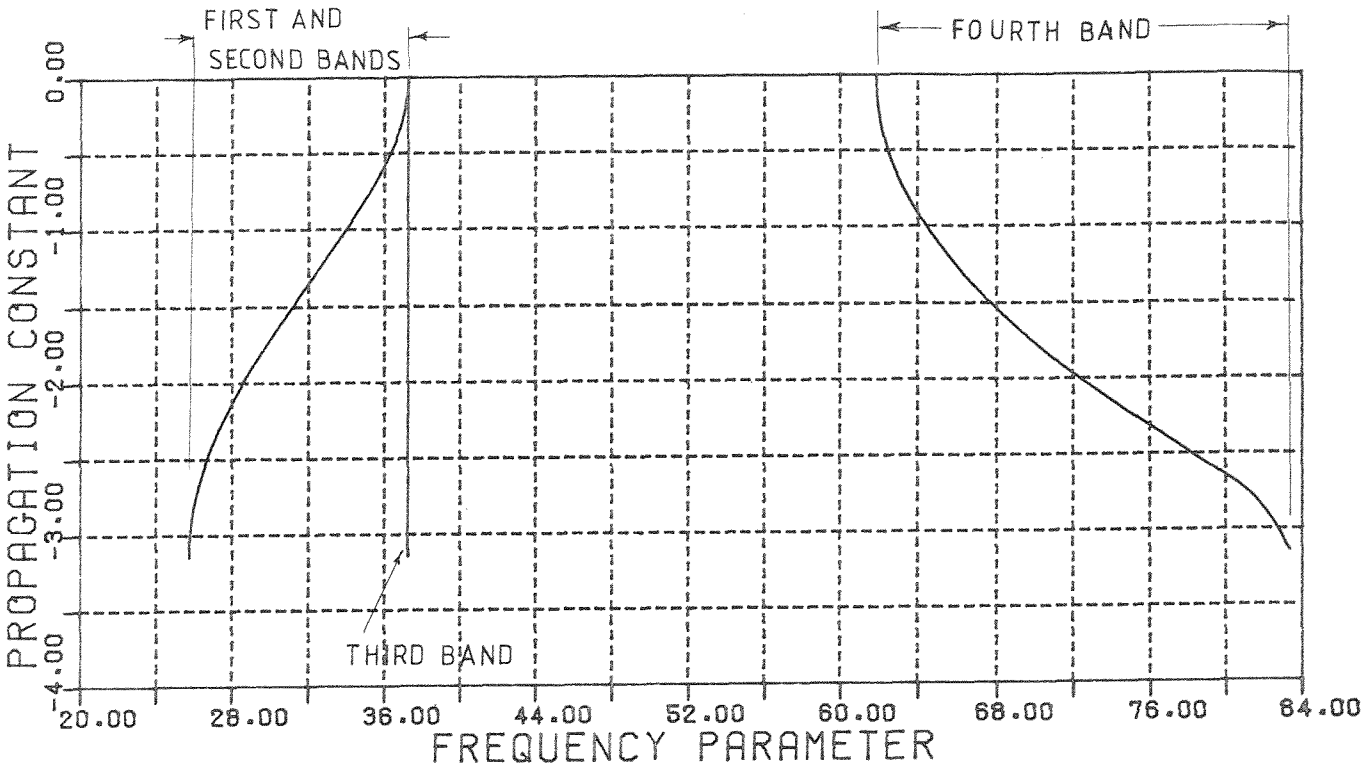

Figure 4.6. Variation of the real propagation constants with frequency, for the three-dimensional periodic plates of figure(4.4), $l_x=l_y=l_z$, for waves propagating along a direction defined by $\alpha=45.^\circ$, $\beta=54.7^\circ$ ($\mu_x=\mu_y=\mu_z$) .

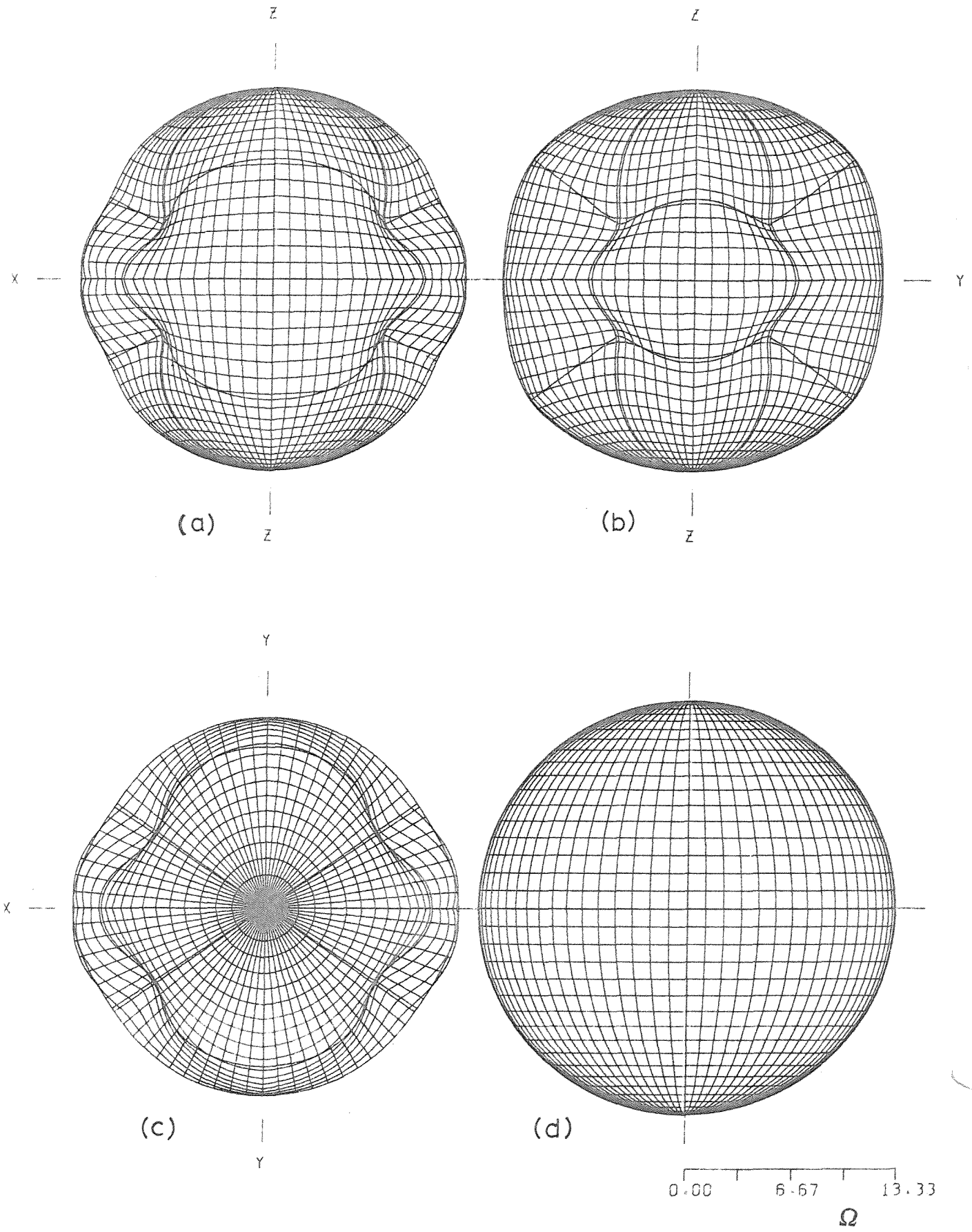

Figure 4.7. Upper and lower bounding surfaces of the first propagation band, for the three-dimensional periodic plates of figure(4.4); $l_x:l_y:l_z$=1.0:1.5:2.0;(a),(b),(c)lower bound;(d)upper bound

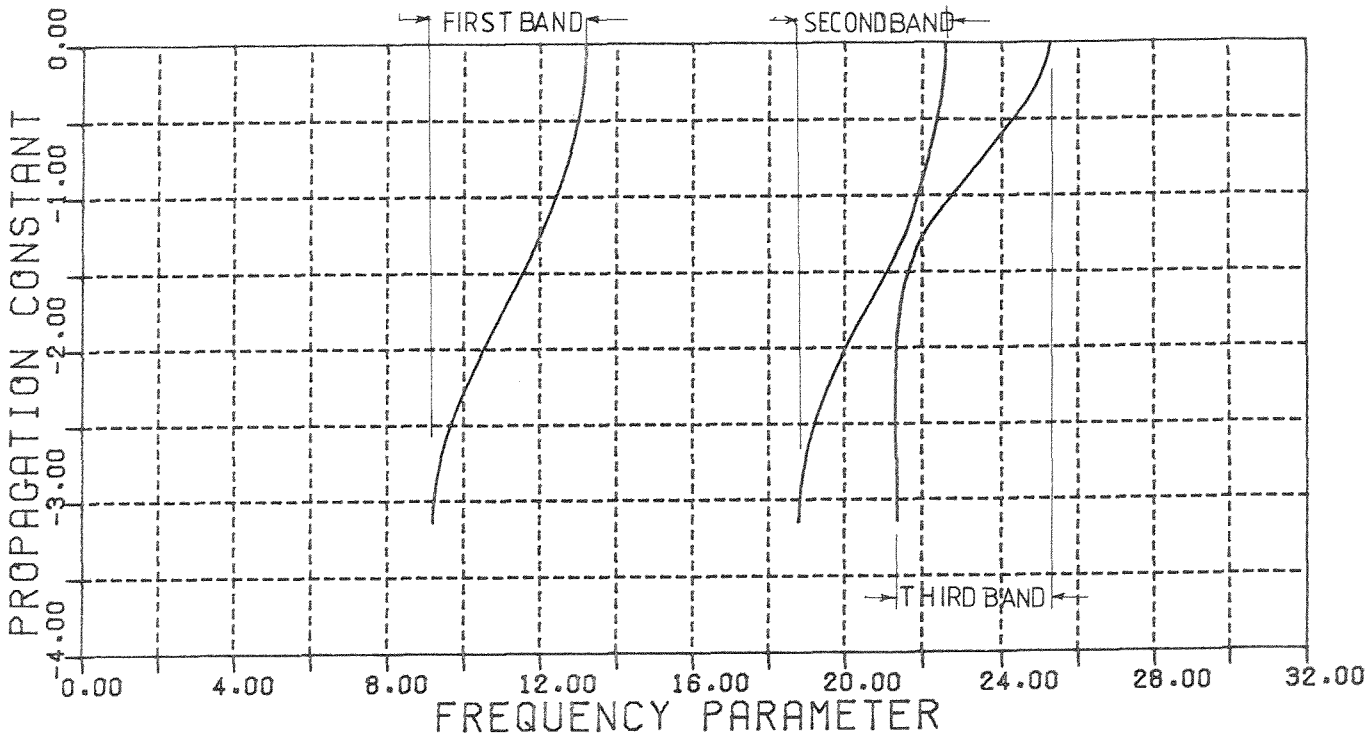

Figure 4.8. Variation of the real propagation constants with frequency, for the three-dimensional periodic plates of figure (4.4), $l_x : l_y : l_z = 1. : 1.5 : 2.$, for waves propagating along a direction defined by $\alpha = 33.7^\circ$, $\beta = 67.4^\circ$ ($\mu_x = \mu_y = \mu_z$).

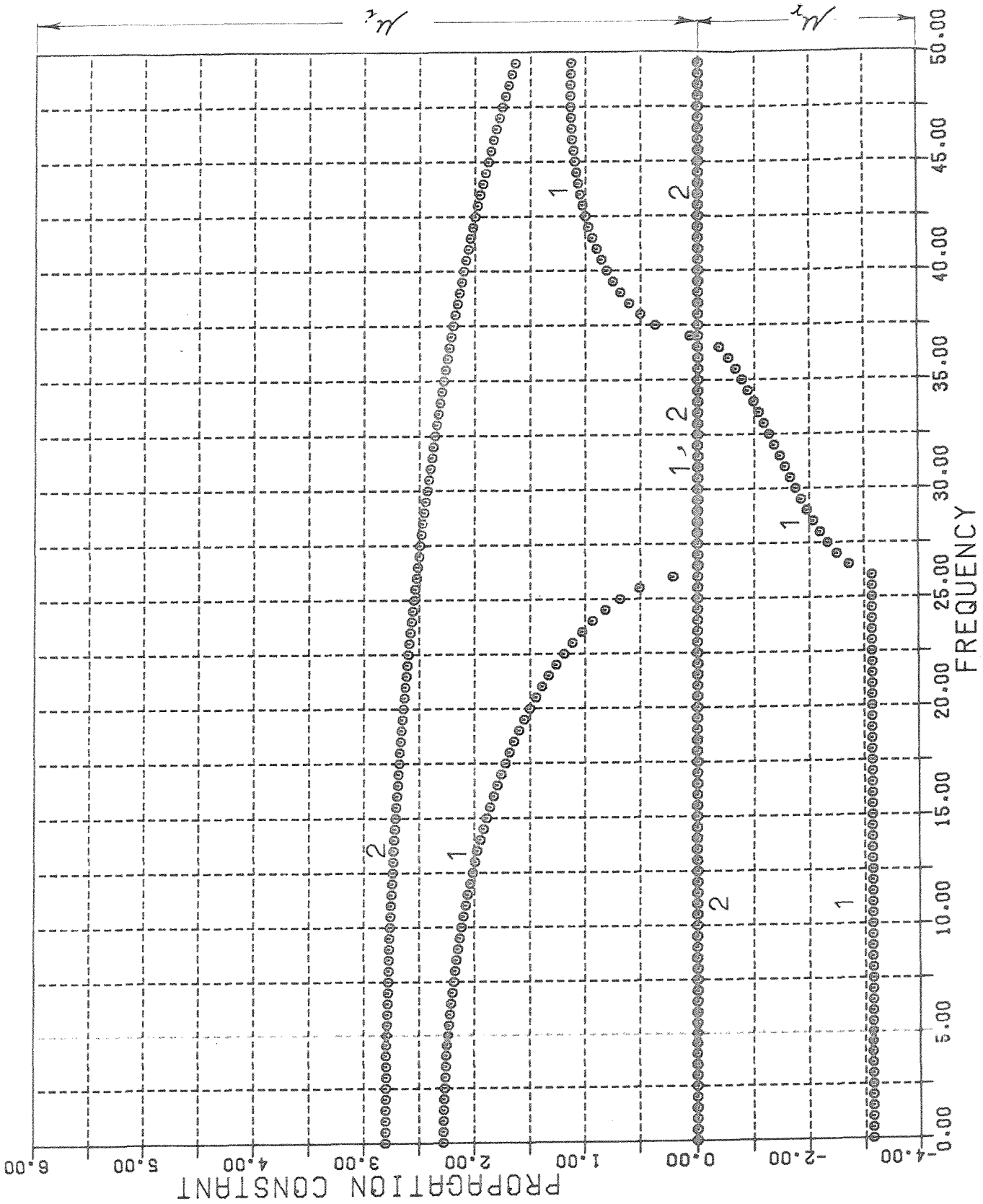

Figure 4.9. Variation of the real and imaginary parts of the propagation constants with frequency, for the thre-dimensional periodic plates of figure (4.4), $l_x = l_y = l_z$, for waves propagating along a direction defined by $\alpha = 45^\circ$, $\beta = 54.7^\circ$ ($\mu_x = \mu_y = \mu_z$).

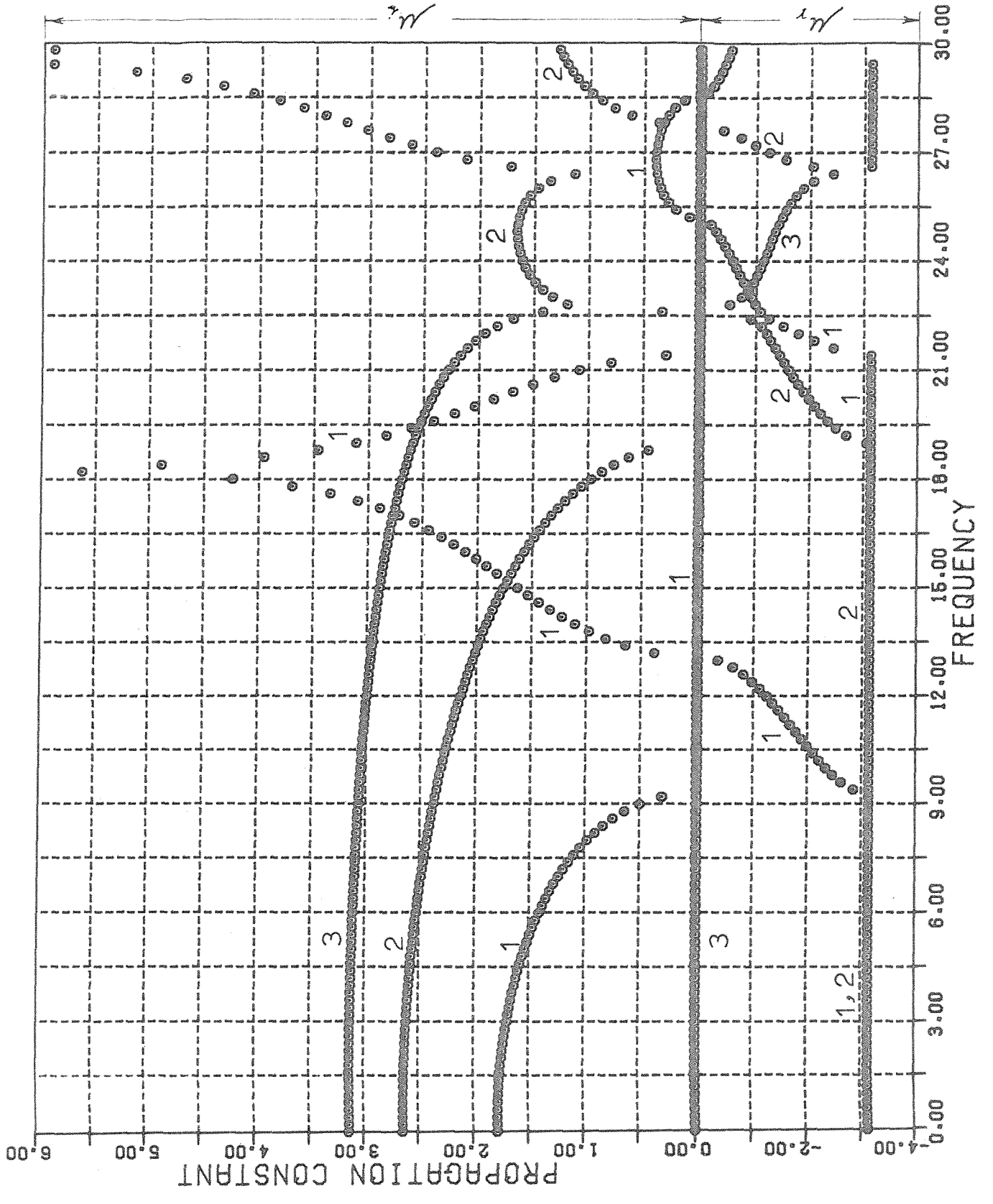

Figure 4.10. Variation of the real and imaginary parts of the propagation constants with frequency, for the three-dimensional periodic plates of figure (4.4) ($l_x : l_y : l_z = 1.0 : 1.5 : 2.0$), for waves propagating along a direction defined by $\alpha = 33.7^\circ$, $\beta = 67.4^\circ$ ($\mu_x = \mu_y = \mu_z$).

CHAPTER V

RESPONSE OF STRUCTURES TO CONVECTED RANDOM PRESSURE FIELDS

5.1 General

The response of a general structure (periodic or non-periodic) to random forces can be calculated using the standard modal method of analysis. This requires modelling the whole structure and finding its natural frequencies and associated normal modes. For the analysis of complex structures using digital computers, such a procedure needs a lot of time and effort for modelling and data preparation. Also the computer time, and storage, required for the analysis can be very large. High modal density and some types of structural damping increase the complexity of the modal analysis |35, 37|.

Many complex structures consist of identical (or nearly so) repetitive units (cells) joined together in a similar manner such as periodically stiffened plates and beams in one and two dimensions. Finding the response of such structures to homogeneous random fields can be greatly simplified if their periodic nature is utilised.

The forced vibration of one-dimensional periodic structures has been recently studied by Mead and Sen-Gupta |29, 30|, Sen-Gupta |57| and Mead and Pujara |34|. They showed that the response of a finite damped periodic structure can be estimated from the response of the infinite structure. For a beam type structure consisting of five periods they find that its average response is very close to the response of the infinite structure while its maximum response is no more than 50% above the response of the infinite structure. Similar results have been obtained experimentally |43|. Lindberg and Olson |24|, Olson |44| and Orris and Petyt |47| used the finite element method to find the response of one-dimensional periodic structures to random pressure fields.

In this chapter a method is presented for using the finite element technique and the periodic structure approach to find the response of any one or two-dimensional periodic structure to random, homogeneous pressure fields. This formulation has the advantage that it can easily analyse any complex periodic structure where only one period of the structure need

be considered. No previous knowledge of the natural frequencies and associated normal modes of the structure is required. Also increased modal density or any type of damping in the structure add no further complication to the analysis.

This analysis is based on the assumption that the structure is considered infinitely periodic in one or two dimensions and that the random excitation can be considered as a sum of harmonic sinusoidally distributed components. The total response of the structure is the sum of the responses due to each of these components acting upon the structure separately. Due to the periodic nature of the structure, the response at any point in one cell (period) of the structure is equal to the response at the corresponding points in other cells multiplied by a phase difference equal to that between the components of the excitation field acting upon the structure at these points.

Most of the computation in this chapter will be concerned with the calculation of the frequency response function, which is the response of the structure to a convected harmonic field with unit amplitude.

5.2 Types of Excitation Fields Considered

In this chapter the response of one and two-dimensional periodic structures to frozen convected random pressure fields and general random homogeneous pressure fields is considered. The response to such pressure fields can be described as follows.

a) Response to frozen convected random pressure fields (acoustic plane wave field)

These are pressure fields that convect over the structure in a certain direction with a constant velocity U_p without change in wave-form. They can be analysed into a continuous frequency spectrum of harmonic components where each component is associated with a wave-number $\underline{a}$ (or $\underline{\kappa}$) given by

$$\underline{a} = \nu/U_p = \frac{\omega}{2\pi U_p} \tag{5.1}$$

or

$$\underline{\kappa} = \frac{\omega}{U_p}$$

where ν is the frequency, ω the angular frequency and $\underline{\kappa}$ is the angular

wave-number where

$$\underline{\kappa} = 2\pi\underline{a}. \tag{5.3}$$

The power spectral density of a response quantity ϕ at any point $\underline{r}$ is given by

$$S_\phi(\underline{r}, \omega) = S_p(\underline{r}, \omega)\,|\phi(\underline{r}, \omega)|^2 \tag{5.4}$$

where $S_p(\underline{r}, \omega)$ is the power spectral density of the pressure field.

$\phi(\underline{r}, \omega)$ is the wave receptance function. It represents the response of the structure at point $\underline{r}$ due to a harmonic wave with unit amplitude, frequency ω and wave-number $\underline{\kappa}$.

The mean square response in the frequency band

$$0 < \omega < \omega_1$$

is given by

$$\sigma_m^2 = \int_0^{\omega_1} S_p(\underline{r}, \omega)\,|\phi(\underline{r}, \omega)|^2 d\omega \tag{5.5}$$

b) Response to general random homogeneous pressure fields.

These fields can be described by a continuous frequency spectrum of harmonic components where each component is associated with a continuous spectrum of wave-numbers (e.g., boundary layer pressure field or diffused sound field). The power spectral density of the response at any point $\underline{r}$ is given by

$$S_\phi(\underline{r}, \omega, \underline{\kappa}) = S_p(\underline{r}, \omega, \underline{\kappa})\,|\phi(\underline{r}, \omega, \underline{\kappa})|^2 \tag{5.6}$$

where $S_p(\underline{r}, \omega, \underline{\kappa})$ is the power spectral density of the pressure field.

The mean square response in the frequency band

$$0 < \omega < \omega_1$$

is given by

$$\sigma_m^2 = \int_0^{\omega_1} \int_0^{\infty} S_p(\underline{r}, \omega, \underline{\kappa}) |\phi(\underline{r}\ \omega, \underline{\kappa})|^2 \, d\kappa d\omega \qquad (5.7)$$

The wave receptance function $\phi(\underline{r}, \omega)$ or $\phi(\underline{r}, \omega, \underline{\kappa})$ can be calculated by means of a finite element analysis. This will be investigated in Sections 5.3 and 5.4.

For a detailed discussion of such pressure fields see |34, 67|.

A typical example of a general random homogeneous pressure field is the boundary layer pressure field. The wave number-frequency spectrum of this field is the double Fourier transform of its space time cross-correlation function |34, 67|. For the calculation of the response of periodic systems, such a field can be expressed in the form

$$S_p(\varepsilon, \Omega) = \frac{S_p(\Omega)}{\pi} \left[\frac{b(CV/\Omega)\{(1 + b^2) + (\varepsilon CV/\Omega)^2\}}{\{b^2 + (1 - \varepsilon CV/\Omega)^2\}\{b^2 + (1 + \varepsilon CV/\Omega)^2\}} \right] \qquad (5.8)$$

(See |34| for the mathematical derivation of this expression)

where

CV : the non-dimensional convection velocity where $\frac{\omega \ell}{U_p} = \frac{\Omega}{CV}$

Ω : the non-dimensional frequency

ε : $= -\kappa.\ell$ where κ is the angular wave-number and ℓ is the periodic length of the structure subjected to the pressure field

b : boundary layer decay parameter

U_p : convection velocity

$S_p(\Omega)$: the power spectral density of the pressure at any point in the field

It should be noted here that the second term in the numerator between the brackets [ ] in (5.8) is (CV/Ω) and not (Ω/CV) as given in |34|.

5.3 Mathematical Formulation for One-dimensional Periodic Systems

Consider a one-dimensional periodic system composed of an infinite number of identical cells (periods) joined together in identical manner, figure (2.1a). Using the finite element technique a cell can be described by a model coupled to its neighbours on either side by a certain number of degrees of freedom and forces, figure (2.1b). The linear equation of

motion of the cell can be written in the form

$$([K] + i\omega[C] - \omega^2[M])\{q\} = \{F\} \tag{5.9}$$

where

$[K]$, $[C]$ and $[M]$ are the stiffness, damping and inertia matrices for the cell,

$\{q\}$ and $\{F\}$ are the degrees of freedom and forces at the different nodes in the cell.

The matrices $[K]$, $[C]$ and $[M]$ and the vectors $\{q\}$ and $\{F\}$ can be partitioned according to the interior, left and right degrees of freedom in the cell, figure (2.1b), hence

$$[K] = \begin{bmatrix} K_{I,I} & K_{I,L} & K_{I,R} \\ K_{L,I} & K_{L,L} & K_{L,R} \\ K_{R,I} & K_{R,L} & K_{R,R} \end{bmatrix} \tag{5.10}$$

Similar expressions can be written for $[M]$ and $[C]$,

$$\{q\} = \begin{Bmatrix} q_I \\ q_L \\ q_R \end{Bmatrix}, \qquad \{F\} = \begin{Bmatrix} F_I \\ F_L \\ F_R \end{Bmatrix}^e + \begin{Bmatrix} 0 \\ F_L \\ F_R \end{Bmatrix}^b \tag{5.11}$$

where e and b denote the exterior and boundary forces respectively.

The boundary forces are the forces of interaction between the cell and its neighbours due to the wave-motion in the structure.

Now consider a harmonic pressure wave with unit amplitude, frequency ω and wave-number $\underline{\kappa}$ propagating across the structure (from left to right). This can be written in the form

$$P(\underline{r}, t) = e^{i(\omega t - \underline{\kappa}\cdot\underline{r})} \tag{5.12}$$

The exterior forces acting on the cells are due to this pressure field and hence the relation between these forces at any point in one cell n and the corresponding point in adjacent cell $n + 1$ can be written as

$$\{F\}^e_{n+1} = \{F\}^e_n e^{-i\underline{\kappa}.\underline{\ell}} = \{F_n\}^e e^{i\varepsilon} \tag{5.13}$$

where

$$\varepsilon = -\underline{\kappa}.\underline{\ell} \tag{5.14}$$

ℓ is the length of the cell (periodic length).

As this pressure wave propagates across the structure it will induce a wave-motion in the structure propagating in the same direction and with the same wave-form as the pressure wave. Therefore the relation between the degrees of freedom and boundary forces at any point in cell n and the corresponding point in cell n+1 is similar to relation (5.13), hence

$$\begin{aligned} \{F_L\}^b_{n+1} &= e^{i\varepsilon}\{F_L\}^b_n \ , \\ \{q_L\}_{n+1} &= e^{i\varepsilon}\{q_L\}_n \end{aligned} \tag{5.15}$$

At the common boundary between cell n and cell n+1 the displacements and exterior forces must be equal while the boundary (interior) forces in equilibrium, hence

$$\begin{aligned} \{q_L\}_{n+1} &= \{q_R\}_n \ , \\ \{F_L\}^e_{n+1} &= \{F_R\}^e_n \ , \\ \{F_L\}^b_{n+1} &= -\{F_R\}^b_n \end{aligned} \tag{5.16}$$

Substituting (5.16) into (5.12) and (5.15) gives

$$\begin{aligned} \{F_R\}^e_n &= e^{i\varepsilon}\{F_L\}^e_n \ , \\ \{F_R\}^b_n &= -e^{i\varepsilon}\{F_L\}^b_n \ , \\ \{q_R\}_n &= e^{i\varepsilon}\{q_L\}_n \end{aligned} \tag{5.17}$$

Relations (5.17) are the same for any cell, and hence the suffix n can be dropped. These relations can be substituted into equation (5.9) to eliminate the forces $\{F_L\}^b$, $\{F_R\}^b$ and $\{F_R\}^e$ and the displacements $\{q_R\}$. This will result in an equation of the form

$$\left(\left[\bar{K}(\varepsilon)\right] + i\omega\left[\bar{C}(\varepsilon)\right] - \omega^2\left[\bar{M}(\varepsilon)\right]\right)\begin{Bmatrix} q_I \\ q_L \end{Bmatrix} = \begin{Bmatrix} F_I(\varepsilon) \\ 2F_L(\varepsilon) \end{Bmatrix}^e \tag{5.18}$$

The matrices $[\bar{K}]$, $[\bar{C}]$ and $[\bar{M}]$ are defined in a similar manner which coincide with the definitions of $[\bar{K}]$ and $[\bar{M}]$ given by (2.16) in Chapter II, Section 2.2.

For most engineering structures the damping matrix $[C]$ can be linearly related to the stiffness and inertia matrices. For aircraft structures it is usual to take

$$\omega\left[C(\varepsilon)\right] = \eta\left[K(\varepsilon)\right] \tag{5.19}$$

where η is called the material loss factor.

However, some times, a different loss factor is assumed for different elements.

The solution of (5.18) is

$$\begin{Bmatrix} q_I \\ q_L \end{Bmatrix} = \left[\left[\bar{K}(\varepsilon)\right] + i\omega\left[\bar{C}(\varepsilon)\right] - \omega^2\left[\bar{M}(\varepsilon)\right]\right]^{-1} \begin{Bmatrix} F_I(\varepsilon) \\ 2F_L(\varepsilon) \end{Bmatrix}^e \tag{5.20}$$

The displacements $\{q_R\}$ are then obtained from equation (5.17).

Equation (5.18) can be formed and solved for different values of the frequency ω and wave-numbers $\underline{\kappa}$ given by (5.2). The response quantities $\{q\}$ can then be substituted in equations (5.4) and (5.5) to find the power spectral density of the response and the mean square response. Also it can be solved for various values of the frequency ω and wave-numbers $\underline{\kappa}$ to find the power spectral density and the mean square response given by equations (5.6) and (5.7).

If the damping is ignored, equation (5.18) can be written in the form

$$(\bar{K}^r + i\bar{K}^i - \omega^2(\bar{M}^r + i\bar{M}^i))\{\bar{q}^r + i\bar{q}^i\} = \{F^r + iF^i\}^e \tag{5.21}$$

Separating the real and imaginary parts and combining the two sets together gives

$$\left(\begin{bmatrix} \bar{K}^r & -\bar{K}^i \\ \bar{K}^i & \bar{K}^r \end{bmatrix} - \omega^2\begin{bmatrix} \bar{M}^r & -\bar{M}^i \\ \bar{M}^i & \bar{M}^r \end{bmatrix}\right)\begin{Bmatrix} \bar{q}^r \\ \bar{q}^i \end{Bmatrix} = \begin{Bmatrix} F^r \\ F^i \end{Bmatrix}^e \tag{5.22}$$

or
$$[D]\{q\} = \{F\}. \tag{5.23}$$

Since the matrices $[\bar{K}]$ and $[\bar{M}]$ are Hermitian, then

$$[\bar{K}^i] = -[\bar{K}^i]^T, \qquad [\bar{M}^i] = -[\bar{M}^i]^T \tag{5.24}$$

Therefore the matrix $[D]$ in equation (5.23) is real and symmetric.

5.4 Mathematical Formulation for Two-dimensional Periodic Systems

Consider a two-dimensional periodic system composed of an infinite number of identical cells joined together in identical manner, figure (3.5a). Using the finite element technique a cell can be represented by a model coupled to its neighbours on all sides and corners, figure (3.5b). The linear equation of motion of the cell is given by equation (5.9), namely,

$$([K] + i\omega[C] - \omega^2[M])\{q\} = \{F\}.$$

The matrices $[K]$, $[C]$ and $[M]$ can be partitioned according to the interior, left, right, bottom, top and corners degrees of freedom in the cell as given by (3.8) (Chapter III, Section 3.3).

The vectors $\{q\}$ and $\{F\}$ can be written as

$$\{q\} = \begin{Bmatrix} q_I \\ q_L \\ q_R \\ q_B \\ q_T \\ q_{LB} \\ q_{LT} \\ q_{RB} \\ q_{RT} \end{Bmatrix}, \qquad \{F\} = \begin{Bmatrix} F_I \\ F_L \\ F_R \\ F_B \\ F_T \\ F_{LB} \\ F_{LT} \\ F_{RB} \\ F_{RT} \end{Bmatrix}^e + \begin{Bmatrix} 0 \\ F_L \\ F_R \\ F_B \\ F_T \\ F_{LB} \\ F_{LT} \\ F_{RB} \\ F_{RT} \end{Bmatrix}^b \tag{5.25}$$

where e and b denote the exterior and boundary forces respectively.

Now consider a harmonic pressure wave with unit amplitude, frequency ω and wave-number $\underline{\kappa}$ travelling across the system at a direction making an angle α to the d_1 axis (the d_1 and d_2 axes are parallel to the sides of the cells, figure (3.1a)). This can be written (at a point $\underline{S}$)

in the form

$$P(\underline{S}, t) = e^{i(\omega t - \underline{\kappa}.\underline{S})} = e^{i(\omega t - \kappa_1 S_1 - \kappa_2 S_2)} \tag{5.26}$$

where κ_1, κ_2 and S_1, S_2 are the components of the wave-number $\underline{k}$ and the position vector $\underline{S}$ (defining the position of the considered point from the origin). The exterior forces acting on the cells are due to this pressure field and hence the relation between these forces at any point in one cell n_1, n_2 (where n_1 and n_2 define the position of the cell along the d_1 and d_2 directions) and the corresponding points in neighbouring cells can be written as

$$\{F\}^e_{n_1+1,n_2} = \{F\}^e_{n_1,n_2} e^{-ik_1\ell_1} = \{F\}^e_{n_1,n_2} e^{i\varepsilon_1}$$
$$\{F\}^e_{n_1,n_2+1} = \{F\}^e_{n_1,n_2} e^{-ik_2\ell_2} = \{F\}^e_{n_1,n_2} e^{i\varepsilon_2} \tag{5.27}$$

where ℓ_1 and ℓ_2 are the dimensions of the cell along the d_1 and d_2 directions,

$$\varepsilon_1 = -k_1\ell_1, \qquad \varepsilon_2 = -k_2\ell_2 \tag{5.28}$$

As this pressure wave propagates across the system it will induce a wave-motion in the structure propagating at the same direction and with the same wave-form as the pressure wave. Therefore the relation between the degrees of freedom and boundary forces at corresponding points in neighbouring cells is similar to relation (5.27).

Now following the analysis given in Chapter III, Section 3.3, we can obtain relations between the degrees of freedom and exterior forces at the boundaries of the cell similar to (3.12). Also considering the equilibrium of the boundary forces results in relations between the boundary forces similar to (3.11), where ε_1 and ε_2 replace μ_1 and μ_2 in these relations. These relations can be used to eliminate all the boundary forces and the degrees of freedom and exterior forces, $\{q_R\}$, $\{F_R\}^e$, $\{q_T\}$, $\{F_T\}^e$, $\{q_{RB}\}$, $\{F_{RB}\}^e$, $\{q_{LT}\}$, $\{F_{LT}\}^e$ and $\{q_{RT}\}$, $\{F_{RT}\}^e$ from equation (5.9). This will result in an equation of the form

$$\left([\bar{K}(\varepsilon_1, \varepsilon_2)] + i\omega[\bar{C}(\varepsilon_1, \varepsilon_2)] - \omega^2[\bar{M}(\varepsilon_1, \varepsilon_2)]\right) \begin{Bmatrix} q_I \\ q_L \\ q_B \\ q_{LB} \end{Bmatrix} = \begin{Bmatrix} F_I \\ 2F_L \\ 2F_B \\ 4F_{LB} \end{Bmatrix}^e \quad (5.29)$$

The matrices $[\bar{K}(\varepsilon_1, \varepsilon_2)]$, $[\bar{C}(\varepsilon_1, \varepsilon_2)]$ and $[\bar{M}(\varepsilon_1, \varepsilon_2)]$ are defined in a similar manner which coincides with the definition of $[\bar{K}(\mu_1, \mu_2)]$ given by (3.20) (Chapter III, Section 3.3). The solution of (5.29) is

$$\begin{Bmatrix} q_I \\ q_L \\ q_B \\ q_{LB} \end{Bmatrix} = \left[\bar{K}(\varepsilon_1, \varepsilon_2) + i\omega\bar{C}(\varepsilon_1, \varepsilon_2) - \omega^2\bar{M}(\varepsilon_1, \varepsilon_2)\right]^{-1} \begin{Bmatrix} F_I \\ 2F_L \\ 2F_B \\ 4F_{LB} \end{Bmatrix}^e \quad (5.30)$$

The remaining displacements $\{q_R\}$, $\{q_T\}$, $\{q_{LT}\}$, $\{q_{RB}\}$ and $\{q_{RT}\}$ are then obtained from relations (3.12).

5.5 Computer Programs and Applications

A general computer program has been written to calculate the response of any one or two-dimensional periodic structure to the two types of excitation given in Section 5.2. One periodic section (cell) of the structure is represented by a finite element model, then the matrices in equations (5.18) for one-dimensional systems or (5.29) for two-dimensional systems are formulated. The wave receptance functions $\phi(\underline{r}, \omega)$ or $\phi(\underline{r}, \omega, k)$ are obtained by solving these sets of equations. The basic flow diagram for the computational procedure is given in Appendix B. The set of equations (5.18) or (5.29) are solved using Crout's factorisation method [65].

5.5.1 Examples of one-dimensional periodic systems

Some of the examples used in Chapter II will be used here. This will enable us to see how to use the curves describing the variation of the propagation constant with frequency, obtained in Chapter II for these examples, to understand and predict their response to random pressure fields.

The first example is the beam on multiple supports at equal distances. At these supports the translational stiffness is infinite and the rotational stiffness $K_r = 4.0$. This example was used in Section 2.3.2 and shown in figures (2.3a, b). Its propagation constant-frequency curve is shown in figure (2.11). To determine the response of this structure to random pressure fields, the generalised forces for a single beam element due to a harmonic pressure wave given by

$$P(\underline{r}, \omega, \underline{k}) = e^{i(\omega t - \underline{k}.\underline{r})} \tag{5.31}$$

must be calculated first. This is given in Appendix C1. The single cell representing one period of the structure, figure (2.3b) is idealised by four beam elements and two rotational spring elements. The beam element and data values used are given in Appendix D1. The distance between the supports (periodic length) is taken equal to unity. The damping matrix is calculated from relation (5.19) where the material loss factor η is taken equal to 0.25. The rotational stiffness K_r at the supports is taken equal to 4.0. The response of the beam to the two types of pressure fields given in Section 5.2 is calculated. Figure (5.1) shows the power spectral density of the displacement at the mid point of the cells due to acoustic plane wave with unit amplitude. Various values for the non-dimensional convection velocity CV of the acoustic wave are chosen. The convection velocity U_p of such a pressure field can be written as

$$U_p = \frac{\nu}{a} = \frac{\omega}{k}$$

where $k = 2\pi a$, $\omega = 2\pi\nu$.

The non-dimensional convection velocity is given by

$$CV = -\frac{\Omega}{\varepsilon} \tag{5.33}$$

where $\varepsilon = -k.\ell$

Ω is the non-dimensional frequency, and

ℓ is the periodic length.

From the graph it can be seen that in each spectrum the response has maximum values at frequencies where the convection velocity of the pressure

field equals the free wave speed (phase velocity) in the beam (coincidence phenomenon). The free wave speed, or phase velocity, v_w, is given by

$$v_w = \frac{\nu}{a} = -\frac{\omega \ell}{\mu} \tag{5.34}$$

The non-dimensional free wave speed V_w is defined as

$$V_w = -\frac{\Omega}{\mu}$$

or in general

$$V_w = -\frac{\Omega}{\mu \pm 2m\pi} \qquad 0 \leq |\mu| \leq \pi \tag{5.35}$$

where m is an integer number and μ is the propagation constant.

The relation between Ω and μ for this example is shown in figure (2.11).

The highest peak occurs when the convection velocity of the pressure wave equals the free wave speed corresponding to the lower bounding frequency of the first propagation band where

$$\Omega = 12.8, \quad \mu = -\pi$$

and hence

$$V_w = 12.8/\pi \simeq 4.0.$$

This frequency coincides with the fundamental natural frequency of the single cell when its coupling degrees of freedom (θ_L and θ_R) are unconstrained. These results are in agreement with the results produced by Mead and Sen-Gupta [30] using closed form solution.

Figure (5.2) shows the response of the beam to the same excitation as before while the material loss factor η is taken equal to 0.02. In this case the maximum response in each spectrum occurs at the same frequency as before but the amplitude of the response is much higher than the previous case (due to the low damping in the beam in this case).

Figures (5.3) and (5.4) show the response due to an acoustic plane wave with convection velocities CV = 2.0 and 4.0 while the damping in the beam is taken equal to zero. Also shown is the response when the material loss factor $\eta = 0.25$ for comparison. In the first figure

(CV = 2.0) the response is infinite at $\Omega \simeq 16.0$. At this point the propagation constant $|\mu| \simeq 2.74$ (see figure (2.11)) where one of the free wave speeds is equal to 2.0. This is obtained from (5.35) where m = 1 and hence

$$|V_w| = \frac{\Omega}{|\mu \pm 2m\pi|} = \frac{16.0}{2.74 + 6.28} \simeq 2.0$$

In the second figure (CV = 4.0) the response is infinite at $\Omega \simeq 12.8$. At this point the propagation constant $|\mu| = \pi$ (see fig. (2.11)) and hence the free wave speed in the beam is

$$V_w = \frac{12.8}{\pi} \simeq 4.0$$

where m is taken equal to zero.

From the above discussion it can be concluded that from the propagation constant/frequency curve one can predict the frequencies at which maximum response occurs when the structure is subjected to an acoustic plane wave with a certain convection velocity.

Figure (5.5a,b,c) (figures 5.5b, c are cross-sections in (5.5a)) shows the power spectral density of displacement at the mid point of the cells due to a general random pressure field ($S_p(\underline{r}, \omega, \underline{k})$) with unit amplitude. From the figure it is clear that the largest response occurs when the wave-number $\underline{k}$ (notice that $|\mu| = |k|\ell = |k|$) and the frequency of the excitation coincide with one of the points on the propagation constant/frequency curve (fig. (2.11)). The highest peak occurs at the lower bounding frequency of the first band where $\Omega = 12.8$ and $|\mu| = \pi$. Figures (5.6a,b) show the power spectral density of the displacement at the cell centres due to a boundary-layer pressure field $S_p(\Omega, \varepsilon)$ calculated from expression (5.8) where the following values are considered.

The non-dimensional convection velocity CV = 4.0, the boundary layer decay parameter b = 0.1, the power spectral density of the pressure at any point in the field $S_p(\Omega) = 1.0$. This boundary layer pressure field is shown in figures (5.7a, b). As can be seen from this figure the pressure spectrum has maximum peaks when $\Omega/\varepsilon = 4.0$ which is the non-dimensional convection velocity of the pressure field in this case.

Now returning to figure (5.6) it is clear that the maximum response occurs at frequencies where the non-dimensional free wave speed in the beam equals to 4.0. This figure is in fact the product of the two figures (5.5) and (5.7). Similar results were produced by Mead and Pujara |34| using a particular series of space harmonics.

The next example is the flat stiffened panel used in Section 2.3.3. This is shown in figure (2.4). The propagation constant/frequency curve is shown in figure (2.12). Appendix C2 gives the formulation for calculating the generalised nodal forces for one element of the panel (strip element) due to a harmonic pressure wave with unit amplitude, frequency ω and wave-number $\underline{\kappa}$. The damping matrix is calculated from relation (5.19) where the material loss factor η is taken equal to 0.25. The displacement response at the mid point of the cells due to acoustic plane wave with unit amplitude is shown in figure (5.8) for various values of the non-dimensional convection velocity CV where

$$CV = U_p \ell \left(\frac{\rho h}{D}\right)^{\frac{1}{2}}$$

The response is shown as a function of the non-dimensional frequency Ω where

$$\Omega = \omega \ell^2 \left(\frac{\rho h}{D}\right)^{\frac{1}{2}}.$$

Here again, similar to the previous example, the maximum response in each spectrum occurs at a frequency where the convection velocity of the pressure field equals the free wave speed (phase velocity) in the panel and the highest peak occurs at the lower bounding frequency of the first propagation band (see figure (2.12)). Similar results were produced in |14| using transfer matrix methods.

5.5.2 Examples of two-dimensional periodic systems

The two examples used in Chapter III, Section 3.4.2 will be used here. These are the flat infinite plates resting on equally spaced orthogonal line supports, figure (3.6a). The same finite element idealisation for the cell representing one period of the system is used here. This was shown in figure (3.6b). The generalised forces for a single plate element due to a harmonic pressure wave with unit amplitude, frequency ω and wave-number $\underline{\kappa}$, are derived in Appendix C3. The damping matrix is

calculated from equation (5.19) where the material loss factor η is taken equal to 0.25.

First the plate with square cells ($\ell_x = \ell_y = 1.0$) is considered. Its response to the two types of pressure fields given in Section 5.2 is calculated. Figures (5.9), (5.10) and (5.11) show the power spectral density of the displacement at the centre of the cells due to an acoustic plane wave with unit amplitude propagating along the x direction, along a direction making 45 degrees to the x axis (preferred direction of propagation) and along a direction making 20 degrees to the x axis. Various values of the convection velocity U_p of the pressure field are chosen. From these graphs it can be seen that the maximum response in each spectrum occurs at a frequency where the convection velocity of the pressure field coincides with the free wave speed (phase velocity) in the plate. The free wave speed V_w can be calculated from the propagation constants/frequency curves shown in figures (3.17) and (3.18) where

$$V_w = \frac{\nu}{|\underline{a}|} = \frac{\omega}{|\underline{\kappa}|} = \frac{\omega}{\sqrt{\kappa_x^2 + \kappa_y^2}} = \frac{\omega}{\sqrt{(\frac{\mu_x}{\ell_x})^2 + (\frac{\mu_y}{\ell_y})^2}}$$

(since $\mu_x = -k_x \ell_x$, $\mu_y = -k_y \ell_y$).

k_x and k_y are the components of the wave-number $\underline{k}$ along the x and y directions respectively. The highest peak for each direction of propagation occurs at the lower bounding frequency of the first propagation band along that direction when the convection velocity of the pressure field coincides with the free wave speed at that frequency. For waves propagating along the x direction the highest peak occurs at $\Omega \simeq 30.0$ (notice that $\Omega = \omega$ for this example) when the convection velocity of the pressure field equals 9.55. At this frequency the free wave speed in the plate is given by

$$V_w = \frac{\omega}{\sqrt{(\frac{\mu_x}{\ell_x})^2 + (\frac{\mu_y}{\ell_y})^2}} \simeq \frac{30.0}{\sqrt{0.0 + \pi 2}} \simeq 9.55$$

(since $\mu_x = \pi$ and $\mu_y = 0.0$ at this point).

Similarly for waves travelling along the preferred direction of propagation the highest peak occurs at $\omega \simeq 20.0$ when the convection velocity of the pressure field $U_p \simeq 4.5$. The free wave speed in the plate at this point is given by

$$V_w = \frac{20.0}{\sqrt{2\pi^2}} \simeq 4.5$$

(since $|\mu_x| = |\mu_y| = \pi$ at this point. See figure (3.17).)

Also for waves travelling at a direction making 20 degrees to the x direction the highest peak occurs at $\omega \simeq 26.2$, when the convection velocity of the pressure field $U_p \simeq 7.8$. (Notice that this frequency is the lower bounding frequency of the first propagation band along this direction, figure (3.18)). At this point the free wave speed in the plate is given by

$$V_w = \frac{26.2}{\sqrt{(\pi)^2 + (1.143)^2}} \simeq 7.8$$

(notice that k_x and k_y, and hence μ_x and μ_y, are restricted inside the first zone, figure (3.4)).

Figures (5.12a,b), (5.13a,b) and (5.14a,b) show the power spectral density of the displacement at the centre of the cells due to a general homogeneous random pressure field with unit amplitude travelling along the three directions discussed above. From these graphs it is clear that the response in each case is largest when the wave-number and the frequency of the pressure field coincide with one of the points on the propagation constants/frequency curves along the direction of propagation (notice that $|\mu_x| = |k_x|\ell_x$ and $|\mu_y| = |k_y|\ell_y$). The maximum response in each graph occurs at the lower bounding frequency of the first band along the direction of propagation of the pressure field. These frequencies can be clearly seen in the polar plot of the propagation constants/frequency curves shown in figure (3.18) where the curve showing the lower bound for the first band gives the frequencies where maximum response occurs for various directions of propagation. The highest peak occurs when the pressure field is propagating along the preferred direction of propagation in the plate as can be seen from figure (5.13).

Figures (5.15) and (5.16) show the response of the plate with rectangular cells ($\ell_x = 1.0$, $\ell_y = 2.0$) due to an acoustic plane wave with unit amplitude travelling along the x direction and along a direction making 26.56 degrees to the x direction (preferred direction of propagation in the plate). Similar to the previous example, the response of the plate is largest when the convection velocity of the acoustic wave coincides with the free wave speed in the plate. The highest peak in each graph occurs at the lower bounding frequency of the first propagation band along the direction of propagation. (The propagation bands for this example are shown in figures (3.25) and (3.26)).

Figures (5.17 a,b) and (5.18a,b) show the response of the plate due to general homogeneous random pressure field with unit amplitude, travelling along the two directions discussed above. Here again, similar to the previous example, the response of the plate is largest when the wave-number and the frequency of the pressure field coincide with one of the points on the propagation constants/frequency curves along the direction of propagation (notice that $|\mu_x| = |k_x|$ and $|\mu_y| = 2|k_y|$ in this case). These curves are shown in figures (3.25) and (3.26). Also the maximum response occurs at the lower bounding frequency of the first band along the direction of propagation. The highest peak occurs at the lower bounding frequency of the first propagation band when the pressure field is propagating along the preferred direction of propagation in the plate.

From the above discussion it can be concluded that from the propagation constants/frequency variation for free waves propagating in the two-dimensional periodic system, one can predict the frequencies at which the response of the structure is largest when it is subjected to pressure fields propagating at various directions. The polar plot of the propagation constants/frequency curves shows these frequencies very clearly.

5.6 Response of General Structures to Random Excitation (Modal Analysis)

In the previous sections of this chapter the analysis has been confined to calculating the response of infinite periodic structures to homogeneous random pressure fields. In this section, the response of general structures (non-periodic or finite periodic structures) to any arbitrary excitation is calculated using finite elements and the modal

method of analysis. The response of some finite periodic structures in one and two dimensions is calculated using this approach and the results are compared with the response of infinite structures presented in previous sections.

5.6.1 Mathematical formulation

First the structure is represented by a finite element model. This gives the differential equation of motion in the matrix form

$$[M]\{q''\} + [C]\{q'\} + [K]\{q\} = \{F\} \tag{5.36}$$

where $[M]$, $[C]$ and $[K]$ are the structure's inertia, damping and stiffness matrices respectively.

$\{q\}$ and $\{F\}$ are the vectors of generalised degrees of freedom and forces respectively.

Equation (5.36) represents a system of simultaneous ordinary differential equations with constant coefficients. For complex structures the matrices in (5.36) can be of large order, and the solution of such a set of equations can be very complicated and time consuming, especially if the response is required for a large range of the excitation forces as usually the case in random response problems.

Equations (5.36) can be transformed into a set of independent equations by using the modal matrix of the undamped system [35, 37]. This modal matrix is obtained by solving the eigenvalue problem of the undamped system. Such a solution can be written in the form

$$[M][V]\left[\omega^2\right] = [K][V] \tag{5.37}$$

where

$\left[\omega^2\right]$ is a diagonal matrix where ω's are the natural frequencies of the undamped system.

$[V]$ is the modal matrix (eigenvectors associated with ω's). This modal matrix can be normalised such that

$$[V]^T[M][V] = [I] \tag{5.38}$$

$$[V]^T[K][V] = \left[\omega^2\right] \tag{5.39}$$

Now if we let

$$\{q\} = [V]\{\eta\} \tag{5.40}$$

where $\{\eta\}$ represents another set of generalised coordinates, then we can write,

$$\begin{aligned} \{q'\} &= [V]\{\eta'\} \\ \{q''\} &= [V]\{\eta''\} \end{aligned} \tag{5.41}$$

Substituting (5.40) and (5.41) into equation (5.36) gives

$$[M][V]\{\eta''\} + [C][V]\{\eta'\} + [K][V]\{\eta\} = \{F\} \tag{5.42}$$

Multiplying (5.42) by $[V]^T$ gives

$$\{\eta''\} + [\bar{C}]\{\eta'\} + [\omega^2]\{\eta\} = \{Q\} \tag{5.43}$$

where

$$[\bar{C}] = [V]^T[C][V] \tag{5.44}$$

$$\{Q\} = [V]^T\{F\} \tag{5.45}$$

In general the matrix $[\bar{C}]$ is non-diagonal. However, in many cases the matrix $[C]$ can be considered as a linear combination of the stiffness and inertia matrices. Hence

$$[C] = a[M] + b[K] \tag{5.46}$$

where a and b are constants, and hence the matrix $[\bar{C}]$ will be a diagonal matrix. In some other cases the off-diagonal terms of $[\bar{C}]$ are small compared with the diagonal terms and it can be approximated as a diagonal matrix. Also for the general case when $[\bar{C}]$ is non-diagonal and the off-diagonal terms are not small there are other methods to transform it into a diagonal matrix. This has been discussed in detail in |35|.

In this section we will consider that the matrix $[C]$ is proportional to the stiffness matrix such that the matrix $[\bar{C}]$ will be given by

$$[\bar{C}] = \begin{bmatrix} \ddots & \\ & 2\xi\omega \\ & & \ddots \end{bmatrix}$$

where ξ is called the modal damping.

Therefore equation (5.43) represents an independent set of equations. Its solution gives the displacements $\{\eta\}$, and hence $\{q\}$ can be obtained from (5.40).

The response of the structure to random pressure fields of the type discussed in Section 5.2 can be obtained by calculating the response to various values of the pressure field components (given by (5.12)) using the modal analysis method as explained above. The power spectral density of the response and the mean square response are then obtained from relations (5.4) and (5.5) or (5.6) and (5.7).

5.6.2 Computer programs and applications.

A general computer program has been written to represent a general structure by a finite element model. The eigenvalue problem of the undamped structure is formulated and solved to calculate the natural frequencies and the modal matrix. Then the matrices in equation (5.43) are formed. This equation is solved to obtain the response of the structure to the two types of excitation given in Section 5.2.

The response of some finite periodic structures in one and two dimensions is investigated here. This will enable us to compare their response to the response of infinite structures presented in previous sections. The following cases are considered.

a. Response of a five bay beam to a frozen convected random pressure field.

The beam is resting on equally spaced point supports having infinite translational stiffness and a rotational stiffness $K_r = 4.0$, figure (5.19). The distance between the supports is taken equal to unity. The structure is represented by a finite element model where each bay is idealised by four beam elements. The beam element and data values used in the analysis are given in Appendix D1. First the natural frequencies and associated normal modes of the undamped structure are calculated (only the first five normal modes are considered. This will be discussed later). Figure (5.20) shows the first five normal modes of the beam.

The modal damping ξ is taken equal to 0.01 (material loss factor $\eta = 2\xi$). The response of the beam to a frozen convected random pressure field with unit amplitude travelling over the beam from left to right with a convection velocity CV = 4.0 is calculated. Figure (5.21) shows the power spectral density of the displacement at the centre point of the bays (numbered 1 to 5 on the graph where bay 1 is on the left end of the structure, figure (5.19)). Since the beam has five bays then its natural frequencies will occur in groups where each group contains five natural frequencies occurring within one of the propagation bands of the infinite structure. Therefore it is enough to consider only the first five natural frequencies and associated normal modes to calculate the response to excitation forces with frequencies within the first propagation band. As can be seen from figure (5.21) the response of the beam has five peaks corresponding to the first five natural frequencies. Also it should be noticed that two of these modes are antisymmetric (see figure (5.20)) and hence contribute nothing to the response at the mid point of the middle bay (bay 3). Comparing these results with the response of the infinite beam discussed in Section 5.5.1, figure (5.2), shows that the maximum response of the finite beam is very close to the maximum response of the infinite beam and occurs at nearly the same frequency (at $\Omega = 13.1$ for the finite beam and at $\Omega = 12.8$ for the infinite beam, which is the lower bounding frequency of the first propagation band, figure (2.11)). Figure (5.22) shows the response to the same excitation as before while the modal damping ξ is taken equal to 0.125 ($\eta = 2\xi = 0.25$). Here, due to the relatively heavy damping in the structure, some of the peaks have disappeared. Also the amplitudes of the response is much lower than before. The maximum response occurs at a frequency close to the first natural frequency of the structure ($\Omega = 13.1$).

Similar to the previous case, comparing the response of this structure to the response of the infinite structure calculated in Section 5.5.1, figure (5.1) shows that the maximum response for both structures occurs at very close frequencies. Also the maximum r.m.s. response of the finite structure is about 6% higher than the maximum r.m.s. response of the infinite structure.

Figure (5.23) shows the response of the beam when the convection velocity of the pressure field is taken equal to ∞ (this represents a

constant pressure field where the wave-number $k = 0.0$). In this case the response of the structure is symmetrical (the response of the first and second bays is identical to the response of the fifth and fourth bays respectively). The maximum response occurs in bay 3 at a frequency close to the upper bounding frequency of the first propagation band (where the maximum response of the infinite structure occurs in this case). Here the maximum r.m.s. response of the finite structure is about 33% higher than the maximum r.m.s. response of the infinite structure.

From the above discussion it can be concluded that calculating the response of the infinite structure can provide a good estimate to the response of finite structures. Similar conclusions are obtained in |30|.

b. Response of two-dimensional finite periodic plates.

The response of flat plates resting on equally spaced orthogonal line simple supports is examined here. The following three cases are considered.

(i) a 5 x 5 bay square plate,
(ii) a 3 x 3 bay square plate,
(iii) a single bay square plate.

First the 5 x 5 bay plate is considered, figure (5.24a). The plate is represented by a finite element model where each bay is idealised by four plate elements only. (This will give 135 degrees of freedom in the system. A better idealisation, that is idealising each bay by a larger number of elements, will result in a very large number of degrees of freedom in the structure and hence cannot be solved easily on the computer.) The plate element and data values used in the analysis are given in Appendix D4. The modal damping ξ is taken equal to 0.125 (material loss factor $\eta = 2\xi = 0.25$). The generalised nodal forces for a single plate element due to a harmonic pressure wave with unit amplitude, frequency ω and wave-number $\underline{\kappa}$ are derived in Appendix C3. The response of the plate to a frozen convected random pressure with unit amplitude travelling over the plate along a direction making 45 degrees to the x direction with convection velocities $CV = 4.5$ and $CV = \infty$ is investigated. First the natural frequencies and associated normal modes of the undamped structure are calculated. The first 25 natural frequencies

and normal modes are considered since they are closely spaced and occur within the first propagation band of the infinite structure. It should be noted here that these natural frequencies can be calculated much more accurately from table 3.6 corresponding to values of the propagation constants μ_x and μ_y given by

$$\mu_x = \frac{m_1 \pi}{N_1} \quad , \quad (N_1 = 5, \quad m_1 = 1,2,\ldots, 5)$$

$$\mu_y = \frac{m_2 \pi}{N_2} \qquad (N_2 = 5, \quad m_2 = 1,2,\ldots, 5)$$

Figure (5.25) shows the power spectral density of the displacement at the centre point of the first, third and fifth bays along the diagonal of the plate (see figure 5.25a)). From this figure it is clear that the maximum response occurs in bay 1 near the first natural frequency of the plate (notice that the first natural frequency obtained using this idealisation is $\Omega = 21.6$, while the more accurate value obtained from the wave propagation results in table 3.6 is $\Omega = 19.8$) which is the lower bounding frequency of the first propagation band shown in figure (3.17). To obtain an accurate comparison between these results and the response of the infinite structure using the periodic structure approach discussed in Section 5.5.2, one cell of the infinite structure is represented by a finite element model using the same idealisation used here (4 plate elements per cell). Its response to the same excitation as above is calculated using the periodic structure approach. This is shown in figure (5.26). Also shown in the figure is the response when the convection velocity of the pressure field is taken equal to ∞. Comparing the response of the finite structure, figure (5.25) and the response of the infinite structure, figure (5.26), shows that the largest response of the infinite structure occurs at a frequency $\Omega = 21.6$ which is the lower bounding frequency of the first propagation band (where the maximum response of the finite structure occurs as discussed above). Also it can be seen that the maximum response of the middle bay (bay 3) is very close to the maximum response of the infinite structure and occurs near the same frequency ($\Omega = 21.6$). Figure (5.27) shows the response of the plate when the convection velocity of the pressure field is taken equal to ∞ (this represents a constant pressure field where the wave-number $\underline{\kappa} = 0$).

Here it can be seen that the response of the different bays is largest within a range of frequencies which coincides with the first propagation band of the infinite structure (see figure (3.17)). The maximum response occurs in the middle bay (bay 3) at a frequency close to the upper bounding frequency of the first propagation band (where the maximum response of the infinite structure occurs, figure (5.26)).

Figures (5.28), (5.29) and (5.30) show the response of a 3 x 3 bay plate and a single bay plate (shown in figures (5.24b,c)) to the same excitation as above. (The plate is idealised, in each case, by four plate elements per bay). Here, similar to the previous case, when the convection velocity of the pressure field is equal to 4.5 the largest response in each case occurs near the lower bounding frequency of the first propagation band. Also it can be seen that the maximum response of the middle bay of the 3 x 3 bay plate is very close to the response of the infinite structure shown in figure (5.26). When the convection velocity of the excitation is equal to ∞, the response of the single bay plate occurs near the lower bounding frequency of the first propagation band ($\Omega = 21.6$) which coincides with the only natural frequency of the plate occurring within the first propagation band. The largest response of the 3 x 3 bay plate occurs in bay 2 (middle bay) at a frequency close to the upper bounding frequency of the first propagation band.

A comparison between these three cases shows that as the number of bays in the finite structure increases, the response of the middle bay is closer to the response of the infinite structure. This can be clearly seen in figures (5.31) and (5.32) showing a comparison between the responses when the convection velocity of the pressure field is taken equal to 4.5 and ∞ respectively.

From the above discussion, similar to the beam example, it can be concluded that knowledge of the response of the infinite structure can provide a good estimate to the response of finite structures.

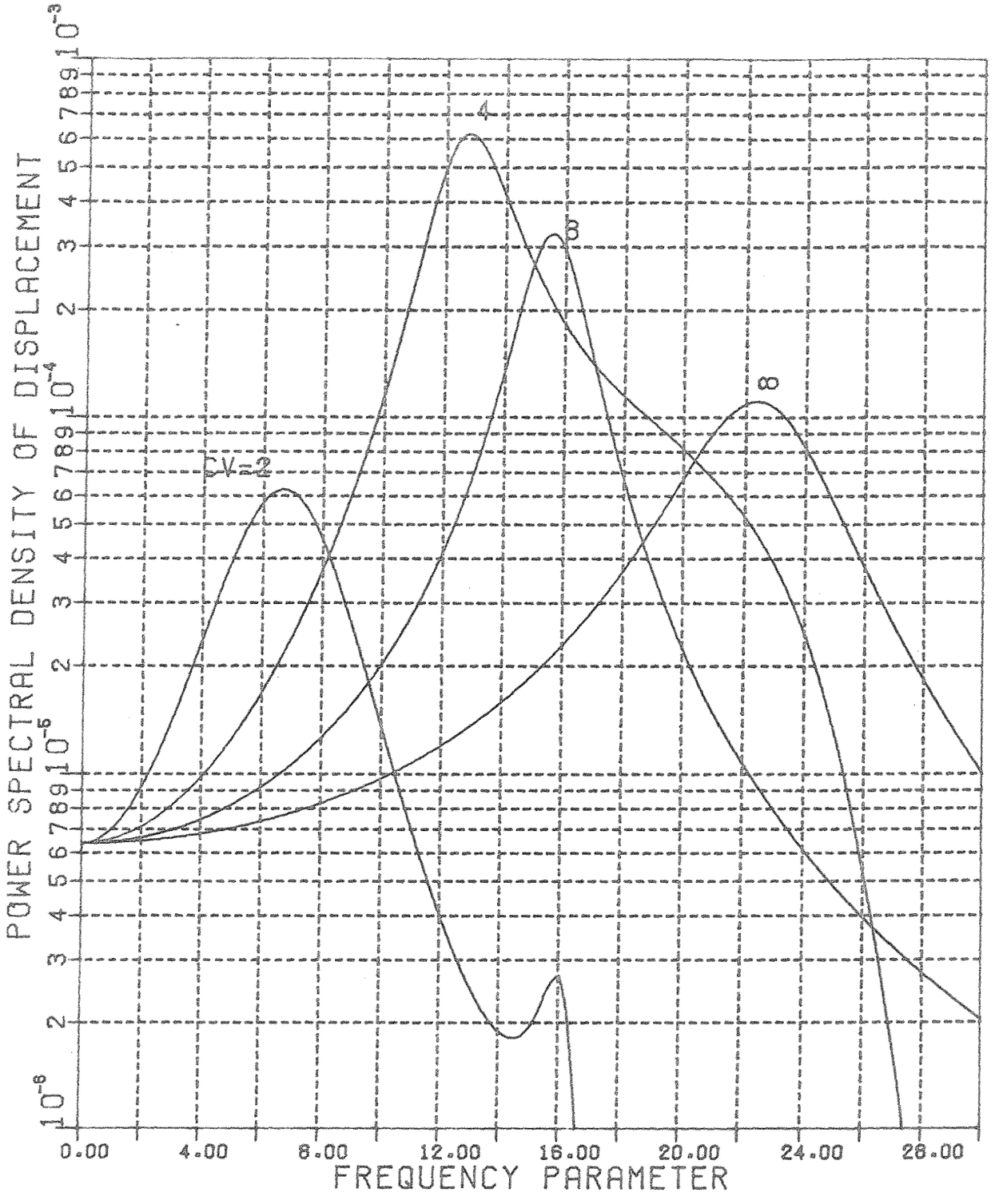

Figure 5.1. Spectra of displacement at bay centres of an infinite beam on periodic point supports with rotational stiffness $K_\gamma=4.0$, $\eta=0.25$, due to random pressure field;frozen convection.

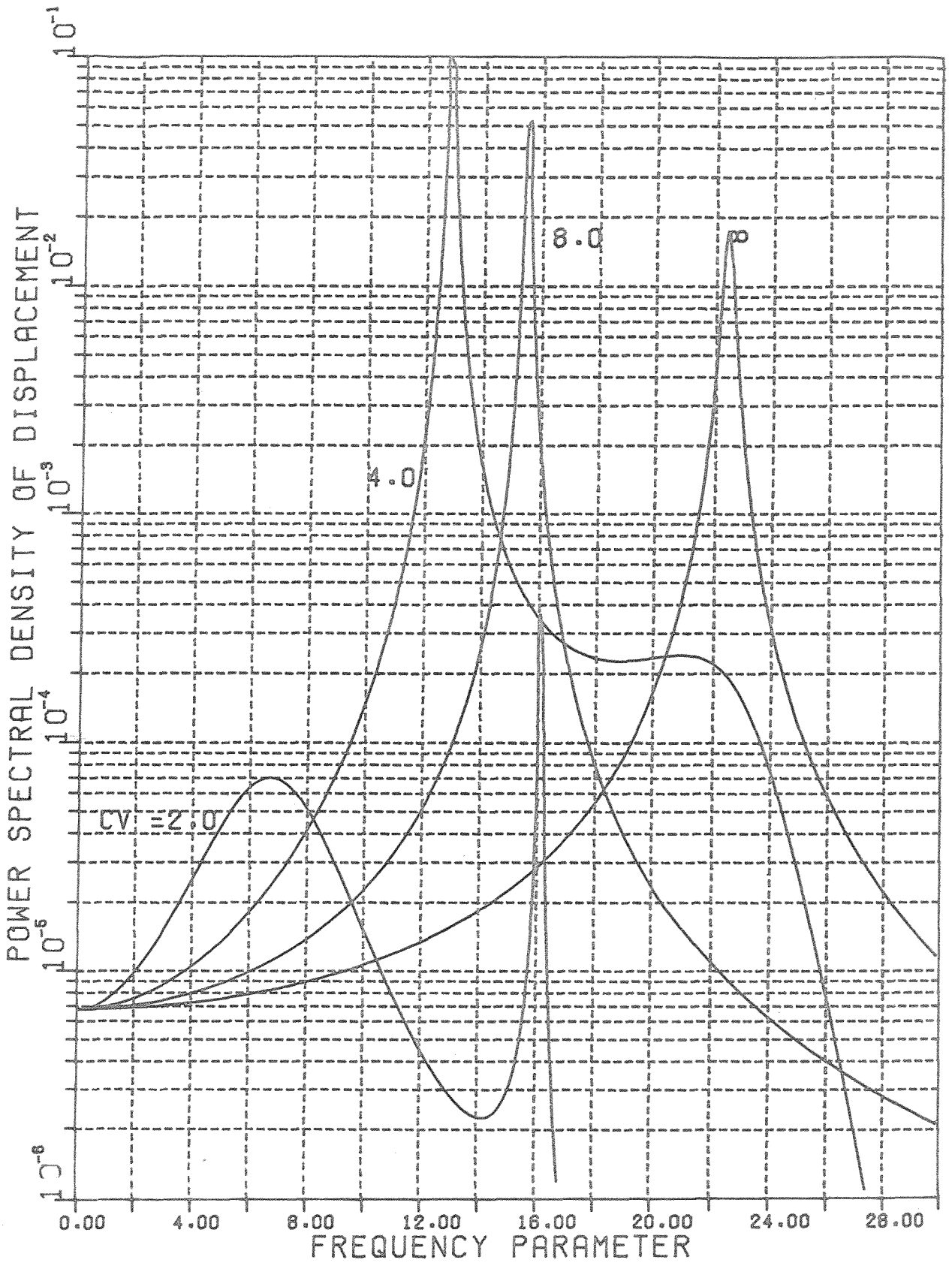

Figure 5.2. Spectra of displacement at bay centres of an infinite beam on periodic point supports with rotational stiffness k_r=4.0, η=0.02, due to random pressure field;frozen convection.

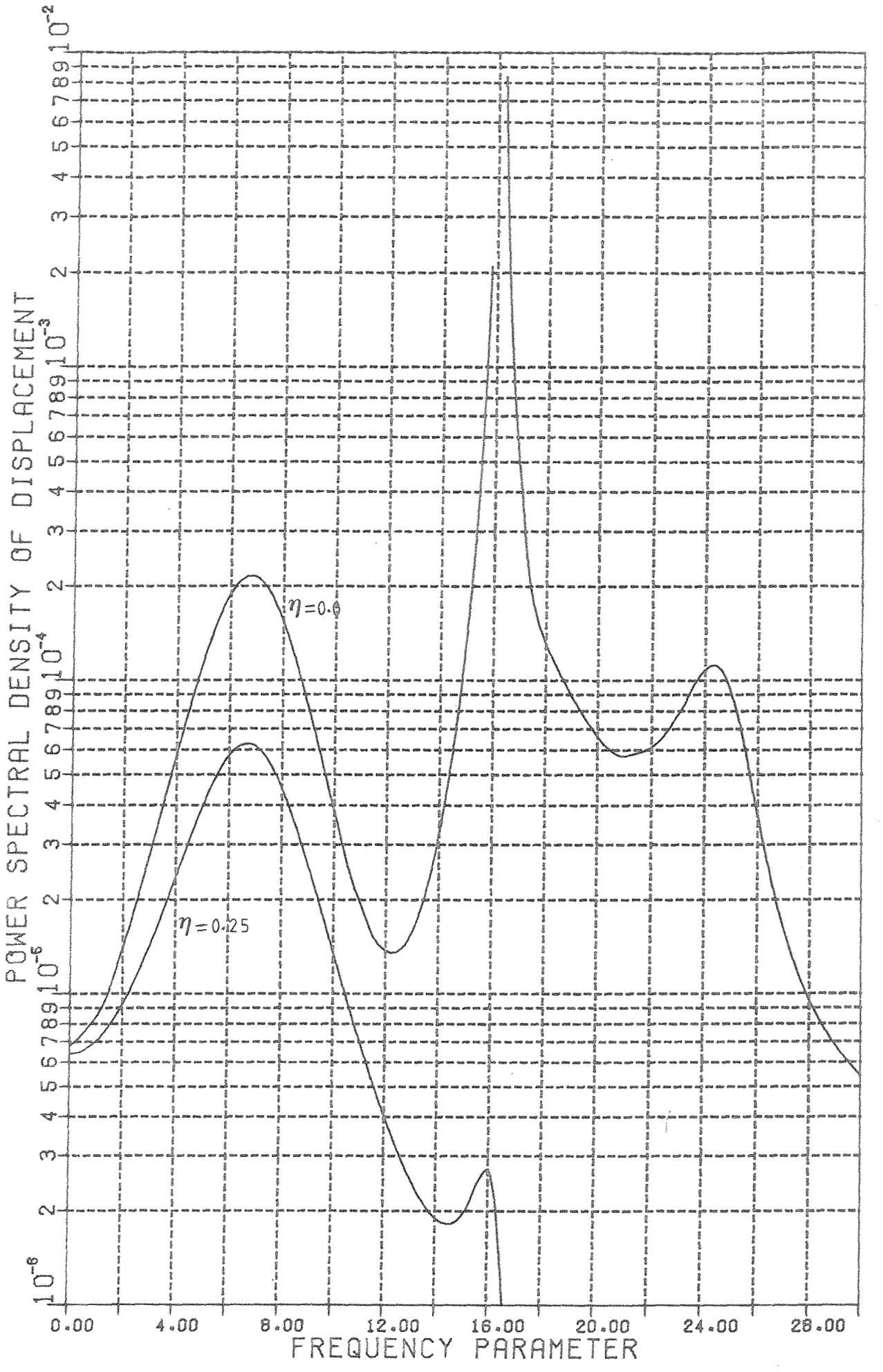

Figure 5.3. Spectra of displacement at bay centres of an infinite beam on periodic point supports with rotational stiffness $k_\gamma=4.0$, due to frozen convected random pressure field , CV=2.0 .

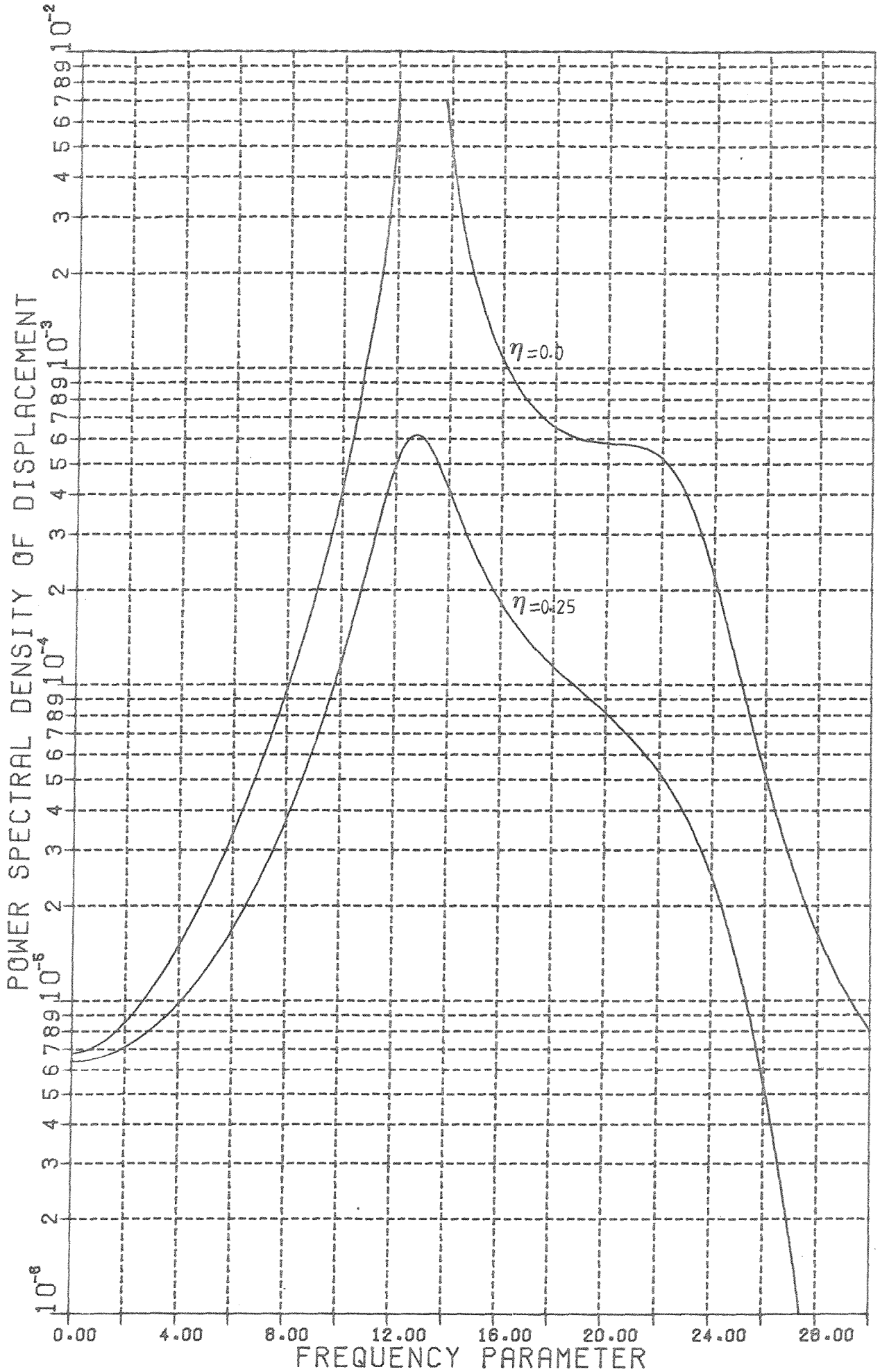

Figure 5.4. Spectra of displacement at bay centres of an infinite beam on periodic point supports with rotational stiffness K_γ=4.0, due to frozen convected random pressure field, CV=4.0 .

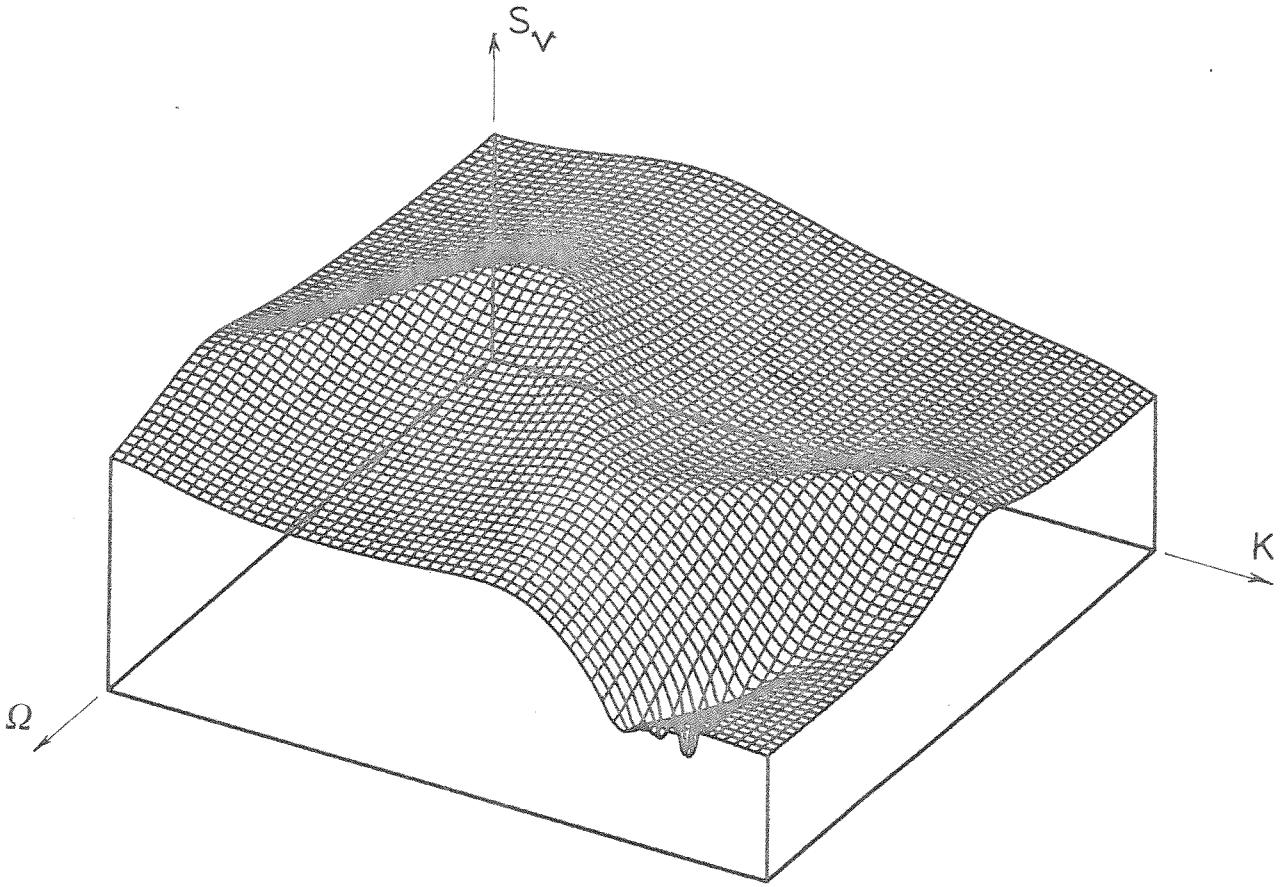

Figure 5.5.(a) Spectra of displacement at bay centres of an infinite beam on periodic point supports with rotational stiffness, $K_\gamma = 4.0$, $\eta = 0.25$, due to general random homogeneous pressure field with unit amplitude .

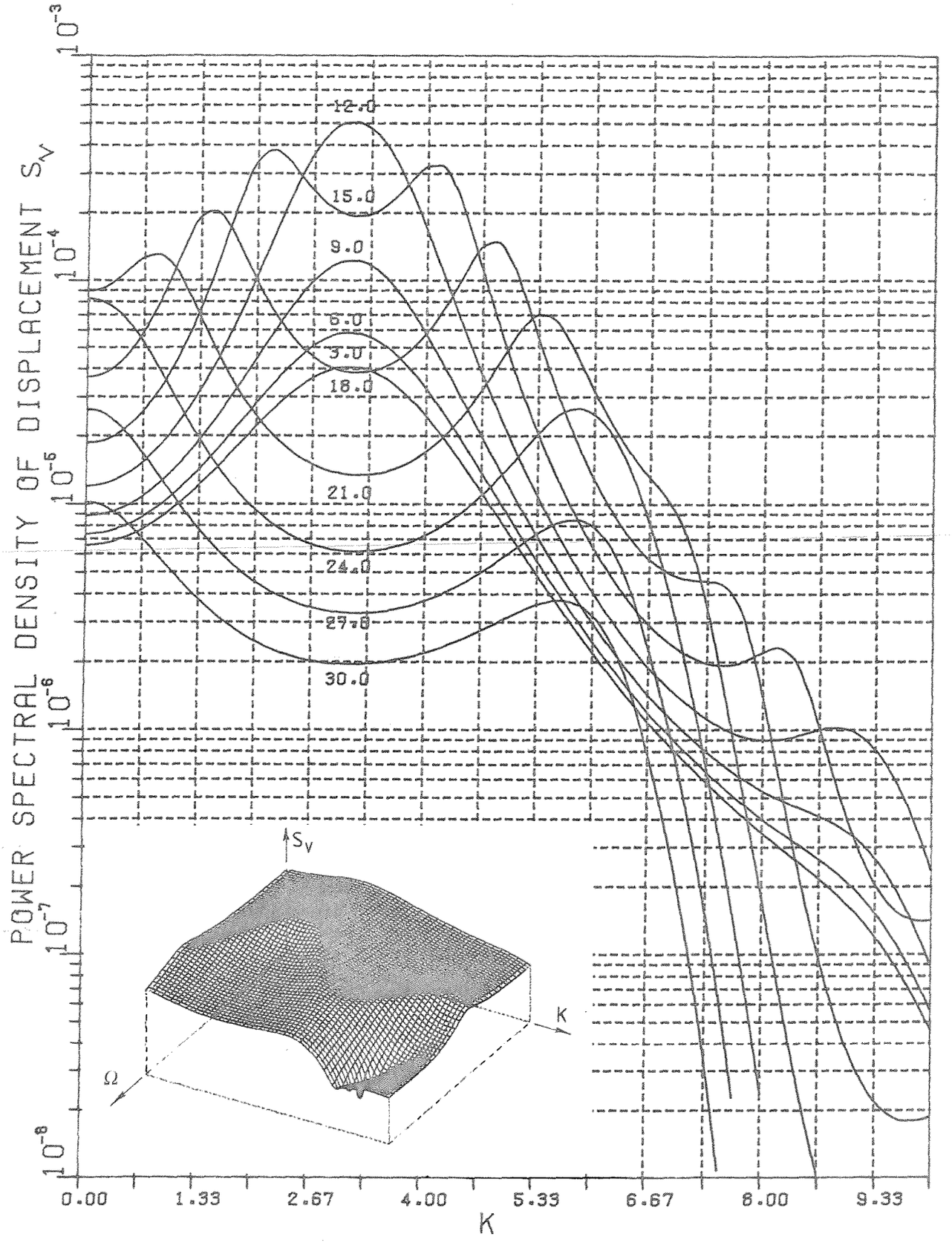

Figure 5.5.(b) Cross-sections in figure(5.5a).Lines of constant frequency .

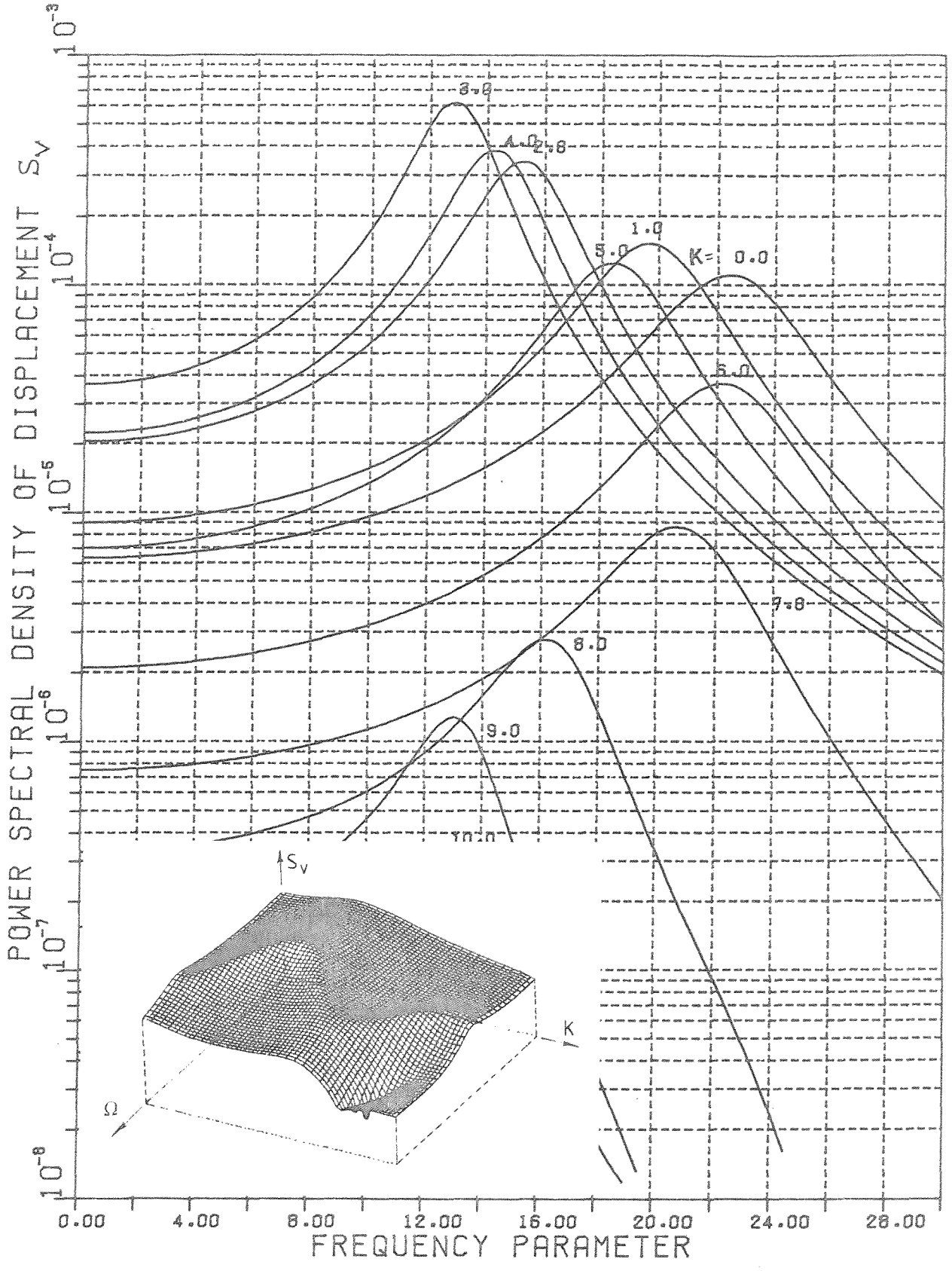

Figure 5.5.(c) Cross-sections in figure(5.5a).Lines of constant wave-number .

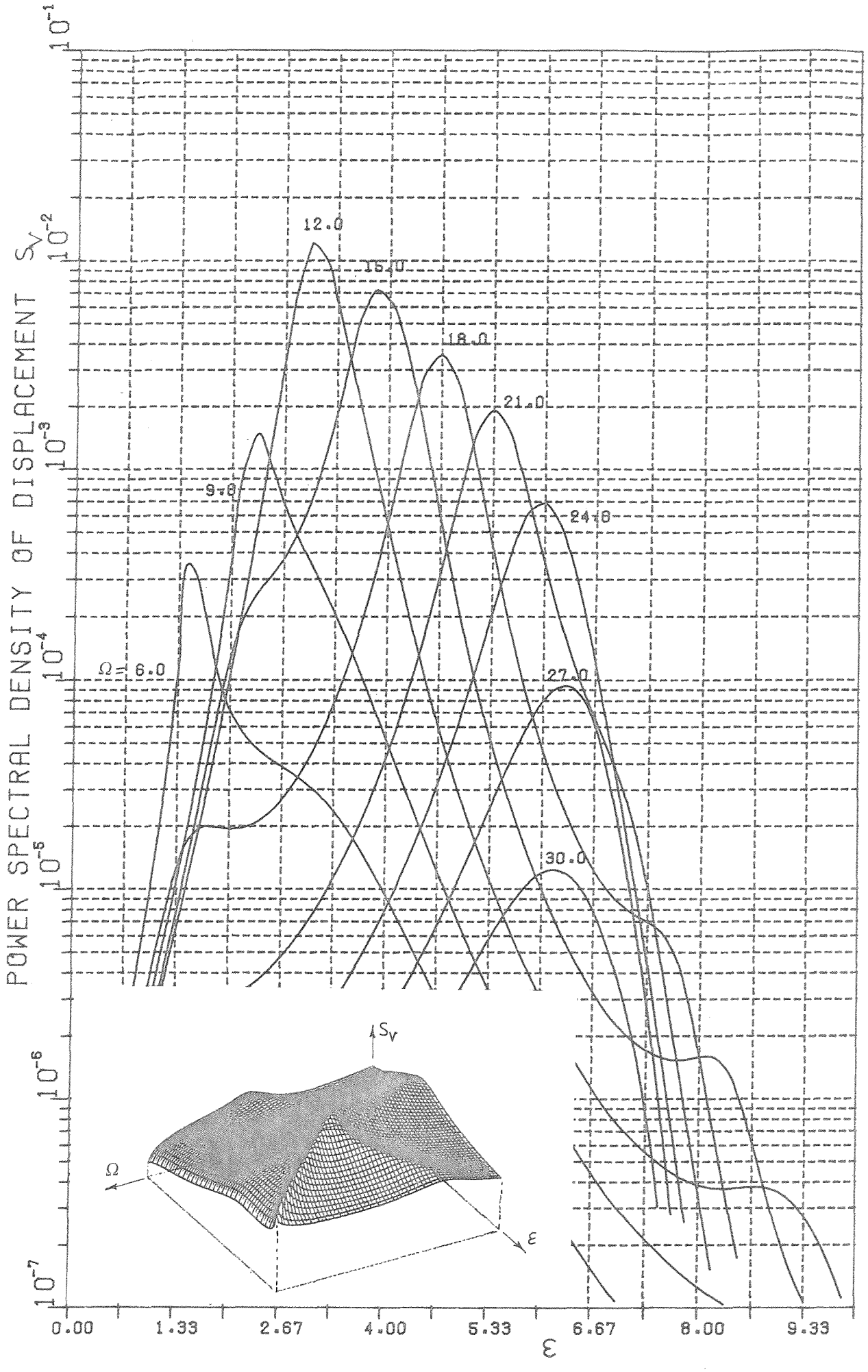

Figure 5.6.(a) Response at bay centres of an infinite beam on periodic point supports, K_y=4.0, η=0.25; due to boundary layer pressure field. Lines of constant frequency.

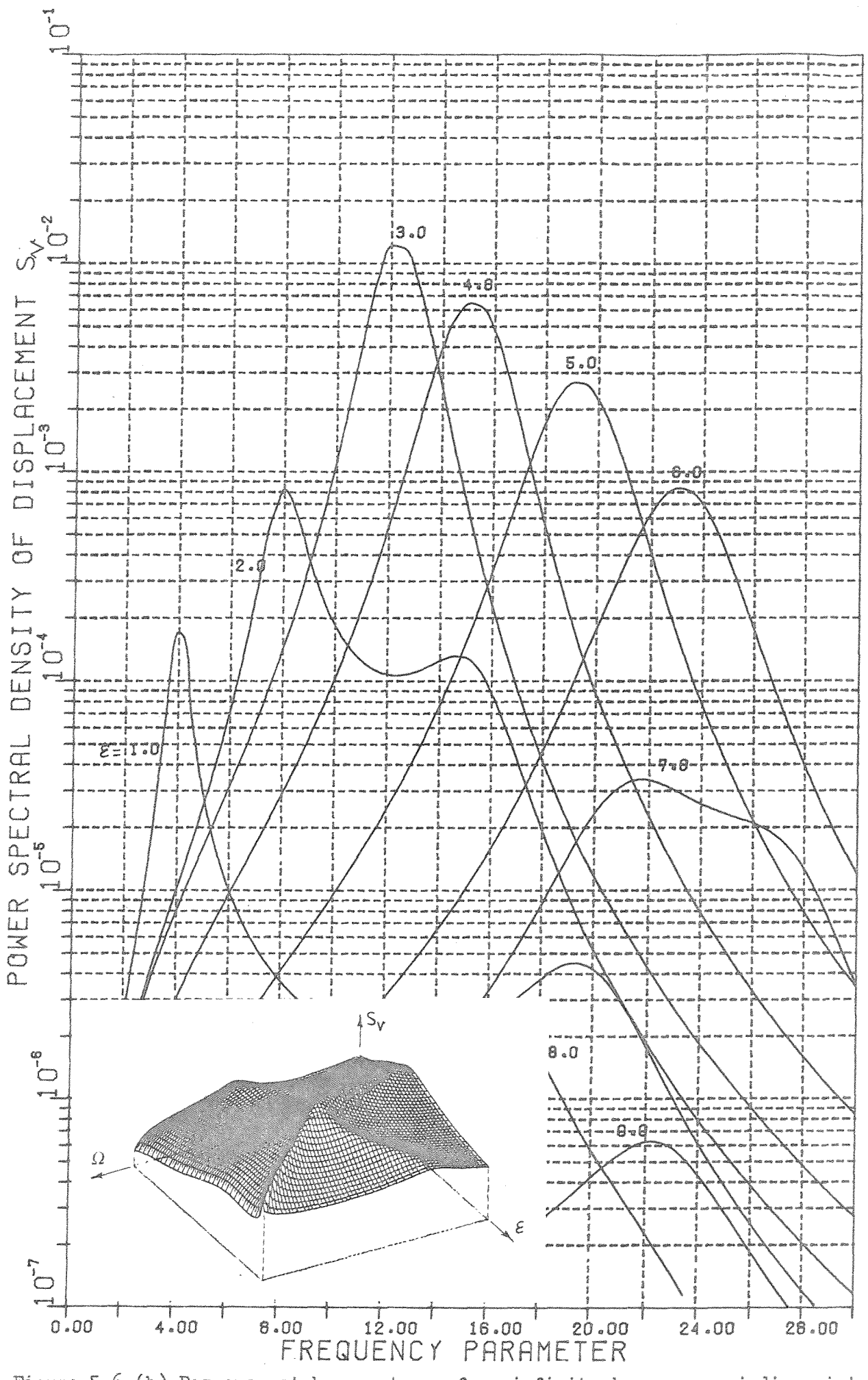

Figure 5.6.(b) Response at bay centres of an infinite beam on periodic point supports, K_r=4.0, η=0.25; due to boundary layer pressure field.

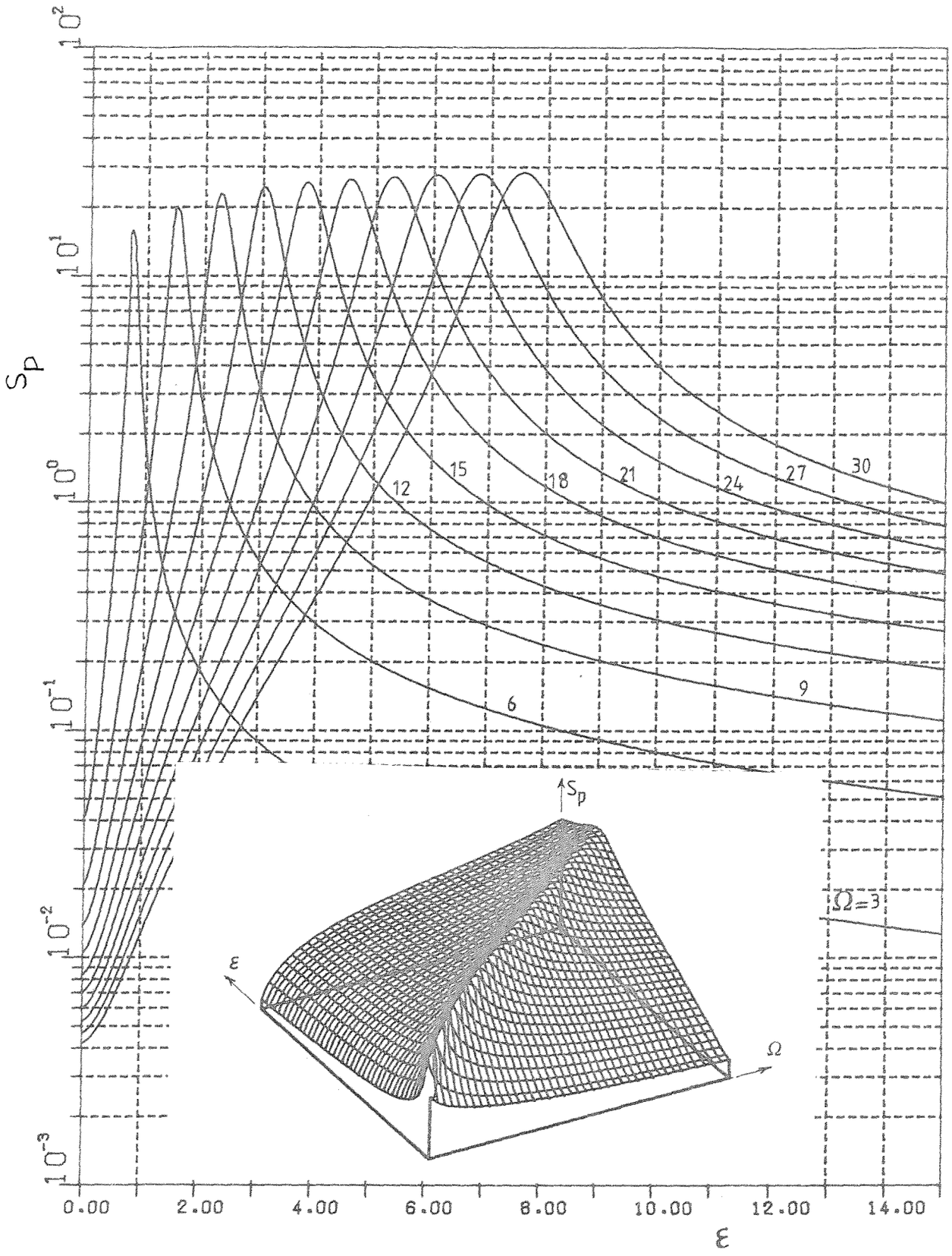

Figure 5.7.(a)The power spectral density of a boundary layer pressure field ,b=0.1,CV=4.0,$S_p(\Omega)$=1.0, ε=-K.1 (see Section 5.2) .

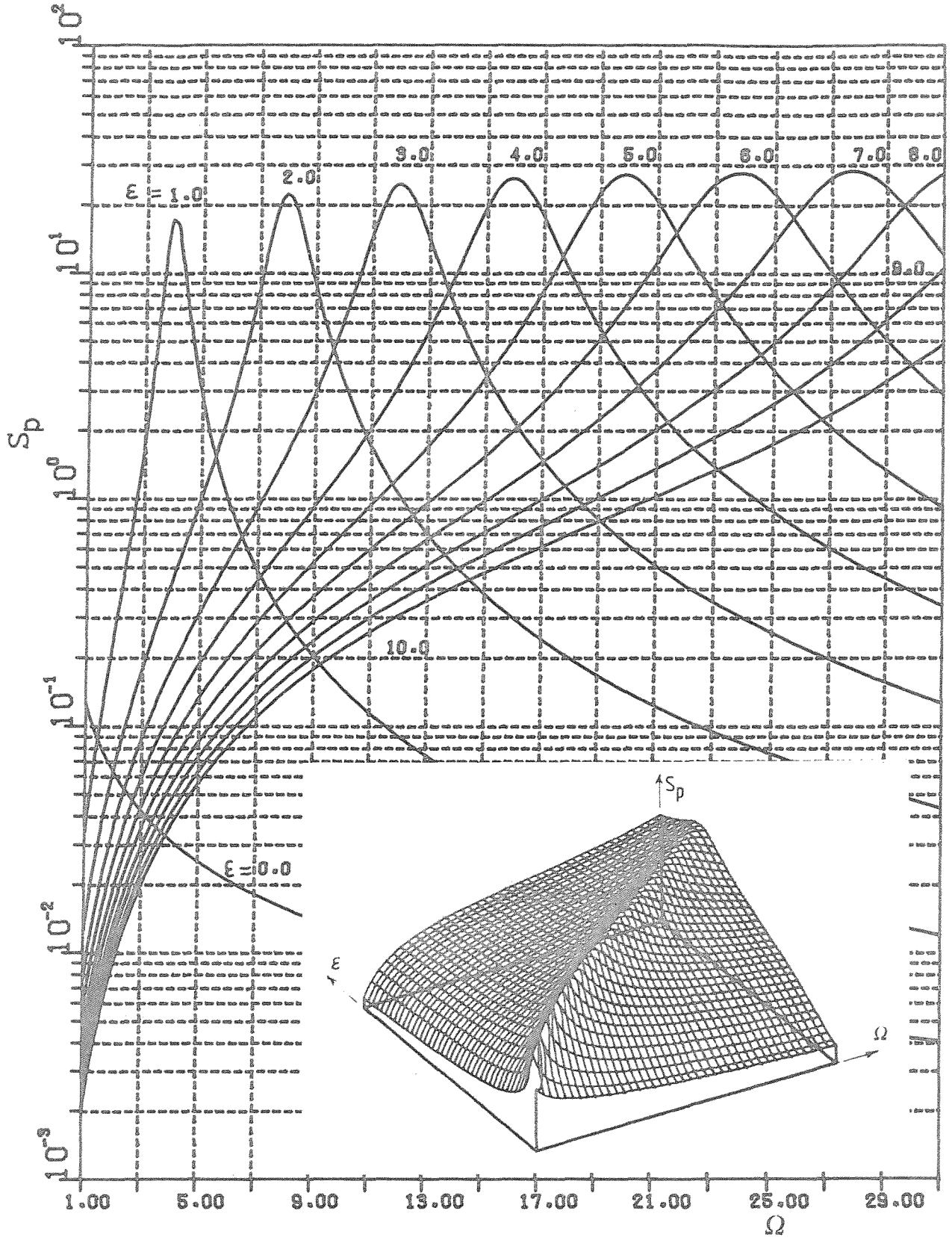

Figure 5.7.(b) The power spectral density of a boundary layer pressure field ,b=0.1,CV=4.0,$S_p(\Omega)$=1.0, ξ=-K.1 (see Section 5.2).

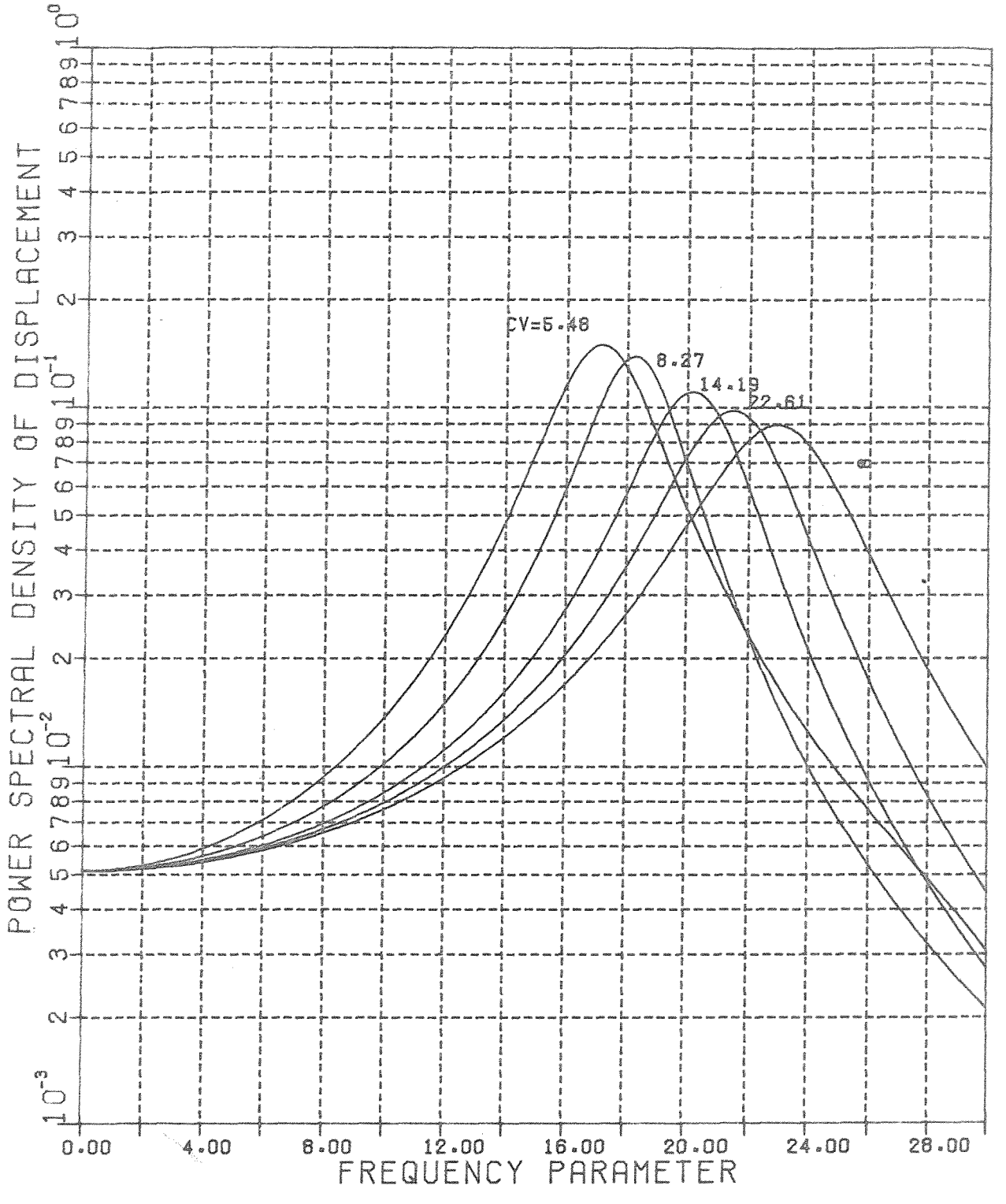

Figure 5.8. Spectra of displacement at bay centres of the infinite periodically stiffened panel shown in figure(2.4),due to frozen convected random pressure field .

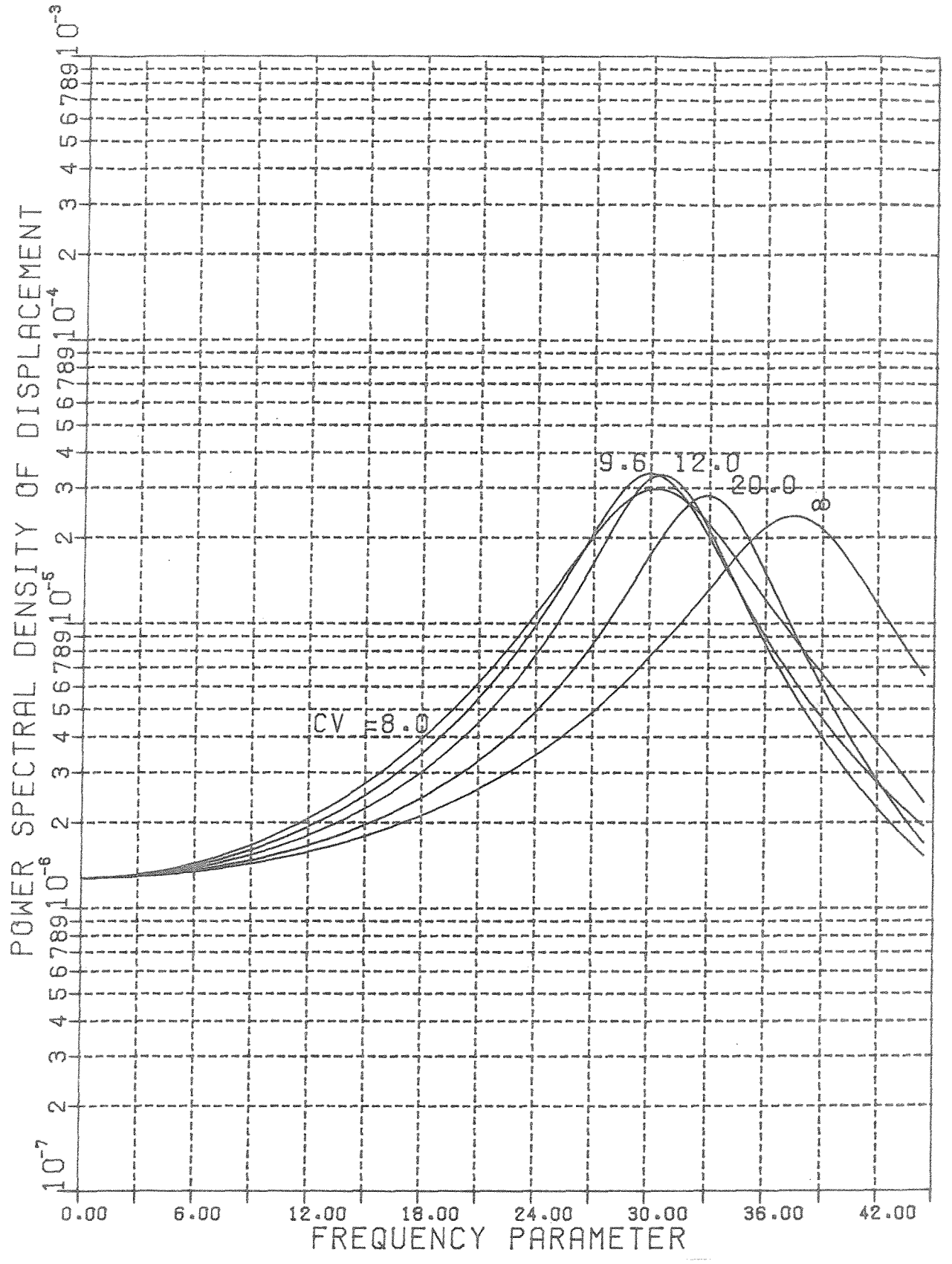

Figure 5.9. Spectra of displacement at bay centres of a two-dimensional periodic plate on simple line supports with square cells due to frozen convected random pressure field propagating along the X direction .

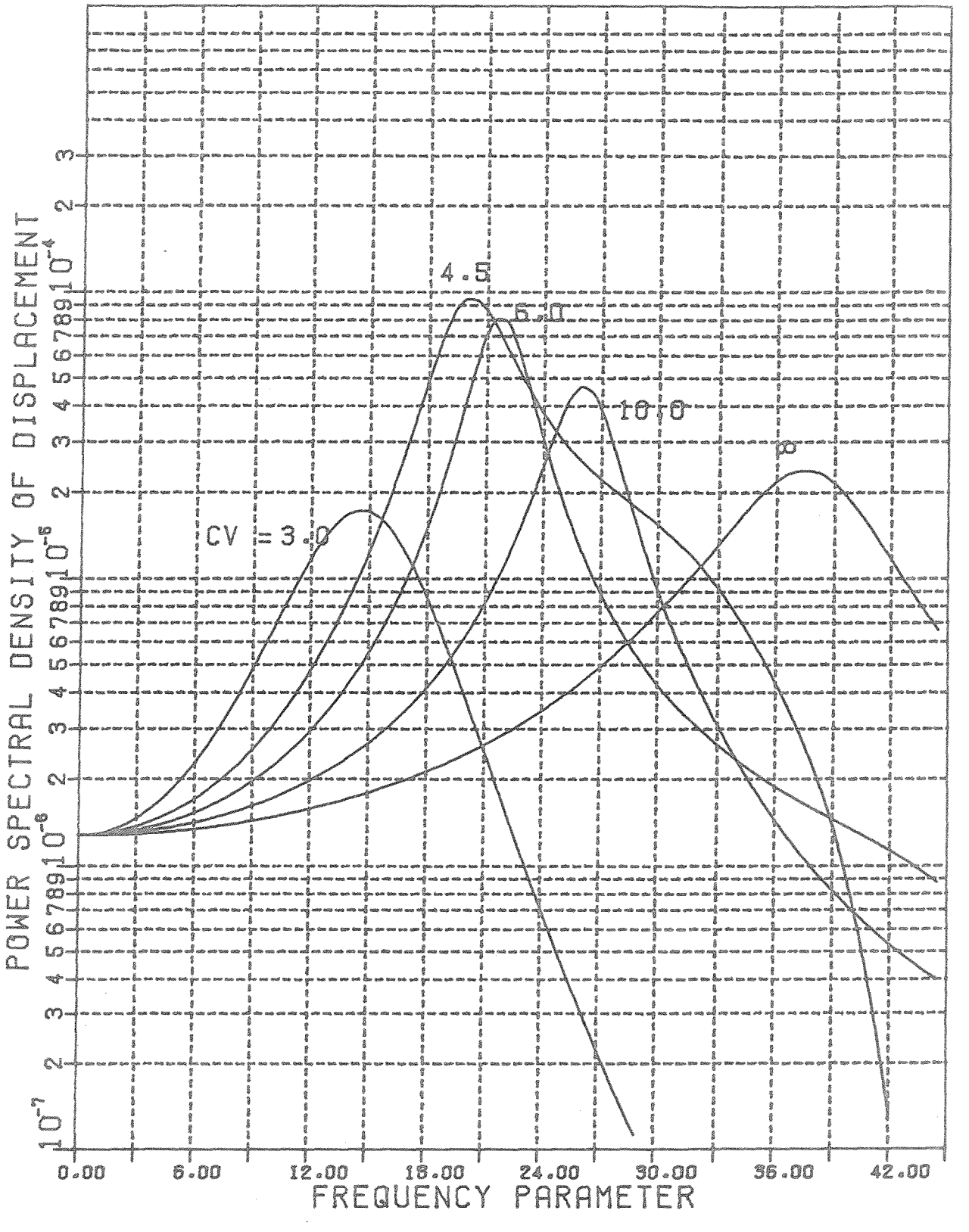

Figure 5.10. Spectra of displacement at bay centres of a two-dimensional periodic plate on simple line supports with square cells due to frozen convected random pressure field propagating in a direction making 45 degrees to the X direction .

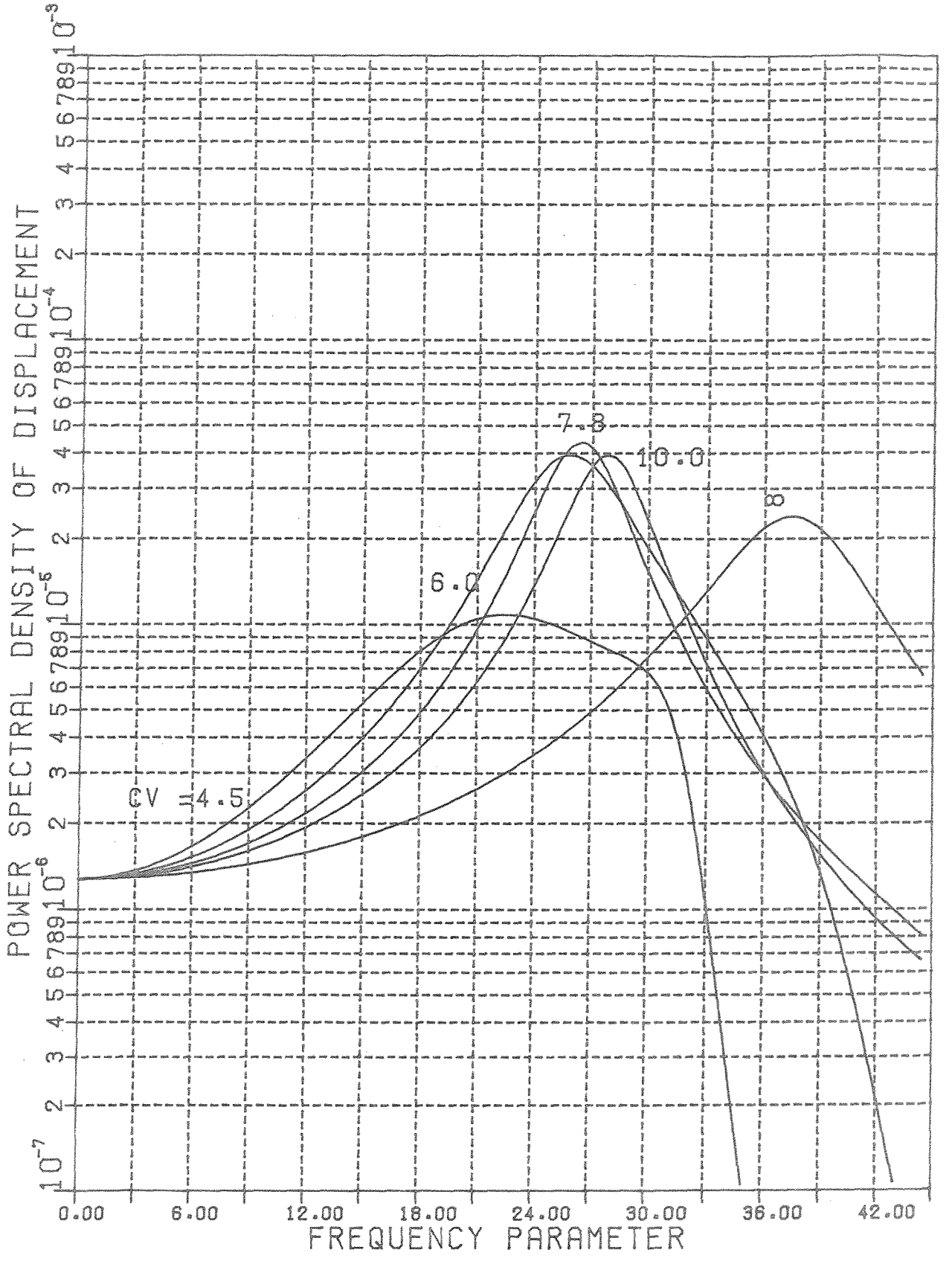

Figure 5.11. Spectra of displacement at bay centres of a two-dimensional periodic plate on simple line suppores with square cells due to frozen convected random pressure field propagating in a direction making 20 degrees to the X direction .

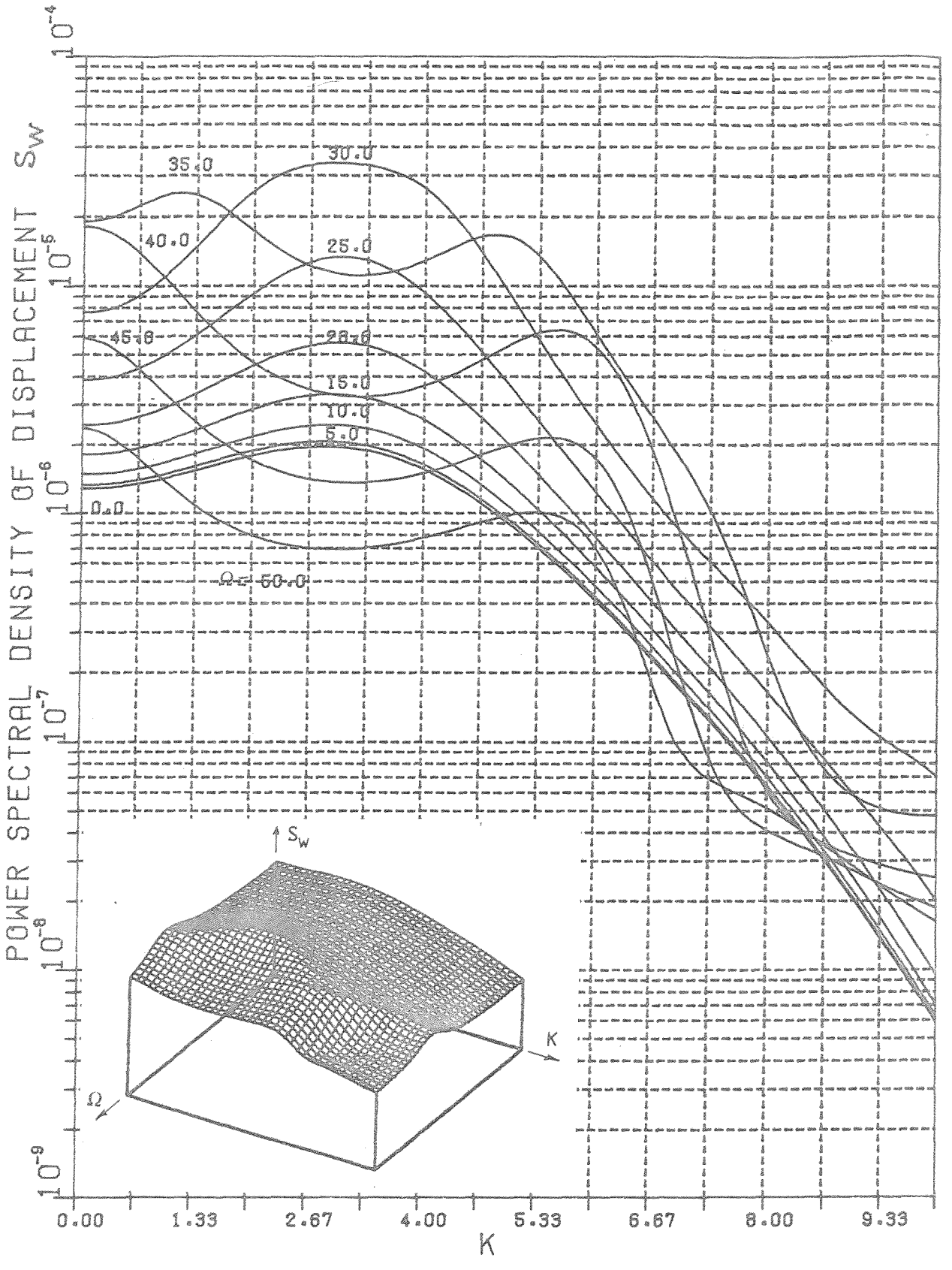

Figure 5.12.(a) Spectra of displacement at cell centres of an infinite two-dimensional periodic plate on simple line supports with square cells, due to general random homogeneous pressure field with unit amplitude propagating along the X direction. Lines of constant frequency .

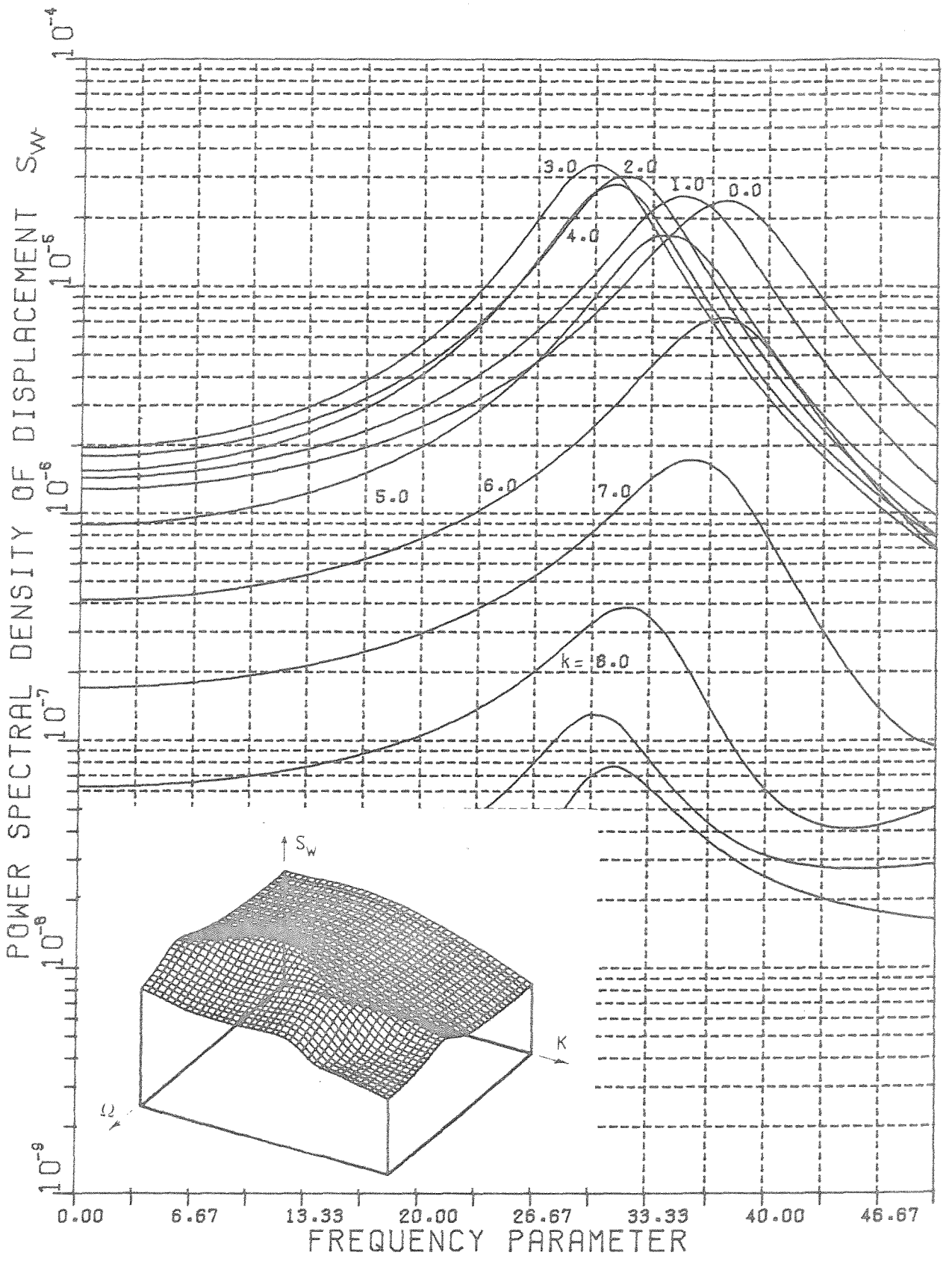

Figure 5.12.(b) Spectra of displacement at cell centres of an infinine two-dimensional periodic plate on simple line supports with square cells,due to general random homogeneous pressure field with unit amplitude propagating along the X direction. Lines of constant wave-number .

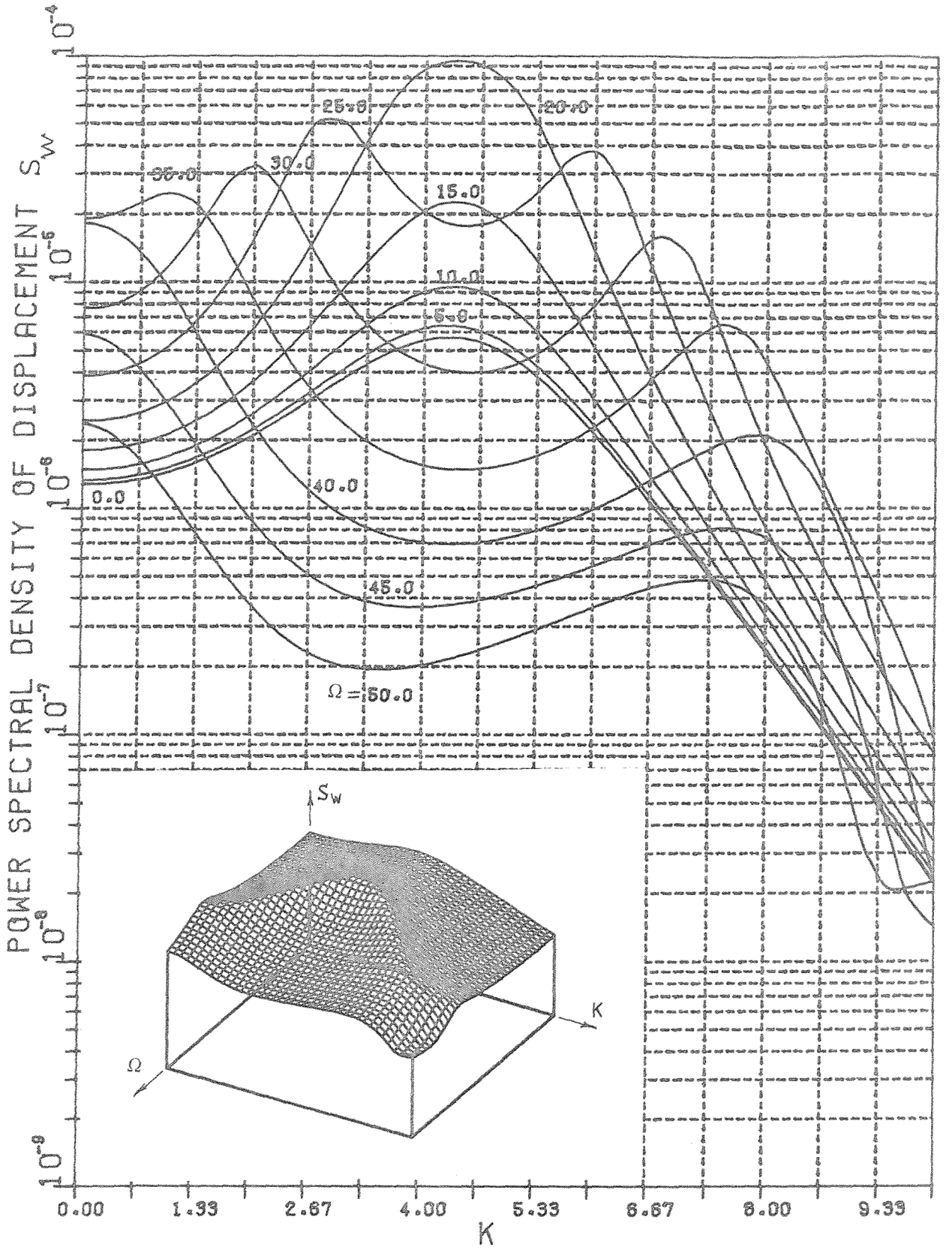

Figure 5.13.(a) Spectra of displacement at cell centres of an infinite two-dimensional periodic plate on simple line supports with square cells,due to general random homogeneous pressure field with unit amplitude propagating along a direction of 45 degrees to the X direction.Lines of constant frequency .

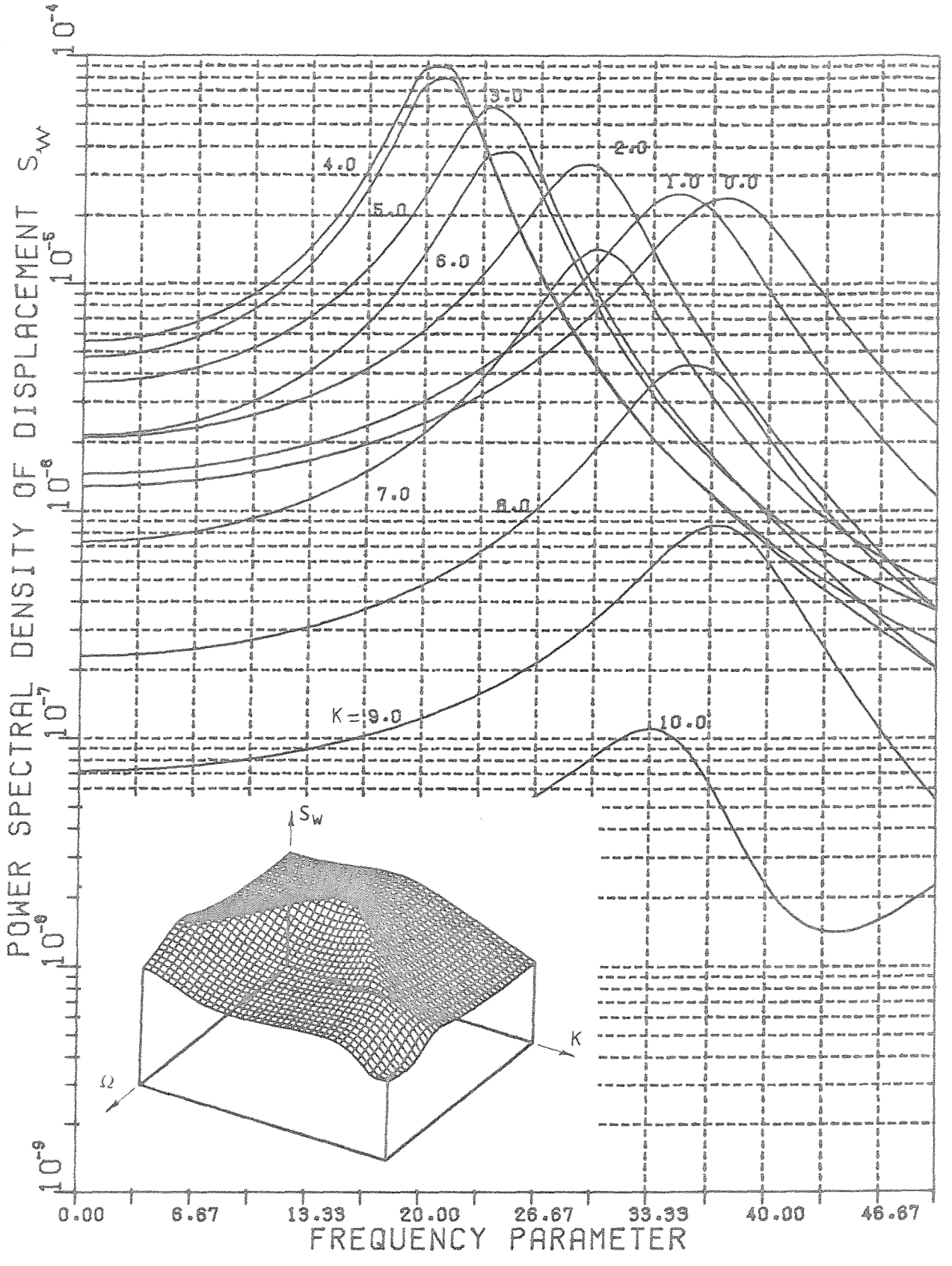

Figure 5.13.(b) Spectra of displacement at cell centres of an infinite two-dimensional periodic plate on simple line supports with square cells, due to general random homogeneous pressure field with unit amplitude propagating along a direction of 45 degrees to the X direction. Lines of constant wave-number.

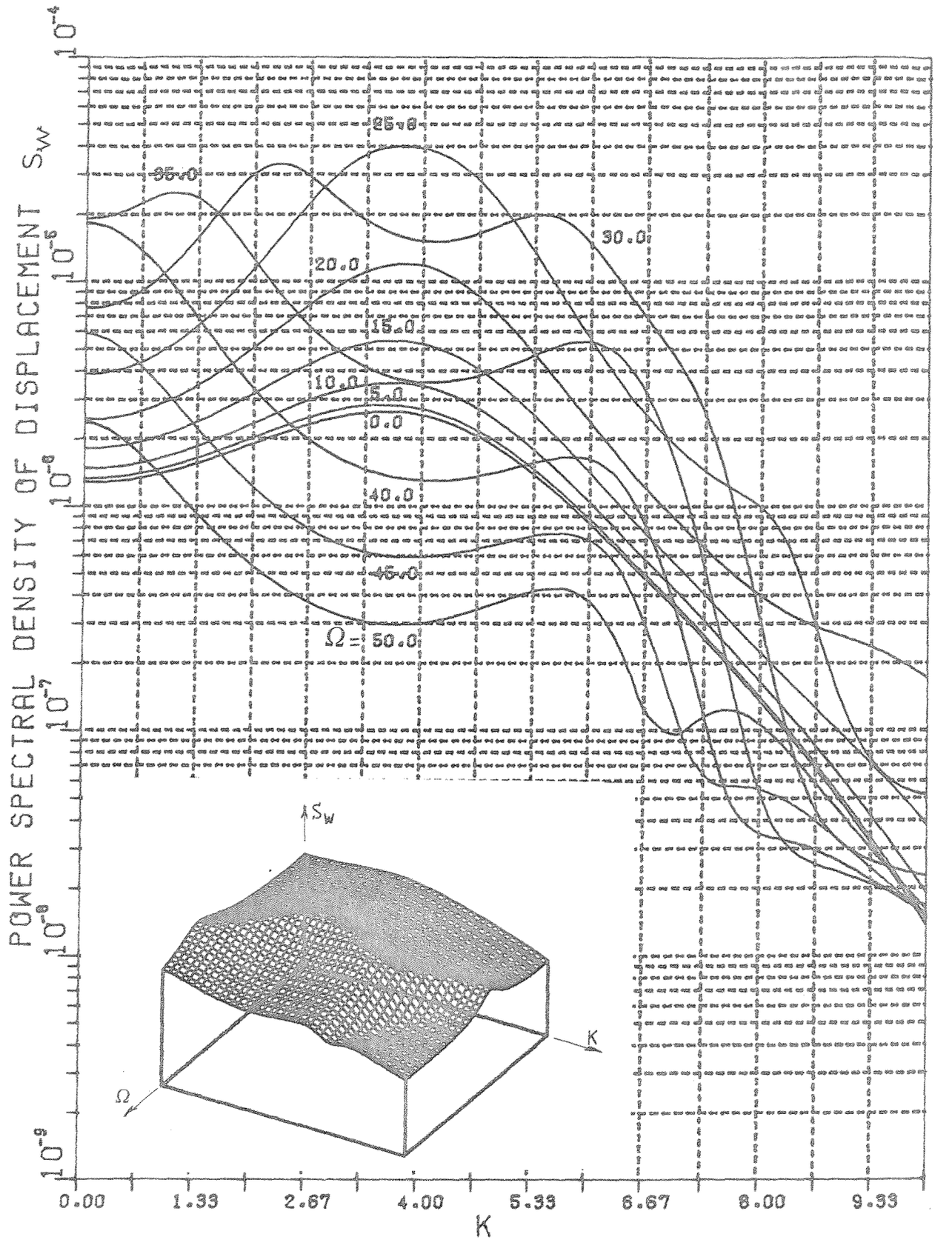

Figure 5.14.(a) Spectra of displacement at cell centres of an infinite two-dimensional periodic plate on simple line supports with square cells ,due to general random homogeneous pressure field with unit amplitude propagating along a direction of 20 degrees to the X direction.Lines of constant frequency.

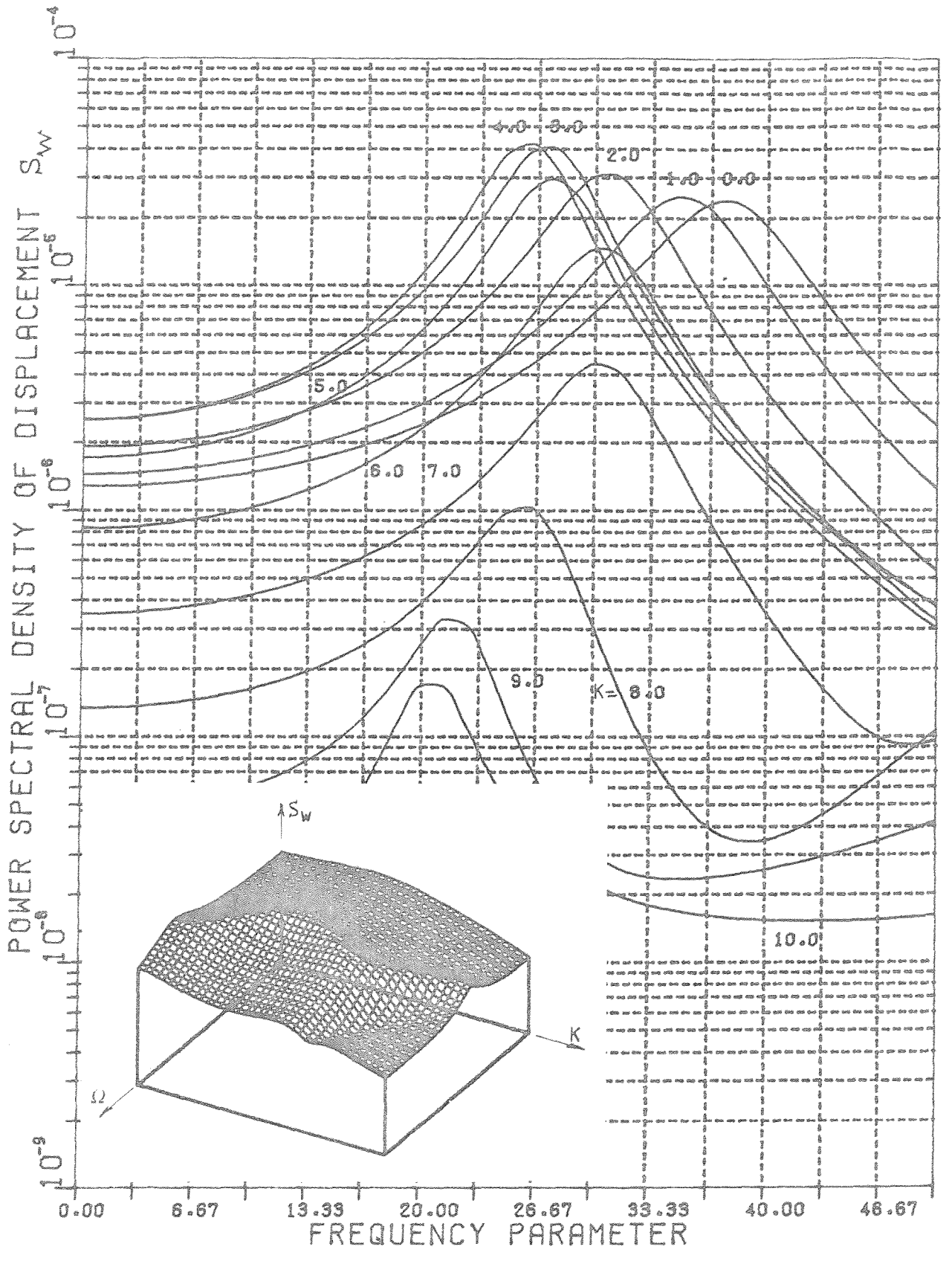

Figure 5.14.(b)Spectra of displacement at cell centres of an infinite two-dimensional periodic plate on simple line supports with square cells,due to general random homogeneous pressure field with unit amplitude propagating along a direction of 20 degrees to the X direction.Lines of constant wave-number.

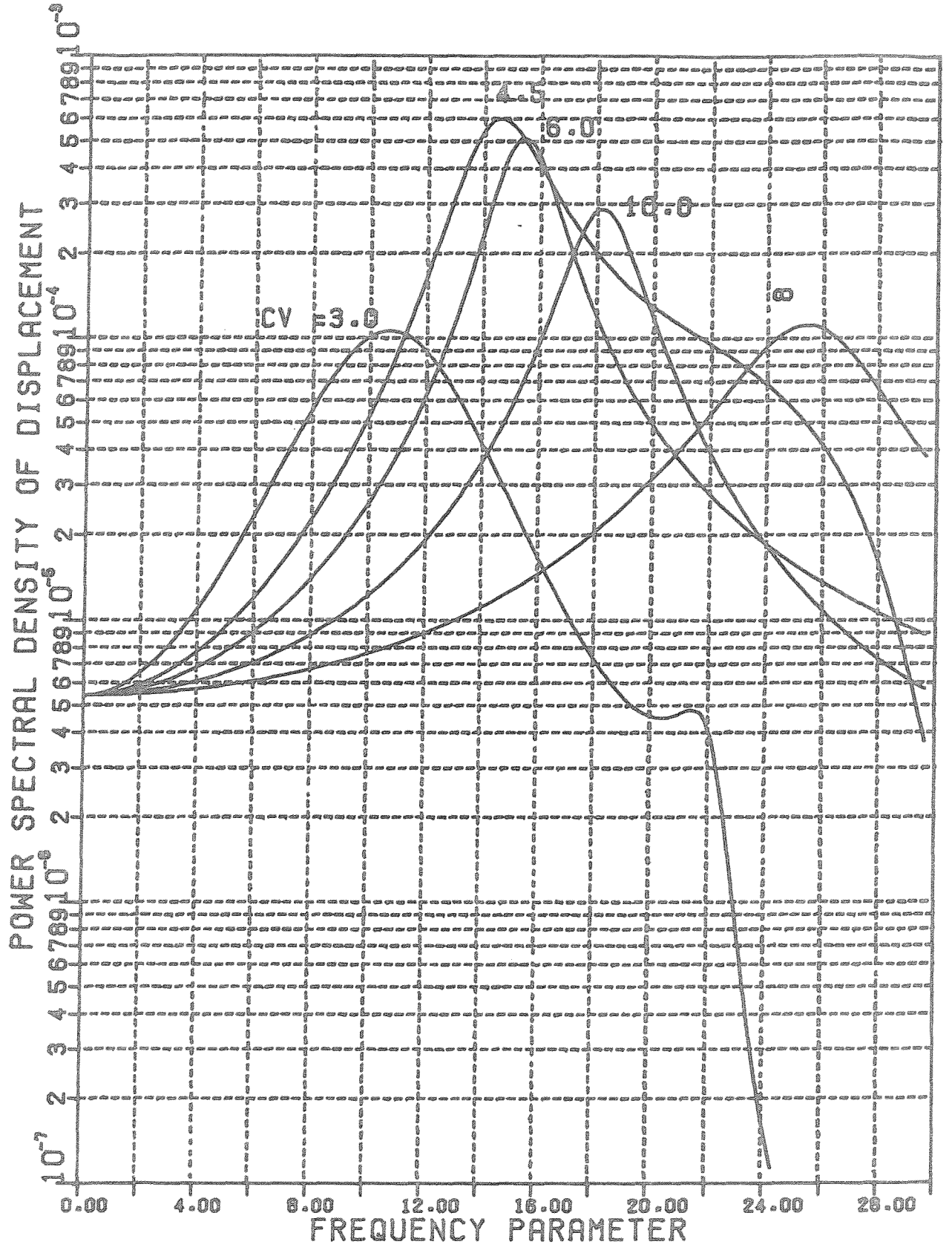

Figure 5.15. Spectra of displacement at cell centres of an infinite two-dimensional periodic plate on simple line supports with rectangular cells(l_x/l_y=.5), due to frozen convected random pressure field propagating along the X direction .

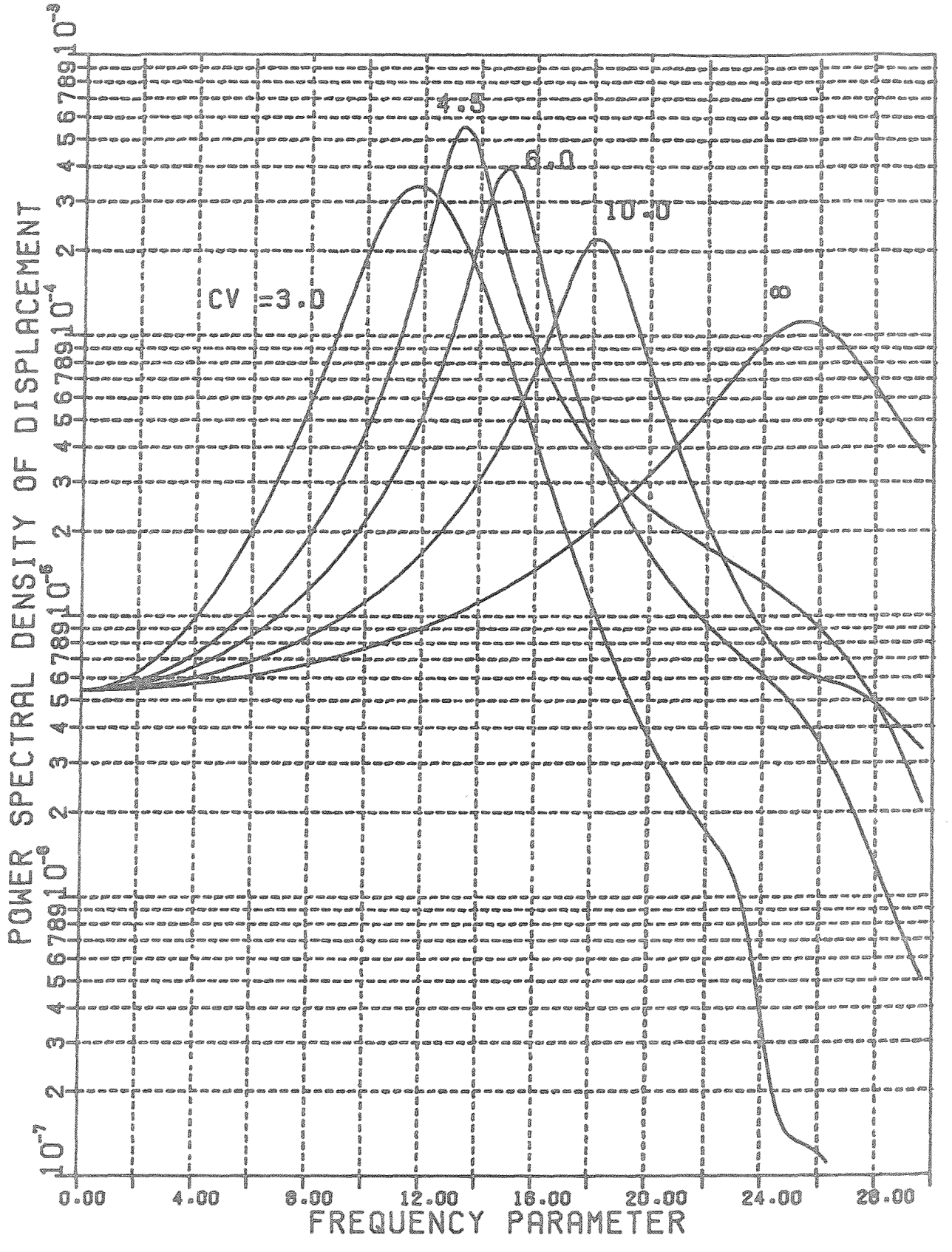

Figure 5.16. Spectra of displacement at cell centres of an infinite two-dimensional periodic plate on simple line supports with rectangular cells(l_x/l_y=.5), due to frozen convected random pressure field propagating along a direction of 26.6 degrees to the X direction.

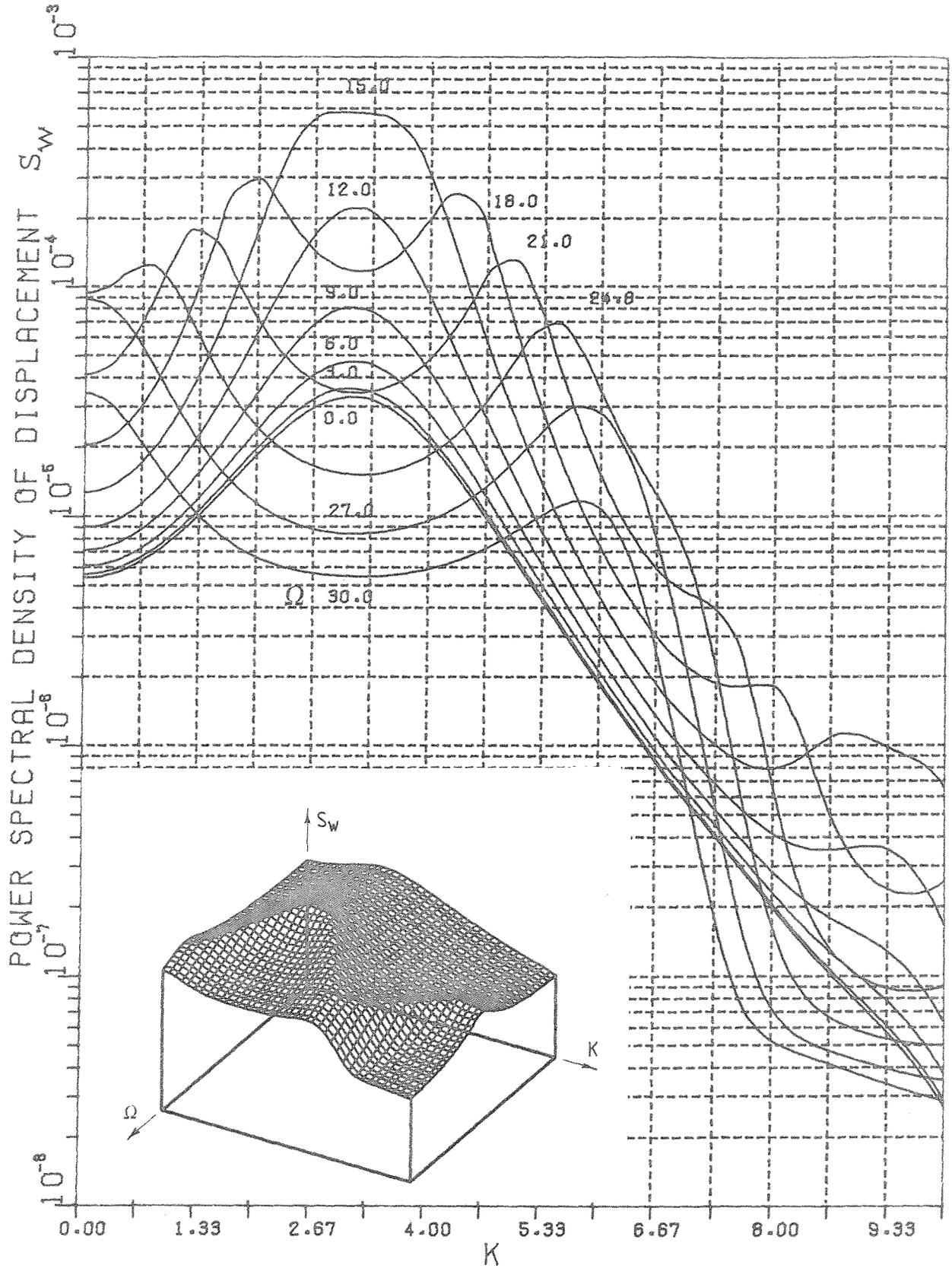

Figure 5.17.(a)Spectra of displacement at cell centres of an infinite two-dimensional periodic plate on simple line supports with rectangular cells(l_x/l_y=0.5),due to general random homogeneous pressure field with unit amplitude propagating along the X direction.Lines of constant frequency.

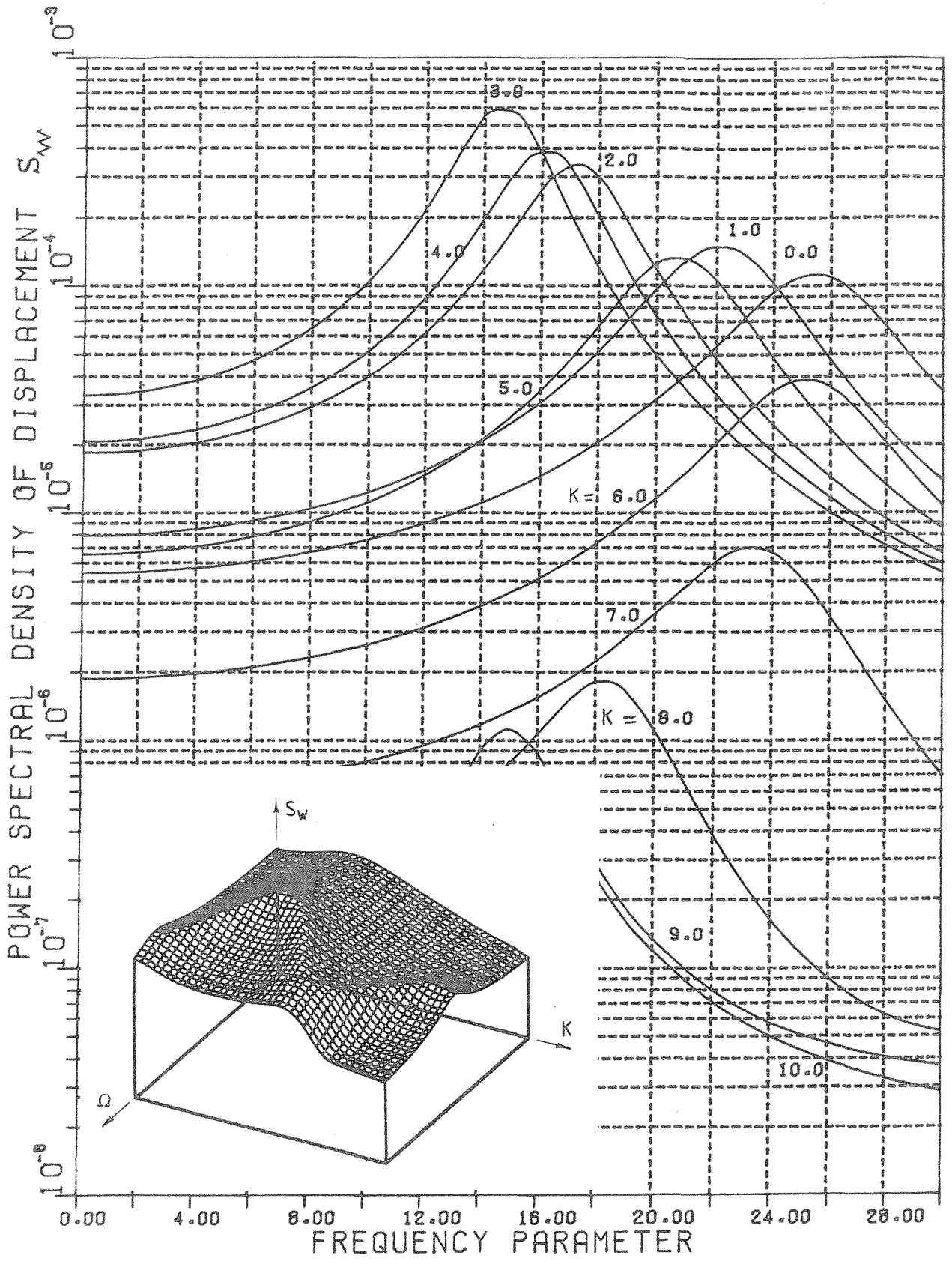

Figure 5.17.(b)Spectra of displacement at cell centres of an infinite two-dimensional periodic plate on simple line supports with rectangular cells(l_x/l_y=0.5),due to general random homogeneous pressure field with unit amplitude propagating along the X direction.Lines of constant wave-number .

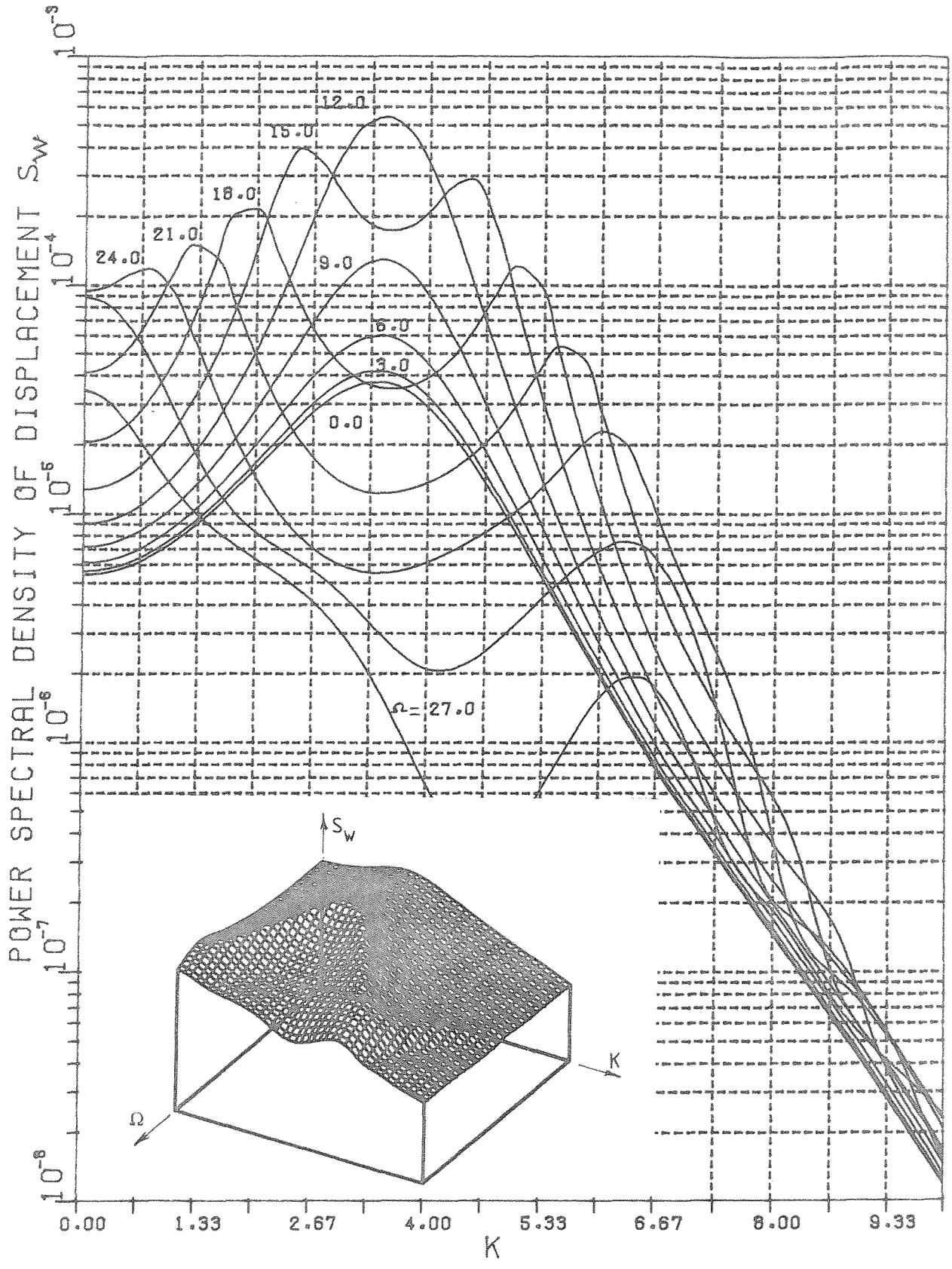

Figure 5.18.(a)Spectra of displacement at cell centres of an infinite two-dimensional periodic plate on simple line supports with rectangular cells(l_x/l_y=.5),due to general random homogeneous pressure field with unit amplitude propagating along a direction of 26.6 degrees to the X axis.Lines of constant frequency .

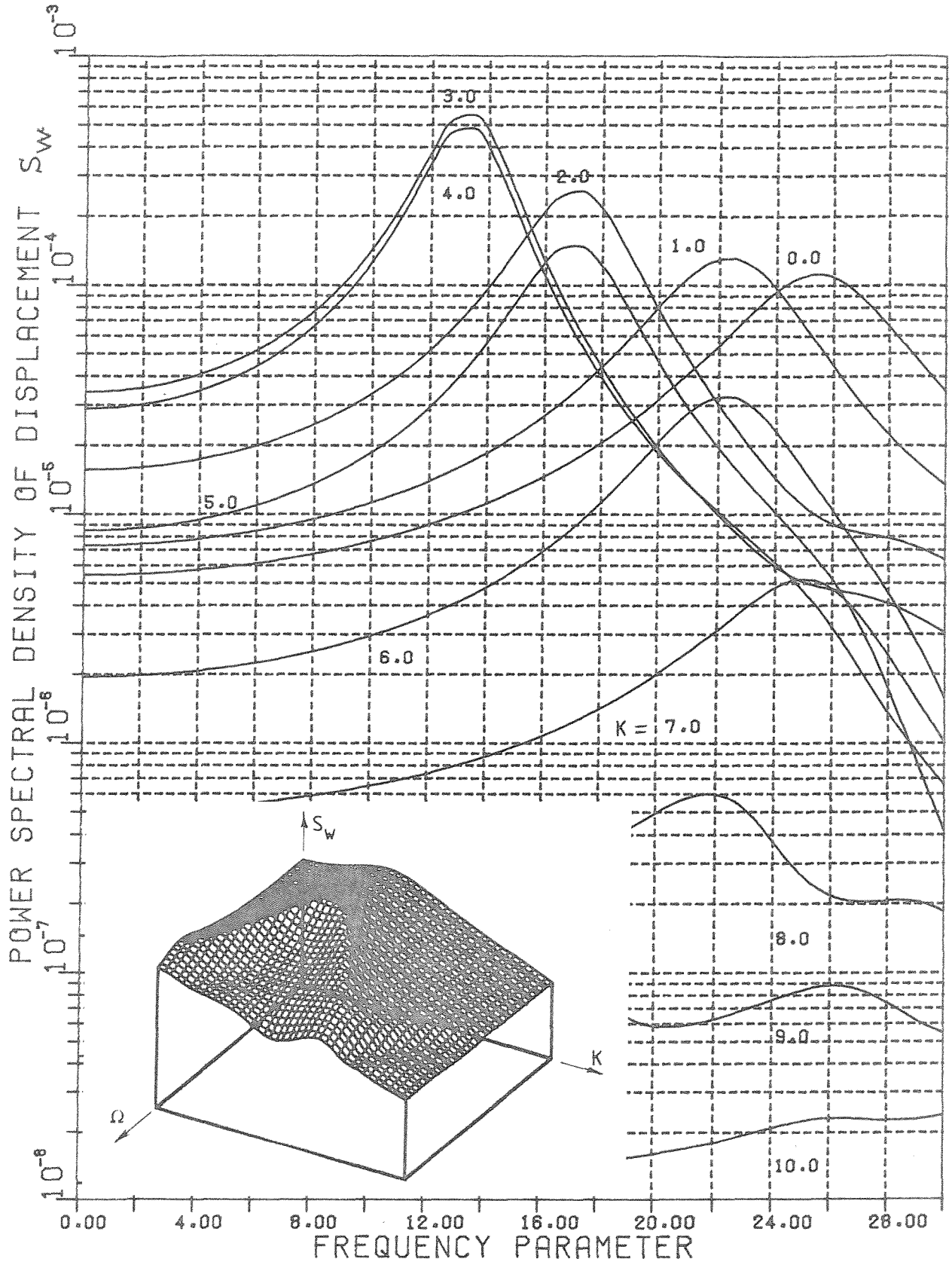

Figure 5.18.(b)Spectra of displacement at cell centres of an infinite two-dimensional periodic plate on simple line supports with rectangular cells(l_x/l_y=.5),due to general random homogeneous pressure field with unit amplitude propagating along a direction of 26.6 degrees to the X direction.Lines of constant wave-number.

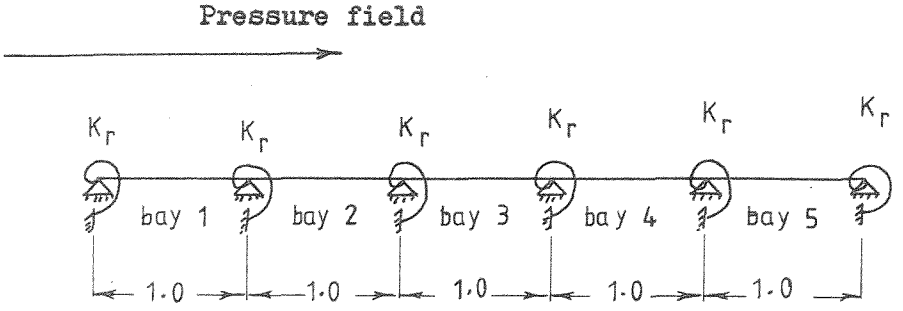

Figure 5.19. A five bay beam on point supports with rotational stiffness subjected to random pressure field .

Ω =13.10

14.19

16.23

18.86

21.32

Figure 5.20. The first five natural frequencies and associated normal modes of the five bay beam shown in figure(5.19), K_r=4.0 .

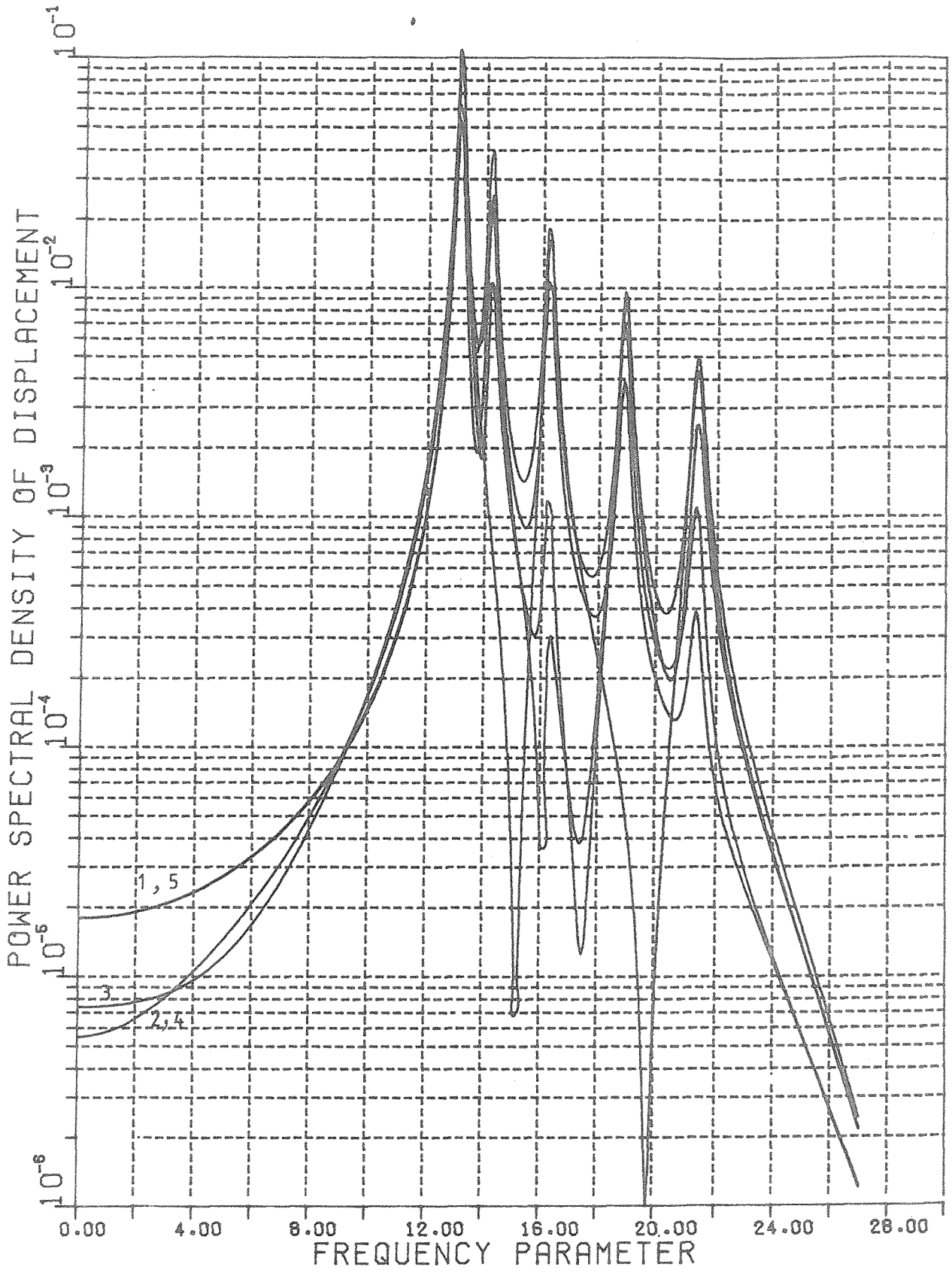

Figure 5.21. Spectra of displacement at bay centres of the five bay beam of figure(5.19), due to frozen convected random pressure field, CV=4.0, K_r=4.0, ξ =0.01 .

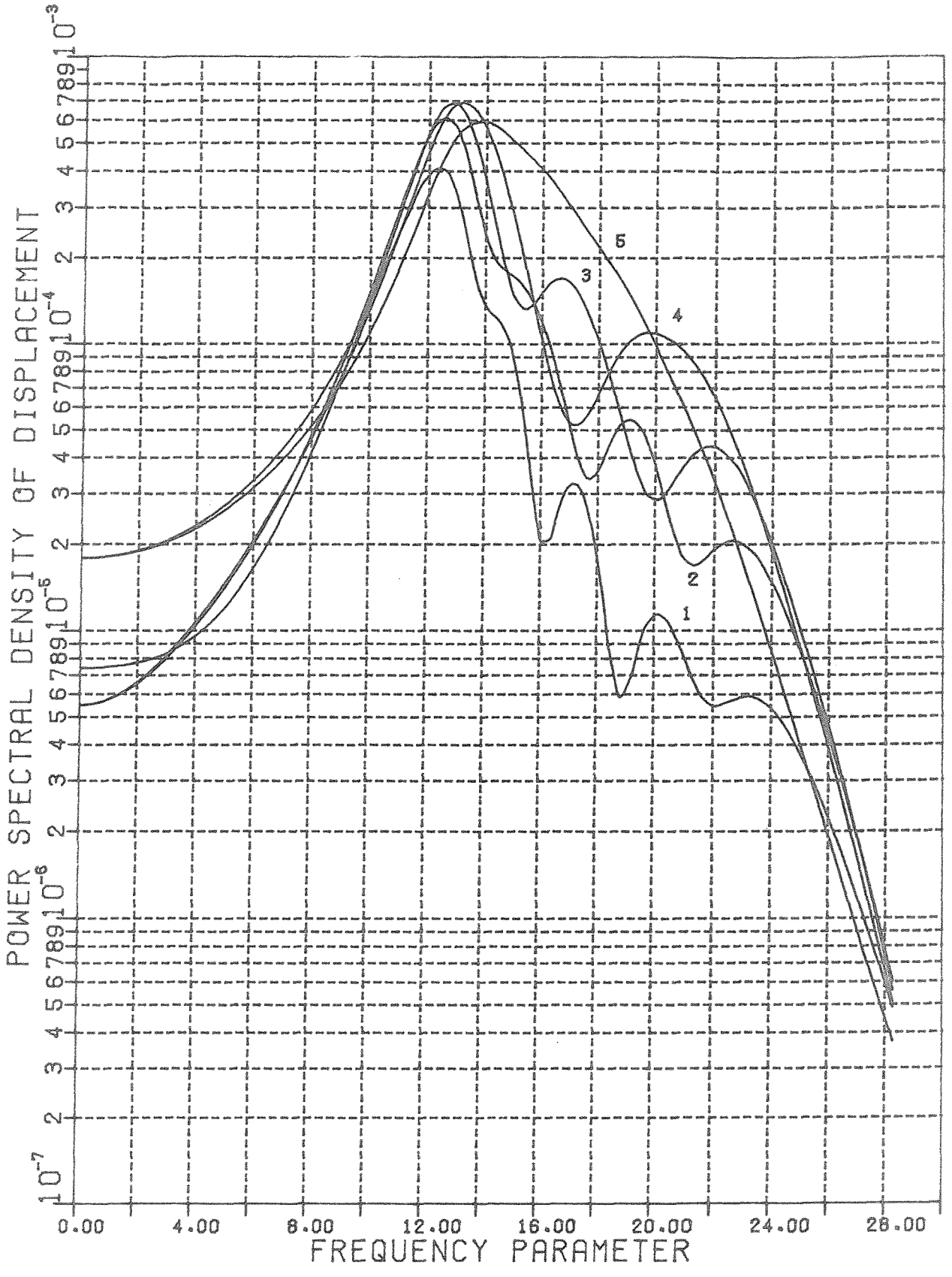

Figure 5.22. Spectra of displacement at bay centres of the five bay beam of figure(5.19), due to frozen convected random pressure field, CV=4., K_r=4.0, ζ=0.125 .

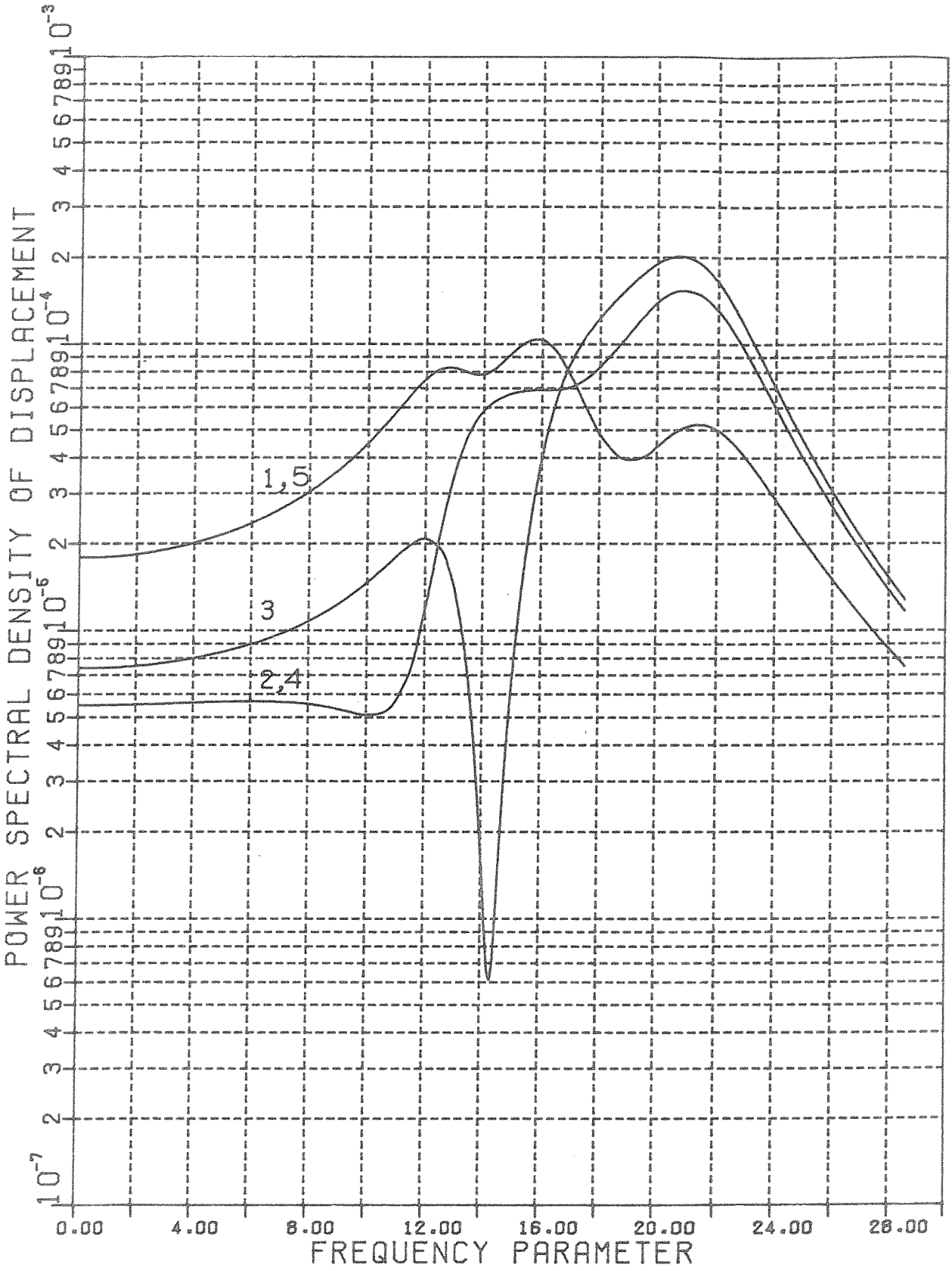

Figure 5.23. Spectra of displacement at bay centres of the five bay beam of figure(5.19), due to frozen convected random pressure field, $CV=\infty, K_r=4.0, \xi=0.125$.

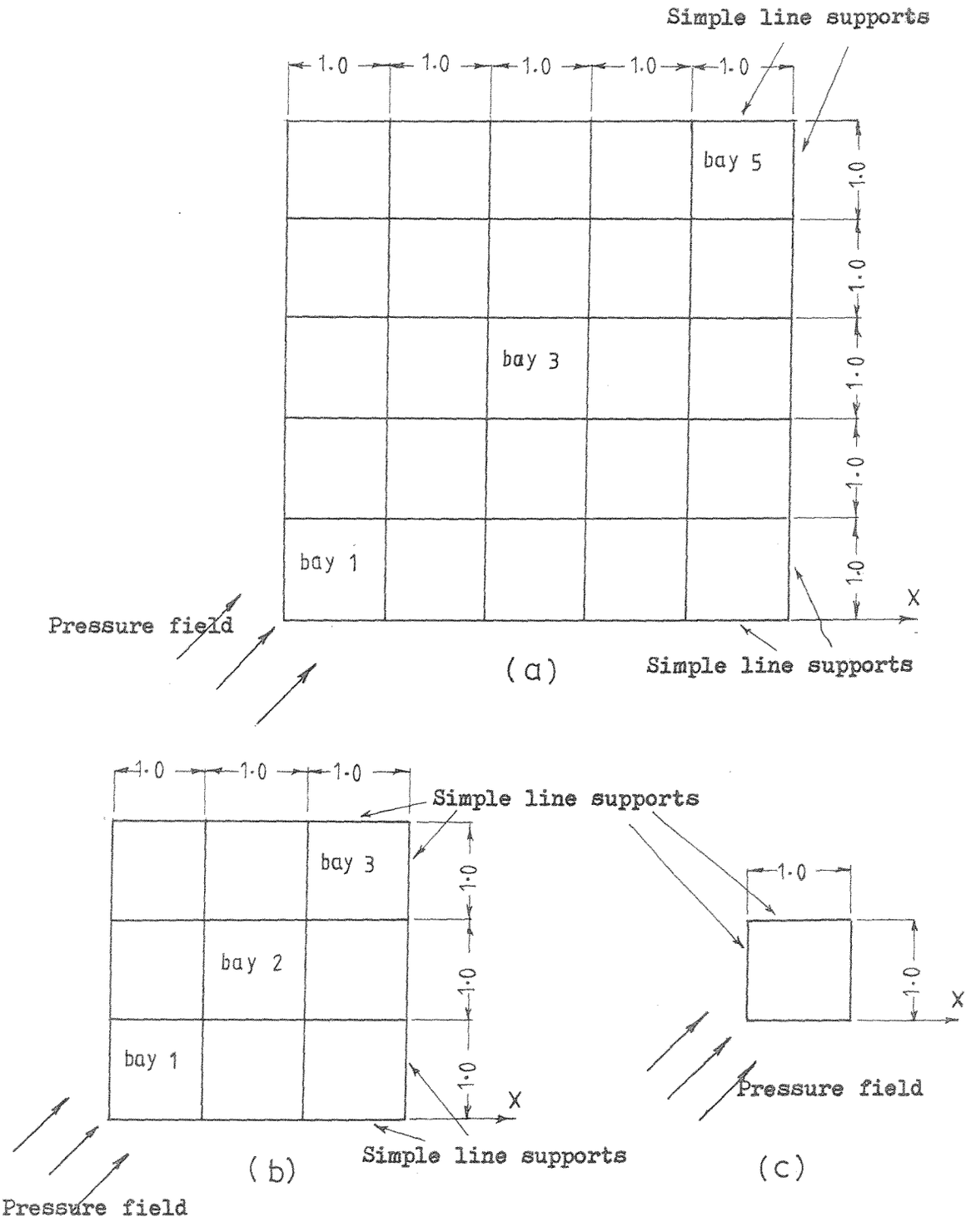

Figure 5.24. Two-dimensional finite periodic plates on simple line supports subjected to random pressure field ;(a)a 5X5 bay plate ;(b) a 3X3 bay plate ;(c) a single bay plate .

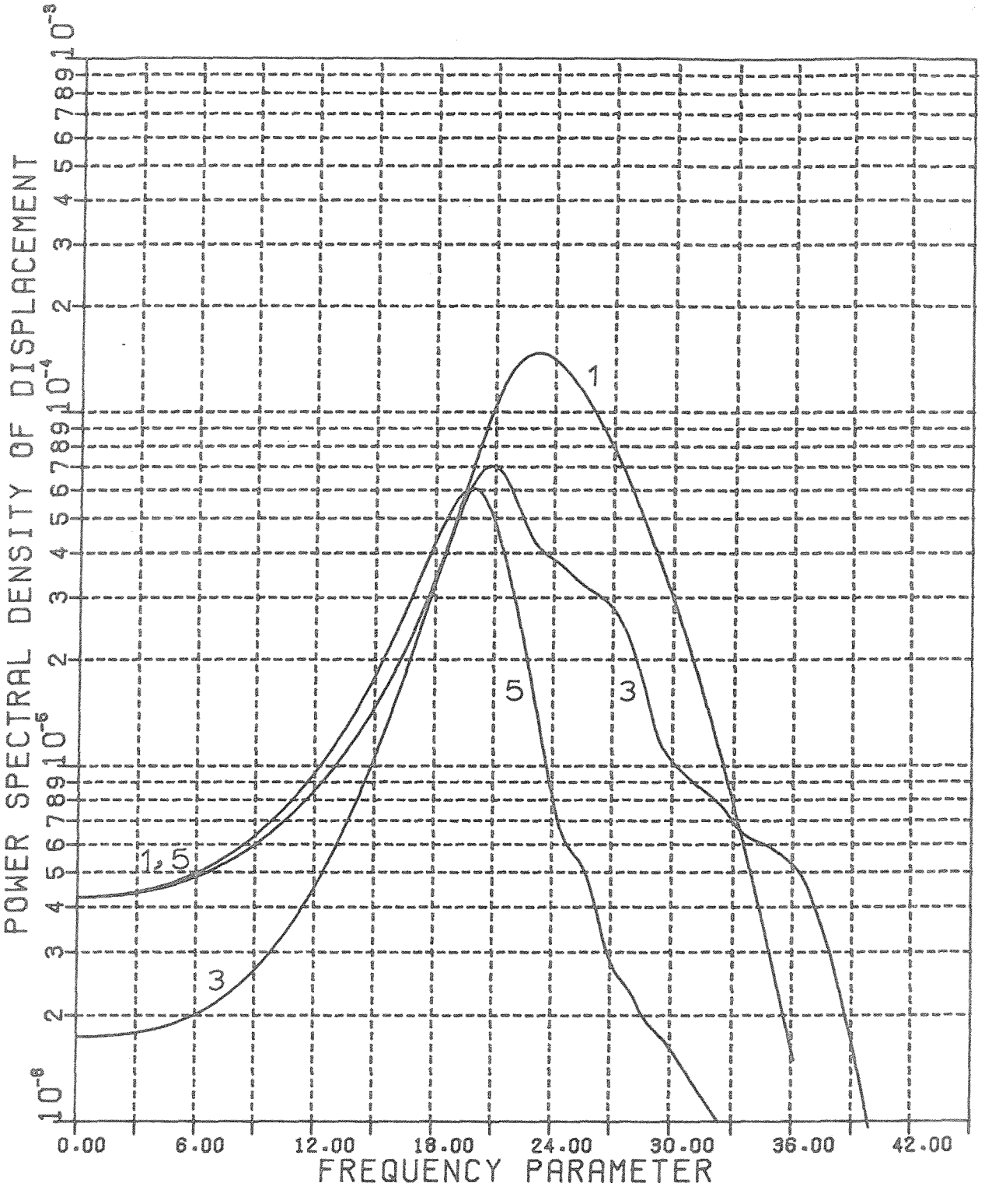

Figure 5.25. Spectra of displacement at bay centres of the 5X5 bay plate of figure(5.24a), due to frozen convected random pressure field propagating along a direction of 45 degrees to the X direction, CV=4.5, ζ =.125 .

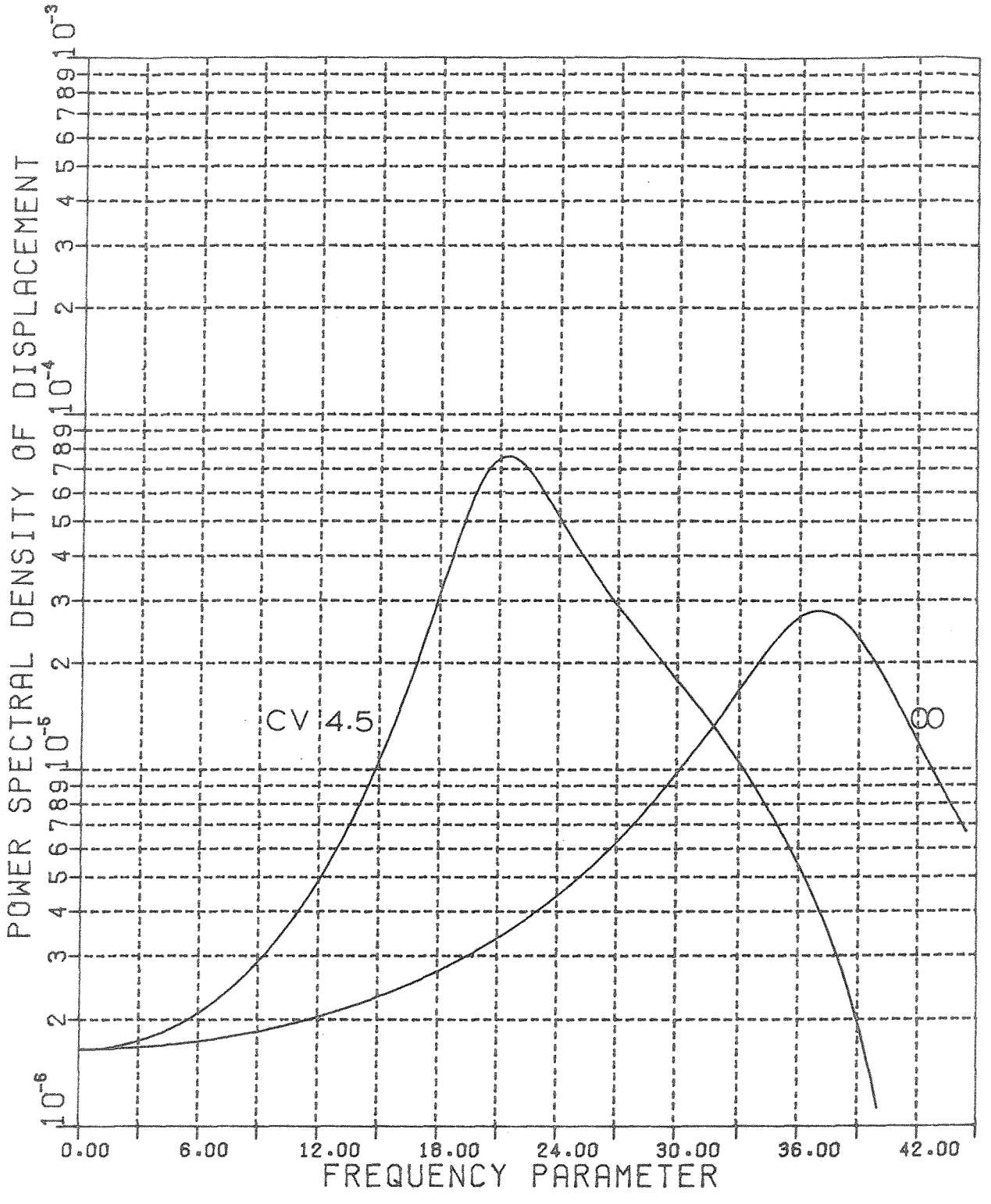

Figure 5.26. Spectra of displacement at cell centres of an infinite two-dimensional periodic plate on simple line supports with square cells, due to frozen convected random pressure field propagating along a direction of 45 degrees to the X direction, $\eta = 0.25$.

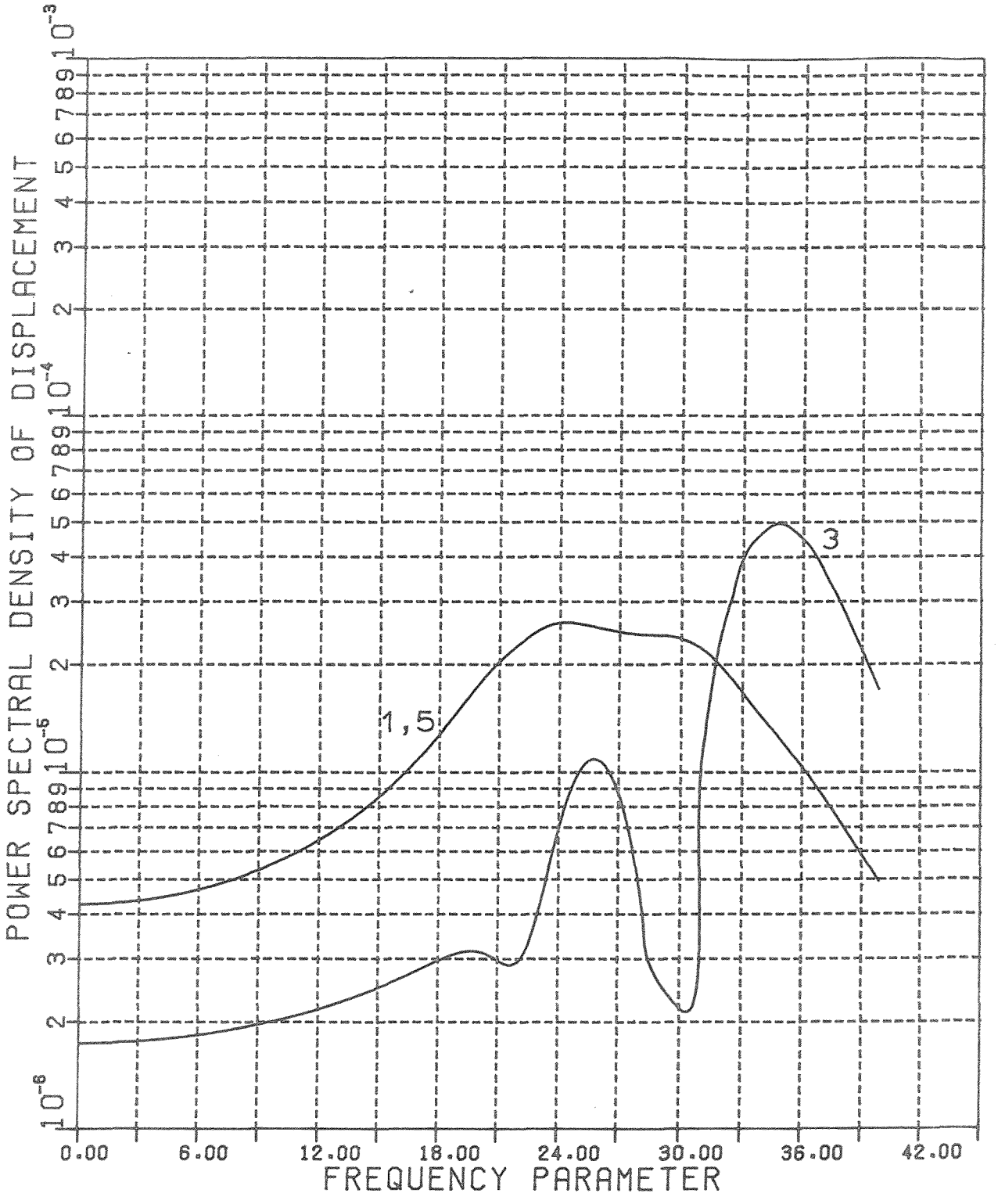

Figure 5.27. Spectra of displacement at bay centres of the 5X5 bay plate of figure(5.24a), due to frozen convected random pressure field, $CV=\infty$, $\xi=0.125$.

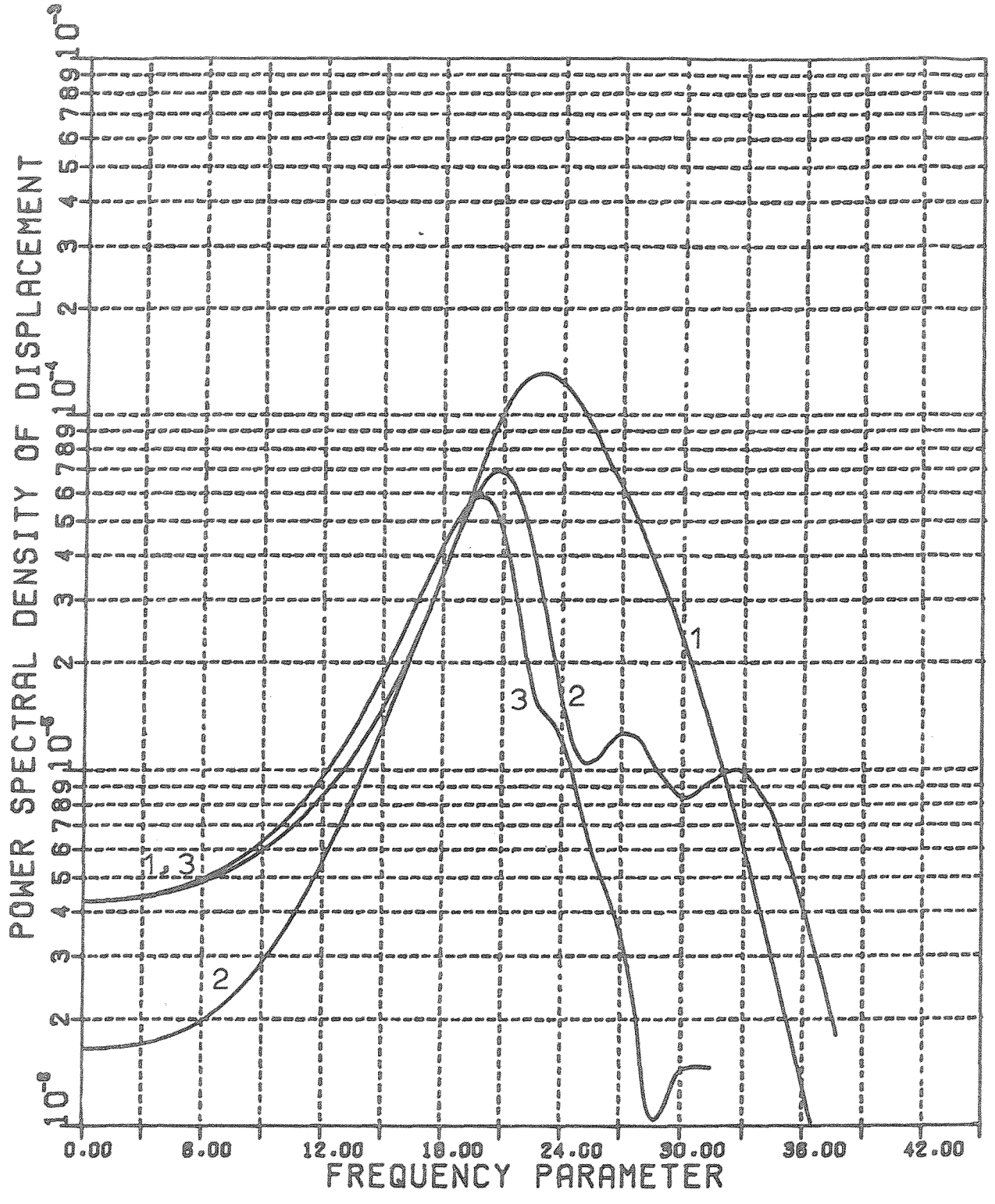

Figure 5.28. Spectra of displacement at bay centres of the 3X3 bay plate of figure(5.24b), due to frozen convected random pressure field propagating along a direction of 45 degrees to the X direction, $CV=4.5$, $\xi=0.125$.

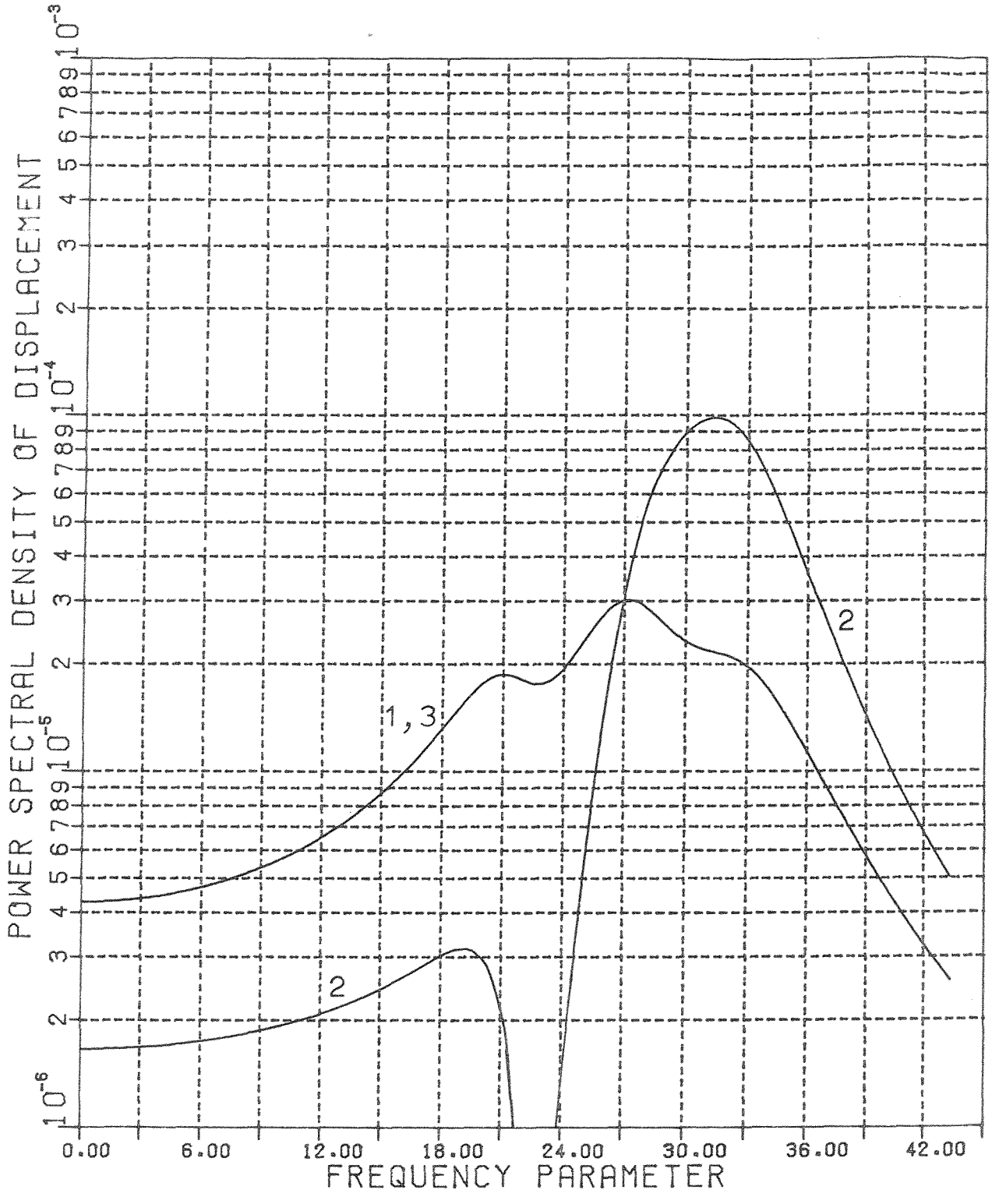

Figure 5.29. Spectra of displacement at bay centres of the 3X3 bay plate of figure(5.24b), due to frozen convected random pressure field, CV=∞, ξ =0.125 .

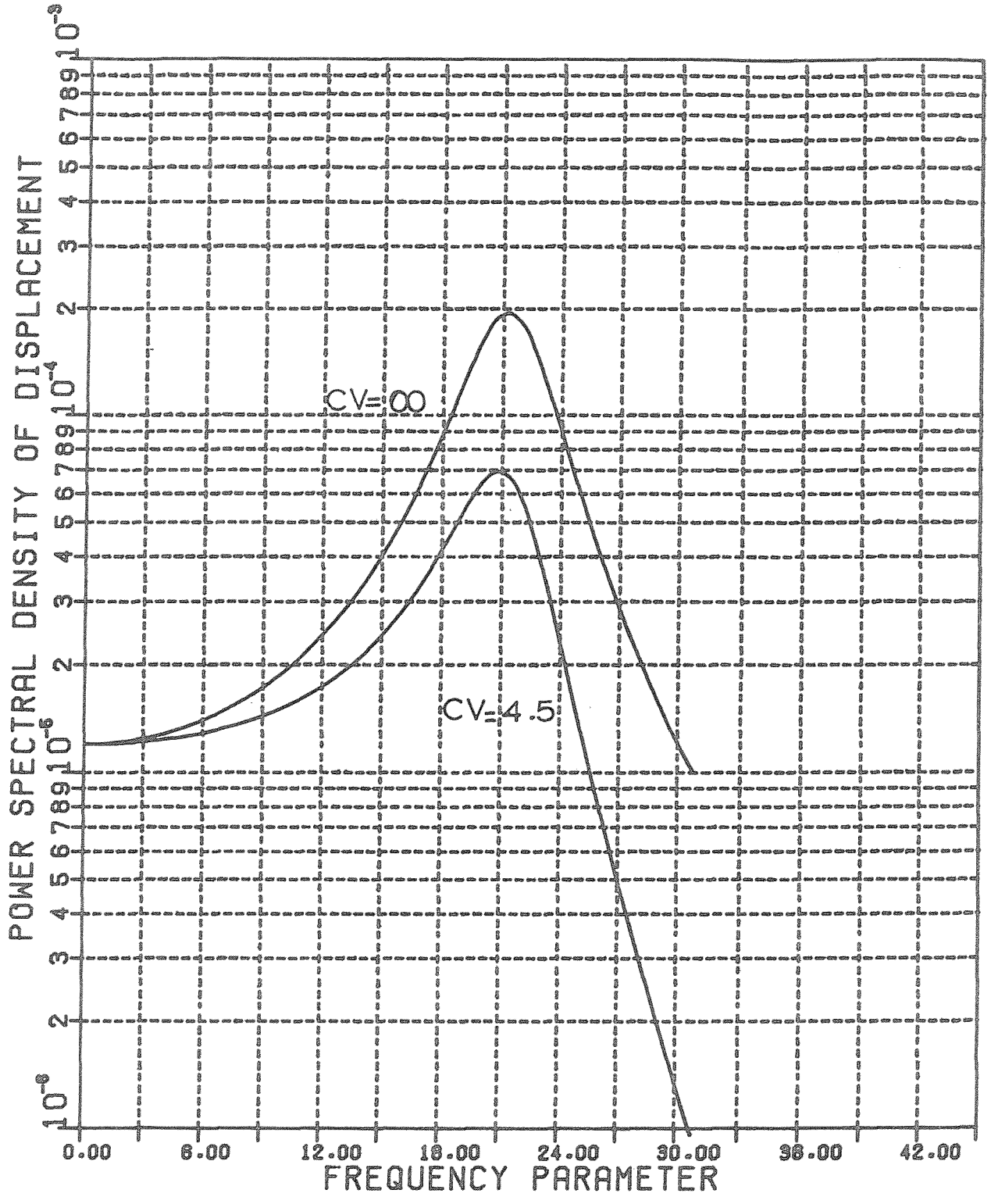

Figure 5.30. Spectra of displacement at the mid point of the simply supported square plate of figure(5.24c), due to frozen convected random pressure field propagating along a direction of 45 degrees to the X direction, ξ=0.125 .

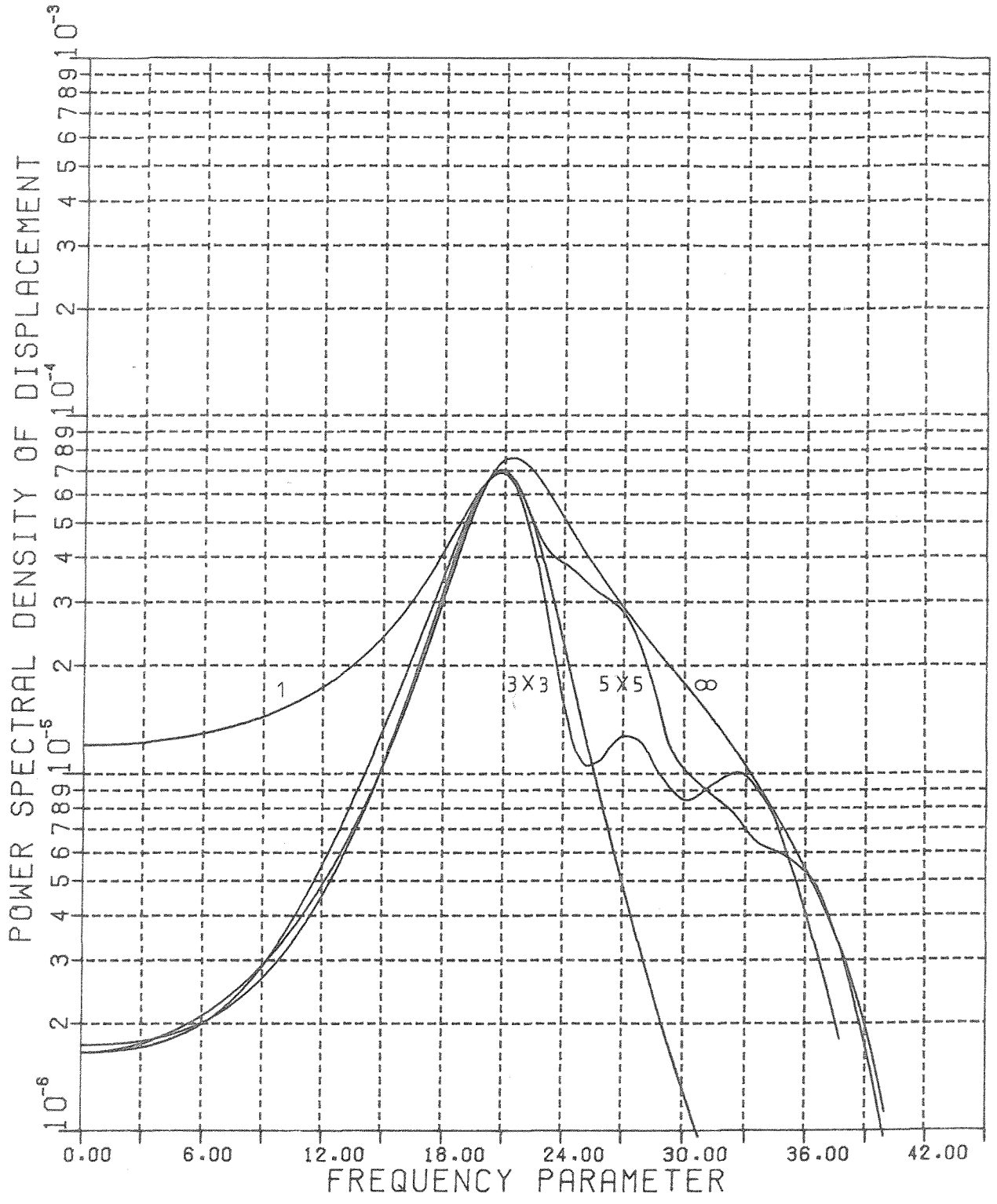

Figure 5.31. Comparison of the response at the cell centres of an infinite two-dimensional periodic plate on simple line supports with square cells and the response at the centre of the middle bay of a 5X5 ,3X3 and a single bay plate of figure(5.24), due to frozen convected random pressure field propagating along a direction of 45 degrees to the X direction, CV=4.5, $\eta = 2\xi = .25$.

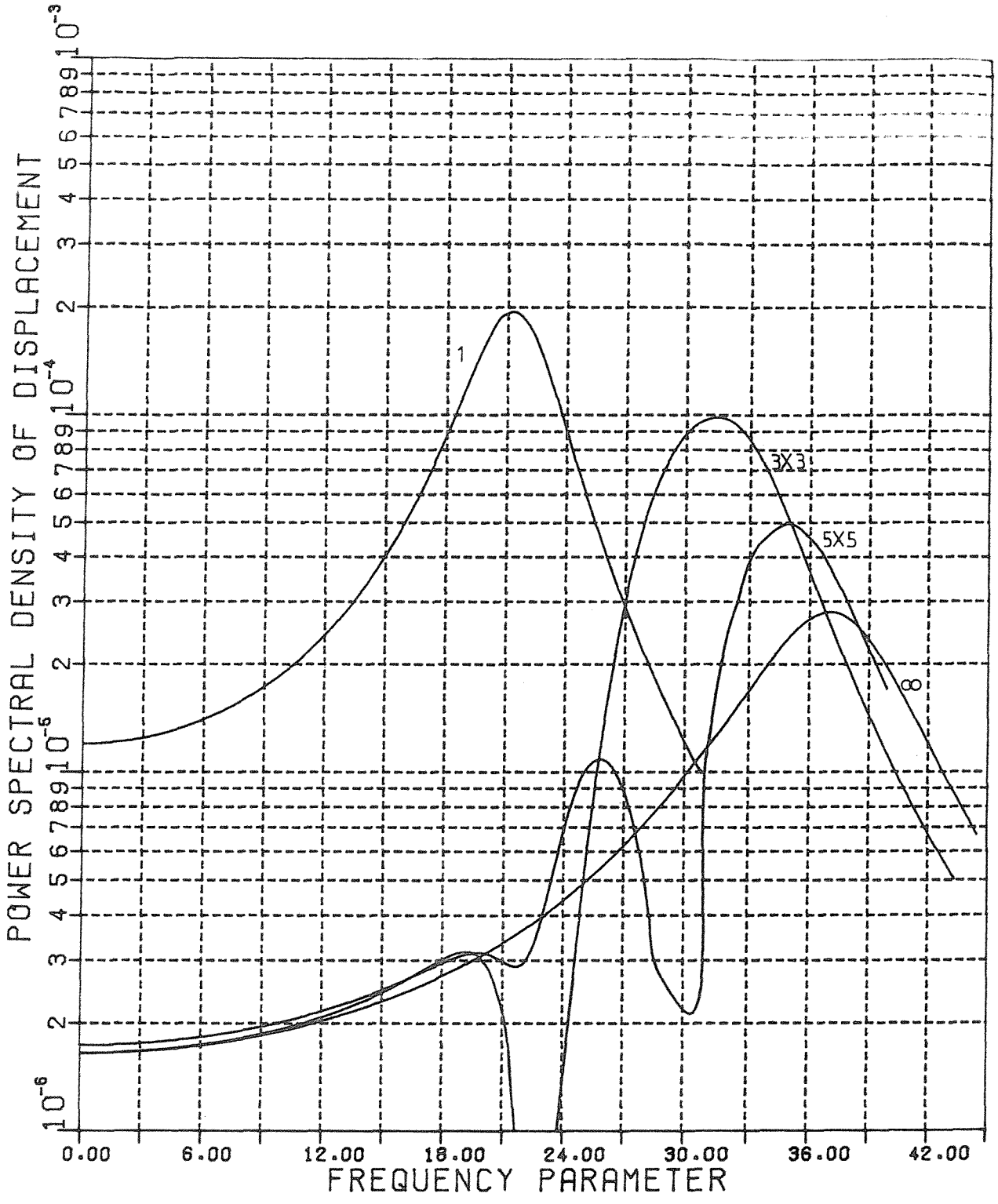

Figure 5.32. Comparison of the response at cell centres of an infinite two-dimensional periodic plate on simple line supports with square cells, and the response at the centre of the middle bay of a 5X5, 3X3 and a single bay plate of figure(5.24), due to frozen convected random pressure field, $CV=\infty$, $\eta=2$ $\xi=0.25$.

CHAPTER VI

CONCLUSIONS AND GENERAL DISCUSSION

The study of the vibration characteristics of periodic structures using the finite element method in conjunction with the periodic structure theory as presented in this work proved to be an efficient and reliable approach for the analysis of complex structures using digital computers. It provided a general procedure to analyse, practically, any periodic structure in one, two and three dimensions making use of existing finite element programs.

The fact that only one period of the structure needs be considered made a considerable saving in computer time and storage. It also simplified modelling the structure making it possible to represent the system by an accurate finite element model.

The basic principles of periodic structure theory has been briefly reviewed and a theoretical background to the finite element method is presented.

Free wave propagation in one-dimensional periodic systems is examined in detail in Chapter II. Matrix formulation for calculating the variation of the propagation constant, whether real or complex, with frequency and finding the associated wave-forms is presented. It is found that one-dimensional periodic structures in general allow propagation within some frequency bands only (called propagation bands). Within these bands waves propagate through the system without attenuation. Their propagation constant is a real quantity. It represents the change in phase in passing from one cell to the next. Outside the propagation bands, waves attenuate as they travel from one cell to the next. The propagation constant corresponding to these waves is a complex quantity where the real part represents the change in phase while the imaginary part represents the attenuation in the amplitude of the wave in passing from one period to the next. The width of the propagation bands and their bounding frequencies are characteristic of the periodic system and depend on its physical properties. Also it is found that the frequency of propagation is a periodic function of the real propagation constant with period 2π. Wave-forms corresponding to various values of the propagation constant have been calculated and

demonstrated on a movie film, produced by the computer, which showed clearly the propagating, standing and attenuating waves.

Very good agreement with exact calculations and other approximate methods has been obtained even when using few elements to represent the basic period of the structure.

The natural frequencies of some finite one-dimensional periodic structures has been estimated from the propagation constant/frequency curve. It is found that the natural frequencies of the finite structure fall into groups. Each group occurs within one of the propagation bands and the number of frequencies in each group equals the number of periods in the structure.

The study of the transition from non-periodic to periodic structures showed clearly the effect of the existence of periodic discontinuities on the propagation of waves in a homogeneous medium.

Two-dimensional periodic systems are examined in Chapter III. We found that two propagation constants were needed to extend the periodic structure theory to analyse two-dimensional systems. Matrix formulation for examining the relation between the propagation constants and frequency of propagation and calculating the corresponding wave-forms is presented and general computer programs are written. It is found that the frequency of propagation is a periodic function of the real propagation constants with periods 2π. Also it is found that propagation occurs within some frequency bands only and that the width of these bands depends on the direction of propagation as well as the physical properties of the system with possible overlapping of the various bands.

The discussion of the zones for two-dimensional systems showed that it is enough to study the variation of the frequency with the propagation constants (or the wave-number) within the first zone only.

The study of flexural waves in two-dimensional plates resting on orthogonal equally-spaced line supports provided a clear understanding of the general behaviour of two-dimensional periodic systems. Standing and travelling waves corresponding to various values of the propagation constants have been obtained and demonstrated on a movie film produced

by the computer. Also we showed how to determine the natural frequencies of some two-dimensional periodic systems from the propagation constants/ frequency curves.

The discussion of the transition from non-periodic to periodic two-dimensional systems showed that it is possible to study wave propagation in homogeneous non-periodic systems using this approach. It also showed a very good agreement between the theoretical calculation and finite element results for flexural wave propagation in infinite flat plates.

Various ways of presenting the variation of the frequency of propagation with the propagation constants are shown. The polar presentation showed clearly the overlapping of the bands and the variation in their width with direction of propagation.

The cases of oblique two-dimensional systems, the point supported plates and the two-dimensional stringer stiffened panels demonstrated the flexibility of this approach to analyse large varieties of problems with great ease and simplicity.

Free wave propagation in three-dimensional periodic systems is investigated in Chapter IV. It is found that three propagation constants were needed to extend the periodic structure theory to analyse three-dimensional systems. Similar to the one and two-dimensional systems, formulation for investigating the variation of the propagation constants with frequency is presented and general finite element programs are written. It is found that the frequency is a periodic function of the real propagation constants with periods 2π. It is also found that three-dimensional periodic systems allow propagation within some frequency bands only. The width of these bands and their bounding frequencies depend on the direction of propagation and the physical properties of the system. The study of waves propagating in three-dimensional plates showed all these characteristics very clearly.

In Chapter V the response of one and two-dimensional infinite periodic structures to random pressure fields is investigated.

For one-dimensional systems it is found that the largest response of the structure occurs within the propagation bands, and the maximum response occurs at the lower bounding frequency of the first band. Therefore knowledge of the propagation constant/frequency variation for the structure can be used to predict the frequencies at which the response is largest.

For two-dimensional systems it is found that the propagation constants/frequency variation in the polar plot shows clearly the frequencies where the response to homogeneous pressure fields is largest. The maximum response occurs at the lower bounding frequencies of the first propagation band.

Finally the response of general structures to random pressure fields using finite elements and the standard modal analysis is presented. The response of finite one and two-dimensional periodic structures showed that such a response can be predicted from the response of infinite structures.

From the above discussion we can summarise the main advantages of using the finite element method and the periodic structure theory to study the dynamical behaviour of periodic structures as follows.

a. Only one period (cell) of the structure need be considered, thus modelling is simplified and the number of degrees of freedom is reduced;

b. Large complex periodic structures of any shape can be automatically analysed without any further mathematical formulation;

c. General computer programs have been written making use of existing finite element routines;

d. Calculation of the response of periodic structures to random pressure fields using the periodic structure approach does not require knowledge of the structure's natural frequencies and normal modes. Also systems with any type of damping can be analysed without any further complication.

The analysis presented in this work is only a step towards a full investigation to understanding the dynamic behaviour of periodic structures, especially in two and three dimensions, using digital computers. Further work should be done to study some of the points mentioned below.

a. Study of the response of periodic structures to concentrated loads and non-homogeneous excitation.

b. The study presented in the previous chapters was restricted to studying plane waves only. It should be extended to study circular wave motion in two dimensions and spherical wave motion in three dimensions.

c. The generalised nodal forces due to harmonic pressure waves should be developed for various existing finite elements.

d. Apply the analysis presented here to investigate the dynamic behaviour of various periodic structures such as stiffened cylinders or acoustically coupled periodic structures, etc.

e. Experiments on models representing various engineering periodic structures such as ship hulls or stiffened cylinders should be carried out.

Although the study presented in this work is applied only to periodic systems composed of beams and plates, it can be used to analyse other periodic systems in physics and engineering.

APPENDIX A

METHODS USED IN SOLVING THE VARIOUS EIGENVALUE PROBLEMS ENCOUNTERED IN CHAPTERS II , III AND IV

i- Eigenvalue problems of the form

$$([A] - \lambda [B]) \{ x \} = 0 \qquad (A.1)$$

where $[A]$ and $[B]$ are real symmetric matrices and $[B]$ is positive definite.

The main steps for solving this eigenvalue problem are as follows

a- Apply Cholesky's symmetric decomposition on the matrix $[B]$,hence

$$[B] = [L][L]^T \qquad (A.2)$$

where $[L]$ is a lower triangular matrix and $[L]^T$ is its transpose.

b- Reduce equation (A.1) into the standard form

$$([C] - \lambda [I]) \{ y \} = 0 \qquad (A.3)$$

where

$$[C] = [L]^{-1} [A] [L]^{-T} \qquad (A.4)$$

$$\{ y \} = [L]^T \{ x \} \qquad (A.5)$$

c- Using Householder's transformation, equation (A.3) can be reduced to the form

$$([D] - \lambda [I]) \{ z \} = 0 \qquad (A.6)$$

where $[D]$ is a symmetric tridiagonal matrix.

d- The eigenvalues of (A.6) are obtained by the method of bisection using Sturm sequencies. The eigenvectors are obtained by applying the inverse iteration process.

e- The eigenvectors $\{ y \}$ are obtained from the vectors $\{ z \}$ by the reverse Householder's process. The eigenvectors $\{ x \}$ of the original equation are then obtained from equation (A.5).

For further details of the above methods see | 2,51 and 64| .

ii- Eigenvalue problems of the form

$$(A_n \lambda^n + A_{n-1} \lambda^{n-1} + \cdots\cdots + A_0) \{x\} = 0 \qquad (A7)$$

where $A_n, A_{n-1}, \ldots\ldots, A_0$ are real square matrices of order N .
Two procedures are applied to solve this eigenvalue problem depending on the properties of the matrices A_n and A_0 .

a- The matrix A_n (or A_0) is non-singular.

If the matrix A_n is non-singular, the eigenvalue problem (A7) can be transformed to a standard eigenvalue problem of the form

$$([C] - \lambda [I]) \{y\} = 0 \qquad (A8)$$

where

$$[C] = \begin{bmatrix} 0 & I & 0 & 0 \\ 0 & 0 & I & 0 \\ 0 & 0 & 0 & I \\ B_0 & B_1 & B_2 & B_3 \end{bmatrix} \qquad \{y\} = \begin{Bmatrix} x \\ \lambda x \\ \lambda^2 x \\ \lambda^3 x \end{Bmatrix} \qquad (A9)$$

where

$$B_i = - A_n^{-1} A_i \qquad (i = 0,1,2,\ldots\ldots, n-1) \qquad (A10)$$

Here we used the case n = 4 for convenience in illustration of the arrays.

The eigenvalue problem (A8) is solved by reduction to Hessenberg form and the QR algorithm [65] .

If A_n is singular but A_0 is non-singular, a similar procedure can be carried out to obtain an eigenvalue problem in $1/\lambda$.

b- The matrices A_n and A_0 are singular.

In this case we observe that the eigenvalues of equation (A7) are those of the system

$$([C] - \lambda [D]) \{y\} = 0 \qquad (A11)$$

where

$$[C] = \begin{bmatrix} 0 & I & 0 & 0 \\ 0 & 0 & I & 0 \\ 0 & 0 & 0 & I \\ -A_0 & -A_1 & -A_2 & -A_3 \end{bmatrix} \qquad (A12)$$

$$[D] = \begin{bmatrix} I & 0 & 0 & 0 \\ 0 & I & 0 & 0 \\ 0 & 0 & I & 0 \\ 0 & 0 & 0 & A_4 \end{bmatrix} \qquad \text{(A13)}$$

where both $[C]$ and $[D]$ are singular matrices.

The eigenvalue problem (A11) can be solved using the QZ algorithm |41,49 and 63| .

APPENDIX B

FLOW DIAGRAMS FOR COMPUTATION

These flow diagrams are for the computational procedures to calculate the variation of the propagation constants(real or complex)with frequency for one,two and three-dimensional periodic systems and their response to random homogeneous pressure fields.

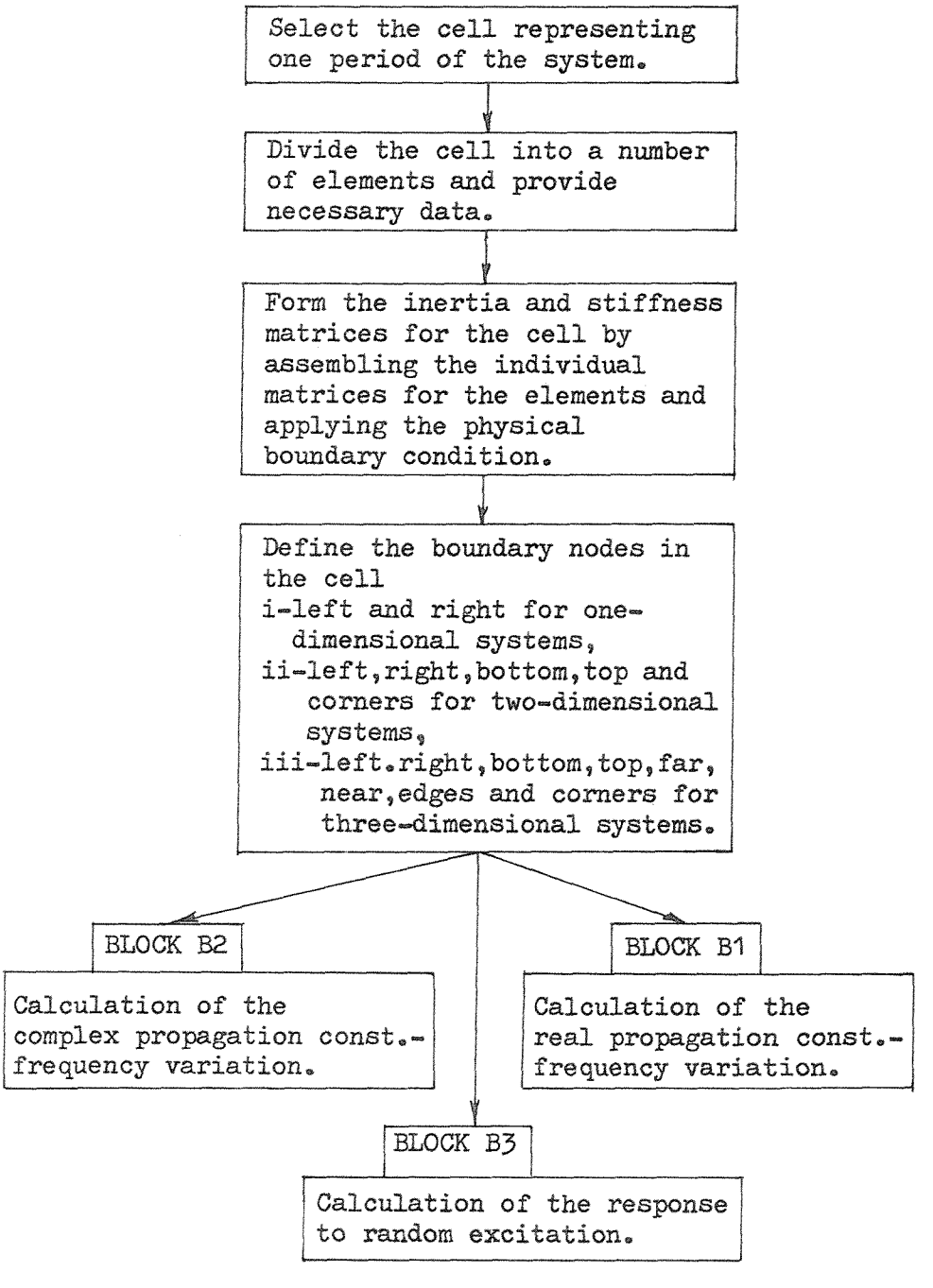

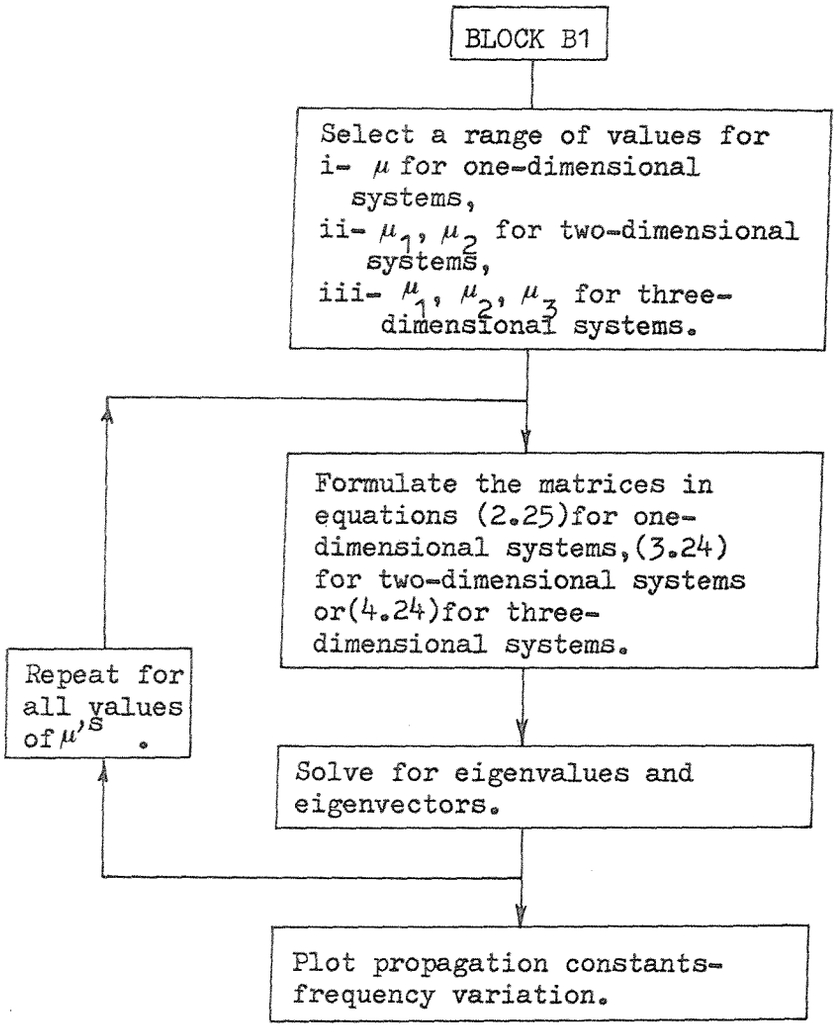
BLOCK B1
Select a range of values for
i- μ for one-dimensional systems,
ii- μ_1, μ_2 for two-dimensional systems,
iii- μ_1, μ_2, μ_3 for three-dimensional systems.
Formulate the matrices in equations (2.25)for one-dimensional systems,(3.24) for two-dimensional systems or(4.24)for three-dimensional systems.
Solve for eigenvalues and eigenvectors.
Plot propagation constants-frequency variation.
Repeat for all values of μ's .

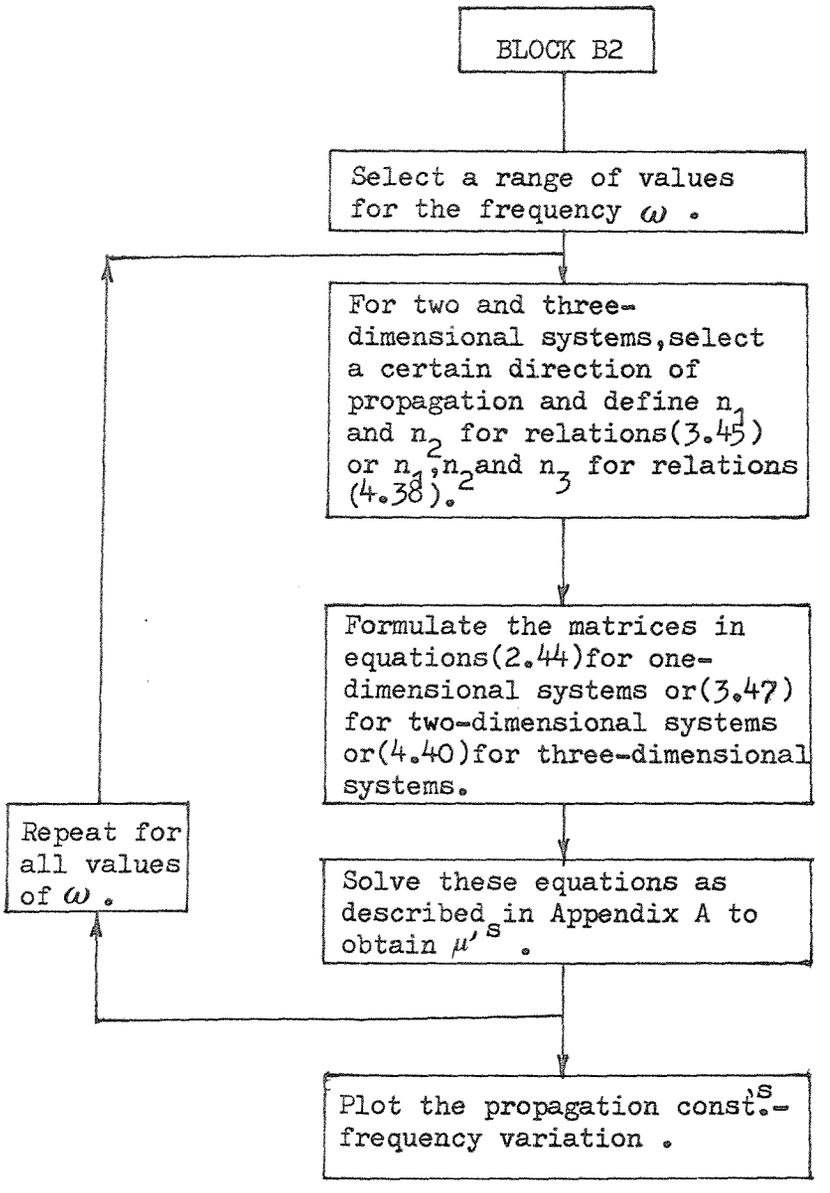
BLOCK B2
Select a range of values for the frequency ω .
For two and three-dimensional systems, select a certain direction of propagation and define n_1 and n_2 for relations (3.45) or n_1, n_2 and n_3 for relations (4.38).
Formulate the matrices in equations (2.44) for one-dimensional systems or (3.47) for two-dimensional systems or (4.40) for three-dimensional systems.
Solve these equations as described in Appendix A to obtain μ'_s .
Repeat for all values of ω .
Plot the propagation const.'s - frequency variation .

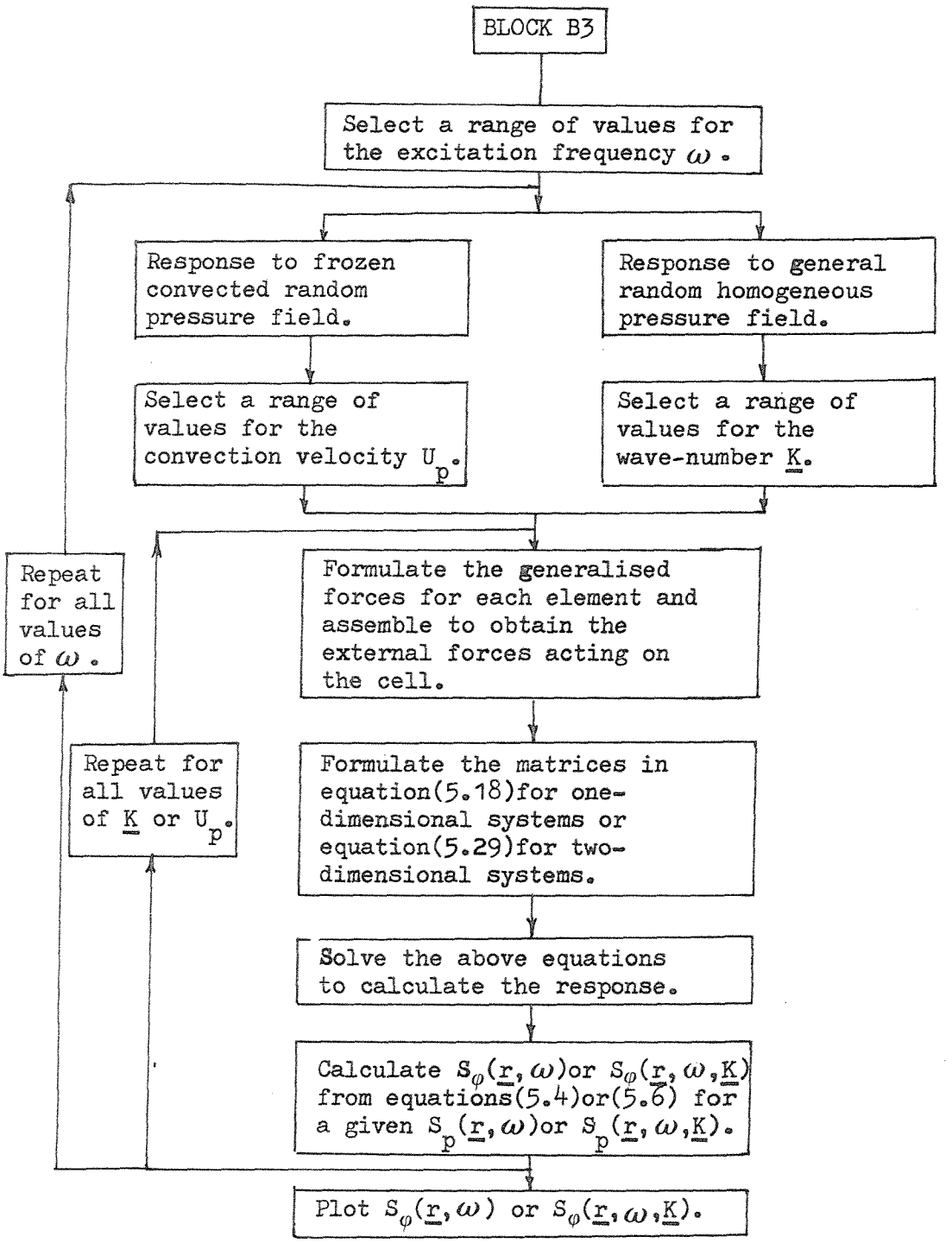
BLOCK B3
Select a range of values for the excitation frequency ω.
Response to frozen convected random pressure field.
Response to general random homogeneous pressure field.
Select a range of values for the convection velocity U_p.
Select a range of values for the wave-number $\underline{K}$.
Repeat for all values of ω.
Formulate the generalised forces for each element and assemble to obtain the external forces acting on the cell.
Repeat for all values of $\underline{K}$ or U_p.
Formulate the matrices in equation(5.18)for one-dimensional systems or equation(5.29)for two-dimensional systems.
Solve the above equations to calculate the response.
Calculate $S_\varphi(\underline{r},\omega)$or $S_\varphi(\underline{r},\omega,\underline{K})$ from equations(5.4)or(5.6) for a given $S_p(\underline{r},\omega)$or $S_p(\underline{r},\omega,\underline{K})$.
Plot $S_\varphi(\underline{r},\omega)$ or $S_\varphi(\underline{r},\omega,\underline{K})$.

APPENDIX C

DERIVATION OF THE GENERALISED NODAL FORCES FOR ELEMENTS USED IN CHAPTER V

C1 Generalised forces for the beam element used in Section 5.5.1 |22,51,52|

The beam is assumed to be lying along the x axis and the pressure wave is travelling over it in the x direction, figure (C.1).

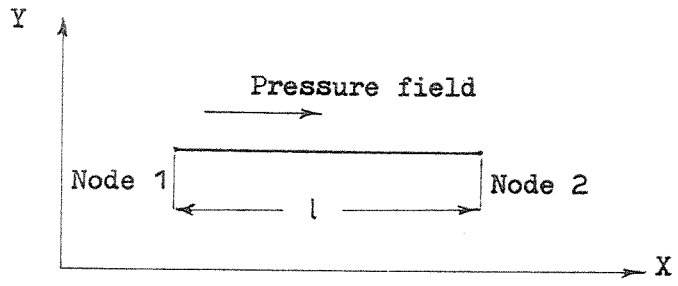

Figure C.1

If the pressure wave is harmonic and having unit amplitude, it can be expressed in the form

$$P(x, t) = e^{i(\omega t - k.x)} \tag{C.1}$$

where

ω is the angular frequency, k the angular wave-number and t the time.

The generalised nodal forces are given by

$$\{f\} = \int_0^{\ell} [N]^T e^{-ikX} dx \tag{C.2}$$

where $[N]$ is the element shape functions, $\ell = X_2 - X_1$ and $x = X - X_1$. X_1 and X_2 are the global coordinates of nodes 1 and 2.

$$[N(x)]^T = \begin{bmatrix} 0 \\ 1 - 3(\frac{x}{\ell})^2 + 2(\frac{x}{\ell})^3 \\ x - 2\frac{x^2}{\ell} + \frac{x^3}{\ell^2} \\ 0 \\ 3(\frac{x}{\ell})^2 - 2(\frac{x}{\ell})^3 \\ -\frac{x^2}{\ell} + \frac{x^3}{\ell^2} \end{bmatrix} \qquad (C.3)$$

The generalised nodal forces $\{f\}$ are obtained by performing the integration in (C.2), hence

$$\{f\} = e^{-ikX_1} \begin{bmatrix} 0 \\ F_1 - \frac{3}{\ell^2} F_3 + \frac{2}{\ell^3} F_4 \\ F_2 - \frac{2}{\ell} F_3 + \frac{1}{\ell^2} F_4 \\ 0 \\ \frac{3}{\ell^2} F_3 - \frac{2}{\ell^3} F_4 \\ -\frac{1}{\ell} F_3 + \frac{1}{\ell^2} F_4 \end{bmatrix} \qquad (C.4)$$

where

$$F_1 = \frac{i}{k}(e^{-ik\ell} - 1),$$

$$F_2 = \frac{e^{-ik\ell}}{k^2}(1 + ik\ell) - \frac{1}{k^2},$$

$$F_3 = \frac{e^{-ik\ell}}{k^3}\{2k\ell + i(k^2\ell^2 - 2)\} + \frac{2i}{k^3}, \qquad (C.5)$$

$$F_4 = \frac{e^{-ik\ell}}{k^4}\{3k^2\ell^2 - 6 + i(k^3\ell^3 - 6k\ell)\} + \frac{6}{k^4}$$

For the case when $k = 0$ we can write

$$\begin{aligned} F_1 &= \ell \ , \\ F_2 &= \tfrac{1}{2}\ell^2 , \\ F_3 &= \tfrac{1}{3}\ell^3 , \\ F_4 &= \tfrac{1}{4}\ell^4 \end{aligned} \qquad \text{(C.6)}$$

C2 Generalised forces for the flat strip element used in Section 5.5.1 [15, 50, 52]

The strip element is lying in the x direction and the pressure wave is travelling over it in the y direction, figure (C.2).

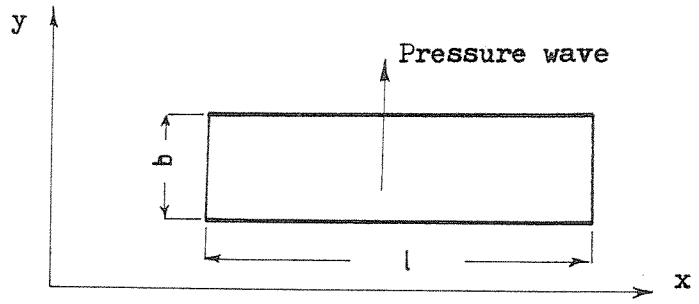

Figure C.2.

The generalised nodal forces become

$$\{f\} = \int_0^b \int_0^\ell X_m(x) \left[N_w(y)\right]^T e^{-iky} \, dx \, dy \qquad \text{(C.7)}$$

where

$y = Y - Y_1$

$b = Y_2 - Y_1$

ℓ = length of strip in the x direction.

Y_1 and Y_2 = global coordinates of nodes 1 and 2

$X_m(x)$ = characteristic functions for a uniform beam.

$$[N_w(y)]^T = \begin{bmatrix} 0 \\ 0 \\ 1 - 3(\frac{y}{b})^2 + 2(\frac{y}{b})^3 \\ y - 2\frac{y^2}{b} + \frac{y^3}{b^2} \\ 0 \\ 0 \\ 3(\frac{y}{b})^2 - 2(\frac{y}{b})^3 \\ -\frac{y^2}{b} + \frac{y^3}{b^2} \end{bmatrix} \qquad (C.8)$$

The generalised nodal forces $\{f\}$ are obtained by performing the integration (C.7), hence

$$\{f\} = I_m e^{-iky} \begin{bmatrix} 0 \\ 0 \\ F_1 - \frac{3}{b^2} F_3 + \frac{2}{b^3} F_4 \\ F_2 - \frac{2}{b} F_3 + \frac{1}{b^2} F_4 \\ 0 \\ 0 \\ \frac{3}{b^2} F_3 - \frac{2}{b^3} F_4 \\ -\frac{1}{b} F_3 + \frac{1}{b^2} F_4 \end{bmatrix} \qquad (C.9)$$

where F_1, F_2, F_3 and F_4 are identical to (C.5) and (C.6) with ℓ replaced by b.

For a strip with simply supported ends, $I_m = 2\ell/m\pi$ for m odd where m is the number of half waves in the x direction.

C3 Generalised forces for the plate bending element used in Sections 5.5.2 and 5.6.2 [15, 51, 52]

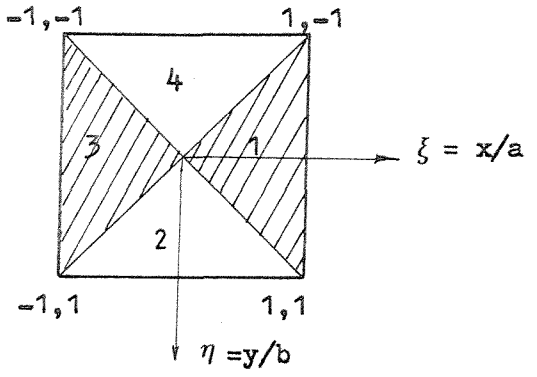

Figure C.3.

Consider a rectangular plate element with dimensions 2a and 2b, figure (C.3). In non-dimensional coordinates ξ, η the displacement field over the plate is given by

$$W(\xi, \eta) = \sum_{i=1}^{12} \alpha_i P_i(\xi, \eta) \qquad (C.10)$$

The functions $P_i(\xi, \eta)$ are defined as follows

$$P_1 = 1$$

$$P_2 = \xi^2$$

$$P_3 = \eta^2$$

$$P_4 = \xi$$

$$P_5 = \xi^3$$

$$P_6 = \begin{cases} \xi^2 - 2\xi + \eta^2 & \text{in region (1)} \\ 2\xi\eta - 2\xi & \text{in region (2)} \\ -\xi^2 - 2\xi - \eta^2 & \text{in region (3)} \\ -2\xi\eta - 2\xi & \text{in region (4)} \end{cases} \qquad (C.11)$$

$$P_7 = \eta$$

$$P_8 = \eta^3$$

$$P_9 = \begin{cases} 2\eta\xi - 2\eta & \text{in region (1)} \\ \eta^2 - 2\eta + \xi^2 & \text{in region (2)} \\ -2\eta\xi - 2\eta & \text{in region (3)} \\ -\eta^2 - 2\eta - \xi^2 & \text{in region (4)} \end{cases}$$

$$P_{10} = \xi\eta$$

$$P_{11} = 3\xi^3\eta + 3\xi\eta^3 - \xi^3\eta^3 - 5\xi\eta$$

$$P_{12} = \begin{cases} \tfrac{1}{4}(\xi^3\eta^3 - \xi^5\eta - 3\xi\eta^3 + 3\xi^3\eta) & \text{in regions (1), (3)} \\ \tfrac{1}{4}(\xi\eta^5 - \xi^3\eta^3 - 3\xi\eta^3 + 3\xi^3\eta) & \text{in regions (2), (4)} \end{cases}$$

The coefficients α are related to the displacements w, θ_x and θ_y at the four corners of the plate by

$$\{\alpha\} = [W]\{q\} \qquad \text{(C.12)}$$

where $\{q\}$ is the vector of nodal degrees of freedom

$$\{q\} = \lfloor w_1, \theta_{x_1}, \theta_{y_1}, \ldots, w_4, \theta_{x_4}, \theta_{y_4} \rfloor$$

and

$$[W] = \begin{bmatrix}
\frac{1}{4} & b/8 & -a/8 & \frac{1}{4} & b/8 & a/8 & \frac{1}{4} & -b/8 & a/8 & \frac{1}{4} & -b/8 & -a/8 \\
0 & 0 & a/8 & 0 & 0 & -a/8 & 0 & 0 & -a/8 & 0 & 0 & a/8 \\
0 & -b/8 & 0 & 0 & -b/8 & 0 & 0 & b/8 & 0 & 0 & b/8 & 0 \\
-\frac{3}{8} & 0 & a/8 & \frac{3}{8} & 0 & a/8 & \frac{3}{8} & 0 & a/8 & -\frac{3}{8} & 0 & a/8 \\
\frac{1}{8} & 0 & -a/8 & -\frac{1}{8} & 0 & -a/8 & -\frac{1}{8} & 0 & -a/8 & \frac{1}{8} & 0 & -a/8 \\
0 & b/8 & 0 & 0 & -b/8 & 0 & 0 & b/8 & 0 & 0 & -b/8 & 0 \\
-\frac{3}{8} & -b/8 & 0 & -\frac{3}{8} & -b/8 & 0 & \frac{3}{8} & -b/8 & 0 & \frac{3}{8} & -b/8 & 0 \\
\frac{1}{8} & b/8 & 0 & \frac{1}{8} & b/8 & 0 & -\frac{1}{8} & b/8 & 0 & -\frac{1}{8} & b/8 & 0 \\
0 & 0 & -a/8 & 0 & 0 & a/8 & 0 & 0 & -a/8 & 0 & 0 & a/8 \\
\frac{1}{4} & 0 & 0 & -\frac{1}{4} & 0 & 0 & \frac{1}{4} & 0 & 0 & -\frac{1}{4} & 0 & 0 \\
-\frac{1}{16} & -\frac{b}{32} & a/32 & 1/16 & b/32 & a/32 & -\frac{1}{16} & b/32 & -\frac{a}{32} & 1/16 & -\frac{b}{32} & -\frac{a}{32} \\
0 & b/8 & a/8 & 0 & -b/8 & a/8 & 0 & -b/8 & -a/8 & 0 & b/8 & -a/8
\end{bmatrix}$$

(C.13)

The generalised forces for the element due to a harmonic pressure wave

$$P(S, t) = e^{i(\omega t - \underline{k}.\underline{s})} \tag{C.14}$$

are given by

$$\{f\} = [W]^T \int_{-1}^{+1}\int_{-1}^{+1} P_i(\xi, \eta) e^{-i\underline{k}.\underline{s}} \, d\xi d\eta \tag{C.15}$$

where $\underline{k}$ is the wave-number.

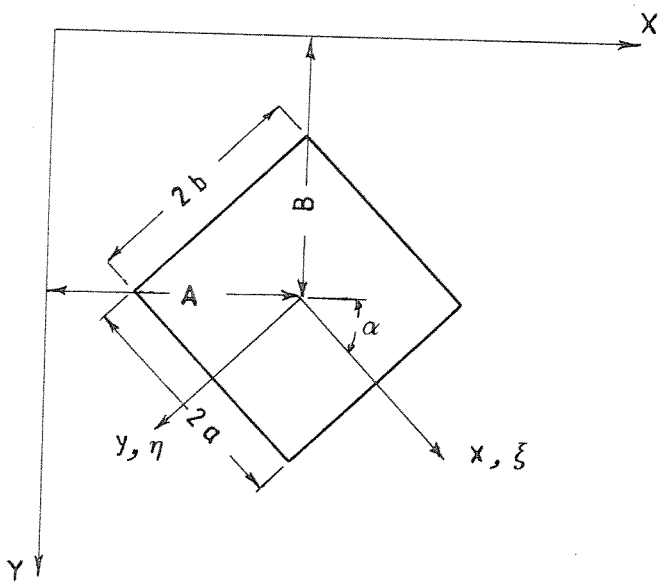

Figure C.4.

If X, Y are the global coordinates and x, y are the local coordinates for the element, figure (C.4), then we can write

$$\begin{aligned} X &= A + x\cos\alpha - y\sin\alpha \\ Y &= B + x\sin\alpha + y\cos\alpha \\ x &= \xi a \\ y &= \eta b \\ \underline{k}.\underline{s} &= k_X.X + k_Y.Y \end{aligned} \tag{C.16}$$

where A and B are the global coordinates of the centre of the element and α is the angle between the local and global coordinates.

Substituting (C.16) into equation (C.15) gives

$$\{f\} = [W]^T \int_{-1}^{+1}\int_{-1}^{+1} \{P_i(\xi, \eta).$$

$$e^{-i\{k_X(A+\xi a\cos\alpha - \eta b \sin\alpha) + k_Y(B + \xi a \sin\alpha + \eta b \cos\alpha)\}} \}d\xi d\eta$$

$$= e^{-i(k_X A+k_Y B)} [W]^T \int_{-1}^{+1}\int_{-1}^{+1} P_i(\xi, \eta)\{e^{-i\xi(k_X a\cos\alpha + k_Y a \sin\alpha)}$$

$$e^{-i\eta(-k_X b \sin\alpha + k_Y b \cos\alpha)} \} \, d\xi d\eta \qquad \text{(C.17)}$$

The nodal forces $\{f\}$ should then be transformed from the local axes to the global axes as explained in Chapter I, equation (1.24).

The integration in (C.17) should be carried out in the four regions of the element shown in fig. (C.3). This can be done in a closed form as follows.

a). $$\int_{x_1}^{x_2} x^n e^{ax} dx = e^{ax} \sum_{i=1}^{n+1} \frac{(-1)^{i+1} n! \, x^{n-i+1}}{a^i (n-i+1)!} \Bigg|_{x_1}^{x_2}$$

$$= \text{FUN1}(a, n, x_1, x_2) \qquad \text{(C.18)}$$

b). $$\int_{y_1}^{y_2}\int_{-y}^{y} x^n y^m e^{ax} e^{by} \, dx \, dy$$

$$= \sum_{i=1}^{n+1} \frac{(-1)^{i+1} n!}{a^i (n-i+1)!} \{ \int_{y_1}^{y_2} e^{(b+a)y} \, y^{m+n-i+1} \, dy$$

$$- \int_{y_1}^{y_2} (-1)^{n-i+1} \, e^{(b-a)y} \, y^{m+n-i+1} \, dy \}$$

$$= \sum_{i=1}^{n+1} \frac{(-1)^{i+1} n!}{a^i (n-i+1)!} \{\text{FUN1}(b+a, m+n-i+1, y_1, y_2)$$

$$+ (-1)^{n-i+2} \, \text{FUN1}(b-a, m+n-i+1, y_1, y_2)\}$$

$$= \text{FUN2}(a, b, n, m, y_1, y_2)$$

where

a, b are real or complex numbers,

x, y are real numbers, and

m, n are integer numbers.

If n = 0

$$\int_{x_1}^{x_2} e^{ax} dx = \frac{e^{ax}}{a} \Bigg|_{x_1}^{x_2}$$

If a = 0

$$\int_{x_1}^{x_2} x^n dx = \frac{x^{n+1}}{n+1} \Bigg|_{x_1}^{x_2}$$

and

$$\int_{y_1}^{y_2} e^{by} y^m \{ \int_{-y}^{y} x^n dx \} dy$$

$$= \int_{y_1}^{y_2} e^{by} y^m \left(\frac{x^{n+1}}{n+1} \Bigg|_{-y}^{y} \right)$$

$$= \int_{y_1}^{y_2} \frac{e^{by}}{n+1} \{ y^{m+n-1} - (-1)^{n+1} y^{m+n+1} \} dy$$

$$= \frac{1}{n+1} \{ \text{FUN1}(b, m+n+1, y_1, y_2) - (-1)^{n+1} \text{FUN1}(b, m+n+1, y_1, y_2) \}$$

$$= 0 \qquad (n \text{ odd})$$

or

$$= \frac{2}{n+1} \text{FUN1}(b, m+n+1, y_1, y_2) \qquad (n \text{ even or zero})$$

Also

$$\int_{-1}^{+1} e^{by} y^m \{\int_{-1}^{+1} e^{ax} x^n \, dx\} dy$$

$$= \int_{-1}^{+1} e^{by} y^m \{FUN1(a, n, -1, +1)\} dy$$

$$= FUN1(a, n, -1, +1) \int_{-1}^{+1} e^{by} y^m \, dy$$

$$= FUN1(a, n, -1, +1).FUN1(b, m, -1, +1)$$

APPENDIX D

FINITE ELEMENTS AND DATA VALUES USED IN THE DIFFERENT EXAMPLES OF THIS WORK

D.1

Two-dimensional beam bending element of constant cross-section |22,51,52| .

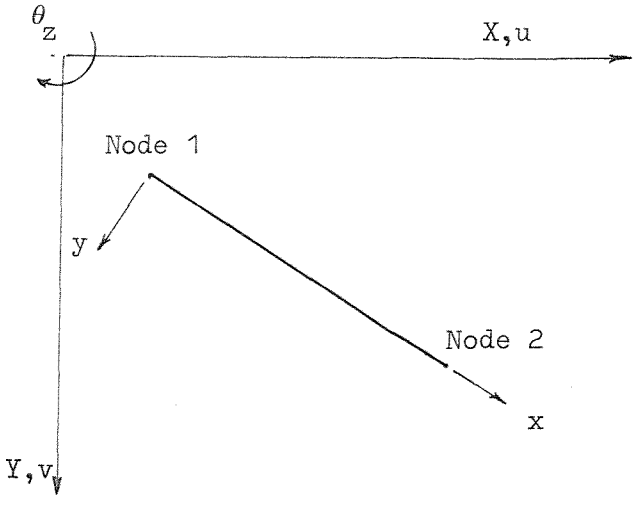

This element has two nodes at the ends. The degrees of freedom at the nodes are u,v and θ_z . The displacements along the axis of the beam vary linearly with x whilst those normal to the axis vary cubically.

Data values used.

A : constant cross-sectional area = 1.0

I_{zz} : second moment of area of the cross-section about the local z axis through the centroid = 1.0

E : Young's modulus = 1.0

ρ : mass per unit volume = 1.0

D.2.

i- Plate element

Finite strip flat shell element |15,50 and 52| .

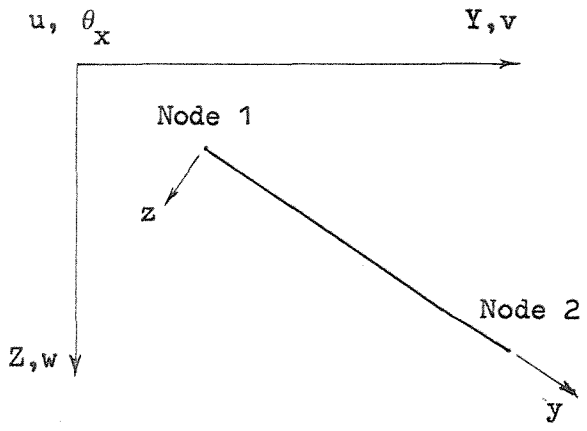

This element has two nodes.The degrees of freedom at each node are u,v,w and θ_x.The variation of displacements in the x direction is the same as the beam function of Appendix D.1. .

Data values used

h : constant plate thickness = 0.04 ins (1.016×10^{-3} m)

ℓ : length in the x direction = 20.0 ins (0.508 m)

σ : Poisson's ration =0.3

E : Young's modulus = 10.5×10^{-3} lb/ins^2 (7.24×10^{10} N/m^2)

ρ : mass per unit volume = 0.26166×10^{-3} lb.sec^2/ins^4(2795.69 kg/m^3)

The plate is considered simply supported at its edges parallel to the y direction .

ii- Beam element

Thin walled open section beam element |15,50,51 and 52| .

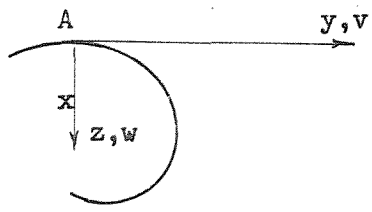

This element has one node only with degrees of freedom u,v,w and θ_x.

Data values used

A : cross-sectional area = 0.2302 ins^2 (0.1485×10^{-3} m^2)

I_{yy}, I_{yz}, I_{zz} : second moments of area of cross-section with respect to axes through attachment point A = 0.179, 0.0, 0.083 ins^4 (0.745×10^{-7}, 0.0, 0.3455×10^{-7} m^4)

a_y, a_z : coordinates of centroid of the cross-section = 0.0, 0.72 ins (0.0, 0.0183 m)

$S_\omega, J_{\omega y}, J_{\omega z}, J_\omega$: warping constants = 0.0, 6.806×10^{-3} ins^5, 0.0, 0.01649 ins^6 (0.0, 7.195×10^{-11} m^5, 0.0, 4.428×10^{-12} m^6)

J : Saint-Venant torsion constant = 2.263×10^{-4} ins^{-4} (9.419×10^{-11} m^4)

G : shear modulus = 4.0×10^6 lb/ins^2 (2.759×10^{10} N/m^2)

E, ρ, ℓ : the same as the shell element .

The distance between stringers is 8.2 ins (0.208 m).

D.3.

i- Plate element

Finite strip singly curved shell element [15,51 and 52] .

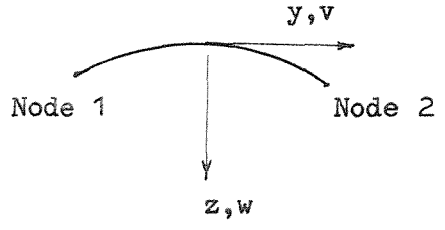

This element has a constant radius of curvature with two nodes.the degrees of freedom at each node are u, u_y, v, v_y, w and w_y . The variation of displacements in the x direction is the same as straight beam functions.

Data values used

h : shell thickness = 0.04 ins (1.016×10^{-3} m)

ℓ : length in x direction = 20.0 ins (0.508 m)

R : radius of curvature = 72.0 ins (1.829 m)

b : arc length(for one element) = 2.05 ins (0.052 m)

σ : Poisson's ratio = 0.3

E : Young's modulus = 10.5×10^6 lb/ins^2 (7.235×10^{10} N/m^2)

ρ : mass per unit volume = 0.26166×10^{-3} $lb.sec^2/ins^4$ (2795.69 kg/m^3)

The shell is considered simply supported at its edges parallel to the y direction .

ii- Stringer element.

The same stringer element used in Appendix D.2. .The arc length between stringers is 8.2 ins (0.208 m).

D.4.

Two-dimensional isotropic rectangular plate bending element |10,51 and 52| .

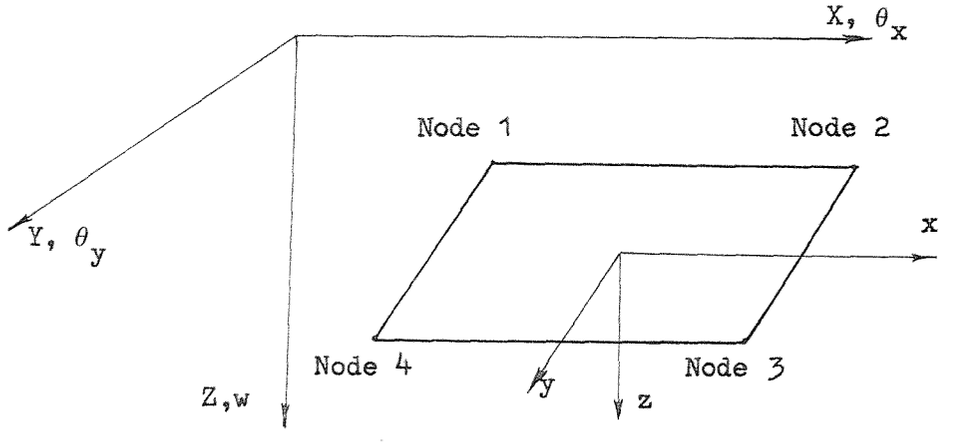

This element has 4 nodes at the corners.The degrees of freedom at the nodes are w, θ_x and θ_y.The lateral displacements vary cubically whilst the normal rotations vary linearly along each edge.

Data values used

h : constant plate thickness = 1.0

σ : Poisson's ration = 0.3

E : Youngs modulus = 10.92 ($D = E.h^3/(12(1-\sigma^2)) = 1.0$)

ρ : mass per unit volume = 1.0

D.5.

Two-dimensional orthotropic quadrilateral plate bending element |45,48,51 and 52| .

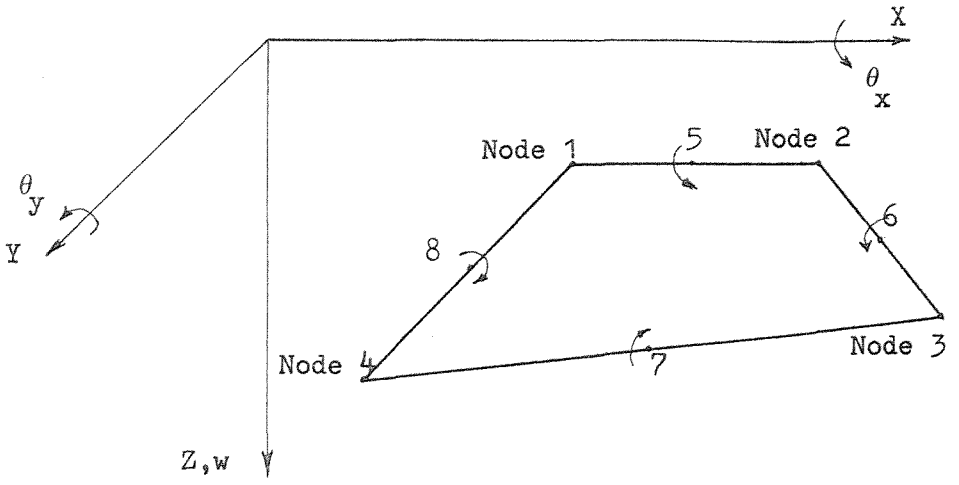

This element has 8 nodes (4 at the corners and 4 at the mid point of the sides).The degrees of freedom at the nodes are w, θ_x, θ_y at nodes 1 to 4 and θ at nodes 5 to 8.The lateral displacements vary cubically and normal rotations vary quadratically along each edge.

Data values used

h : constant plate thickness = 1.0

β : angle betweeen material and global XY axes

D_x, D_y, D_1, D_{xy} : orthotropic plate constants referred to material axes (for isotropic material $D_x=D_y=D = E.h^3/(12(1-\sigma^2))$, $D_1 = \sigma D$, $D_{xy} = \frac{1}{2}(1-\sigma).D$ = 1.0,1.0,0.3,0.35

ρ : mass per unit volume = 1.0

D.6.

i- Plate element

Two-dimensional orthotropic quadrilateral plate bending element. This is the same element described in Appendix D.5 .

Data values used.

h = 0.028 ins (1.016×10^{-3} m)

β = 0.0

$D_x = D_y$ = 21.1 lb.ins (2.385 N.m)

D_1 = 6.33 lb.ins (0.7154 N.m)

D_{xy} = 7.385 lb.ins (0.8347 N.m)

ρ = 0.26165×10^{-3} lb.sec^2/ins^4 (2795.69 kg/m^3)

ii- Stringer element

Two-dimensional grillage element with thin walled open section |51,52| .

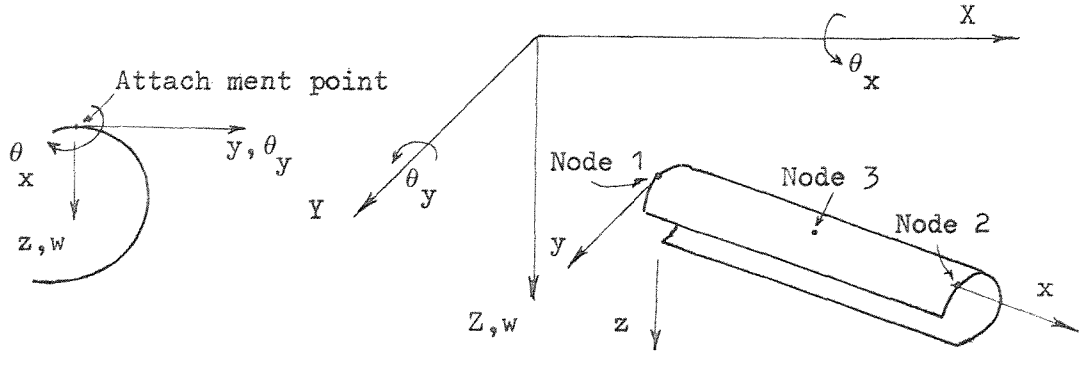

This element has three nodes(two at the ends and one at mid-point along the x direction).The degrees of freedom at the nodes are w, θ_x and θ_y at nodes 1 and 2 and θ at node 3.

Data values used.

The plate is stiffened by channel section frames and Z section stringers. The distance between the frames is 9 ins (0.2286 m) and the distance between the stringers is 4.5 ins (0.1143 m).

Stringer data.

a_y, a_z : coordinates of centroid of the cross-section = 0.318,0.318 ins (8.077×10^{-3} , 8.077×10^{-3} m)

C_y, C_z : coordinates of the shear centre of the cross-section
= 0.425 ,0.425 ins (0.018 ,0.018 m)

A : cross-sectional area = 0.05862 ins^2 (3.782×10^{-5} m^2)

I_{yy}, I_{yz}, I_{zz} : second moments of area of cross-section with respect to axes through attachement point = 0.01722,0.01232,0.01074ins^4 (7.168×10^{-9},5.128×10^{-9},4.47×10^{-9} m^4)

ω_A : warping function with pole at shear centre evaluated at attachement point = 0.0499

$J_{\omega A}$: warping constant with pole at shear centre = 5.06×10^{-4} ins^5 (5.35×10^{-12} m^5)

J : Saint Venant torsion constant = 1.573×10^{-5} ins^4 (6.547×10^{-12} m^4)

E : Young's modulus = 10.5×10^6 lb/ins^2 (7.235×10^{10} N/m^2)

G : shear modulus = 4.0×10^6 lb/ins^2 (2.759×10^{10} N/m^2)

ρ : mass per unit volume = 2.6165×10^{-4} $lb.sec^2/ins^4$ (2795.69 kg/m^3)

Data values for frames.

a_y, a_z = 0.214,1.25 ins (5.44×10^{-3},3.18×10^{-2} m)

C_y, C_z = 0.516,1.25 ins (0.0131,010318 m)

A = 0.1145 ins^2 (7.385×10^{-5} m^2)

I_{yy}, I_{yz}, I_{zz} = 0.28094,0.0306,0.00786 ins^4 (1.169×10^{-7},1.274×10^{-8}, 3.272×10^{-9} m^4)

$J_{\omega A}$ = 0.052189 ins^5 (5.518×10^{-10} m^5)

J = 2.78×10^{-5} ins^4 (1.157×10^{-11} m^4)

E,G,ρ = the same as the stringers .

D.7.

Three-dimensional orthotropic quadrilateral plate bending element |45,48,51 and 52| .

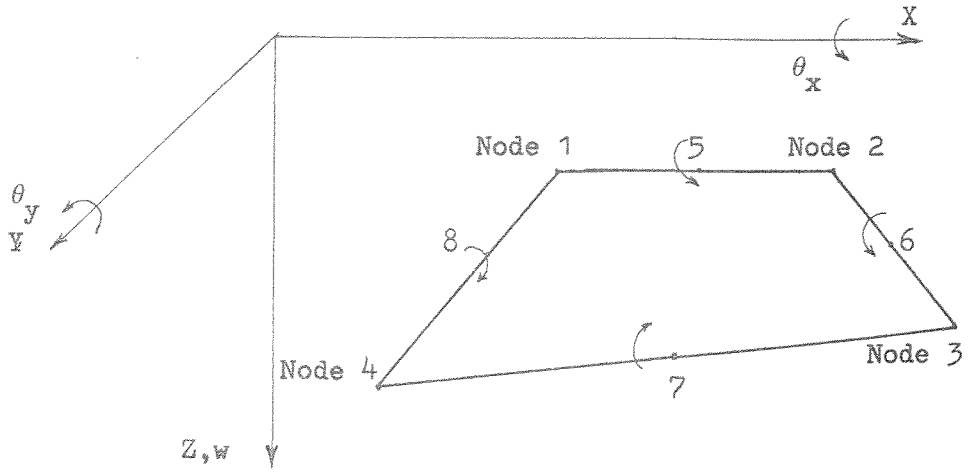

This element has 8 nodes(4 at the corners and 4 at the mid point of the sides).The degrees of freedom at the nodes are u,v,w, θ_x, θ_y and θ_z at nodes 1 to 4 and θ at nodes 5 to 8.The lateral displacements vary cubically and normal rotations vary quadratically along each edge.

Data values used.

h : constant plate thickness = 1.0

β : angle between material and global XY axes = 0.0

D_x, D_y, D_1, D_{xy} : orthotropic plate constants referred to material axes (for isotropic material $D_x = D_y = D = E.h^3/(12(1-\sigma^2))$, $D_1 = \sigma D$ and $D_{xy} = \frac{1}{2}(1-\sigma)D$)
= 1.0 , 1.0 , 0.3 , 0.35 .

ρ : mass per unit volume = 1.0 .

REFERENCES

1. Abrahamson,A.L. 'Flexural wave mechanics- an analytical approach to the vibration of periodic structures forced by convected pressure fields'. J.Sound Vib.(1973)28,247-258.

2. Bishop,R.,Gladwell,G. and Michaelson,S. 'The Matrix Analysis of Vibration'. Cambridge University Press,1965.

3. Brillouin,L. 'Wave Propagation in Periodic Structures'. Dover Publications,1953.

4. Brillouin,L. 'Wave propagation and Group Velocity'. Academic Press,1960.

5. Brobovnitski,Yu.I. and Maslov,V.P. 'Propagation of flexural waves along a beam with periodic point loading'. Soviet-Physics-Acoustics,1966.

6. Clarkson,B.L.and Mead,D.J. 'High frequency vibration of aircraft structures'. J.Sound Vib.(1973)28,487-504.

7. Clarkson,B.L.and Ford,R.D. 'The response of a typical aircraft structure to jet noise'. J.Roy.Aero.Soc. Vol.66.No.31(1962).

8. Crandall,S.H.and Mark,W.D. 'Random Vibration in Mechanical Systems'. Academic Press,1963.

9. Crandall,S.H. 'Random Vibration'. M.I.T.Press.1963.

10. Deak,A.L.and Pian,T.H.H. 'The application of the smooth-surface interpolation technique to the finite element analysis of thin plates'. Aeroelastic and Structures Research Laboratory Report,M.I.T.,1966.

11. Denke,P.H.,Eide,G.R. and Pickard,J. 'Matrix difference equation analysis of vibrating periodic structures'. AIAA Journal,1965,Vol.13.No.2.pp.160-166.

12. Eastham,M.S.P. 'The Spectral Theory of Periodic Differential Equations'. Scottish Academic Press,1973.

13. Engles,R.C.and Meirovitch,L. 'Response of periodic structures by modal analysis'. J.Sound Vib.(1978)56(4),481-493.

14. Espindola,J.J. 'Numerical Methods in Wave Propagation in Periodic Structures'.Ph.D.Thesis, University of Southampton,1974.

15. Fleischer,C.C. 'Dynamic Analysis of Curved Structures'. Ph.D.Thesis,University of Southampton,1973.

16. French,A.P. 'Vibration and Waves'.M.I.T.Introductory Physics Series.Nelson,London.1971.

17. Ford,R.D. 'The Response of Structures to Jet Noise'. Ph.D.Thesis,University of Southampton,1962.

18. Gladwell,G. and Tabb. 'Finite element analysis of the axisymmetric vibration of cylinders'. J.Sound Vib.(1972), 22(2),143-156.

19. Heckel,M.A. 'Wave propagation in beam-plate systems'. J.Acoust.Soc.Am.(1961),33(5),640-651.

20. Heckel,M.A. 'Investigations on the vibrations of grillages and other simple beam structures'.J.Acoust. Soc.Am.(1964),36,pp 1335-1343.

21. Kinsler,L.E. and Frey,A.R. 'Fundamental of Acoustics'.(Second Edition) John Wiley&Sons,Inc.,1962.

22. Leckie,F.A. and Lindberg,G.M. 'The effect of lumped parameters on beam frequencies'.Aeronautical quarterly(1963) pp 224-240.

23. Lin,Y.K. 'Free vibration of continuous skin stringer panels'.J.Applied Mechanics(1960)27(4)669-676.

24. Lindberg,G.M. and Olson,M.D. 'A numerical approach to random response problems'.National Research Council of Canada,Aero.Report LR.479.

25. Mead,D.J. 'Some theorems relating to wave propagation in periodic systems'.Institute of Sound and Vibration Research Memo.507,1974,

26. Mead,D.J. 'The Effect of Certain Damping Treatments on the Response of Idealised Aeroplane Structures Excited by Noise'.Ph.D.Thesis, Southampton University,1963.

27. Mead,D.J.and Wilby,E.W. 'The random vibration of a multi-supported heaviley damped beam'.Shock and Vibration Bulletin(1966),35(3),45-54.

28. Mead,D.J. 'Vibration response and wave propagation in periodic structures'.Paper No.70-WA/DE-3. Proc.ASME. winter annual meeting New York, N.Y.(1970).

29. Mead,D.J.and Sen-Gupta,G. 'Wave group theory applied to the analysis of forced vibrations of rib-skin structures'. Paper No.D.3,Proceedings Symp.Struct. Dynamics,Loughborough,1970.

30. Mead,D.J.and Sen-Gupta,G. 'Wave group theory applied to the response of finite structures'.Paper No.Q. Proc.Conf. on current developments in sonic fatigue, Southampton,1970.

31. Mead,D.J. 'Free wave propagation in periodically supported infinite beams'. J.Sound Vib. (1970)11(2) 181-197.

32. Mead,D.J. 'A general theory of harmonic wave propagation in linear periodic systems with multiple coupling'.J.Sound Vib.(1973)27(2) 235-260.

33. Mead,D.J. 'Wave propagation and natural modes in periodic systems'.I-Mono-coupled systems, II- Multi-coupled systems with and without damping. J.Sound Vib.(1975)40(1) 1-18 and 19-39

34. Mead,D.J.and Pujara,K.K. 'Space harmonic analysis of periodically supported beams:response to convected random loading'.J.Sound Vib.(1971)14(4), 525-541.

35. Meirovitch,L. 'Analytical Methods in Vibration'. Macmillan, New-York,1967 .

36. Meirovitch,L. 'Methods of Analytical Dynamics'. McGraw Hill, New-York,1970 .

37. Meirovitch,L. 'Elements of Vibration Analysis'. McGraw Hill, New-York,1975 .

38. Meirovitch,L.and Engels,R.C. 'Response of periodic structures by Z transform method'.American Institute of Aeronautics Journal(1977)15,167-174 .

39. Mercer,C.A. 'Response of a multi-supported beam to a random pressure field'.J.Sound Vib.(1965) 2(3)293-306 .

40. Miles,J.W. 'Vibration of beams on many supports'. Proc.Am.Soc.Civil Eng.Vol.82,n EM1,1-9(1956).

41. Moler,C.B.and Stewart,G.W. 'An algorithm for gemeralised matrix eigen-problems'.SIAM.J.Num.Anal.,Vol.10(1973)241-256.

42. Newland,D.E. 'Random Vibrations and Spectral Analysis'. Longman Group Ltd. London,1975 .

43. O'Keefe,J.M. 'A Study of the Forced Response of a Highly Damped Periodic Structures'. M.Sc.Thesis, University of Southampton,1971 .

44. Olson,M.D. 'A consistent finite element method for random response problems'.Int.J.of Computers and Structures(1972)2,163-180 .

45. Orris,R.M.and Petyt,M. 'A finite element study of the vibration of trapezoidal plates'.J.Sound Vib.(1973)27, 325-344 .

46. Orris,R.M.and Petyt,M. 'A finite element study of harmonic wave-propagation in periodic structures'. J.Sound Vib.(1974)33(2)223-236 .

47. Orris,R.M.and Petyt,M. 'Random response of periodic structures by a finite element technique'.J.Sound Vib.(1973) 27(2),235-260.

48. Orris,R.M. 'A Finite Element Study of the Vibration of Skin-Rib Structures'.Ph.D.Thesis, University of Southampton,1974 .

49. Peters,G.and Wilkinson,J.H. 'A.x=λ.B.x and the generalised eigenproblem'. SIAM J.Numr.Anal.Vol.7 No.4(1970)

50. Petyt,M. 'Finite strip analysis of flat skin-stringer structures'.J.Sound Vib.(1977)54(4)533-547.

51. Petyt,M. 'SPADAS Theoretical Manual'. Institute of Sound and Vibration Research,1974 .

52. Petyt,M.and Abdel-Rahman,A.Y. 'SPADAS Users Manual'. Institute of Sound and Vibration Research,1974 .

53. Pujara,K.K. 'Vibration of and Sound Radiation from some Periodic Structures under Convected Loads'. Ph.D.Thesis,University of Southampton,1970.

54. Salama,A.L.and Petyt,M. 'Dynamic response of packets of blades by the finite element method'.Paper No.77 DET-70, Design Eng.Tech.Conf.,Am.Soc.Mech.Eng.Sept., 1977.

55. Sen-Gupta,G. 'Natural flexural waves and normal modes of periodically supported beams and plates'. J.Sound Vib.(1970)13(1),89-101 .

56. Sen-Gupta,G. 'Natural frequencies of periodic skin-stringer structures using wave approach'. J.Sound Vib.(1971)16(4),567-580 .

57. Sen-Gupta,G. 'Dynamics of Periodically Stiffened Structures using a Wave Approach'.Ph.D.Thesis, University of Southampton,1970 .

58. Ting,E.C. 'On the natural frequencies of continuous beam structures'.J.Sound Vib.(1978)57(3), 457-459 .

59. Thomson,W.T. 'Theory of Vibration with Applications'. Prentice Hall,Inc.,1972 .

60. Ungar,E.E. 'Steady state response of one-dimensional periodic flexural systems'.J.Acoust.Soc. Am.(1966)39(5) 887-894 .

61. Warburton,G.B. 'The vibration of rectangular plates'.Proc. Inst.Mech.Eng.London(1954) 168,371-384 .

62. Warburton,G.B. 'The Dynamical Behaviour of Structures'. Second Edition, Pergamon Press,1977 .

63. Ward,R.C. 'An extension of the QZ algorithm for solving the generalised matrix eigenvalue problem'. Techmical note NASA TN D-7305, 1973 .

64. Wilkinson,J.H. 'The Algebraic Eigenvalue Problem'. The Clarendon Press, Oxford,1965 .

65. Wilkinson,J.H. and Reinsch,C. 'Handbook for Automatic Computation'.Vol.II Linear Algebra,pp.93-110,339-358 and 359-371.

66. Williams,F.W. 'Natural frequencies of repetitive structures'. Quart.Journ.Mech.and Applied Math.,Vol.XXIV, Pt.3,1971.

67. Wills,J.A.B. 'Measurements of the wave-number frequency spectrum of wall pressure beneath a turbulent boundary layer'.Natn.Phys.Lab. Aero.Rep.1224, 1967 .

68. Wittrick,W.H.and Williams,F.W. 'A general algorithm for computing the natural frequencies of elastic structures'.Quart. Journ.Mech.and Applied Math.,Vol.XXIV Pt.3, 1971.

69. Zienkiewicz,O.C. 'The Finite Element Method'.Third Edition McGraw Hill,1977 .